

# **Continuous-flow methodologies for deuteration of haloarenes, *N*-acetylation and amide formation reactions**

**PhD Thesis**

By

**György Orsy**

Supervisors:

Prof. Dr. Ferenc Fülöp

Dr. István Mándity



University of Szeged

Institute of Pharmaceutical Chemistry

Szeged

2020

# Table of Contents

List of publications and lectures.....	iii
Papers related to the thesis .....	iii
Scientific lectures related to the thesis .....	iv
Abbreviations .....	v
1. INTRODUCTION AND AIM .....	1
2. LITERATURE SURVEY .....	3
2.1. Concepts of flow chemistry.....	3
2.2. Deuterium labelled compounds, haloarenes in organic chemistry, hydrogenation and deuteration reactions .....	6
2.2.1. Deuterium labelled compounds in medical therapy .....	6
2.2.2. Haloarenes in organic chemistry and catalytic metal-mediated hydrogenation/deuteration reactions .....	8
2.3. The significance of the acetyl functional group and acetylation reactions in organic chemistry .....	11
2.3.1. The significance of the acetyl functional group and acetylation reaction.....	11
2.3.2. Acetylation methodologies in organic chemistry.....	13
2.4. Amide bond formation in organic chemistry .....	17
2.4.1. The importance of the amide bond.....	17
2.4.2. The strategies for amide bond formation .....	19
2.4.3. Amide bond formation with boronic acid and carbon disulfide.....	21
3. EXPERIMENTAL SECTION .....	24
3.1. General information .....	24
3.2. General Procedure for the Flow Reactions.....	24
3.2.1. General aspects of the CF deuteration in H-Cube® device .....	24
3.2.2. General aspects of the CF acetylation and amidation in a “home-made” reactor.....	25
4. RESULTS AND DISCUSSION .....	26
4.1. Deuteration of haloarenes in H-Cube® CF device .....	26
4.1.1. Optimization.....	26
4.1.2. Scope and scale-up experiments .....	28
4.2. <i>N</i> -acetylation of amines in a “home-made” CF reactor with acetonitrile .....	32
4.2.1. Optimization.....	32

4.2.2. Scope and scale-up experiments .....	35
4.3. Direct amide formation in a “home-made” CF reactor mediated by carbon disulfide.....	38
4.3.1. Optimization.....	39
4.2.3. Scope and scale-up experiments .....	43
5. SUMMARY .....	46
Acknowledgements .....	48
References .....	49
Appendix .....	56

## List of publications and lectures

### Papers related to the thesis

- I. **György Orsy**, Ferenc Fülöp, István M. Mándity:  
Continuous-flow catalytic deuterodehalogenation carried out in propylene carbonate  
*Green Chem.*, 2019, **21**, 956-961. IF.: 9.480
- II. **György Orsy**, Ferenc Fülöp, István M. Mándity:  
N-Acetylation of Amines in Continuous-Flow with Acetonitrile-No Need for  
Hazardous and Toxic Carboxylic Acid Derivatives  
*Molecules*, 2020, **25**, 1985. IF.:3.267
- III. **György Orsy**, Ferenc Fülöp, István M. Mándity:  
Direct amide formation in a continuous-flow system mediated by carbon disulfide  
*Catal. Sci. Technol.*, 2020, DOI: 10.1039/d0cy01603a IF.: 5.721

### Other papers

- IV. Loránd Kiss, Eniko Forró, **György Orsy**, Renáta Ábrahádi, Ferenc Fülöp:  
Stereo- and Regiocontrolled Syntheses of Exomethylene Cyclohexane  $\beta$ -Amino Acid  
Derivatives  
*Molecules*, 2015, **20**, 21094-102. IF.:3.267

*Cumulative impact factor: 21.735*

## Scientific lectures related to the thesis

1. **György Orsy**, Ferenc Fülöp, István M. Mándity:  
*Haloarének katalitikus deuterálása áramlásos reaktorban*  
Szegedi Ifjú Szerves Kémikusok Támogatásáért Alapítvány, a SZAB Szerves és Gyógyszerkémiai Munkabizottsága és a Magyar Kémikusok Egyesülete Csongrád Megyei Csoportja 16. tudományos előadójelentése  
Hungary, Szeged, 2017
2. **György Orsy**, Ferenc Fülöp, István M. Mándity  
*Catalytic deuterodehalogenation of haloarenes in continuous-flow*  
7th BBBB International Conference on Pharmaceutical Sciences  
Hungary, Balatonfüred, 2017
3. **György Orsy**, Ferenc Fülöp, István M. Mándity  
*Direct amide formation in continuous-flow system mediated by carbon disulfide*  
United Kingdom, Cambridge, 2018

## Abbreviations

4-PBA	4-phenylbutyric acid
Ac	acetyl
APT	attached proton test
BA	benzylamine
Boc	<i>tert</i> -butoxycarbonyl
CF	continuous-flow
CoA	coenzyme A
D	deuterium incorporation value
DMAP	4-dimethylaminopyridine
DMSO	dimethyl sulfoxide
DNA	deoxyribonucleic acid
FDA	Food and Drug Administration
FER	ferrierite
GC	gas chromatography
HMG	$\beta$ -hydroxy $\beta$ -methylglutaryl
HPLC	high performance liquid chromatography
JAK	Janus kinase
MS	mass spectrometry
NMDA	<i>N</i> -methyl-D-aspartate
NMR	nuclear magnetic resonance
p	pressure
PBSAC	polymer-based spherical activated carbon
PC	propylene carbonate
Pd/BaSO <sub>4</sub>	palladium on barium sulfate
Pd/C	palladium on charcoal
PDA	poly-dopamine
PDE4	phosphodiesterase-4

PPAR- $\gamma$	peroxisome proliferator-activated receptor gamma
STAT	signal transducer and activator of transcription
T	temperature
ZPE	zero-point

# 1.INTRODUCTION AND AIMS

Since The Industrial Revolution, chemical manufacturing is still using the traditional batch chemistry methodology, the general principle of which has been around for hundreds of years and remained virtually unchanged in that time. Chemical batch processes are reactions carried out in single vessels. In case of multistep syntheses, batch reactions usually require significant manual labour, as the reaction products from each step must be processed separately (start–stop batch processing). Chemical production has traditionally been the process of the production of fine chemicals,<sup>1</sup> pesticides<sup>2</sup> and medical drugs.<sup>3</sup> At the start of the 21<sup>st</sup> century, technical and economic innovations led to a paradigm shift. The traditional chemical process model has undergone a tremendous change in a particular direction: continuous process. The driving force behind this effort of paradigm shift is minimizing waste, improving sustainability, and safety standards, finding economic and selective ways to earn greater yields and profit.<sup>4</sup>

The field of flow chemistry has garnered considerable attention over the past two decades,<sup>5</sup> scientists around the world report a huge number of publications accessing continuous-flow (CF) chemistry techniques. The most significant adoption of flow technology is in pharmaceutical industry.<sup>6</sup> The new technology has the ability to facilitate the discovery of new medicines, high-speed development and optimization of scale-up of potential drug candidates. CF processing can permit special reaction conditions, such as highly pressurized and superheating reactions. Furthermore, it permits better safe use of unstable and/or toxic reagents, allowing atom-efficient reagents to be better exploited, it can help exploration of atom-economical reactions.<sup>7, 8</sup> The CF chemistry is a versatile tool of not just the laboratory users, a kind of opportunity that can be used in any possible area of synthetic chemistry.<sup>9</sup>

Our aim was to apply continuous-flow in three types of different reactions to improve efficiency, to make them more green, more selective and as safe as possible. Highlighting the reactions where we had applied the flow chemistry technology, we investigated the following areas in CF: (i) catalytic deuterodehalogenation of haloarenes in H-Cube® device, (ii) *N*-acetylation of amines with acetonitrile as solvent and acetyl group source, (iii) direct amide formation mediated by carbon disulfide.

Deuterium-labelled compounds have a wide range of applications such as in mass spectrometry as internal standards<sup>10</sup>, in different hydrogen-deuterium exchange mechanistic studies of several chemical reactions<sup>11</sup> and it can be a useful protecting group.<sup>12</sup> Nowadays, they



are considered in medical applications, especially, the deuterated aryl moiety in approved medical drugs have high therapeutic values due to improved pharmacokinetic properties.<sup>13</sup> The first deuterated compound is deutetrabenazine that has entered clinical practice in 2017.<sup>14</sup> This success has resulted in more than 10 deuterated drugs being presently under clinical trials for various diseases.<sup>15</sup>

The *N*-acetylation is a fundamental chemical reaction in organic chemistry.<sup>16</sup> This reaction is utilized in drug research and preparation and has importance in polymer chemistry and agrochemical productions.<sup>17-20</sup> The acetyl functional group is utilized in peptide synthesis and in several organic syntheses.<sup>21</sup> Importantly, acetylation is a major regulatory process in post-translational protein modification and it has a major impact on regulation of DNA expression in all life forms.<sup>22</sup> The general method to produce an *N*-acetylated amine is performed by acetic anhydride or acetyl chloride as the acetylation agent in the presence of acidic or basic catalysts in organic medium, nevertheless, even utilizing these reagents with various Lewis acids.<sup>23, 24</sup> Moreover, these reagents are harmful to health.<sup>25</sup>

One of most ubiquitous chemical linkages is the amide bond in nature.<sup>26</sup> It is a spine-like bond in peptides/proteins, natural and synthetic polymers<sup>27</sup>. The amide bond is an important functional group in a huge number of different types of medical drugs such as local anaesthetics, nonsteroidal anti-inflammatories, antibiotics and therapeutic peptides.<sup>28-31</sup> Amide compound synthesis includes two main strategies: one is the use of coupling reagents, the other is the use of the activation agent for the carboxylic acid starting material. Both methods suffer from many drawbacks, such as generating a large amount of side-products and the purification of the desired amide product is difficult.<sup>32</sup>

## 2. LITERATURE SURVEY

### 2.1. Concepts of flow chemistry

CF technology has affected many fields over the last decades, found application for the production of many highly valuable intermediates and products on industry and laboratory scales.<sup>33</sup> Classic chemical batch synthesis had to face a variety of problems known since organic chemical products were introduced in industry at the end of the 19<sup>th</sup> century. The major challenges are in the fields of plant security, sustainable production, temperature and efficient mixing control in batch vessels, there is still a demand for improved solutions. The new approach was found to replace the limited batch vessel technology by a more flexible and efficient alternative: flow chemistry technology.<sup>35</sup> This technology offers many advantages over classical batch technology, including great improvements in energy efficiency, reliability, scalability, reaction yield and speed, and finer process control.<sup>36</sup>

In flow chemistry, the chemical reaction is carried out with a continuous supply of starting substrate and reagents. Reagents are continuously pumped through the reactor and they are mixed and exposed to reaction parameters. The transformation takes place, the product forms and the product is continuously isolated. Depending on the reaction, a wide range of technologies can be integrated such as a heating or cooling system, oscillator, electrochemical reactor, microwave unit, photoreactor, ultrasound apparatus. An added advantage of flow chemistry is that work-up and purification can be linked and performed in-line, as part of an integrated process. The flow reactor has the capabilities of a modern concept in which classical problems of large scale synthesis.<sup>37, 38</sup>

There are a few fundamental differences between classical batch and CF systems. In flow processes, the ratio of parameters such as flow rate molarity are used to set the specific stoichiometry. The reaction time is determined by the time a batch is stirred under fixed conditions, however, in flow processes, the reaction time is determined by the residence time; the time the reactants spend in the reactor zone where the reaction occurs. Residence time is calculated by the ratio of the tube volume of reactor and the reaction flow rate. The precise controlling of the residence time is a crucial factor of flow processes, because the reaction kinetics can be controlled by the flow rates of the material streams. The flow rates will influence the residence time of the reaction and have a strong impact on the outcome of transformation. Inside of flow reactor channel,

each portion is defined by a specific concentration of the starting materials and products. Thus, the reaction profile must be defined within space rather than time. The steady state is an important parameter that defines a condition where all parameters remain unchanged at a certain point in time that is a desired condition in the reactor zone to achieve the most excellent transformation.<sup>39, 40</sup>

The major advantages of flow technology are the excellent mass and heat transfer properties compared classical batch reactions (Figure 1).<sup>41, 42</sup>

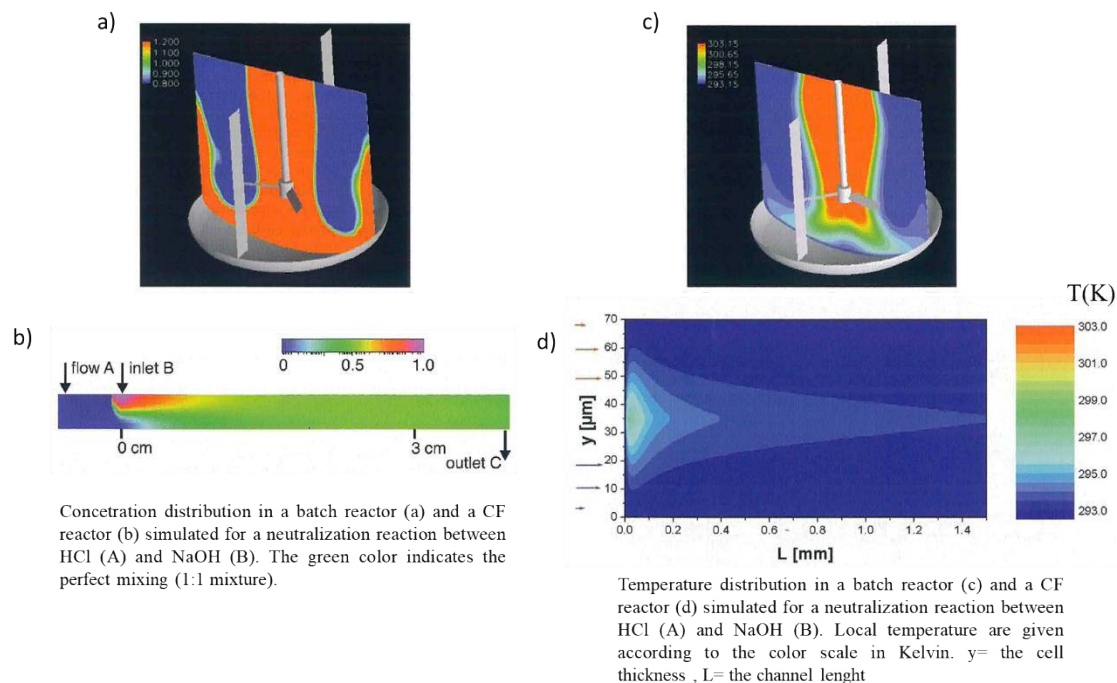


**Figure 1.** Concentration and temperature profiles in a batch reactor (a, c) and a CF reactor (b, d)<sup>42</sup>

Generally, the mixing is often achieved by mechanical stirring in chemical reaction vessels and the fluid motion is mainly turbulent flow at high Reynolds numbers that means the fluid motion is characterized by chaotic changes in pressure and flow velocity. Thus, the mixing is often unsatisfactory. In contrast, flow reactors operate at low Reynolds numbers, where the mixing can occur through diffusion between laminar flow layers. According to Fick's law, in case of flow reactor scales, the velocity of diffusion depends on the channel diameter, which suggests that miniaturization of the axial dimensions can definitely enhance the mass transfer in flow stream.<sup>42</sup>

In many chemical processes, reaction temperature has to be controlled in a certain range. It is a key element to suppress undesired side-reactions. The heat is exchanged via the reactor surface

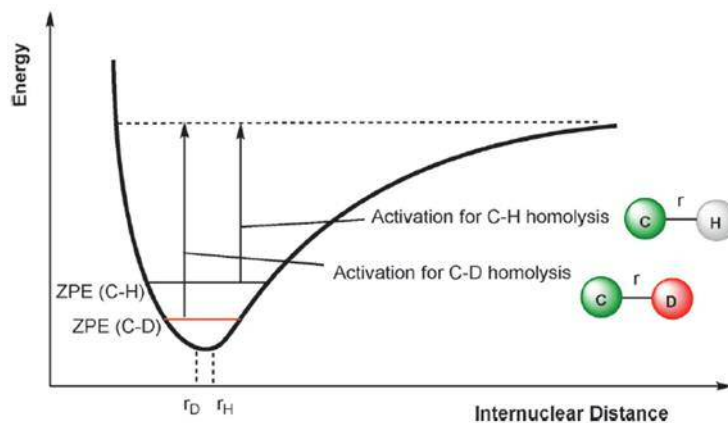
depends on surface area-to-volume ratio in batch reactions. Flow reactors have a very large surface area-to-volume ratio due to tiny channels parameters.<sup>43</sup> Therefore, the heat exchange is much faster than conventional batch reactors. The highly controlled heat transfer allows a homogeneous and narrow temperature distribution which influence the yield, selectivity, and reaction time.<sup>44</sup>

## 2.2. Deuterium labelled compounds, haloarenes in organic chemistry, hydrogenation and deuteration reactions

### 2.2.1. Deuterium labelled compounds in medical therapy

Deuterium is a stable isotope of hydrogen, not radioactive, and found in extremely small amounts in nature; the natural abundance of deuterium is 0.0156% in the oceans of Earth.<sup>45</sup> Deuterated water is produced in very large quantities, it is used to slow down fast neutrons and thus act as a neutron modulator in nuclear reactors.<sup>46</sup> Nowadays, the notable application is the use of deuterium in drug design.<sup>47</sup>

The reason for usefulness of the deuterium isotope in drug design is the primarily the deuterium kinetic isotope effect. The C-D bond is shorter than the C-H bond in a molecule which results in a lower vibrational frequency. Thus, the cleavage of this bond needs a larger activation energy (Scheme 1).<sup>48</sup>



**Scheme 1.** The lower zero-point energy (ZPE) results in a higher activation energy for C-D bond homolysis<sup>48</sup>

The primary deuterium kinetic isotope effect has been utilized to understand many kinds of reaction mechanisms. Incorporation of deuterium into active pharmaceutical molecules has resulted in more stable substrates for metabolic degradation that remain active for a longer time in the body. Moreover, deuteration of a soft-spot in the active pharmaceuticals can reduce the formation of unwanted metabolites. The substitution of hydrogen with deuterium at the chiral center of a chiral pure compound can stabilize it, for example, in case of *d*<sub>1</sub>-Telaprevir.<sup>15</sup>

Deuteration is a useful strategy to affect pharmacokinetic and metabolic profiles of active pharmaceuticals. This property can be a potential new tool in next generation medical drugs as deuterium-labelled compounds, in order to deliver improved therapeutic alternatives.<sup>49</sup> So far however, only one deuterium-labelled compound, deutetrabenazine<sup>50</sup> has been approved by the US Food and Drug Administration (FDA) as a treatment for Huntington’s disease. It has a longer half-life than the non-deuterated form of tetrabenazine, which had been approved earlier for the same indication. Deuterium incorporation at key positions in the tetrabenazine molecule leads to a longer drug half-life, less frequent daily dosing and a more favorable side effect profile. Numerous potential drug candidates are now in clinical trials for various indications (Table 1).<sup>51</sup>

**Table 1.** *Examples of deuterated compounds in clinical trials for various indications.*<sup>51</sup>

Drug maker	Drug name	Deuterium-modified drug	Target	Indication	Status
Avanir/Concert	AVP-786	Dextromethorphan	NMDA glutamate receptor	Alzheimer’s disease agitation symptoms	Phase 3
				Depression/schizophrenia	Phase 2
Concert	CTP-543	Ruxolitinib	JAK/STAT	Hair loss (alopecia areata)	Phase 2
Vertex	CTP-656	Kalydeco (ivacaftor)	cystic fibrosis transmembrane conductor regulator	Cystic fibrosis	Phase 2
DeuteRx	DRX-065	Pioglitazone (deuterated form)	PPAR- $\gamma$	Non-alcoholic steatohepatitis/adrenoleukodystrophy	Phase 1
Retrotope	RT001	Linoleic acid	Cell membrane	Freidreich’s ataxia	Phase 1/2
BMS	BMS-986165	New molecular entity	Tyrosine kinases	Psoriasis	Phase 2
Celgene/Concert	CT-730	Apremilast	PDE4	Inflammatory disorders	Phase 1
Vertex	VX-984	Doxorubicin	DNA-dependent protein kinase	Solid tumors	

The effects of deuterium exposure on living organism have been well studied. It was shown that D<sub>2</sub>O has low systematic toxicity. Unicellular microorganisms can be grown in full deuterated conditions, and lower organisms such as fish and tadpoles can survive at least 30% D<sub>2</sub>O levels. Higher organisms such as mice, rats and dogs can tolerate without any visible harmful effects from long-term replacement of 10-15% of body-fluid hydrogen with deuterium. However, more than 25% D<sub>2</sub>O levels are toxic to them. Humans can tolerate levels of 15-23% deuterium replacement in whole body plasma without evident adverse effects.<sup>52, 53</sup>

### 2.2.2. Haloarenes in organic chemistry and catalytic metal-mediated hydrogenation/deuteration reactions

Halogenated aromatic compounds (haloarenes) are very important and versatile compounds with many applications in laboratory chemistry and industrial application.<sup>54</sup> Although, the polyhalogenated derivatives are of particular interest and importance because they bioaccumulate in the food web and exhibit high toxicity, mutagenicity and carcinogenicity.<sup>55-60</sup> Therefore, it is urgent to develop an efficient and economic method to detoxify them in sustainable way. Several methods have been developed for the removal the halogen atom from halogenated aromatic molecules such as chemical oxidation,<sup>61</sup> photochemical degradation,<sup>62</sup> ultrasonic irradiation,<sup>63</sup> electrolysis,<sup>64</sup> microbial degradation,<sup>65</sup> incineration<sup>66</sup> and catalytic metal-mediated hydrodehalogenation.<sup>67</sup> Of these methods, the catalytic metal-mediated hydrodehalogenation reaction is the most selective and non-destructive treatment for transforming toxic material into much less toxic compounds for sustainable purpose. Metal-mediated hydrodehalogenation is almost equivalent to the catalytic hydrogenation process, in general, threatening with hydrogen gas source or hydrogen is transferred from donor molecules such as formic acid, isopropanol etc. in presence of a catalyst,<sup>68</sup> usually nickel,<sup>67, 69</sup> palladium,<sup>67, 70</sup> rhodium,<sup>71, 72</sup> ruthenium,<sup>73, 74</sup> gold<sup>75</sup> based catalysts.

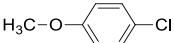
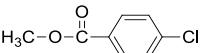
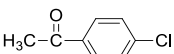
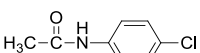
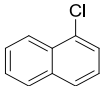
Depending on the catalysts' consistence they are classified into two broad classes: homogeneous and heterogeneous catalysts.

Homogeneous catalysts are soluble transition metal complexes used in reactions where the catalyst is in the same phase as the reactants; in solution. An advantage of this type is that the catalyst mixes into the reaction mixture, allowing a high degree of interaction between catalyst and reactants, to achieve the same rate milder conditions can be used and so it is possible to achieve greater chemoselectivity, regioselectivity, and/or enantioselectivity.<sup>76, 77</sup> However, after the reaction, the catalysts are often difficult to separate and may have issues at high temperatures.

One of them useful method of hydrodehalogenations of aryl chlorides under homogeneous conditions is demonstrated by Logan *et al.*<sup>78</sup> They examined the reduction of a series of aryl chlorides in refluxing methanol under argon, using 2 equiv of sodium formate as the hydride source, 2 mol% of Pd(OAc)<sub>2</sub> as the soluble transition metal complex, and 4 mol% of [1,1'-biphenyl]-2-yl-di-tert-butylphosphine as the Buchwald biphenyl ligand. The combination of Pd(OAc)<sub>2</sub> and Buchwald ligand was attractive, because both the palladium source and ligand are air-stable and

are commercially available. A few examples of the successful application of this method, with substrates bearing electron-donating, electron-withdrawing, or neutral functional groups, were reported (Table 2).

**Table 2.** Homogeneous catalytic hydrogenation of aryl chlorides by Logan et al.<sup>78</sup>

Entry	Aryl Chloride	Time (h)	Yield (%) <sup>a</sup>
1		3	99
2		1.5	97
3		2	100
4		3	97
5		4	95

<sup>a</sup>Gc yields, average of two runs

Heterogeneous catalysts have the advantage of being stable, reusable, and easy to separate.<sup>79, 80</sup> Especially supported palladium catalyst, which can be used not only in batch synthesis, but also in continuous-flow technology. The major breakthrough of continuous-flow (CF) technologies to organic chemistry and the fine chemical industry has appeared in the field of catalytic hydrogenation triggered by the invention of the hydrogenation device.<sup>81</sup>

In 2006, Darvas et al.<sup>82</sup> developed a continuous-flow high pressure device (H-Cube®) for use in high-throughput novel hydrogenation reductions such as nitroreduction, debenzylation, reduction of alkenes, alkynes and cyanides. The device consists of a built-in hydrogen generator that can produce *in situ* hydrogen gas from water by electrolysis. It was designed for mixing of liquid phase, the gas phase, and the solid catalyst phase to increase efficiency. The use of continuous-flow technology allows high-throughput hydrogenation, making the hydrogenation



process safer and more efficient than novel heterogeneous hydrogenation reactions. A few examples of the successful application of this method, were reported (Figure 2).

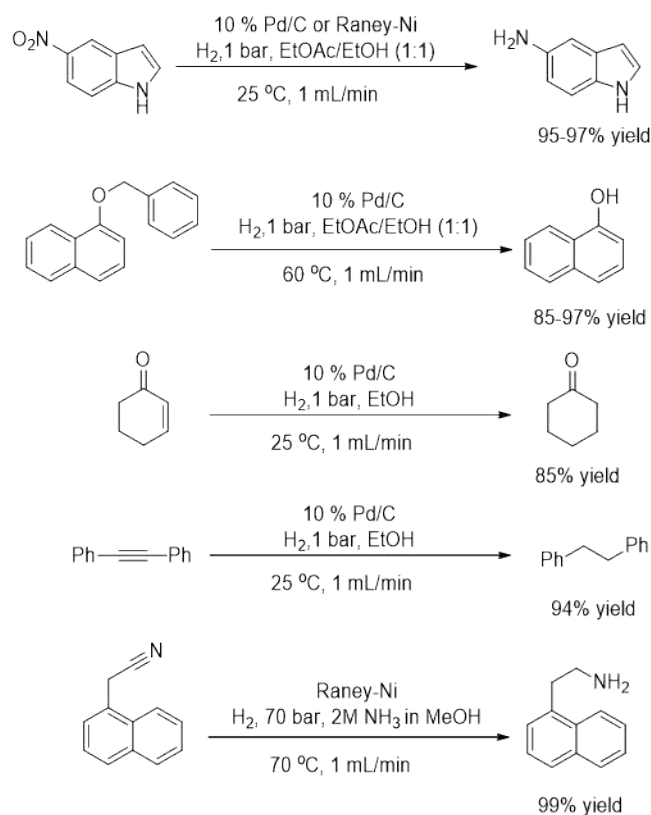


**Figure 2.** Catalytic hydrogenation reactions in *H-Cube*<sup>®</sup> device by Darvas *et al.*<sup>82</sup>

In recent years, the high interest in the medical application of deuterated compounds has resulted in a plethora of studies on the preparation of deuterated substances by hydrogen-deuterium exchange.<sup>83-87</sup> The most easy way to incorporate deuterons into molecules is by replacing hydrogen atoms. Such a transformation occurs in the presence of a suitable deuterium source such as D<sub>2</sub>O, D<sub>2</sub> gas or deuterated protic solvents. The general method for hydrogen-deuterium exchange is divided into pH-dependent hydrogen-deuterium exchange and metal catalyzed hydrogen-deuterium exchange (homogeneous/heterogeneous catalysis).<sup>88</sup> Not only can deuterium be incorporated into a molecule by hydrogen-deuterium exchange, it can also be achieved via halogen-deuterium exchange or catalytic deuteration.<sup>89-91</sup> Here, we have primarily focused on the heterogeneous metal catalyzed halogen-deuterium exchange reaction, because it is the most effective way to furnish deuterated aryl moiety compounds.

In 2009, Mándity et al.,<sup>92</sup> used heavy water to produce deuterium gas to develop an efficient and fast deuteration method in the H-Cube® reactor. They have established a deuteration procedure for alkenes, alkynes and  $\beta$ -amino acid derivatives which possess a double bond (Figure 3). The process was faster than literature methods, offered excellent yields and deuterium incorporation ratios.

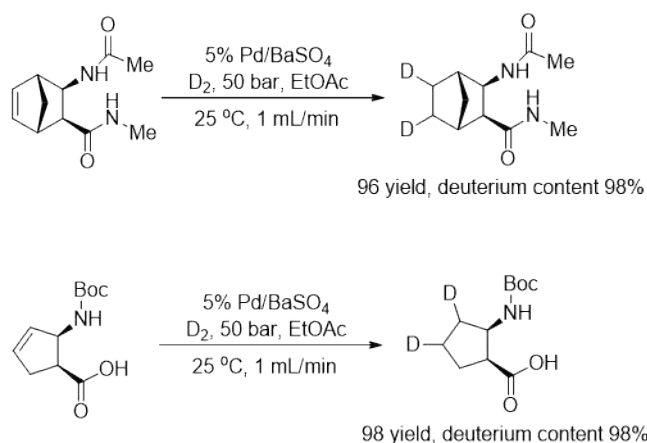
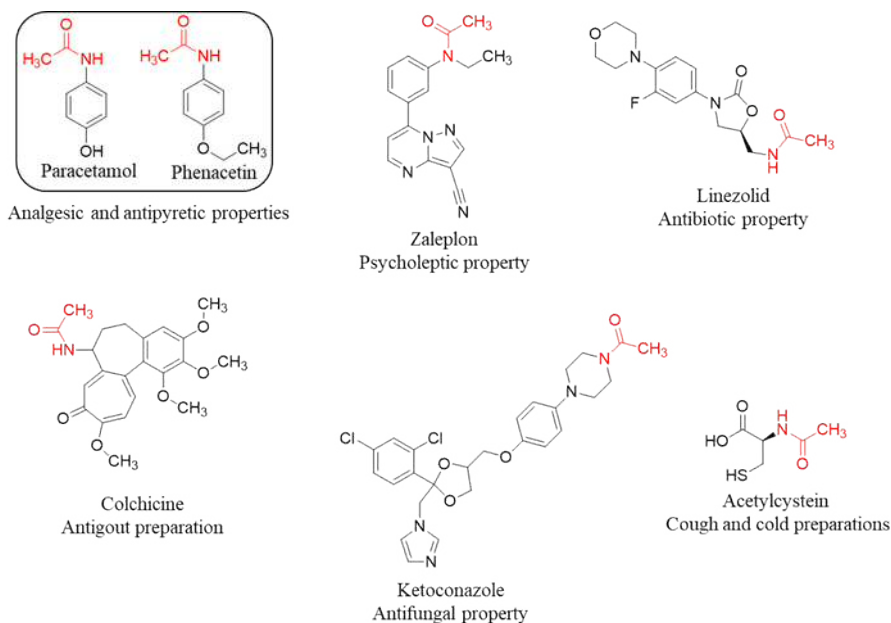


**Figure 3.** Deuteration of  $\beta$ -amino acids in H-Cube® by Mándity et al.<sup>92</sup>

## 2.3. The significance of the acetyl functional group and acetylation reactions in organic chemistry

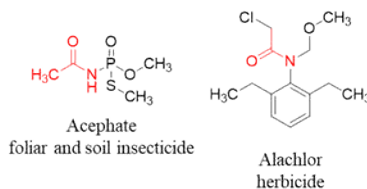
### 2.3.1. The significance of the acetyl functional group and acetylation reaction

The best-known acetamide drugs are paracetamol and phenacetin, synthesized in the late 1880s, for their mild analgesic/antipyretic properties. Initially, phenacetin was discarded in favor of paracetamol because the latter drug was less toxic.<sup>93</sup> Paracetamol has been used for many decades, with more than 27 billion doses sold in 2009. It is used to treat many conditions such as headache, muscle aches, arthritis, colds and fever but has no effect on the underlying inflammation.<sup>94</sup> The acetamide moiety can be found in a wide range of active pharmaceutical compounds for various indications (Scheme 2).



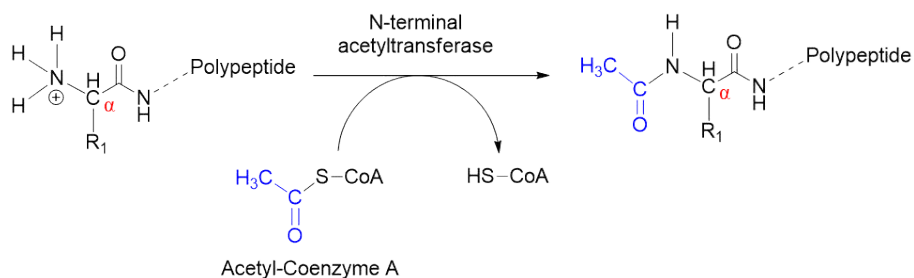
**Scheme 2.** A few examples for acetamide compounds which are approved drugs

Another important utilization of the acetamide compounds is in agrochemical application, is chemical product used in agriculture.<sup>95</sup>



**Scheme 3.** Two examples for acetamide compounds in agrochemical using

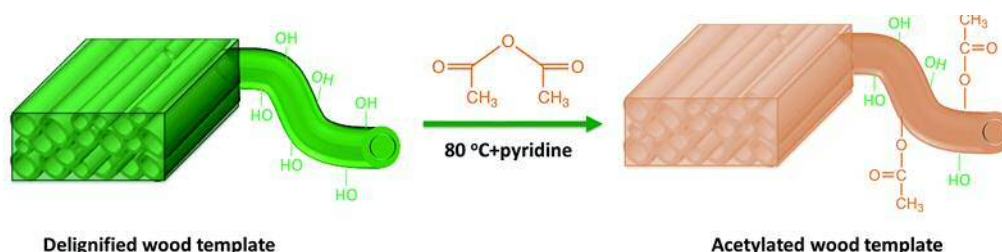
In cell biology, acetylation is one of the most important reactions and has been studied intensively. Protein acetylation is a kind of post-translational modification in which the acetyl group from acetyl coenzyme A is transferred by N-terminal acetyltransferases to a specific site on a polypeptide chain. Especially, N-terminal acetylation is a crucial regulation of a huge number of proteins. This process plays an important role in the synthesis, stability and localization of proteins in eukaryotic cells.<sup>22, 96-98</sup>



**Scheme 4.** N-terminal acetylation by N-terminal acetyltransferase enzyme

Acetylation is a very common metabolic reaction to process the xenobiotic molecules such as drugs or other chemicals in living organism. This “phase II” biotransformation is responsible for the conjugation of activated xenobiotic metabolites with an acetyl group. The conjugated products have increased molecular weight and tend to be less active.<sup>99</sup>

Since the early 20<sup>th</sup> century, acetylation of wood was researched to upgrade the durability of the material. The structure of wood is a porous three dimensional biopolymer composite assembled of an interconnecting matrix of cellulose, hemicellulose and lignin. Water layers build up this composite and the cell walls in wood have hydroxyl groups accessible to moisture with water due to hydrogen bonding. This high water content offers an opportunity for microorganisms to colonize and begin the process of rotting and mold growth. If these hydroxyl groups are substituted with a more hydrophobic groups, the bonded functional group can expand the cell wall to its elastic limit. The substituted hydrophobic groups reduce the water content of the wood and will be no longer a medium for microorganism growth. The acetylation of cell wall hydroxyl groups can achieve these properties. The increased acetyl content in wood also causes an improvement of dimensional stability and durability.<sup>100-102</sup>



**Scheme 5.** A sustainable acetylation method of wood by Li *et al.*<sup>101</sup>

### 2.3.2. Acetylation methodologies in organic chemistry

The generally method to access an *N*-acetylated amine is performed by acetic anhydride or acetyl chloride as acetylation agent in the presence of an acidic or basic catalyst in organic medium; numerous such strategies have been developed.<sup>103-105</sup> Among them, one of the promising methods is that Sharley *et al.*<sup>106</sup> This is a cheap and simple method for the acetylation of a broad range of amines using catalytic acetic acid and esters as the acyl source instead of anhydride derivatives. This method needs a low acetic acid catalyst loading (10 mol%) and afforded a wide variety acetamid products in excellent yields at temperatures ranging from 80-120 °C.

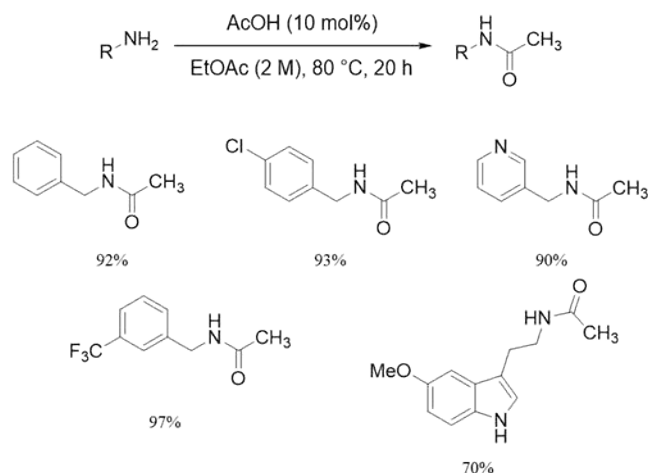


**Figure 4.** Acetylation reaction of amines and a few examples by Sharley *et al.*<sup>106</sup>

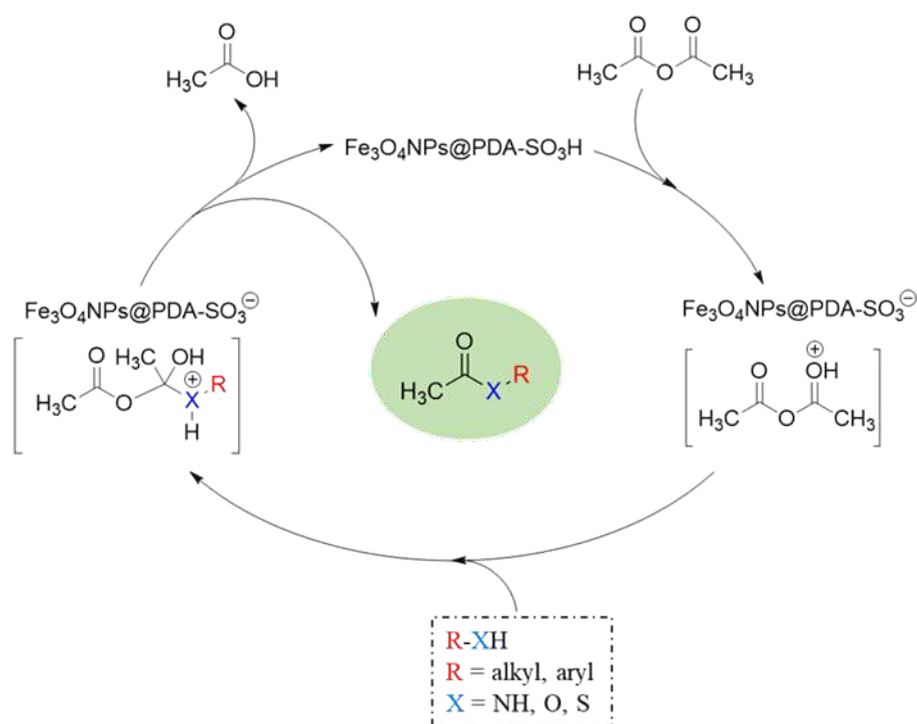
An another promising acetylation reaction has been reported by Yadav *et al.*,<sup>107</sup> who presented a new, economical and simple method for the acetylation of amines, alcohols and phenols with Ac<sub>2</sub>O/AcCl as the acyl source and KF-Al<sub>2</sub>O<sub>3</sub> as the acidic catalyst. KF-Al<sub>2</sub>O<sub>3</sub> catalyst has been used for the O-alkylation of phenols and alcohols, β-elimination, Michael addition, aldol condensation. This method, relying on substituting organic soluble acidic catalysts for a solid, is a highly efficient process and faster than most used methods.

**Table 3.** Acetylation of amines promoted by KF-Al<sub>2</sub>O<sub>3</sub> in toluene by Yadav *et al.*<sup>107</sup>

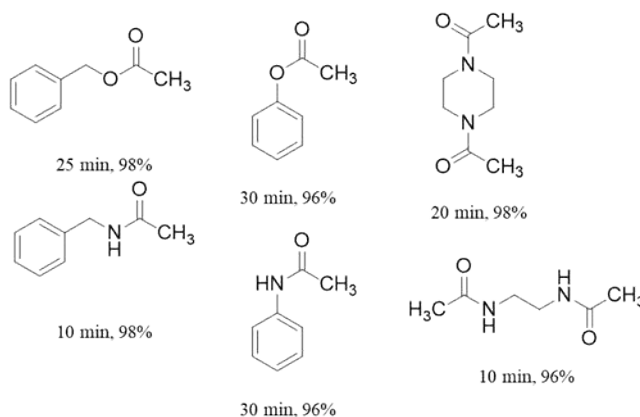
Entry	Substrate	Ac <sub>2</sub> O/AcCl	Reaction time (h)	Yield (%)
1	<i>tert</i> -Butyl amine	Ac <sub>2</sub> O	0.2	92
2	Morpholine	Ac <sub>2</sub> O	0.2	95
3	4-Chloroaniline	Ac <sub>2</sub> O	0.1	96
4	4-Nitroaniline	Ac <sub>2</sub> O	4	97

In recent years, most scientists have been making a large effort to develop the green and sustainable processes and have been focusing on the environmental impact of chemistry, including reducing consumption of technological approaches to reduce pollution. Due to increasing demand, a large number of studies have been published in recent years. In one of them, Veisi *et al.*<sup>108</sup> have developed a novel core-shell nanocatalyst for the acetylation of alcohols, phenols, amines and thiols with acetic anhydride. This catalyst was a polydopamine-coated Fe<sub>3</sub>O<sub>4</sub> nanoparticles (Fe<sub>2</sub>O<sub>3</sub>@PDA). The PDA can serve as an adhesion layer to immobilize biological molecules,

amine- and mercapto functionalized self-assembled monolayer and metal films. The generated  $\text{Fe}_3\text{O}_4@\text{PDA}$  nanstructure was further sulfonated using chlorosulfonic acid to make polydopamine sulfonic acid-functionalized magnetic  $\text{Fe}_3\text{O}_4$  nanoparticles with a core/shell nanostructure as a solid acid nanocatalyst. This kind of catalyst can replace soluble acids and can be considered a green chemistry approach. It has a high catalytic activity under mild reaction conditions and the removal of catalyst is easy due to the magnetic property of  $\text{Fe}_3\text{O}_4$  nanoparticles. The nanocatalyst could be recycled in 10 runs without any significant loss of activity.



**Scheme 6.** Plausible reaction mechanism of  $\text{Fe}_3\text{O}_4@\text{PDA}-\text{SO}_3\text{H}$ -catalyzed acetylation by Veisi et al.<sup>108</sup>

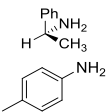
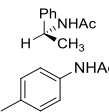


**Figure 5.** A few products of *O,N*-acetylation with acetic anhydride under solvent free conditions in the presence of  $Fe_3O_4@PDA-SO_3H$  reported by Veisi *et al.*<sup>108</sup>

Chavan *et al.*<sup>109</sup> developed a catalytic acetylation process for alcohols, thiols and amines with zeolite H-FER (protonated form of ferrierite) under solvent-free conditions. Application of an inorganic solid porous zeolite as a heterogeneous catalyst for organic synthesis has garnered attention due to its unique properties such as selectivity, acidic or basic nature and thermal stability. The activity of these catalysts is based on the Brønsted acid function and their ability to donate a proton. The advantage of these solid zeolite catalysts are well known, such as stability, ease of removal, lack of corrosion and environment hazards, recovery and regeneration are a simple procedures. They carried out this reaction with the use of acetic anhydride as the acetylation agent. In table 4, several alcohols, phenols, amines and thiols underwent acetylation in excellent yields.

**Table 4.** Direct acetylation of alcohols, phenols, thiols and amines with acetic anhydride over Zeolite H-FER by Chavan *et al.*<sup>109</sup>

Entry	Reactant	Product	Reaction time (h)	Yield (%)
1			2	98
2			2	98
3			1.5	99
4			2	95
5			5	5
6			5	5

7		2	2
8		2	2

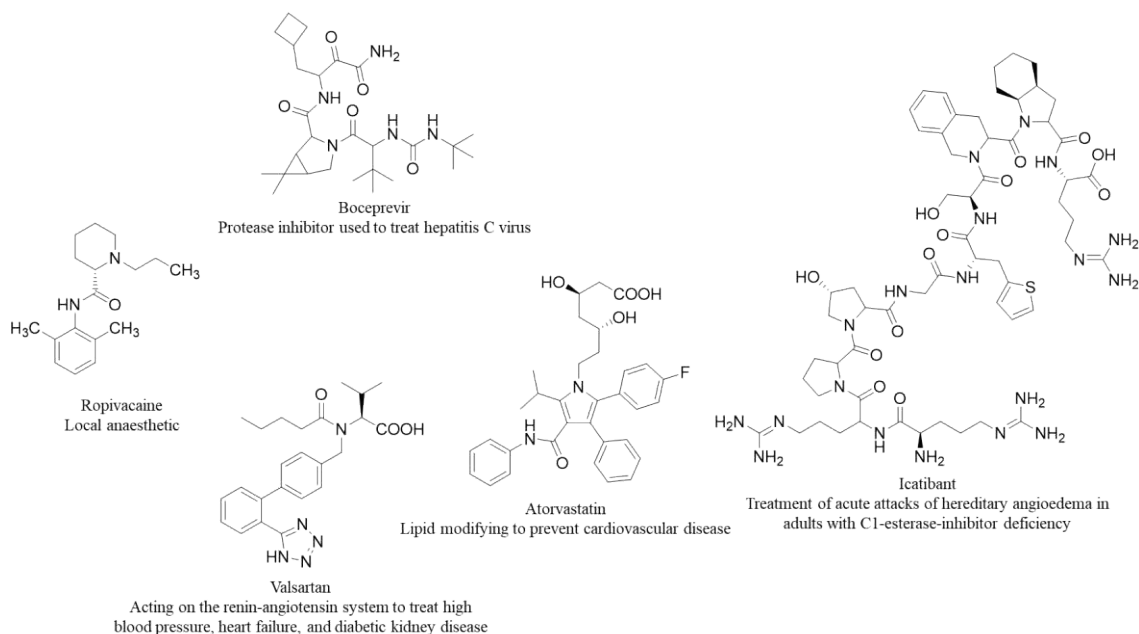
## 2.4. Amide bond formation in organic chemistry

### 2.4.1. The importance of the amide bond

The amide bond is one of the most important chemical connections in nature and organic chemistry.<sup>26</sup> Amide bonds form the backbones of peptides and proteins; linear polymers built by linking natural  $\alpha$ -amino acids between their amino and carboxylic groups to form the primary structure of a biomolecule. In the amide structure, the electrons are partially delocalized over the N-C-O bond, thus exhibiting a partial double bond characteristic. Therefore, the three bonds around the nitrogen atom form a planar structure. The planarity and rigidity of the peptide chain are accounted for by the fact that free rotation is not possible around double bonds. Most peptides and proteins exist in the *trans* configuration due to the much higher thermodynamic stability of the *trans* isomer. These facts are responsible for 3D structures adopted by peptides, proteins and natural or artificial polyamides.<sup>110, 111</sup>

The amide bond can be found in a huge number of medicinal products, from small molecules to therapeutic peptides and antibodies.<sup>112-115</sup> For example, atorvastatin<sup>116</sup> is a statin which is an HMG-CoA reductase inhibitor medication used to prevent cardiovascular disease in high risk patients and treat abnormally high lipid levels. It was the top selling drug worldwide in 2003.<sup>117</sup> From a chemical view point, therapeutic peptides have a broad range of structures, showing their size and complexity.





### Scheme 7. A few examples of amide drugs

Medicinal chemistry has been focusing on the design and synthesis of bioactive compounds that have the potential to become drugs,<sup>118</sup> Brown and Boström<sup>119</sup> reported an analysis of chemical reactions used in 2014 medical chemistry, and three decades ago (1984). The analysis revealed that of the most frequently used were amide bond formation, Suzuki-Miyaura coupling, and  $S_NAr$  reactions, due to commercial availability of reagents, high chemoselectivity, and a pressure on delivery. Figure 6. shows the occurrence of a particular production reaction (or last step reaction), plotted as the percentage of appearance in at least one manuscript.

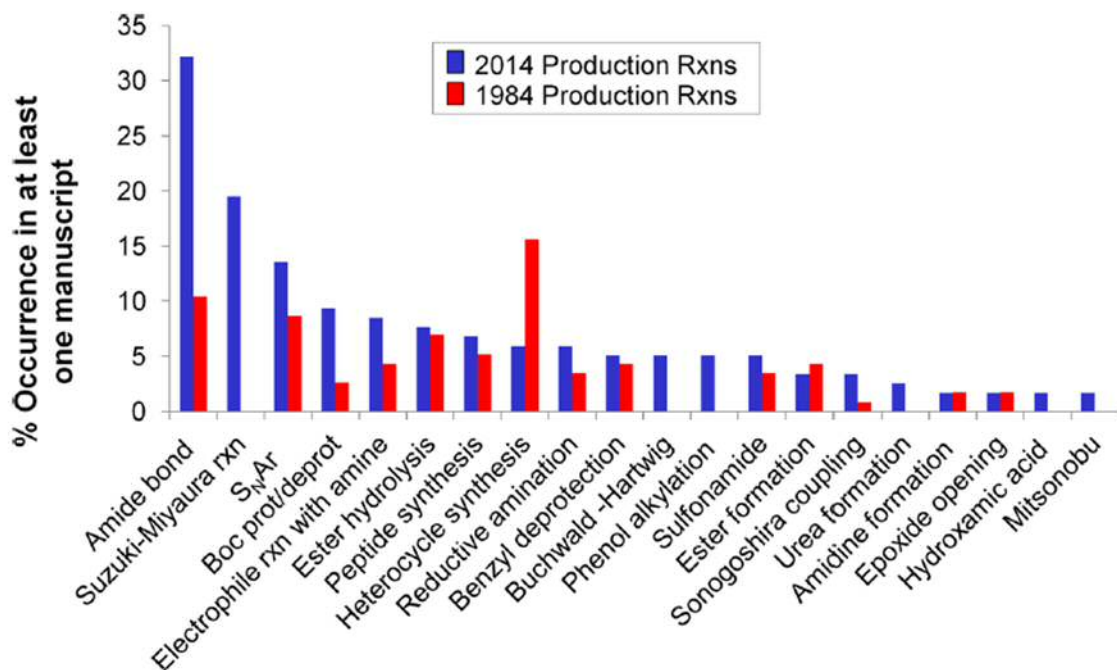


**Figure 6.** Representative data set was taken from 1984,  $n = 114$ , and 2014 in *Journal of Medicinal Chemistry*,  $n = 118$ , from analysis of Brown and Boström<sup>119</sup>

#### 2.4.2. The strategies for amide bond formation

The development of efficient amide formation methods continues to be a challenging scientific pursuit. The amide bond has a favorable thermodynamic stability, therefore, reaction between a free carboxylic acid and an amine requires a large activation energy to overcome the thermodynamic barrier of salt formation. The initial step is direct thermal dehydration that provides a stable ammonium carboxylate salt that then slowly collapses at high temperatures (over 180 °C) to form the amide molecule. This harsh reaction condition is not compatible with most functionalized substrate molecules.<sup>120, 121</sup> Hence, instead of this direct method, the popular methods have been utilizing coupling reagents,<sup>122, 123</sup> oxidative agents,<sup>124, 125</sup> metal<sup>126</sup> and non-metal<sup>127</sup> catalysts. Transamidation<sup>128</sup> and carbonylation<sup>129, 130</sup> reactions may provide attractive methods of the amide bond formation.

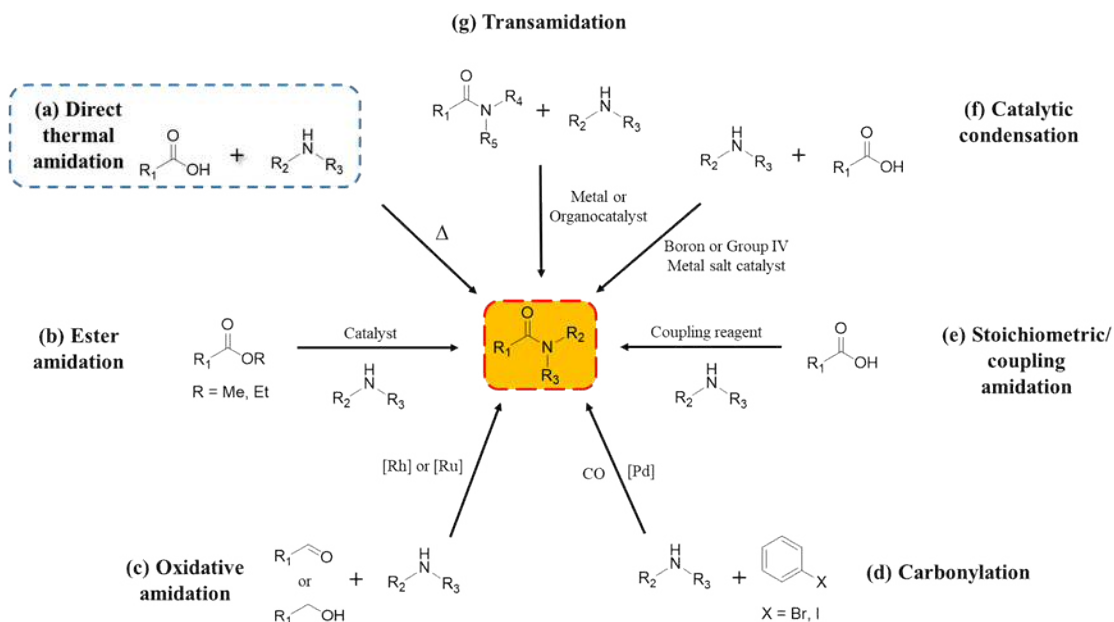


**Figure 7.** The most used amidation methods and a few new developments<sup>131</sup>

Strategies for amide synthesis<sup>131</sup> are shown in Figure 7. The direct thermal amidation reaction (a) is rarely employed as it requires high temperature. Alternative catalytic approaches exist such as amidation of esters (b), oxidative amidation of primary alcohols or aldehydes (c), and carbonylation of aryl halides (d). The most popular syntheses of amide compounds are the stoichiometric or coupling amidation reaction (e) *via* a condensation reaction of a carboxylic acid and an amine, mediated by a stoichiometric activating reagent. These activating reagents are generally, carbonic anhydrides, mixed anhydrides, acid chlorides or active esters. Following activation, the subsequent condensation reaction only requires removal of a water. A potential method is the use of a catalyst for mediating direct amidation under milder reaction conditions (f). Boron-based catalysts and those derived from group (IV) metals are employed as Lewis acids due to their strongly electrophilic nature granted by a vacant p-orbital into which electrons can be received. A special reaction of in the field of amide chemistry is an amidemetathesis or transamidation (g), this process would exchange the constituents of two different amide groups. Although secondary and tertiary amides are extremely inert under normal conditions, they must be activated in the presence of aluminum,<sup>132</sup> zirconium<sup>133</sup> or hafnium<sup>134</sup> catalysts to undergo transamidation reaction.

Another view of non-classical routes is the use of amine surrogate reactions in amide formation.<sup>135</sup> The amine reaction partners are replaced by isocyanates,<sup>136</sup> isonitriles,<sup>137</sup> 1'-

carbonyldiimidazoles,<sup>138, 139</sup> thioamides,<sup>140, 141</sup> dithiocarbamates,<sup>142</sup> sulfonamides,<sup>143</sup> azides,<sup>144</sup> tertiary amines,<sup>145</sup> imines,<sup>146</sup> hydroxyl amines<sup>147-150</sup> or halogeno-amines.<sup>151</sup>

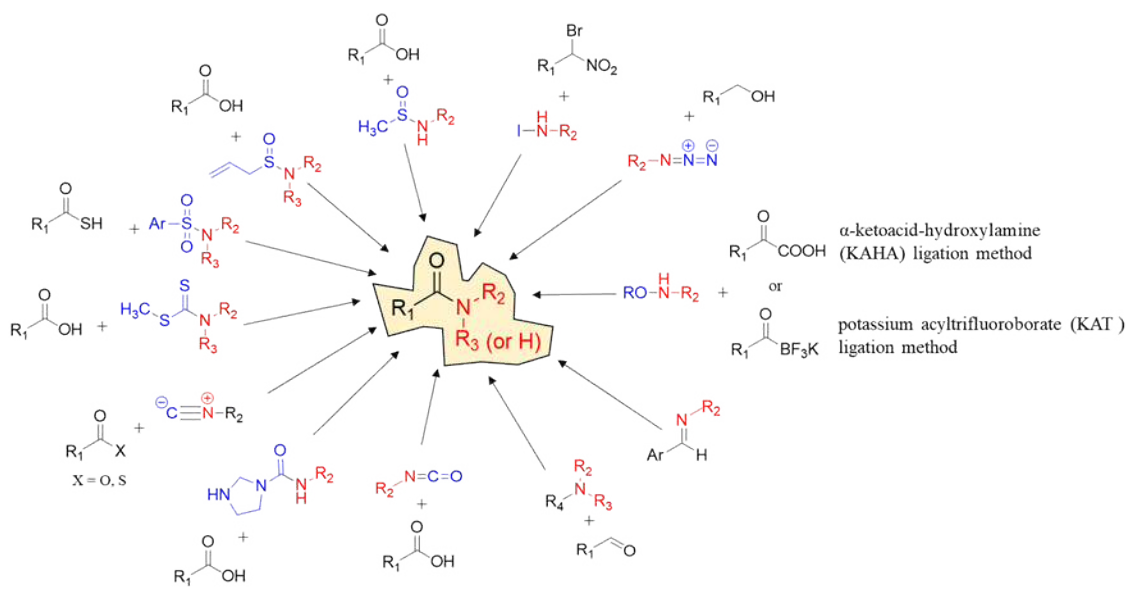


**Figure 8.** Overview of potential amine surrogate methods<sup>135</sup>

#### 2.4.3. Amide bond formation with boronic acid and carbon disulfide.

There are several catalytic routes to form amide compounds, one attractive example relies on catalytic boronic acid derivatives. Ishihara *et al.*<sup>152</sup> reported that arylboronic acids containing electron-withdrawing groups, (*e.g.* 3,4,5-trifluorobenzeneboronic acid and 3,5-bis(trifluoromethyl)benzeneboronic acid), act as highly efficient catalysts in amidation reactions between free carboxylic acids and amines. They investigated the catalytic activities of various arylboronic acids (5 mol%), which promote the model reaction of 4-phenylbutyric acid with 3,5-dimethylpiperidine in toluene at reflux under anhydrous conditions (4-Å molecular sieves). They found that the most effective catalyst for the amidation reaction is the 3,4,5-trifluorobenzeneboronic acid. They explored the generality and scope of 3,4,5-trifluorobenzeneboronic acid-catalyzed amidation.

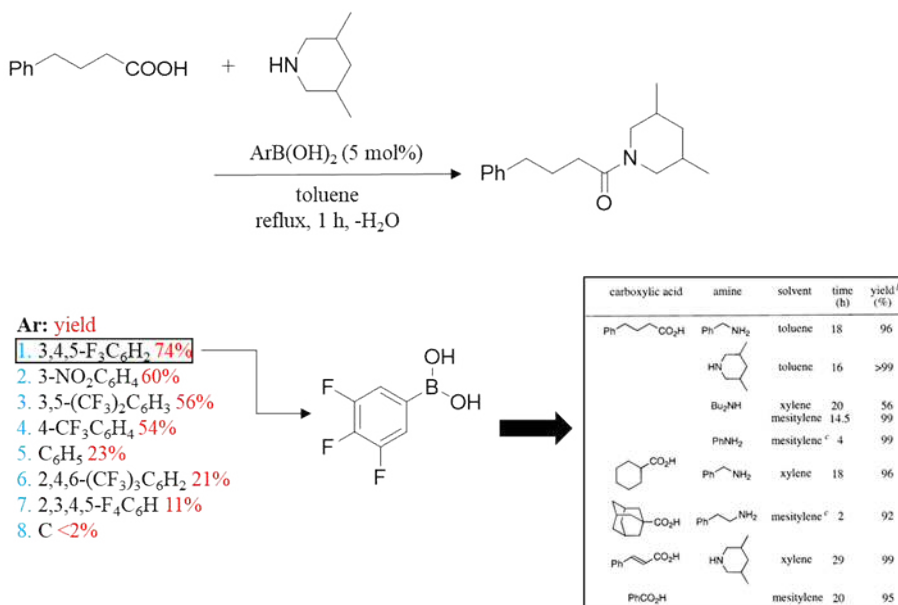


**Figure 9.** Overview of Ishimure *et al.* experiment<sup>152</sup>

These facts demonstrated that arylboronic acid derivatives as Lewis acid catalysts are practical and useful for catalytic amide formation.

Carbon disulfide (CS<sub>2</sub>) is a reagent and a powerful building block in preparative processes. It has been utilized in the manufacturing of viscose rayon, cellophane, carbon tetrachloride, and is even used as solvent in extraction processes. Leman *et al.*<sup>153-155</sup> reported a study that CS<sub>2</sub> promotes peptide bond formation in modest yields (up to ~20%) in prebiotic conditions. From  $\alpha$ -amino acids carbon disulfide initially yields aminoacyl dithiocarbamate, which in turn generate reactive 2-thio-5-oxazolidine intermediates. These are able to polymerize to generate oligopeptides. The 2-thio-5-oxazolidine intermediates are the thio variants of *N*-carboxyanhydrides have been studied under prebiotic conditions and have been proposed to be a universal activated form of amino acids. This study proves that carbon disulfide can act as a condensing agent. Similarly to carbon disulfide

the related carbonyl sulfide (COS), was also reported to mediate condensation reactions of monomeric  $\alpha$ -amino acids.

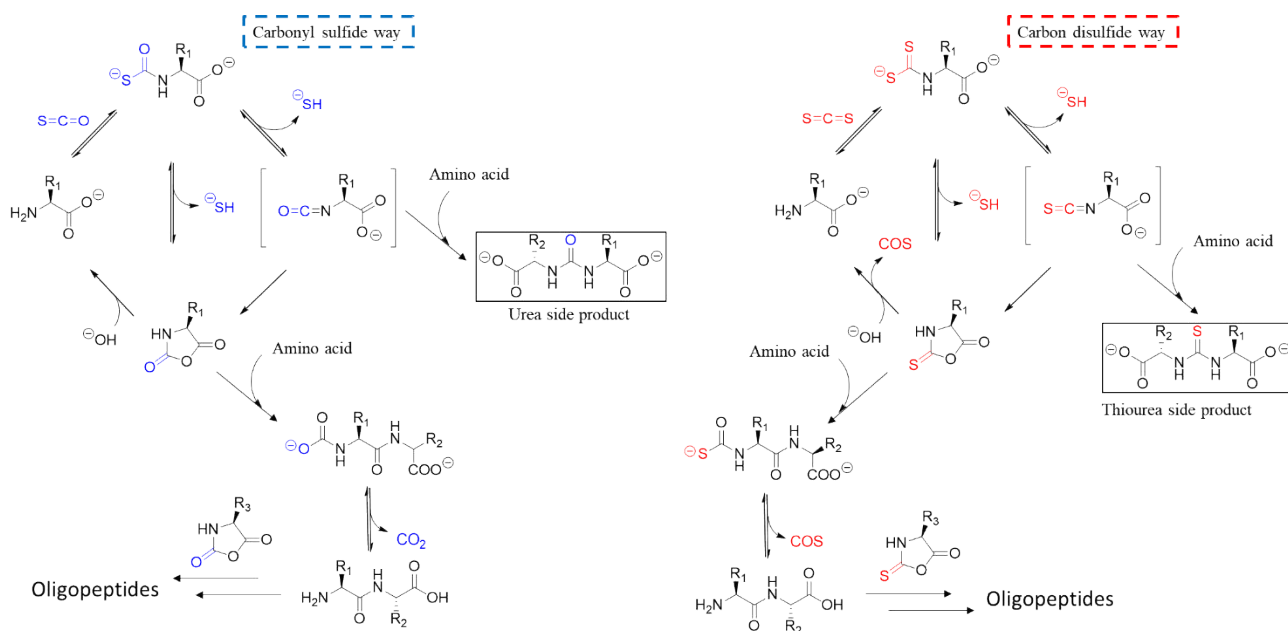


**Figure 10.** Proposed mechanism for CS<sub>2</sub> and COS-mediated peptide formation by *Leman et al.*<sup>153-155</sup>

## 3. EXPERIMENTAL SECTION

### 3.1. General information

All solvents and reagents were of analytical grade and used directly without further purification. 5% Pd/C and 5% Pd/BaSO<sub>4</sub> catalysts used in this study were purchased from Sigma-Aldrich, while D<sub>2</sub>O (>99.9%) was from Merck; HPLC-grade solvents from VWR were used without purification. The propylene carbonate was bought from Acros Organics. The cartridge containing 5% Pd/PBSAC was filled in-house. Fe, Cu, Fe<sub>2</sub>O<sub>3</sub>, Boric acid, AlCl<sub>3</sub>, Al<sub>2</sub>O<sub>3</sub> (for chromatography, activated, neutral, Brockmann I, 50–200 μm, 60 Å) catalysts, carbon disulfide (anhydrous, ≥99%) reagent and organic bases (trimethylamine, pyridine, 4-(dimethylamino)pyridine) used in this study were purchased from Sigma-Aldrich, while acetonitrile (100, 0%) was HPLC LC MS-grade solvents from VWR International.

All melting points were determined on a Jasco SRS OptiMelt apparatus and are uncorrected. Analytical thin-layer chromatography was performed on Merck silica gel 60 F254 plates and flash column chromatography on Merck silica gel 60. The products obtained were characterized by NMR spectroscopy. <sup>1</sup>H-NMR, APT-NMR and <sup>13</sup>C-NMR spectra were recorded on a Bruker Avance DRX 400 spectrometer, in DMSO-d<sub>6</sub> as solvent, at 400.1 MHz. Chemical shifts (δ) are expressed in ppm and are internally referenced (<sup>1</sup>H NMR: 2.50 ppm in DMSO-d<sub>6</sub>). Conversion and deuterium incorporation values were determined *via* the <sup>1</sup>H-NMR spectra of the crude materials. Deuterium contents were determined from the relative intensities of the <sup>1</sup>H-NMR indicator signals. A PerkinElmer 341 polarimeter was used for the determination of optical rotations.

### 3.2. General Procedure for the Flow Reactions

#### 3.2.1. General aspects of the CF deuteration in H-Cube® device

The CF deuteration reactions were carried out in an H-Cube® reactor (ThalesNano Inc.) with D<sub>2</sub>O as deuterium source. The catalyst cartridge (with internal dimensions of 30×4 mm) was filled with ca. 100 mg of the heterogeneous hydrogenation catalyst. It was then placed into a thermostat unit controlled by a Peltier system, up to a maximum of 100 °C. The pressure of the system was set by a backpressure regulator to a maximum of 100 bar, and the CF of the solution of the starting material was provided by an HPLC pump (Knauer WellChrom K-120). For the CF

reactions, 3 mg mL<sup>-1</sup> solution of the appropriate starting material was prepared in propylene carbonate. The solution was homogenized by sonication for 5 min and then pumped through the CF reactor under the set conditions. After the completion of the reaction, the reaction mixture was collected, diluted with water, freeze and lyophilized. Conversion and deuterium incorporation values were determined via the <sup>1</sup>H-NMR spectra of the crude materials. Deuterium contents were determined from the relative intensities of the <sup>1</sup>H-NMR indicator signals.

### *3.2.2. General aspects of the CF acetylation and amidation in a “home-made” reactor*

The CF acetylation reactions were carried out in a home-made flow reactor consisting of an HPLC pump (Jasco PU-987 Intelligent Prep. Pump), a stainless steel HPLC column as catalyst bed (internal dimensions 250mm L × 4.6 ID × ¼ in OD), a stainless steel preheating coil (internal diameter 1 mm and length 30 cm) and a commercially available backpressure regulator (Thalesnano back pressure module 300™ to a maximum of 300 bar). Parts of the system were connected with stainless steel tubing (internal diameter 1 mm). The HPLC column was charged with 4 g of the alumina catalyst. It was then placed into a gas chromatography (GC) oven unit (Carlo Erba HR 5300 up to maximum a 350 °C). For the CF reactions, 100 mM solution of the appropriate starting material was prepared in acetonitrile. The solution was homogenized by sonication for 5 min and then pumped through the CF reactor under the set conditions. After the completion of the reaction, the reaction mixture was collected and the rest solvent was evaporated by a vacuum rotary evaporator. Conversion was determined via the <sup>1</sup>H-NMR spectra of the crude materials.



## 4. RESULTS AND DISCUSSION

### 4.1. Deuteration of haloarenes in H-Cube® CF device

As detailed in the Literature Survey *Section 2.2.2*, catalytic hydrogenation is a fast and simple reaction in an H-Cube® device. Furthermore, metal catalyzed hydrodehalogenation is well known in literature.<sup>156, 157</sup> However, deuterodehalogenation reaction of aromatic compounds in CF reactor cannot be found in literature. Thus, we aimed to utilize the CF deuteration technology to carry out the first deuterohalogenation of halogenated aromatic compounds in an H-Cube® device. The experimental set-up of H-Cube® device allows precise controlling of temperature, pressure and flow rate.

#### 4.1.1. Optimization

The H-Cube® device consists a pump to provide the feed for the reaction mixture, a built in hydrogen generator, a catalyst cartridge, where the reaction occurs, a backpressure regulator and a thermostat to control the pressure and temperature. The cartridge is filled with catalyst and the output was collected in a flask. The necessary deuterium gas for the reaction was generated by the electrolysis of heavy water inside the system.

For the initial optimization study, the deuterodehalogenation reaction of 4-bromoacetanilide was chosen as a test reaction. The complete reaction parameter optimization is shown in Table 5.

**Table 5.** Reaction parameter optimization for the CF deuterodehalogenation reaction.

Entry	Solvent	Catalyst	T (°C)	p (bar)	Conc. (mg mL <sup>-1</sup> )	D (%)	Conv.(%)
1	EtOAc	5% Pd/BaSO <sub>4</sub>	25	50	1	n.d.	0
2	EtOAc	5% Pd/BaSO <sub>4</sub>	25	100	1	n.d.	4
3	EtOAc	5% Pd/BaSO <sub>4</sub>	100	100	1	n.d.	13
4	EtOAc	5% Pd/C	100	100	1	81	48
5	EtOAc	5% Pd/PBSAC	100	100	1	92	87
6	PC	5% Pd/PBSAC	100	100	1	96	99
7	PC	5% Pd/PBSAC	100	100	3	96	99
8	PC	5% Pd/PBSAC	100	100	4	97	94

The starting compound concentration was 1 mg mL<sup>-1</sup> in ethyl acetate, utilizing 5% Pd/BaSO<sub>4</sub> catalyst in the cartridge at a temperature of 25 °C and a pressure of 50 bar with flow rate of 1 mL min<sup>-1</sup>. No trace of the desired product was observed under these conditions (entry 1). This was only improved to 13% conversion by heating the reaction to 100 °C and raising the pressure to 100 bar (entry 3). In favor of the production of desired product, the catalyst was changed to charcoal-supported 5% Pd/C. This change could improve the conversion of 48%, while the deuterium incorporation value of the product was found to be 81% (entry 4). To increase the conversion and deuterium incorporation value of desired product, we turned our attention to the novel polymer-based spherical activated carbon (PBSAC) supported catalyst. Because the most regular solid supported catalysts are not suitable for CF devices due to their small particle sizes in low micrometer range and they can block the flow line.<sup>158-160</sup> Nowadays, PBSAC has been introduced as a solid support for CF catalytic hydrogenation.<sup>161-163</sup> With 5% Pd/PBSAC catalyst 87% conversion and 92% deuterium incorporation were observed at 100 °C temperature and 100 bar pressure (entry 5). According to the recent GSK solvent selection guide, the greenest solvent today is propylene carbonate (PC),<sup>164</sup> which can be synthesized in a highly atom-efficient way from propylene oxide and carbon dioxide with prominently low energy consumption.<sup>165</sup> Moreover, PC has already been used for several important reactions.<sup>166-171</sup> However, CF literature results on the suitability of PC solvent in CF reactor and its use in catalytic deuteration is practically unexplored.<sup>172, 173</sup> The solvent was changed for PC, complete conversion was obtained while the deuterium incorporation value was 96% at 100 °C temperature and 100 bar pressure (entry 6). The effect of the concentration was also tested that resulted without the loss of conversion and deuterium incorporation, the concentration can be increased to 3 mg mL<sup>-1</sup> (entry 8). However, any decrease of the temperature or the pressure resulted in lower yields, while the deuterium incorporation level did not change significantly (Figure 11).

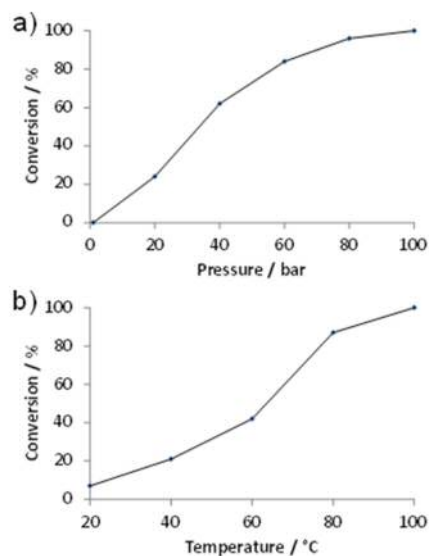
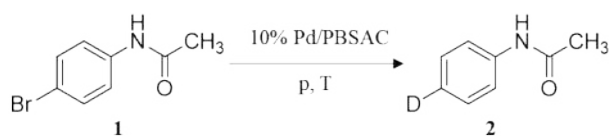


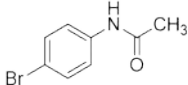
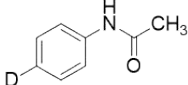
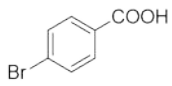
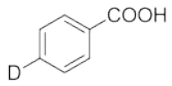
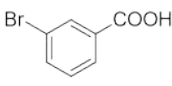
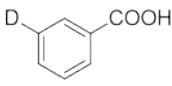
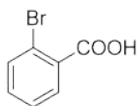
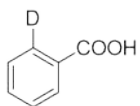
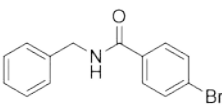
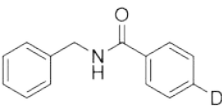
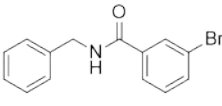
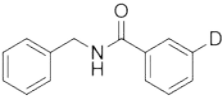
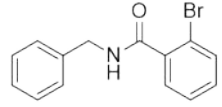
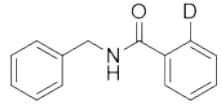
**Figure 11.** The effect of pressure (a) and temperature (b) on the reaction conversion catalysed by PBSAC-supported 10% Pd. The effect of the pressure was measured at 100 °C, while the effect of temperature was determined at 100 bar.

#### 4.1.2. Scope and scale-up experiments

With the optimized reaction conditions in hand, we planned to investigate the scope and limitations of the reaction. The reaction was tested first with various benzoic acids possessing a bromo substituent in positions 4 (**3**), 3 (**5**) and 2 (**7**). As shown in Table 6, for these regioisomers complete conversions were observed with >95% deuterium incorporation in the case of **3** and **5**. Especially, for **7**, *ortho* substituted acetanilide, only marginal deuterium incorporation was achieved. It was probably due to the steric proximity of the functional groups. Thus, the starting material was dissolved in deuterated methanol, the solution was evaporated to dryness, and the product was applied in the deuteration reaction and then the deuterium incorporation value increased to 97%. The further set of test compounds, aromatic amides **9**, **11**, and **13**, were investigated possessing a bromo substituent in positions 2, 3 and 4, respectively. We have achieved excellent conversion and deuterium incorporation value in all cases, except for compound **13**. It was the same steric proximity of the functional groups as described for **7**, thus a similar deuterated

methanol pre-treatment increased the deuterium incorporation value to 98% for compound **14**. Debenzylation by reductive cleavage over palladium metal catalysts with molecular hydrogen is a general method in organic chemistry, however, no debenzylolation was observed for compounds **9**, **11**, and **13**. This is a notable advantage of the method allowing the deuteration of molecules containing the benzyl moiety.

**Table 6.** Results of the optimized deuteration reaction of several bromine-substituted compounds.

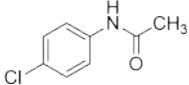
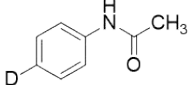
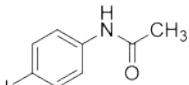
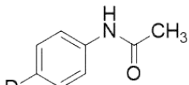
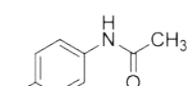
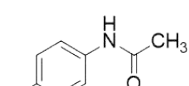
Entry	Substrate	Product	D (%)	Yield (%)
1			96	96
	<b>1</b>	<b>2</b>		
2			96	97
	<b>3</b>	<b>4</b>		
3			95	95
	<b>5</b>	<b>6</b>		
4			98 <sup>[a]</sup>	94
	<b>7</b>	<b>8</b>		
5			97	98
	<b>9</b>	<b>10</b>		
6			96	94
	<b>11</b>	<b>12</b>		
7			98 <sup>[a]</sup>	95
	<b>13</b>	<b>14</b>		

[a] reached by deuterated methanol treatment

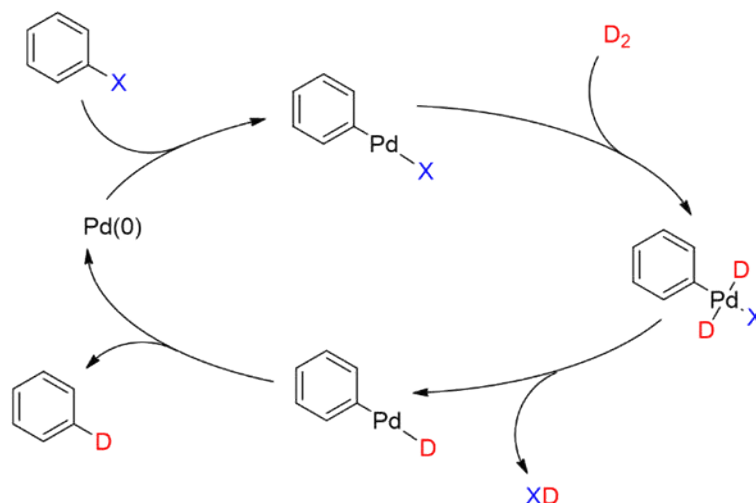
The other halogen-substituted compounds were also tested by the optimized deuterodehalogenation reaction (Table 7). In the reaction of *para* chlorine-substituted acetanilide **15**, total conversion was observed with a high deuterium incorporation value. Importantly, the *para*

iodine-substituted acetanilide **16** gave only a 30% conversion, when we repeated the reaction with the catalyst used in the first reaction, no conversion was observed. Obviously, compound **16** poisoned the PBSAC catalyst. The reaction fluorine-containing acetanilide compound **17** shows that fluorine substituent remained intact and no conversion was observed.

**Table 7.** Results of the optimized deuteration reaction with substrates possessing chlorine, iodine and fluorine acetanilide analogs.

Entry	Substrate	Product	D (%)	Yield (%)
1	 <b>15</b>	 <b>2</b>	96	96
2	 <b>16</b>	 <b>2</b>	n.d.	30
3	 <b>17</b>	 <b>2</b>	n.d.	0

The scope of the deuteration reaction can be explained by the proposed mechanism of the reaction (Scheme 8). The cyclic catalytic process started with the oxidative addition of the aryl halide to a Pd(0) species. According to the literature results this reaction does not proceed for aryl fluorides,<sup>174</sup> this fact supports our observation for fluorinated compounds. The iodinated compounds poisoned the Pd catalyst that can be explained by the elimination of the iodide ion which is known to poison the Pd catalyst.<sup>175</sup>



**Scheme 8.** Proposed reaction mechanism for the catalytic deuterodehalogenation

We focused on the context of green chemistry criteria, catalyst reusability. Therefore, the robustness of our deuteration reaction was also tested (Figure 12). We repeated the deuterodehalogenation reaction of compound **1** 10 times with the same catalyst bed. In the first 6 cycles, the conversion did not change notably. After run of 7, considerable decreases in the catalytic activity was observed.

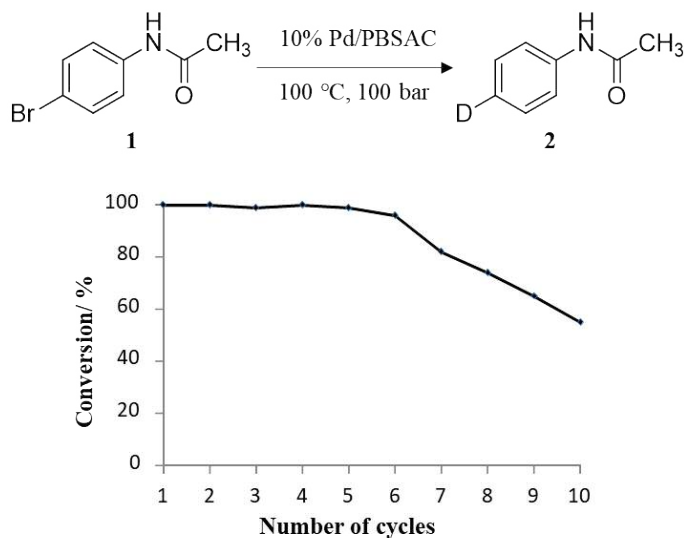


**Figure 12.** Robustness of the CF deuterodehalogenation investigated in the reaction of 4-bromoacetanilide (compound **1**). The same reaction was repeated 10 times on the same 10% Pd/PBSAC catalyst.

Since the catalyst activity did not decrease significantly until 5 cycles and one cycle was carried out with 100 mg of compound **1**, thus, after the pumping of 500 mg of **1** compound through the system, the catalyst cartridge was replaced by a new one. In this way, we carried out with deuteration of 1.5 g of compound **1**, the product **2** was isolated with 95% yield and 96% deuterium incorporation value.

#### 4.2. *N*-acetylation of amines in a “home-made” CF reactor with acetonitrile

As detailed in Section 2.3.2, the general acetylation reagents are acetic anhydride and acetyl chloride, combination with various Lewis acids<sup>23, 176, 177</sup> and/or in neat form,<sup>24</sup> these methods have various drawbacks. The acetyl chloride is considered to be a genotoxic agent and the acetic anhydride is a major irritant.

Flow chemistry technology offers a number of benefits, a wide range of reaction are much faster in flow processes, and fewer substrates and reagents are required. In addition, more efficient and selective reactions can be carried out in CF system as detailed in Section 2.4.2. These properties can help to improve the acetylation reaction to be a simple and sustainable process.

Acetonitrile is a polar aprotic solvent and is generally used in various fields of chemistry as eluent. However, it is rarely used as reagent in organic chemistry. A few studies on acetonitrile as an acylation agent have been reported, for example Saikia *et al.*, presenting an attractive attempt to achieve *N*-acylated aromatic amines with acetonitrile as reagent and solvent with several Lewis acids (e.g. FeCl<sub>3</sub>, InCl<sub>3</sub>, Mn(OAc)<sub>2</sub>, Cu(OAc)<sub>2</sub>). Taking these facts into account, we aimed to develop a CF acetylation method, applying acetonitrile solvent as an acetylation agent with a Lewis acid catalyst.

##### 4.2.1. Optimization

The reactions were carried out in a home-made CF reactor, containing of an HPLC pump that transport the starting material dissolved in acetonitrile. The reaction mixture is feed into a fillable HPLC column that is filled with solid catalyst. Additionally, there is a GC oven and an in-line back pressure regulator in the system to regulate the temperature and pressure of the reaction,

and a 30 cm coil to preheat the reaction mixture before enter into the reaction zone. The schematic outline of the home-made reactor used in this study is shown in Figure 13.

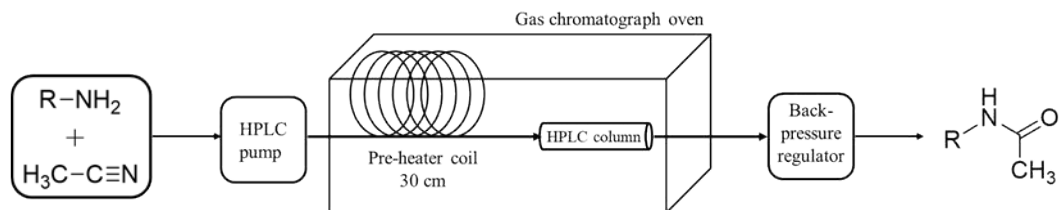
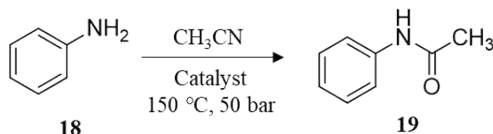


**Figure 13.** Schematic representation of the home made CF reactor used in the acetylation study.

Firstly, we planned to find what is the most useful solid Lewis acid catalyst for the CF acetylation, the catalyst screen was carried out. The aniline was utilized as a test compound, and acetonitrile was used both as solvent and reagent. The complete study of different Lewis acids is shown in Table 7.

**Table 8.** Lewis acids screen in CF acetylation



Entry	Lewis acids	Solvent	Conversion (%)
1	Fe <sub>2</sub> O <sub>3</sub>	Acetonitrile	0
2	Boric acid	Acetonitrile	3
3	AlCl <sub>3</sub>	Acetonitrile	19
4	Al <sub>2</sub> O <sub>3</sub>	Acetonitrile	64

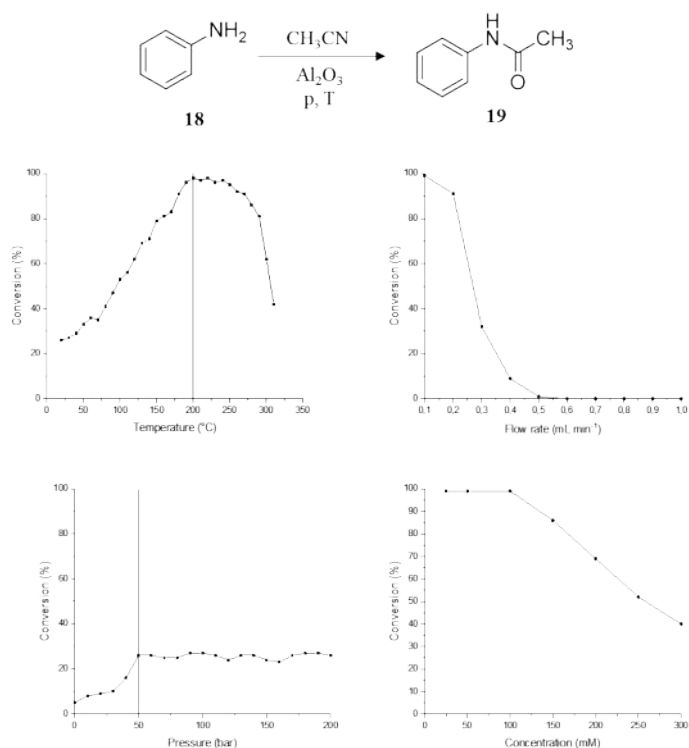
Conditions: 150 °C, 50 bar, 0.1 mL min<sup>-1</sup>, 27 min residence time in flow synthesis

The catalyst screen study shows that the most promising Lewis acid was Al<sub>2</sub>O<sub>3</sub>, other catalyst offered lower yields or no amide product formation was observed. Thus, the further parameter optimization was carried out with Al<sub>2</sub>O<sub>3</sub> as solid catalyst.

The test compound (**18**) was dissolved in acetonitrile in a concentration of 100 mM, utilizing Al<sub>2</sub>O<sub>3</sub> powder as catalyst at a temperature of 25 °C and pressure of 10-100 bar with 0.1 mL min<sup>-1</sup> flow rate and 27 min residence time. The optimization study did not show any pressure dependency and a moderate conversion of 27% was observed without any pressure dependence. The effect of temperature on the conversion rate was tested at 50 bar pressure, increasing the temperature to 100 °C initiated the product formation with 53% conversion. When applying a



higher temperature, the conversion of the product improved and it was found that the optimal temperature is 200 °C (Figure 14a). By applying higher temperature of 200 °C resulted in lower conversion values. The acetonitrile solvent was in its supercritical state ( $T_c=275$  °C,  $P_c=48$  bar) due to the significant solvent expansion produced under supercritical conditions. Above 275 °C, the conversion values of product (**19**) decreased significantly. The effect of pressure on reaction was tested (Figure 14b), the results show that a modest pressure (50 bar) is needed to increase the reaction conversion. The further pressure increase did not influence the product (**19**) formation. The flow rate was also tested (Figure 14c), the results indicated that the optimum flow rate is 0.1 mL min<sup>-1</sup>. The use of a higher flow rate on the reaction resulted in lower conversion values. The effect of concentration on the reaction was tested too (Figure 14d), by applying a higher concentration of 100 mM resulted in the decreased conversion.

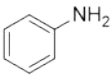
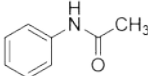
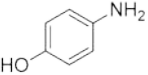
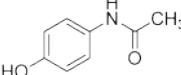
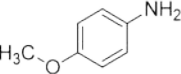
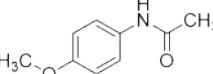
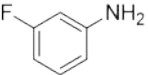
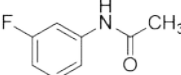
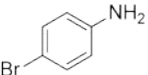
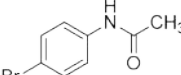
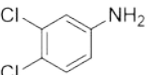
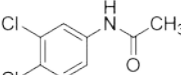
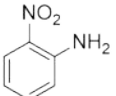
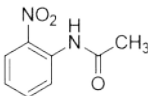
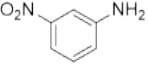
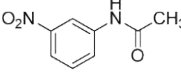
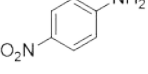
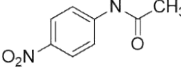


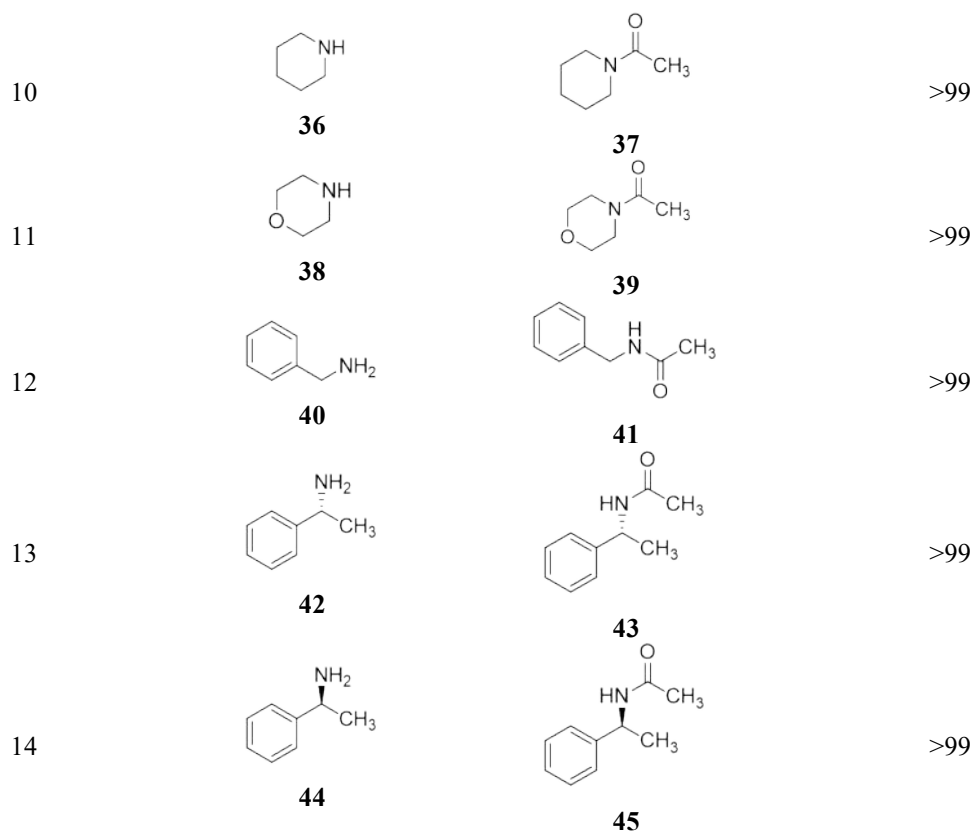
**Figure 14.** The effect of temperature (a), pressure (b), flow rate (c) and concentration (d) on the reaction conversion catalyzed by Al<sub>2</sub>O<sub>3</sub> powder. The effect of the pressure was measured at room temperature and the effect of temperature was determined at 50 bar, while the effect of the flow rate and concentration was analyzed at optimized conditions.

#### 4.2.2. Scope and scale-up experiments

With the optimized reaction conditions (200 °C, 50 bar, 0.1 mL min<sup>-1</sup> in flow rate, 27 min residence time) in hand, we planned to investigate the scope of aniline derivatives (Table 9). The aniline derivatives containing either electron-donating or electron-withdrawing groups were selected. The reactions were carried out in a single run and the products were analyzed by <sup>1</sup>H and <sup>13</sup>C NMR spectroscopy. Column chromatography purification of the product was only needed for compound **23**, for the others, only a simple evaporation of acetonitrile was needed.

**Table 9.** Scope of the acetylation reaction of various aromatic amines.

Entry	Substrate	Product	Yield (%)
1	 <b>18</b>	 <b>19</b>	>99
2	 <b>20</b>	 <b>21</b>	93
3	 <b>22</b>	 <b>23</b>	51
4	 <b>24</b>	 <b>25</b>	>99
5	 <b>26</b>	 <b>27</b>	>99
6	 <b>28</b>	 <b>29</b>	95
7	 <b>30</b>	 <b>31</b>	0
8	 <b>32</b>	 <b>33</b>	0
9	 <b>34</b>	 <b>35</b>	0



*Conditions: 200 °C, 50 bar, 0.1 mL min<sup>-1</sup> flow rate, 27 min residence time.*

The 4-aminophenol (**20**) was acetylated with excellent yield and the drug substance paracetamol (**21**) was gained with quantitative yield after recrystallization. Lower yield was achieved for 4-methoxyaniline (**22**), and the acetylated product was isolated after column chromatography with a 51% yield. For the halogen substituted aniline derivatives (**24**, **26** and **28**) excellent yields were observed. For the nitroaniline derivatives (**30**, **32** and **34**) no conversion was observed and only the starting materials were isolated. The highly electron-withdrawing nature of the nitro group that reduces the nucleophilicity of the amino group might explain the absence of product formation. Aliphatic primary and secondary amines were also tested. The primary benzylic amine (**40**) was converted to the corresponding acetamide (**41**) with excellent yield. When secondary amines, piperidine (**36**) and morpholine (**38**) were examined, the acetylated derivatives (**37**, **39**) were isolated with quantitative yields. The stereoselective property of this reaction was also tested with acetylation reaction carried out for the two enantiomers of 1-phenylethanamine (**42**, **44**). For both enantiomers the acetylated derivative was achieved with quantitative yield and the complete retention of the enantiomeric purity. The isolated products (**43**, **45**) were investigated

by optical rotation and was found to be identical to literature data, so that the heat-induced racemization was not observed.

The catalyst reusability is an important property in sustainable chemical reactions, thus this property was also tested. It was found that the activity of the catalyst did not decrease significantly until 10 cycles and one cycle was carried out with 20 mg of benzylamine (**40**). The excellent result<sup>178</sup> of catalyst reusability study opened the way to scale up the reaction, which was tested with the same reaction. The process could be scale up to 2 g of benzylamine (**40**) without the significant decrease of the conversion. The *N*-benzylacetamide product (**41**) was isolated with 94% yield after recrystallization. The reaction was completed within 28 hours, this is considerably faster than what has been reported with already known technology. Results are shown in Figure 15.

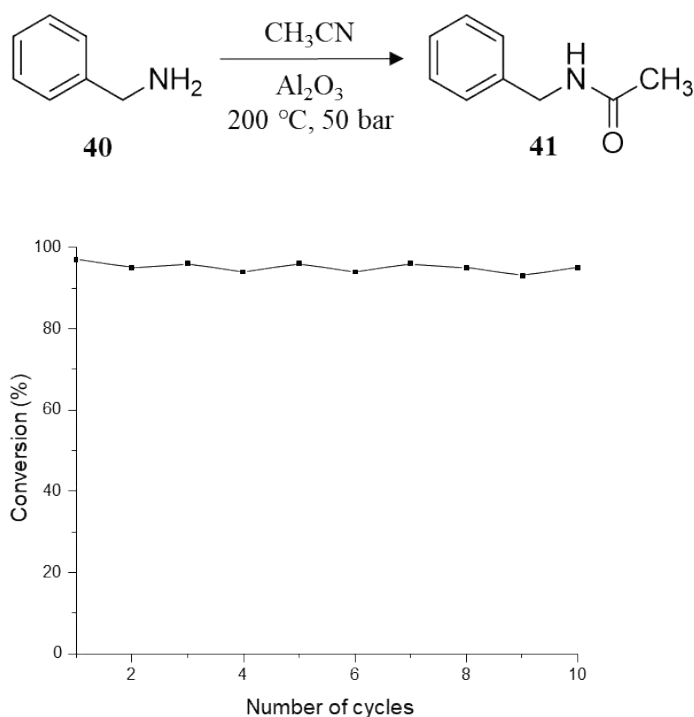
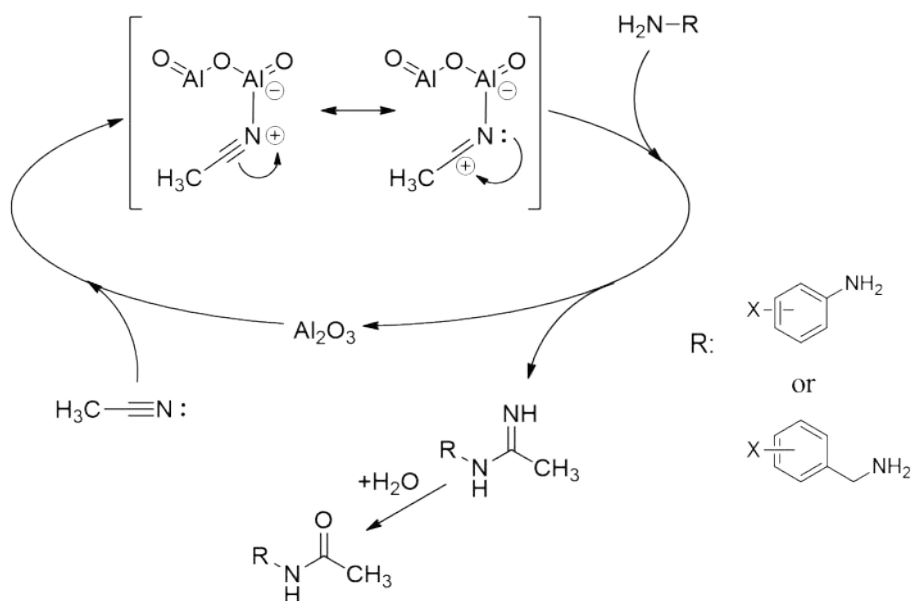


**Figure 15.** Robustness of acetylation of the benzylamine (**40**), the same reaction was repeated 10 times on the same Al<sub>2</sub>O<sub>3</sub> catalyst.

According to literature data,<sup>178-182</sup> these results can be explained by the proposed reaction mechanism (Scheme 9). The key step is the coordination of the lone electron pair of the nitrogen atom of the cyanide group, which yields a positive charge. The positive charge of the cyanide group can be localized on the carbon atom due to mesomeric structures. Thus, this positively charged carbon atom might be attacked by the lone pair electron of the amine resulting amidine, which is further hydrolyzed to form the acetamide as shown in Scheme 9. The origin of the water might be the residual water content of the solvent and/or the Al<sub>2</sub>O<sub>3</sub> catalyst. The addition of extra amount of water in the reaction mixture decreased the conversion of the reaction.



**Scheme 9.** *The proposed reaction mechanism of catalytic acetylation.*

#### 4.3. Direct amide formation in a “home-made” CF reactor mediated by carbon disulfide

As detailed in Section 2.4.2, there are plenty of strategies to provide amide compounds, therefore, there are only a limited number of direct amidation methods without coupling or activating agents. There is a demand for a general technique to access amides in an uncomplicated, environmentally friendly, and efficient way. The CF technology offers many advantages over regular batch operation as detailed in Section 2.1. The section 2.4.3. proved that carbon disulfide might be an attractive coupling agent for amide synthesis. We aimed to utilize CF technology in amide formation reaction with carbon disulfide as a coupling agent.

### 4.3.1. Optimization

The reactions were carried out in the same home-made CF reactor that we used in the *N*-acetylation study in section 4.2.1., Figure 16 shows the schematic illustration of the amidation process.

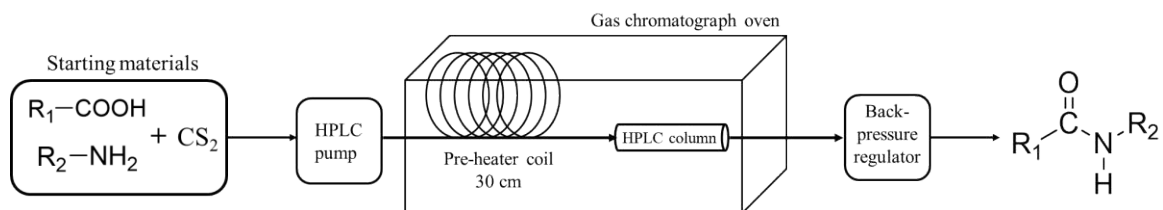


**Figure 16.** Schematic illustration of flow amidation reactor.

We selected a model reaction for the optimization that utilizing benzylamine and 4-phenylbutyric acid as substrates dissolved in acetonitrile to provide a 100 mM solution. According to the study *N*-acetylation conditions and parameters, a high temperature and a modest pressure were used. The trial was performed without any catalyst or reagent at 200°C temperature and 50 bar pressure with a flow rate of 0.1 mL min<sup>-1</sup> and a residence time of 27 min. As expected, no trace of the desired amide product was observed (Table 12, entry 1). According to 2.4.2. the strategies of amide bond formation section, Lewis acids were used in amidation reaction as catalyst. A same result was observed when the reaction was repeated under the same conditions in the presence of Al<sub>2</sub>O<sub>3</sub> as Lewis catalyst (Table 12, entry 2).

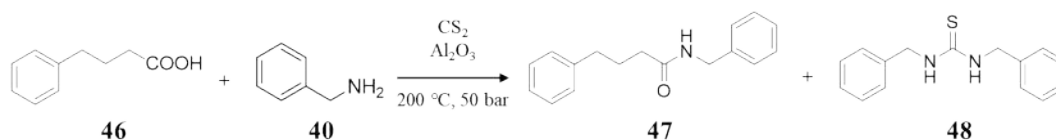
**Table 10.** Screen of the alternative catalysts.

Entry	Lewis acid	Reagent	Solvent	Conversion into 47 (%)
1	boric acid	CS <sub>2</sub>	acetonitrile	2%
2	Fe	CS <sub>2</sub>	acetonitrile	3%
3	Cu	CS <sub>2</sub>	acetonitrile	17%
4	Fe <sub>2</sub> O <sub>3</sub>	CS <sub>2</sub>	acetonitrile	10%
5	NiO	CS <sub>2</sub>	acetonitrile	4%
6	CuO	CS <sub>2</sub>	acetonitrile	40%
7	Al <sub>2</sub> O <sub>3</sub>	CS <sub>2</sub>	acetonitrile	53%

1 equiv. 4-phenylbutyric acid (100 mM), 1 equiv. benzyl amine (100 mM), Reagent: 1.5 equiv. CS<sub>2</sub> Condition: 200 °C, 50 bar, 0.1 mL min<sup>-1</sup>, 27 min residence time

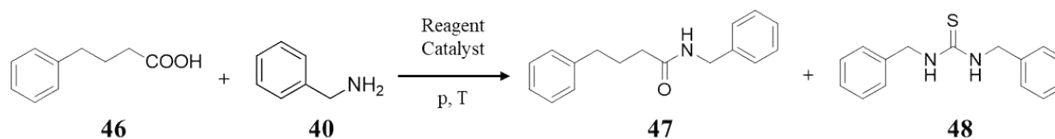
However, a low conversion of 22% was observed when 1.5 equivalent of carbon disulfide was used as an additive along with numerous byproducts (Table 12, entry 3). Furthermore, several Lewis acids were tested too (Table 10, entry 7) and the most promising Lewis acid catalyst was Al<sub>2</sub>O<sub>3</sub> and a significant increase in conversion of 53% was achieved. (Table 12, entry 4). The effect of the solvent on the reaction outcome was also tested. Several solvents were investigated but acetonitrile was found to be the most suitable (Table 11, entry 5).

**Table 11.** Direct amide bond formation in a range of solvents.



Entry	Solvent	Conversion into 47 (%)
1	Water	0%
2	Methanol	31%
3	Isopropanol	10%
4	Toluene	43%
5	Acetonitrile	53%
6	Dichloromethane	0%
7	Dimethylsulfoxide	4%

1 equiv. 4-phenylbutyric acid (100 mM), 1 equiv. benzyl amine (100 mM), Lewis acid: alumina, Reagent: 1.5 equiv. CS<sub>2</sub> Condition: 200 °C, 50 bar, 0.1 mL min<sup>-1</sup>, 27 min residence time

**Table 12.** The model reaction and optimization of amide reaction in flow reactor.

Entry	Substrates	Lewis	Reagent	Solvent	Condition	Conversion into
1	4-PBA + BA			acetonitrile	200 °C 0.1 mL min <sup>-1</sup> 50 bar	0%
2	4-PBA + BA	Al <sub>2</sub> O <sub>3</sub>		acetonitrile	200 °C 0.1 mL min <sup>-1</sup> 50 bar	0% <sup>[a]</sup>
3	4-PBA + BA		CS <sub>2</sub>	acetonitrile	200 °C 0.1 mL min <sup>-1</sup> 50 bar	22%
4	4-PBA + BA	Al <sub>2</sub> O <sub>3</sub>	CS <sub>2</sub>	acetonitrile	200 °C 0.1 mL min <sup>-1</sup> 50 bar	53% <sup>[b]</sup>
5	4-PBA + BA	Al <sub>2</sub> O <sub>3</sub>	CS <sub>2</sub> Pyridine	acetonitrile	200 °C 0.1 mL min <sup>-1</sup> 50 bar	58%
6	4-PBA + BA	Al <sub>2</sub> O <sub>3</sub>	CS <sub>2</sub> Triethylamine	acetonitrile	200 °C 0.1 mL min <sup>-1</sup> 50 bar	62%
7	4-PBA + BA	Al <sub>2</sub> O <sub>3</sub>	CS <sub>2</sub> DMAP	acetonitrile	200 °C 0.1 mL min <sup>-1</sup> 50 bar	>99%

4-PBA : 4-phenylbutyric acid, BA: benzylamine, DMAP : 4-(dimethylamino)pyridine ,CS<sub>2</sub> : carbon disulfide,  
<sup>[a]</sup>Acetylation side reaction was only observed, <sup>[b]</sup> 31% urea formation.

For a higher conversion, organic bases, such pyridine and trimethylamine, in catalytic amount were added to the starting substrate mixture. However, we achieved only slight improvements of conversions (Table 12, entry 5,6), although the formation of thiourea side product was not observed. However, when we used the 4-dimethylaminopyridine (DMAP) as organic base full conversion was observed (Table 12, entry 7). By a simple filtration on a silica gel plug, the additive was removed. Conversions were calculated using the relative signal intensities of the carboxylic acid starting compound in <sup>1</sup>H NMR spectra.

To find the optimal condition for the flow synthesis, we tested the effect of temperature on the outcome of the reaction under established conditions. First, we carried out a reaction at room temperature and we did not observe the desired product. The increase of the temperature to 110 °C resulted a low 9% conversion. Further increase of temperature significantly influenced the conversion, the optimal temperature was found to be 200 °C where >99% conversion was observed. However, reactions at higher temperatures than 200 °C provided lower conversions (Figure 17a). The effect of pressure was tested at 200 °C temperature, the optimal value was found to be 50 bar



reaching full conversion. Raising the pressure higher than 50 bar did not influence the conversion (Figure 17b). A test about flow rate gave an optimum value of 0.1 mL min<sup>-1</sup>, any increase in the flow rate resulted in decreasing conversions (Figure 17c). Analyzing the effect of concentration on reaction outcome indicated full conversions at lower concentrations, the use of higher concentrations of the starting materials resulted in lower conversions (Figure 17d).

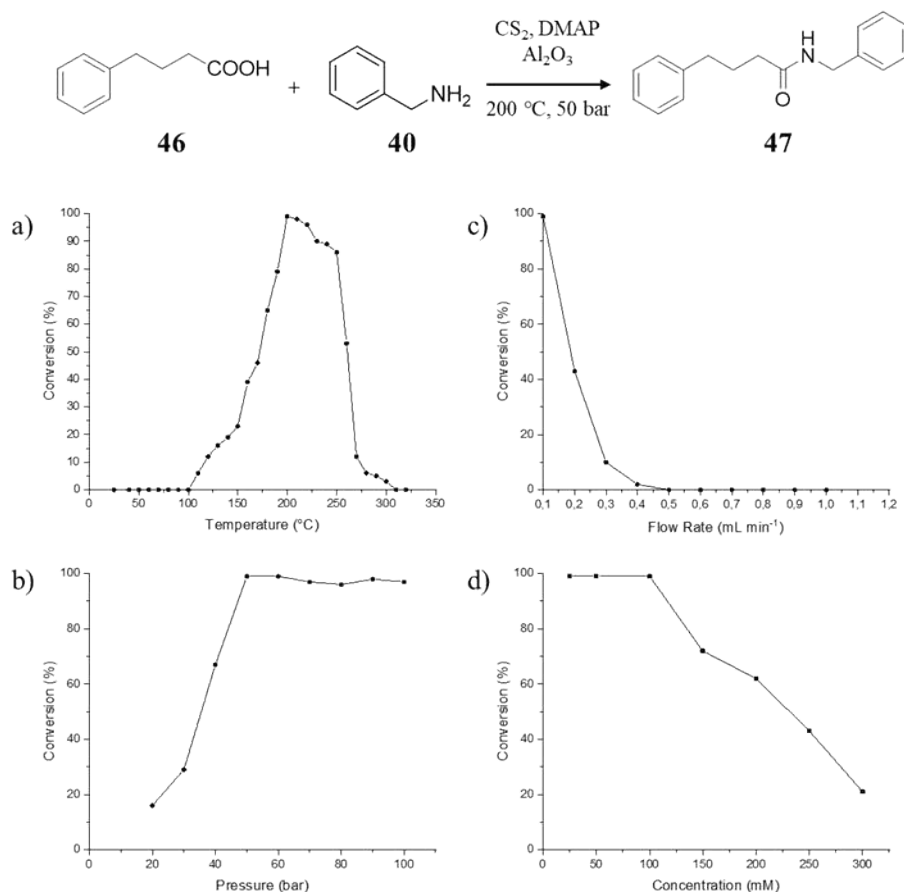


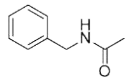
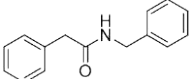
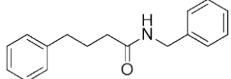
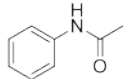
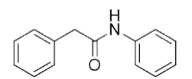
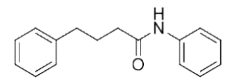
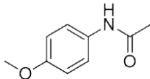
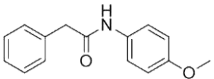
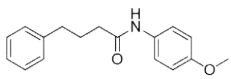
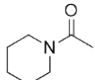
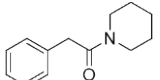
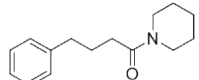
**Figure 17.** The effect of temperature (a), pressure (b), flow rate (c), and concentration of the starting materials (d) on the reaction conversion catalyzed by Al<sub>2</sub>O<sub>3</sub>. The effect of the pressure was measured at room temperature, the influence of temperature was determined at 50 bar, while the effect of the flow rate and concentration was analyzed under the optimized conditions.

Finally, the results about changing the quantity of carbon disulfide show that the optimal amount is 1 equiv.: lower amounts resulted in decreased conversion, whereas higher amounts did not have any significant effect.

### 4.2.3. Scope and scale-up experiments

Impressed by the successful flow amide reaction of model substrates, we expanded the scope of the reaction testing various aromatic and aliphatic substrates. By the use of optimal condition (200 °C, 50 bar, 0.1 mL min<sup>-1</sup>, 27 min residence time), we achieved high yields for 15 different carboxylic acids and five amines including primary aromatics and aliphatic and secondary aliphatic amines. All reactions were carried out in a single run, after filtration through a silica gel plug and vacuum evaporation of the solvent, the products were analyzed by <sup>1</sup>H, <sup>13</sup>C and APT NMR spectroscopy without any further purification. These facts make the process prominently green and sustainable and the isolation of the products is clearly simple. The amide products and the corresponding isolated yield are shown in Table 13. In all products, the NMR experiment showed full conversions.

**Table 13.** Substrate scope of amide formation with isolated yield data.

Substrates	acetic acid	phenylacetic acid	4-phenylbutyric acid
benzylamine			
	<b>41</b>	<b>49</b>	<b>47</b>
	98%	96%	98%
aniline			
	<b>19</b>	<b>50</b>	<b>51</b>
	98%	95%	96%
<i>p</i> -anisidine			
	<b>23</b>	<b>52</b>	<b>53</b>
	97%	95%	94%
piperidine			
	<b>37</b>	<b>54</b>	<b>55</b>
	98%	97%	96%

morpholine			
	<b>39</b>	<b>56</b>	<b>57</b>
	97%	98%	97%

Each reaction was 1 equiv. carboxylic acid (100 mM), 1 equiv. amine (100 mM), Lewis acid: Al<sub>2</sub>O<sub>3</sub>, Reagent: 1 equiv. CS<sub>2</sub>, Adduct: 1 equiv. DMAP and conditions: 200 °C, 50 bar, 0.1 mL min<sup>-1</sup>, 27 min residence time

We tested the catalyst reusability with 30 mg of the model starting substrates. The Figure 18 shows that the activity of the catalyst did not decrease significantly after 30 cycles. This result leads the way to scale up the reaction using the model reaction. A scale-up reaction was carried out and 2 grams of product were isolated after ca. 13 hours working time.

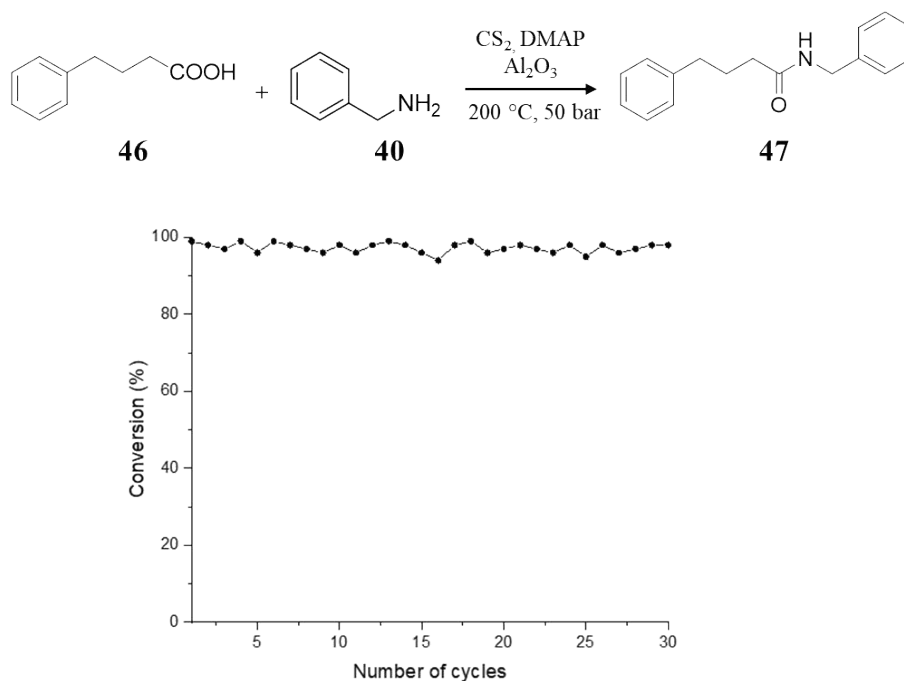


**Figure 18.** Robustness of the amide formation reaction was investigated in the reaction of model substrates. The same reaction was repeated 30 times on the same catalyst.

According to literature data<sup>183-185</sup> and these results, we can establish a reaction mechanism. The mechanism starts with reaction of the amine (Rm-1) and carbon disulfide (CS<sub>2</sub>). This reaction provides an *N*-alkyldithiocarbamic acid (Rm-2), which decomposes by releasing hydrogen sulfide (H<sub>2</sub>S) and affords an isothiocyanate (Rm-3). According to literature data,<sup>186-188</sup> we propose that the

isothiocyanate (Rm-3) might be a key element in the direct amidation reaction. In absence of an organic base, the formation of thiourea side product (Rm-5) was observed. However, if DMAP was present in catalytic amount, the formation of the thiourea side product (Rm-5) was suppressed and only the desired amide product (Rm-7) was detected. The effect of organic base in the reaction can be explained by the deprotonation of the carboxylic acid providing protonated DMAP and Rm-4<sup>-</sup>. The deprotonated carboxylic acid (Rm-4<sup>-</sup>) is more nucleophilic and reacts more rapidly with isothiocyanate (Rm-3) than the amines. The formation of amide product (Rm-7) can be explained by the two mesomeric forms of intermediate Rm-6. Furthermore, the necessity to use a catalytic amount of DMAP can be interpreted too, since the last step, when Rm-7<sup>-</sup> transforms to Rm-7, is a fast protonation reaction. We propose that, as indicated, protonated DMAP (<sup>+</sup>DMAP) is involved in the last product forming step. Then DMAP is protonated and the process starts again, it plays a key role in proton shuffling.

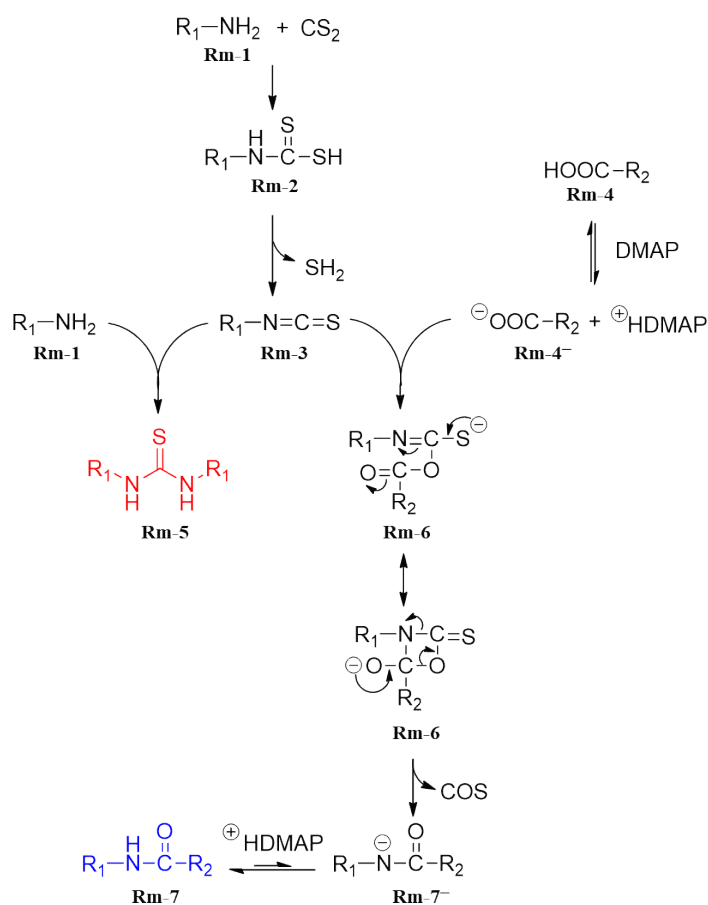


**Figure 19.** The proposed mechanism for the  $\text{Al}_2\text{O}_3$ -catalyzed amide coupling with carbon disulfide.

## 5. SUMMARY

On the basis of earlier results, we have developed heterogeneous catalytic CF methodologies for three different reactions. Each of these processes are time and cost efficient, as it utilizes cheap reagent and catalyst and its considerably fast.

The first CF deuterohalogenation reaction was developed, harsh reaction conditions (100 °C and 100 bar), a novel spherical support (PBSAC) and PC as a solvent were necessary to achieve complete conversions with concomitant >95% deuterium incorporation values. Notably, PC allowed the use of an increased (3 times higher) concentration of the reactants with considerably faster reactions. Importantly, molecules containing the benzyl group were also deuterated without any trace of debenzylation. Chloro- and bromo-substituted substrates provided excellent results, however, the iodine substituent poisoned the catalyst, while the fluorine substituent remained intact. Thus, selective flow deuteration can be performed in the presence of a fluorine substituent. The supported palladium catalyst showed moderate reusability.

A sustainable and selective CF *N*-acetylation was developed, the well-known, cheap and non-toxic Lewis acid alumina was used as catalyst. Furthermore, the acetylation reagent was acetonitrile, which is an industrial side-product with a modest price and it is considerably milder than those for the regular carboxylic acid derivatives used for acetylation. Under the optimized conditions, we have achieved good and excellent conversions of aromatic acetamides (**19**, **21**, **23**, **25**, **27**, **29**, **31**, **33** and **35**), except for nitro substituted compounds, where no conversion was reached. Importantly, the painkiller drug substance paracetamol was gained with high yield. Mainly complete conversions were also achieved of primary (**41**, **43** and **44**) and secondary aliphatic acetamides (**37**, **39**). During the course of the reaction no racemization was observed for either enantiomer of enantiomerically pure 1-phenylethylamine (**42**, **44**).

The direct amide synthesis from carboxylic acids and amines was established in a CF reactor, the synthesis is time and cost efficient and applied acetonitrile as solvent, which is an industrial side-product and utilized additives, alumina and carbon disulfide, are broadly used in several industrial processes too. With the optimized conditions, the reaction was extended to preparation of 15 diverse amides (**19**, **23**, **37**, **39**, **41**, **47**, and **49-57**). In general, full conversions and excellent yields were achieved, without the need of any intensive purification step. The utilized

alumina catalyst showed excellent reusability. Additionally, the reaction was successfully scaled up to 2-gram quantity synthesized in ca. 13 hours. These facts prove this methodology could become broadly applicable for direct amide synthesis utilizing the industrially reliable continuous technology.

## Acknowledgements

This work was carried out in the Institute of Pharmaceutical Chemistry, University of Szeged, during the years 2015-2019. Throughout the working of this dissertation I have received a great deal of support and assistance.

I am honored to be of the recipients of the Gedeon Richter Ltd. Scholarship.

I would first like thank my supervisor, *Prof. Dr. Ferenc Fülöp*, for his professional guidance of my work, his useful advice and constructive criticism.

My special thanks are also due to my co-supervisor, *Dr. István Mándity*, his honest thoughts helped me through many difficulties in my scientific work.

I am grateful to all of my colleagues at the Institute of Pharmaceutical Chemistry for their help and encouragement.

I would like to express my warmest thanks to my family and my friends, without whom I would not have been able to complete my PhD studies, and without whom I would not have made it through.

## References

1. A. J. J. Straathof, S. Panke and A. Schmid, *Current Opinion in Biotechnology*, 2002, **13**, 548-556.
2. R. De la Cruz Quiroz, S. Roussos, D. Hernández, R. Rodríguez, F. Castillo and C. N. Aguilar, *Critical Reviews in Biotechnology*, 2015, **35**, 326-333.
3. T. Bruckdorfer, O. Marder and F. Albericio, *Current pharmaceutical biotechnology*, 2004, **5**, 29-43.
4. D. A. Sandoval-Chávez and M. G. Beruvides, *The Engineering Economist*, 1998, **43**, 107-124.
5. G. S. Calabrese and S. Pissavini, *AIChE Journal*, 2011, **57**, 828-834.
6. C. Wiles and P. Watts, *Green Chem.*, 2012, **14**, 38-54.
7. M. Baumann, T. S. Moody, M. Smyth and S. Wharry, *Organic Process Research & Development*, 2020, DOI: 10.1021/acs.oprd.9b00524.
8. S. G. Koenig and H. F. Sneddon, *Green Chemistry*, 2017, **19**, 1418-1419.
9. M. Plutschack, B. Pieber, K. Gilmore and P. Seeberger, *Chemical Reviews*, 2017, **117**.
10. E. Stokvis, H. Rosing and J. H. Beijnen, *Rapid Communications in Mass Spectrometry*, 2005, **19**, 401-407.
11. E. M. Simmons and J. F. Hartwig, *Angewandte Chemie International Edition*, 2012, **51**, 3066-3072.
12. M. E. Wood, S. Bissiriou, C. Lowe and K. M. Windeatt, *Organic & Biomolecular Chemistry*, 2008, **6**, 3048-3051.
13. T. G. Gant, *Journal of Medicinal Chemistry*, 2014, **57**, 3595-3611.
14. C. Schmidt, *Nature Biotechnology*, 2017, **35**, 493-494.
15. T. Pirali, M. Serafini, S. Cargnin and A. A. Genazzani, *Journal of Medicinal Chemistry*, 2019, **62**, 5276-5297.
16. A. Amić and M. Molnar, *Organic Preparations and Procedures International*, 2017, **49**, 249-257.
17. A. E. Carlos, O.-V. Jorge, V. Andrés, S. Dieter and S. Joachim, *Zeitschrift für Naturforschung B*, 2009, **64**, 969-972.
18. V. Farina, J. T. Reeves, C. H. Senanayake and J. J. Song, *Chemical Reviews*, 2006, **106**, 2734-2793.
19. K. Nakazono, K. Fukasawa, T. Sato, Y. Koyama and T. Takata, *Polymer Journal*, 2010, **42**, 208-215.
20. G. Xu, D. Tang, Y. Gai, G. Wang, H. Kim, Z. Chen, L. T. Phan, Y. S. Or and Z. Wang, *Organic Process Research & Development*, 2010, **14**, 504-510.
21. A. Isidro-Llobet, M. Álvarez and F. Albericio, *Chemical Reviews*, 2009, **109**, 2455-2504.
22. B. K. Hansen, R. Gupta, L. Baldus, D. Lyon, T. Narita, M. Lammers, C. Choudhary and B. T. Weinert, *Nature Communications*, 2019, **10**, 1055.
23. R. Alletti, W. S. Oh, M. Perambuduru, Z. Afrasiabi, E. Sinn and V. P. Reddy, *Green Chemistry*, 2005, **7**, 203-206.
24. N. Deka, A.-M. Mariotte and A. Boumendjel, *Green Chemistry*, 2001, **3**, 263-264.
25. D. J. Snodin, *Organic Process Research & Development*, 2010, **14**, 960-976.
26. V. R. Pattabiraman and J. W. Bode, *Nature*, 2011, **480**, 471-479.
27. J. Puiggali and J. A. Subirana, *Journal of Peptide Science*, 2005, **11**, 247-249.



28. A. P. Davenport, C. C. G. Scully, C. de Graaf, A. J. H. Brown and J. J. Maguire, *Nature Reviews Drug Discovery*, 2020, DOI: 10.1038/s41573-020-0062-z.
29. D. B. Scott, A. Lee, D. Fagan, G. M. Bowler, P. Bloomfield and R. Lundh, *Anesth Analg*, 1989, **69**, 563-569.
30. L. Peikova and B. Tsvetkova, *Pharmacia*, 2013, **60**, 37-45.
31. K. Shah, J. Gupta, N. Chauhan, N. Upmanyu, S. Shrivastava and P. Mishra, *The Open Medicinal Chemistry Journal*, 2017, **11**, 146-195.
32. H. Sigel and R. B. Martin, *Chemical Reviews*, 1982, **82**, 385-426.
33. R. Porta, M. Benaglia and A. Puglisi, *Organic Process Research & Development*, 2016, **20**, 2-25.
34. K. F. Jensen, *AIChE Journal*, 2017, **63**, 858-869.
35. M. B. Plutschack, B. Pieber, K. Gilmore and P. H. Seeberger, *Chemical Reviews*, 2017, **117**, 11796-11893.
36. J. Wegner, S. Ceylan and A. Kirschning, *Advanced Synthesis & Catalysis*, 2012, **354**, 17-57.
37. M. Trojanowicz, *Molecules*, 2020, **25**.
38. M. Baumann, *Organic & Biomolecular Chemistry*, 2018, **16**, 5946-5954.
39. J. Wegner, S. Ceylan and A. Kirschning, *Chemical Communications*, 2011, **47**, 4583-4592.
40. J.-i. Yoshida, Y. Takahashi and A. Nagaki, *Chemical Communications*, 2013, **49**, 9896-9904.
41. N. Kockmann and D. M. Roberge, *Chemical Engineering and Processing: Process Intensification*, 2011, **50**, 1017-1026.
42. T. Schwalbe, V. Autze and G. Wille, *CHIMIA*, 2002, **56**, 636-646.
43. T. Fukuyama, M. T. Rahman, M. Sato and I. Ryu, *Synlett*, 2008, **2008**, 151-163.
44. K. Golbig, A. Kursawe, M. Hohmann, S. Taghavi-Moghadam and T. Schwalbe, *Chemical Engineering Communications*, 2005, **192**, 620-629.
45. J. J. Katz, *Scientific American*, 1960, **203**, 106-117.
46. J. A. Ayres and C. A. Trilling, *Nuclear Engineering and Design*, 1971, **14**, 363-389.
47. A. Mullard, *Nature Reviews Drug Discovery*, 2016, **15**, 219-221.
48. J. Atzrodt, V. Derdau, W. J. Kerr and M. Reid, *Angewandte Chemie International Edition*, 2018, **57**, 1758-1784.
49. R. D. Tung, *Future Medicinal Chemistry*, 2016, **8**, 491-494.
50. M. Dean and V. W. Sung, *Drug design, development and therapy*, 2018, **12**, 313-319.
51. E. M. Russak and E. M. Bednarczyk, *The Annals of pharmacotherapy*, 2019, **53**, 211-216.
52. S. L. Harbeson and R. D. Tung, in *Annual Reports in Medicinal Chemistry*, ed. J. E. Macor, Academic Press, 2011, vol. 46, pp. 403-417.
53. E. Flaumenhaft, S. Bose, H. L. Crespi and J. J. Katz, in *International Review of Cytology*, eds. G. H. Bourne and J. F. Danielli, Academic Press, 1965, vol. 18, pp. 313-361.
54. M. M. Häggblom, V. K. Knight and L. J. Kerkhof, *Environmental Pollution*, 2000, **107**, 199-207.
55. M. Yang and X. Zhang, *Environmental science & technology*, 2013, **47**, 10868-10876.
56. P. Jeschke, *Pest management science*, 2017, **73**, 1053-1066.
57. C. J. Millow, S. A. Mackintosh, R. L. Lewison, N. G. Dodder and E. Hoh, *PloS one*, 2015, **10**, e0127205.
58. Z. Zhang, Q. Zhu, C. Huang, M. Yang, J. Li, Y. Chen, B. Yang and X. Zhao, *Water Research*, 2020, **170**, 115283.

59. Y. Fan, S. J. Chen, Q. Q. Li, Y. Zeng, X. Yan and B. X. Mai, *Environmental pollution (Barking, Essex : 1987)*, 2020, **263**, 114400.
60. D. Henschler, *Angewandte Chemie International Edition in English*, 1994, **33**, 1920-1935.
61. C. P. Huang, C. Dong and Z. Tang, *Waste Management*, 1993, **13**, 361-377.
62. A. Dwivedi, *Scientific Reviews and Chemical Communications*, 2012, **2**, 41-65.
63. K. Teo, Y. Xu and C. Yang, *Ultrasonics sonochemistry*, 2001, **8**, 241-246.
64. S. Rondinini and A. Vertova, 2009, DOI: 10.1007/978-0-387-68318-8\_12, pp. 279-306.
65. D. Ghosal, I. S. You, D. K. Chatterjee and A. M. Chakrabarty, *Science (New York, N.Y.)*, 1985, **228**, 135-142.
66. G. Bonizzoni, *Pure and Applied Chemistry*, 1999, **71**, 1879-1887.
67. X. Ma, S. Liu, Y. Liu, G. Gu and C. Xia, *Scientific Reports*, 2016, **6**, 25068.
68. F. Alonso, I. P. Beletskaya and M. Yus, *Chemical Reviews*, 2002, **102**, 4009-4092.
69. M. Weidauer, E. Irran, C. Someya, M. Haberberger and S. Enthaler, *Journal of Organometallic Chemistry*, 2013, **729**, 53.
70. M. S. Viciu, G. A. Grasa and S. P. Nolan, *Organometallics*, 2001, **20**, 3607-3612.
71. M. L. Buil, M. A. Esteruelas, S. Niembro, M. Oliván, L. Orzechowski, C. Pelayo and A. Vallribera, *Organometallics*, 2010, **29**, 4375-4383.
72. M. Dell'Anna, V. Gallo, P. Mastroilli and G. Romanazzi, *Molecules (Basel, Switzerland)*, 2010, **15**, 3311-3318.
73. T. You, Z. Wang, J. Chen and Y. Xia, *The Journal of Organic Chemistry*, 2017, **82**, 1340-1346.
74. M. E. Cucullu, S. P. Nolan, T. R. Belderrain and R. H. Grubbs, *Organometallics*, 1999, **18**, 1299-1304.
75. Y. Wang, Q. Zhu, Y. Wei, Y. Gong, C. Chen, W. Song and J. Zhao, *Applied Catalysis B: Environmental*, 2018, **231**, 262-268.
76. D. J. Cole-Hamilton, *Science (New York, N.Y.)*, 2003, **299**, 1702-1706.
77. J. E. Lyon, L. E. Rennick and J. L. Burmeister, *Product R&D*, 1970, **9**, 2-20.
78. M. E. Logan and M. E. Oinen, *Organometallics*, 2006, **25**, 1052-1054.
79. V. V. Lunin and E. S. Lokteva, *Russian Chemical Bulletin*, 1996, **45**, 1519-1534.
80. J. Pritchard, G. A. Filonenko, R. van Putten, E. J. M. Hensen and E. A. Pidko, *Chemical Society Reviews*, 2015, **44**, 3808-3833.
81. M. Irfan, T. N. Glasnov and C. O. Kappe, *ChemSusChem*, 2011, **4**, 300-316.
82. R. V. Jones, L. Godorhazy, N. Varga, D. Szalay, L. Urge and F. Darvas, *Journal of Combinatorial Chemistry*, 2006, **8**, 110-116.
83. S. Shi, R. Li, L. Rao and Z. Sun, *Green Chemistry*, 2020, **22**, 669-672.
84. S. Kar, A. Goeppert, R. Sen, J. Kothandaraman and G. K. Surya Prakash, *Green Chemistry*, 2018, **20**, 2706-2710.
85. B. M. Ahmed and G. Mezei, *The Journal of Organic Chemistry*, 2018, **83**, 1649-1653.
86. Y. Ding, S. Luo, C. Weng and J. An, *The Journal of Organic Chemistry*, 2019, **84**, 15098-15105.
87. M. Pohjoispää, R. Mera-Adasme, D. Sundholm, S. Heikkinen, T. Hase and K. Wähälä, *The Journal of Organic Chemistry*, 2014, **79**, 10636-10640.
88. J. Atzrodt, V. Derdau, T. Fey and J. Zimmermann, *Angewandte Chemie (International ed. in English)*, 2007, **46**, 7744-7765.
89. C. S. Donald, T. A. Moss, G. M. Noonan, B. Roberts and E. C. Durham, *Tetrahedron Letters*, 2014, **55**, 3305-3307.

90. M. Janni and S. Peruncheralathan, *Organic & Biomolecular Chemistry*, 2016, **14**, 3091-3097.
91. M. Kuriyama, N. Hamaguchi, G. Yano, K. Tsukuda, K. Sato and O. Onomura, *The Journal of Organic Chemistry*, 2016, **81**, 8934-8946.
92. I. M. Mándity, T. A. Martinek, F. Darvas and F. Fülöp, *Tetrahedron Letters*, 2009, **50**, 4372-4374.
93. S. P. Clissold, *Drugs*, 1986, **32 Suppl 4**, 46-59.
94. S. Groudine and S. Fossum, *Journal of PeriAnesthesia Nursing*, 2011, **26**, 74-80.
95. L. G. Copping, in *Chemistry and Technology of Agrochemical Formulations*, ed. D. A. Knowles, Springer Netherlands, Dordrecht, 1998, DOI: 10.1007/978-94-011-4956-3\_2, pp. 8-40.
96. Y. Kori, S. Sidoli, Z.-F. Yuan, P. J. Lund, X. Zhao and B. A. Garcia, *Scientific Reports*, 2017, **7**, 10296.
97. C. Choudhary, B. T. Weinert, Y. Nishida, E. Verdin and M. Mann, *Nature Reviews Molecular Cell Biology*, 2014, **15**, 536-550.
98. E. Verdin and M. Ott, *Nature Reviews Molecular Cell Biology*, 2015, **16**, 258-264.
99. J. Caldwell, in *Xenobiotic Conjugation Chemistry*, American Chemical Society, 1986, vol. 299, ch. 1, pp. 2-28.
100. R. M. Rowell, R. E. Ibach, J. McSweeney and T. Nilsson, *Wood Material Science & Engineering*, 2009, **4**, 14-22.
101. Y. Li, X. Yang, Q. Fu, R. Rojas, M. Yan and L. Berglund, *Journal of Materials Chemistry A*, 2018, **6**, 1094-1101.
102. R. M. Rowell and J. P. Dickerson, in *Deterioration and Protection of Sustainable Biomaterials*, American Chemical Society, 2014, vol. 1158, ch. 18, pp. 301-327.
103. E. F. V. Scriven, *Chemical Society Reviews*, 1983, **12**, 129-161.
104. E. Vedejs and S. T. Diver, *Journal of the American Chemical Society*, 1993, **115**, 3358-3359.
105. A. R. Gholap, K. Venkatesan, T. Daniel, R. J. Lahoti and K. V. Srinivasan, *Green Chemistry*, 2003, **5**, 693-696.
106. D. D. Sanz Sharley and J. M. J. Williams, *Chemical Communications*, 2017, **53**, 2020-2023.
107. V. K. Yadav, K. Ganesh Babu and M. Mittal, *Tetrahedron*, 2001, **57**, 7047-7051.
108. H. Veisi, S. Taheri and S. Hemmati, *Green Chemistry*, 2016, **18**, 6337-6348.
109. S. P. Chavan, R. Anand, K. Pasupathy and B. S. Rao, *Green Chemistry*, 2001, **3**, 320-322.
110. C. H. Görbitz, *Current Opinion in Solid State and Materials Science*, 2002, **6**, 109-116.
111. A. Thomas, S. Deshayes, M. Decaffmeyer, M. H. Van Eyck, B. Charlotheaux and R. Brasseur, *Proteins: Structure, Function, and Bioinformatics*, 2006, **65**, 889-897.
112. S. Marqus, E. Pirogova and T. J. Piva, *Journal of Biomedical Science*, 2017, **24**, 21.
113. K. Fosgerau and T. Hoffmann, *Drug Discovery Today*, 2015, **20**, 122-128.
114. J. L. Lau and M. K. Dunn, *Bioorganic & Medicinal Chemistry*, 2018, **26**, 2700-2707.
115. F. Albericio and H. G. Kruger, *Future Med Chem*, 2012, **4**, 1527-1531.
116. A. P. Lea and D. McTavish, *Drugs*, 1997, **53**, 828-847.
117. C. A. Jackevicius, M. M. Chou, J. S. Ross, N. D. Shah and H. M. Krumholz, *The New England journal of medicine*, 2012, **366**, 201-204.
118. J. Boström, D. G. Brown, R. J. Young and G. M. Keserü, *Nature Reviews Drug Discovery*, 2018, **17**, 709-727.
119. D. G. Brown and J. Boström, *Journal of Medicinal Chemistry*, 2016, **59**, 4443-4458.

120. R. M. Al-Zoubi, O. Marion and D. G. Hall, *Angewandte Chemie International Edition*, 2008, **47**, 2876-2879.
121. B. S. Jursic and Z. Zdravkovski, *Synthetic Communications*, 1993, **23**, 2761-2770.
122. E. Valeur and M. Bradley, *Chemical Society Reviews*, 2009, **38**, 606-631.
123. W. Zhang and Y. Lu, *QSAR & Combinatorial Science*, 2006, **25**, 724-727.
124. A. J. A. Watson, A. C. Maxwell and J. M. J. Williams, *Organic Letters*, 2009, **11**, 2667-2670.
125. W.-J. Yoo and C.-J. Li, *Journal of the American Chemical Society*, 2006, **128**, 13064-13065.
126. C. L. Allen and J. M. J. Williams, *Chemical Society Reviews*, 2011, **40**, 3405-3415.
127. A. A. Lamar and L. S. Liebeskind, *Tetrahedron Letters*, 2015, **56**, 6034-6037.
128. S. E. Eldred, D. A. Stone, S. H. Gellman and S. S. Stahl, *Journal of the American Chemical Society*, 2003, **125**, 3422-3423.
129. L. Troisi, C. Granito, F. Rosato and V. Videtta, *Tetrahedron Letters*, 2010, **51**, 371-373.
130. R. J. Perry and B. D. Wilson, *The Journal of Organic Chemistry*, 1996, **61**, 7482-7485.
131. M. T. Sabatini, L. T. Boulton, H. F. Sneddon and T. D. Sheppard, *Nature Catalysis*, 2019, **2**, 10-17.
132. E. Bon, D. C. H. Bigg and G. Bertrand, *The Journal of Organic Chemistry*, 1994, **59**, 4035-4036.
133. N. A. Stephenson, J. Zhu, S. H. Gellman and S. S. Stahl, *Journal of the American Chemical Society*, 2009, **131**, 10003-10008.
134. M. Shi and S. C. Cui, *Synthetic Communications*, 2005, **35**, 2847-2858.
135. R. M. de Figueiredo, J.-S. Suppo and J.-M. Campagne, *Chemical Reviews*, 2016, **116**, 12029-12122.
136. K. Sasaki and D. Crich, *Organic Letters*, 2011, **13**, 2256-2259.
137. X. Wu, J. L. Stockdill, P. K. Park and S. J. Danishefsky, *Journal of the American Chemical Society*, 2012, **134**, 2378-2384.
138. C. Larrivé-Aboussafy, B. P. Jones, K. E. Price, M. A. Hardink, R. W. McLaughlin, B. M. Lillie, J. M. Hawkins and R. Vaidyanathan, *Organic Letters*, 2010, **12**, 324-327.
139. R. M. de Figueiredo, J.-S. Suppo, C. Midrier and J.-M. Campagne, *Advanced Synthesis & Catalysis*, 2017, **359**, 1963-1968.
140. T. Messeri, D. D. Sternbach and N. C. O. Tomkinson, *Tetrahedron Letters*, 1998, **39**, 1669-1672.
141. A. Pourvali, J. R. Cochrane and C. A. Hutton, *Chemical Communications*, 2014, **50**, 15963-15966.
142. K. N. Kumar, K. Sreeramamurthy, S. Palle, K. Mukkanti and P. Das, *Tetrahedron Letters*, 2010, **51**, 899-902.
143. T. Messeri, D. D. Sternbach and N. C. O. Tomkinson, *Tetrahedron Letters*, 1998, **39**, 1673-1676.
144. Z. Fu, J. Lee, B. Kang and S. H. Hong, *Organic Letters*, 2012, **14**, 6028-6031.
145. Y. Li, F. Jia and Z. Li, *Chemistry – A European Journal*, 2013, **19**, 82-86.
146. H.-A. Seo, Y.-H. Cho, Y.-S. Lee and C.-H. Cheon, *The Journal of Organic Chemistry*, 2015, **80**, 11993-11998.
147. D. Mazunin, N. Brogiere, M. Zenobi-Wong and J. W. Bode, *ACS Biomaterials Science & Engineering*, 2015, **1**, 456-462.
148. H. Noda, G. Erős and J. W. Bode, *Journal of the American Chemical Society*, 2014, **136**, 5611-5614.

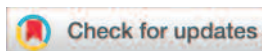
149. F. Rohrbacher, A. Zwicky and J. W. Bode, *Chemical Science*, 2017, **8**, 4051-4055.
150. G. N. Boross, S. Shimura, M. Besenius, N. Tennagels, K. Rossen, M. Wagner and J. W. Bode, *Chemical Science*, 2018, **9**, 8388-8395.
151. B. Shen, D. M. Makley and J. N. Johnston, *Nature*, 2010, **465**, 1027-1032.
152. K. Ishihara, S. Ohara and H. Yamamoto, *The Journal of Organic Chemistry*, 1996, **61**, 4196-4197.
153. L. J. Leman and M. R. Ghadiri, *Synlett*, 2017, **28**, 68-72.
154. L. Leman, L. Orgel and M. R. Ghadiri, *Science (New York, N.Y.)*, 2004, **306**, 283-286.
155. L. J. Leman, Z. Z. Huang and M. R. Ghadiri, *Astrobiology*, 2015, **15**, 709-716.
156. T. N. Glasnov and C. O. Kappe, *Advanced Synthesis & Catalysis*, 2010, **352**, 3089-3097.
157. P. J. Cossar, L. Hizartidis, M. I. Simone, A. McCluskey and C. P. Gordon, *Organic & Biomolecular Chemistry*, 2015, **13**, 7119-7130.
158. A. Borodziński and G. C. Bond, *Catalysis Reviews*, 2008, **50**, 379-469.
159. M. Jin, H. Liu, H. Zhang, Z. Xie, J. Liu and Y. Xia, *Nano Research*, 2011, **4**, 83-91.
160. G. Neri, M. G. Musolino, C. Milone, D. Pietropaolo and S. Galvagno, *Applied Catalysis A: General*, 2001, **208**, 307-316.
161. H. Klefer, M. Munoz, A. Modrow, B. Böhringer, P. Wasserscheid and B. J. M. Etzold, *Chemical Engineering & Technology*, 2016, **39**, 276-284.
162. S. Fichtner, J. Hofmann, A. Möller, C. Schrage, J. M. Giebelhausen, B. Böhringer and R. Gläser, *Journal of Hazardous Materials*, 2013, **262**, 789-795.
163. B. Böhringer, O. Guerra Gonzalez, I. Eckle, M. Müller, J.-M. Giebelhausen, C. Schrage and S. Fichtner, *Chemie Ingenieur Technik*, 2011, **83**, 53-60.
164. R. K. Henderson, C. Jiménez-González, D. J. C. Constable, S. R. Alston, G. G. A. Inglis, G. Fisher, J. Sherwood, S. P. Binks and A. D. Curzons, *Green Chemistry*, 2011, **13**, 854-862.
165. M. North, R. Pasquale and C. Young, *Green Chemistry*, 2010, **12**, 1514-1539.
166. P. Lenden, P. M. Ylioja, C. González-Rodríguez, D. A. Entwistle and M. C. Willis, *Green Chemistry*, 2011, **13**, 1980-1982.
167. B. Pieber and C. O. Kappe, *Green Chemistry*, 2013, **15**, 320-324.
168. P. Neubert, S. Fuchs and A. Behr, *Green Chemistry*, 2015, **17**, 4045-4052.
169. H. L. Parker, J. Sherwood, A. J. Hunt and J. H. Clark, *ACS Sustainable Chemistry & Engineering*, 2014, **2**, 1739-1742.
170. B. Yu, Z.-F. Diao, C.-X. Guo, C.-L. Zhong, L.-N. He, Y.-N. Zhao, Q.-W. Song, A.-H. Liu and J.-Q. Wang, *Green Chemistry*, 2013, **15**, 2401-2407.
171. S. B. Lawrenson, R. Arav and M. North, *Green Chemistry*, 2017, **19**, 1685-1691.
172. B. Schäffner, V. Andrushko, J. Holz, S. P. Verevkin and A. Börner, *ChemSusChem*, 2008, **1**, 934-940.
173. J. Bayardon, J. Holz, B. Schäffner, V. Andrushko, S. Verevkin, A. Preetz and A. Börner, *Angewandte Chemie International Edition*, 2007, **46**, 5971-5974.
174. J. L. Kiplinger, T. G. Richmond and C. E. Osterberg, *Chemical Reviews*, 1994, **94**, 373-431.
175. A. P. Phillips, *Journal of the American Chemical Society*, 1950, **72**, 1850-1852.
176. O. A. El Seoud, A. Koschella, L. C. Fidale, S. Dorn and T. Heinze, *Biomacromolecules*, 2007, **8**, 2629-2647.
177. G. Bartoli, R. Dalpozzo, A. De Nino, L. Maiuolo, M. Nardi, A. Procopio and A. Tagarelli, *Green Chemistry*, 2004, **6**, 191-192.
178. Á. Molnár and A. Papp, *Coordination Chemistry Reviews*, 2017, **349**, 1-65.

179. M. Brahmayya, S.-Y. Suen and S. A. Dai, *Journal of the Taiwan Institute of Chemical Engineers*, 2018, **83**, 174-183.
180. T.-S. Jiang and G.-W. Wang, *Organic Letters*, 2013, **15**, 788-791.
181. W. B. Jang, W. S. Shin, J. E. Hong, S. Y. Lee and D. Y. Oh, *Synthetic Communications*, 1997, **27**, 3333-3339.
182. U. P. Saikia, F. L. Hussain, M. Suri and P. Pahari, *Tetrahedron Letters*, 2016, **57**, 1158-1160.
183. F. E. Critchfield and J. B. Johnson, *Analytical Chemistry*, 1956, **28**, 430-436.
184. W.-D. Rudolf, *Journal of Sulfur Chemistry*, 2007, **28**, 295-339.
185. N. Sun, B. Li, J. Shao, W. Mo, B. Hu, Z. Shen and X. Hu, *Beilstein journal of organic chemistry*, 2012, **8**, 61-70.
186. R. N. Ram, P. Kumar and A. K. Mukerjee, *Journal of Chemical Education*, 1983, **60**, 508.
187. V. Delaveau, Z. Mouloungui and e. A. Gaset, *Synthetic Communications*, 1996, **26**, 2341-2348.
188. W. R. Vaughan, M. V. Andersen, H. S. Blanchard, D. I. McCane and W. L. Meyer, *The Journal of Organic Chemistry*, 1955, **20**, 819-822.

# Appendix

**I**





Cite this: *Green Chem.*, 2019, **21**, 956

Received 11th October 2018,  
Accepted 11th January 2019

DOI: 10.1039/c8gc03192d

rsc.li/greenchem

## Continuous-flow catalytic deuterodehalogenation carried out in propylene carbonate†

György Orsy,<sup>a</sup> Ferenc Fülöp<sup>\*a,b</sup> and István M. Mándity<sup>ID \*a,c,d</sup>

A selective continuous-flow (CF) deuterodehalogenation approach is described performed in propylene carbonate, which is considered as one of the greenest solvents. Various CF technologies are known for hydrodehalogenation reactions; however, they are not directly transferable for deuteration transformations. A novel spherical activated carbon-supported palladium catalyst has been found to be useful for the catalytic deuterodehalogenation of haloarenes. After careful reaction parameter optimization, complete conversion was achieved for bromine- and chlorine-substituted haloarenes. Nonetheless, no deuterium exchange was observed for the fluorine substituent, while iodine-substituted compounds poisoned the catalyst. Importantly, deuterated compounds were obtained with a rate of 3 mg min<sup>-1</sup> and the catalyst showed reasonable reusability. Moreover, benzylic amides were also deuterated without any debenzoylation side-reaction.

### Introduction

Deuterated compounds are of considerable current interest since they have a wide range of biomedical, chemical and medicinal applications.<sup>1–10</sup> They are used in mass spectrometry as internal standards<sup>1,11,12</sup> and can be applied in mechanistic studies,<sup>13–15</sup> and deuterium can also be used as a protecting group.<sup>4,16</sup> Most importantly, nowadays deuterium-labelled compounds are considered as medicines of the future,<sup>17,18</sup>

Deutetrabenazine,<sup>19,20</sup> the first deuterium-labelled compound, has recently been approved by the FDA<sup>21,22</sup> and the deuterated aryl moiety in molecules might lead to next-generation drugs due to high therapeutic values.<sup>22</sup> Deuterium labelling increased the pharmacokinetic properties of the parent molecule through the kinetic isotope effect. There are deuterated drug molecules under clinical phase trials for diseases such as Alzheimer's disease, cystic fibrosis, Friedreich's ataxia, and psoriasis.<sup>22</sup>

The major breakthrough of continuous-flow (CF) technologies to organic chemistry and the fine chemical industry has appeared in the field of catalytic hydrogenation triggered by the invention of the H-Cube® reactor.<sup>23</sup> It consists of a pump delivering the liquids, a built-in hydrogen generator producing hydrogen gas from water and a catalyst cartridge, where the reaction occurs. The cartridge is filled with supported catalysts, which is a crucial factor in CF hydrogenation reactions. In addition, there is a thermostat and a pressure regulator in the system to control the temperature and pressure of the reaction. Nowadays, such reactors are widely used in organic chemistry laboratories.<sup>24–44</sup> By simply changing the water in the reservoir for heavy water and using aprotic solvents, CF deuteration reactions can be carried out.<sup>45–48</sup> A schematic outline of the reactor used in this study is shown in Fig. 1.

In regular batch operations, solid supports with small particle sizes in the low micrometer range are used, since they offer high catalytic activity.<sup>49–51</sup> However, such catalysts are not suitable for CF devices, since they can block the flow line. Thus, the search for novel solid supports is of considerable current interest. Recently, polymer-based spherical activated carbon (PBSAC) has been introduced as a solid support for CF catalytic hydrogenation.<sup>52–54</sup> This polystyrene-derived solid support offers a high surface, which is necessary for high catalytic activity. Furthermore, because of its spherical nature, it is prominently compatible with CF conditions without any observable pressure increase in the flow line during the synthetic operation.

In reaction design, the appropriate choice of solvent is another crucial factor. A suitable solvent can enhance the reac-

<sup>a</sup>Institute of Pharmaceutical Chemistry, University of Szeged, Eötvös u. 6, H-6720 Szeged, Hungary. E-mail: fulop@pharm.u-szeged.hu,

mandity.istvan@pharma.semmelweis-univ.hu, mandity.istvan@ttk.mta.hu

<sup>b</sup>Research Group of Stereochemistry of the Hungarian Academy of Sciences, Dóm tér 8, H-6720 Szeged, Hungary

<sup>c</sup>Department of Organic Chemistry, Faculty of Pharmacy, Semmelweis University, Hógyes Endre u. 7, H-1092 Budapest, Hungary

<sup>d</sup>MTA TTK Lendület Artificial Transporter Research Group, Institute of Materials and Environmental Chemistry, Research Center for Natural Sciences, Hungarian Academy of Sciences, Magyar Tudósok krt. 2, 1117 Budapest, Hungary

† Electronic supplementary information (ESI) available: General experimental setup, <sup>1</sup>H and <sup>13</sup>C NMR spectra. See DOI: 10.1039/c8gc03192d

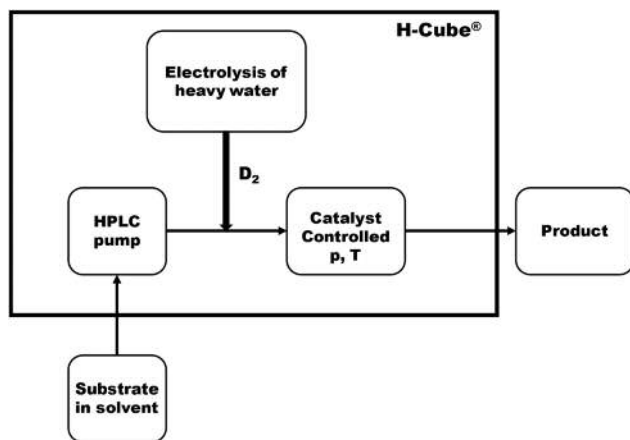


Fig. 1 Schematic illustration of the reactor used for the dehalodeuteration reaction.

tion rate, might stabilize transition states, allows the appropriate concentration of reagents, *etc.* Moreover, solvents used today should be as sustainable as possible.<sup>55</sup> According to the recent GSK solvent selection guide, the greenest solvent today is propylene carbonate (PC),<sup>56</sup> which can be synthesized in a highly atom-efficient way from propylene oxide and carbon dioxide with prominently low energy consumption.<sup>57</sup> PC has already been used for several important reactions;<sup>58–63</sup> however, its use in catalytic deuteration is practically unexplored.<sup>64,65</sup>

Herein we report the first CF deuterodehalogenation of aromatic compounds performed by the use of a PBSAC-supported Pd catalyst in PC as a prominent green solvent. In addition, not only ethyl acetate used traditionally was replaced by a more sustainable solvent, but a higher concentration of the reagents could also be achieved in PC, thus allowing a higher space–time yield and lower solvent consumption.

## Results and discussion

Hydrodehalogenation of aromatic compounds was carried out in CF without difficulties.<sup>27,66,67</sup> Thus, we aimed to implement our CF deuteration technology developed previously to perform deuterodehalogenation reactions selecting 4-bromoacetanilide as a test compound. The complete reaction parameter optimization is shown in Table 1. The starting material was dissolved in ethyl acetate (EtOAc) at a concentration of 1 mg mL<sup>-1</sup>, utilizing 5% Pd/BaSO<sub>4</sub> as the catalyst at a temperature of 25 °C and a pressure of 50 bar with a flow rate of 1 mL min<sup>-1</sup>. No conversion was observed under these conditions. An increase in the pressure to 100 bar provided a marginal increase in conversion. Still, the utilization of 100 °C with 100 bar resulted only in 13% conversion. To increase the performance of our system, the catalyst was changed to charcoal-supported 5% Pd/C. This afforded a significantly improved conversion of 48%, while the deuterium incorporation value of the product was found to be a promising 81%. Next, we turned our attention toward the novel PBSAC supported catalyst.<sup>52,54</sup>

Table 1 Reaction parameter optimization for the CF deuterodehalogenation reaction

Solvent	Catalyst	<i>T</i> (°C)	<i>p</i> (bar)	Conc. (mg mL <sup>-1</sup> )	<i>D</i> (%)	Conv. (%)
EtOAc	A	25	50	1	n.d.	0
EtOAc	A	25	100	1	n.d.	4
EtOAc	A	100	100	1	n.d.	13
EtOAc	B	100	100	1	81	48
EtOAc	C	100	100	1	92	87
PC	C	100	100	1	96	99
PC	C	100	100	3	96	99
PC	C	100	100	4	97	94

A: 5% Pd/BaSO<sub>4</sub>; B: 5% Pd/C; C: 5% Pd/PBSAC.

With this catalyst 87% conversion and 92% deuterium incorporation were observed at 100 bar pressure and 100 °C temperature. Finally, the solvent was optimized and it was changed for PC according to the GSK solvent selection guide and CF literature results on the suitability of PC in CF. Importantly, complete conversion was obtained while the deuterium incorporation value was 96% at 100 bar pressure and 100 °C temperature. The effect of the concentration of the starting material on the reaction outcome was also tested. The results revealed that without the loss of conversion and deuterium incorporation, the concentration can be increased to 3 mg mL<sup>-1</sup>.

However, the decrease in either the pressure or the temperature resulted in lower yields (Fig. 2), while the deuterium incorporation level did not change significantly.

The scope of the reaction was tested first with various bromine-substituted aromatic compounds. Benzoic acids possessing a bromo substituent in positions 4 (**3**), 3 (**5**) and 2 (**7**) were examined under the optimized conditions. As shown in Table 2, for these regioisomers complete conversions were achieved with >95% deuterium incorporation in the case of **3** and **5**. However, for **7**, where the bromine is in the *ortho* position, only marginal deuterium incorporation was observed. We envisaged that intramolecular bromine–hydrogen exchange occurs due to the steric proximity of the functional groups. Thus, the starting material was dissolved in deuterated methanol, the solution was evaporated to dryness, and the product was utilized immediately in the deuteration reaction. By this simple treatment, the deuterium incorporation value increased to 97%.

Next, a further set of test compounds, namely, aromatic amides **9**, **11** and **13**, were investigated possessing a bromo substituent in positions 4, 3 and 2, respectively. Excellent deuterium incorporation and conversion were achieved in all cases, except for compound **13**. Here again the same intramolecular bromine–hydrogen exchange was surmised as described for **7**; thus a similar deuterated methanol pre-treatment was carried out. The deuterium incorporation value, in this way, increased to 98%.

Importantly, no debenzoylation was observed for compounds **9**, **11** and **13**. This is a significant further advantage of the method allowing the deuteration of molecules containing the benzyl moiety.

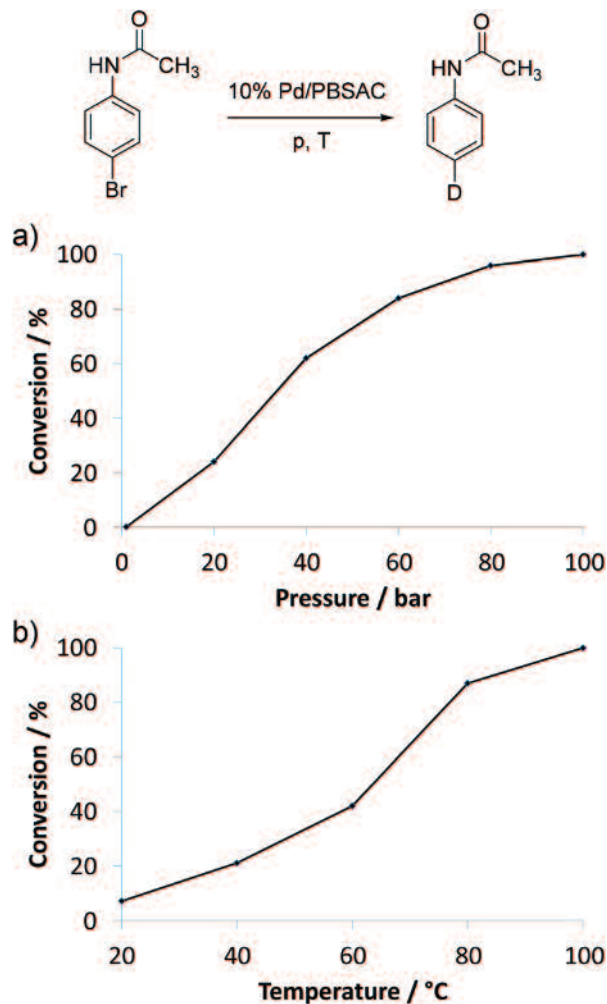


Fig. 2 The effect of pressure and temperature on the reaction conversion catalysed by PBSAC-supported 10% Pd. The effect of pressure was measured at 100 °C, while the effect of temperature was determined at 100 bar.

To further broaden the scope of the developed deuterodehalogenation reaction, aromatic compounds with other halogen substituents were also tested (Table 3).

In the reaction of chlorine-substituted acetanilide **15**, full conversion was achieved with a high deuterium incorporation value. Surprisingly, the corresponding iodine-substituted derivative (**16**) gave only a mere 30% conversion. However, by repeating the reaction with the catalyst used in the first trial, no conversion was observed. Obviously, compound **16** poisoned the catalyst. Compound **17** was selected to test the effect of the fluorine substituent. The results show that the fluorine substituent remained intact and no conversion was observed.

These results can be explained by the proposed mechanism of the reaction (Scheme 1).<sup>68</sup> A key step is the oxidative addition of the aryl halide to a Pd(0) species. According to the literature results this reaction does not proceed for aryl fluorides,<sup>69</sup> which supports our observation for fluorinated compounds. The poisoning of the catalyst in the case of iodinated

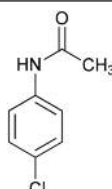
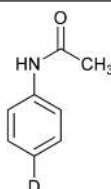
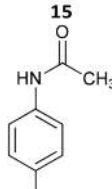
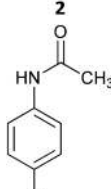
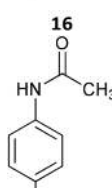
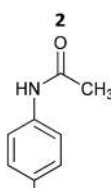
Table 2 Results of the deuteration reaction of several bromine-substituted model compounds

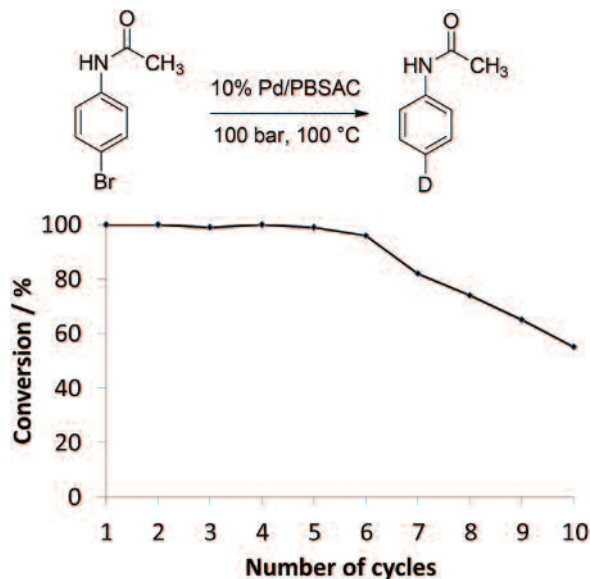
Entry	Substrate	Product	D (%)	Yield (%)
1			96	96
2			96	97
3			95	95
4			98 <sup>a</sup>	94
5			97	98
6			96	94
7			98 <sup>a</sup>	95

<sup>a</sup> Achieved by pre-treating the starting molecule with deuterated methanol.

compounds can be explained by the elimination of the iodide ion. According to the literature results the iodide ion is known to poison the Pd catalyst.<sup>70</sup>

**Table 3** Results of the deuteration reaction with substrates possessing chloro, iodo and fluoro substituents

Entry	Substrate	Product	D (%)	Yield (%)
1			96	96
2			n.d.	30
3			n.d.	0

**Fig. 3** Robustness of the CF deuteration investigated in the reaction of **1**. The same reaction was repeated 10 times on the same catalyst.

The product (**2**) was isolated with 95% yield and the data showed 96% deuterium incorporation.

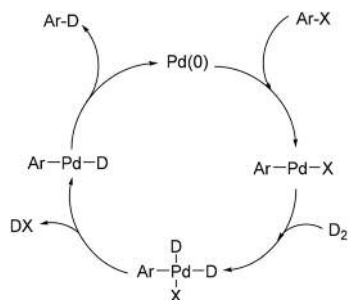
## Conclusions

In conclusion, we have developed the first CF deuteration reaction induced by palladium. Surprisingly, the conditions described previously for CF hydrodehalogenations were not suitable for deuteration. Harsh reaction conditions (100 bar and 100 °C), a novel spherical support (PBSAC) and PC as a solvent were necessary to obtain complete conversions with concomitant >95% deuterium incorporations. Importantly, PC allowed the use of an increased (3 times higher) concentration of the reactants with considerably faster reactions. Test compounds possessing bromine substituents in different positions provided excellent results, except the 2-bromo-substituted compounds. In these cases, deuteromethanol pre-treatment was necessary, due to intramolecular halogen-hydrogen exchange. Importantly, molecules containing the benzyl group were also deuterated without any trace of debenzilation. Chloro-substituted derivatives also provided excellent results. However, the iodine substituent poisoned the catalyst, while the fluorine substituent remained intact. Thus, selective deuteration can be performed in the presence of a fluorine substituent. The catalyst under these harsh reaction conditions showed moderate reusability.

## Experimental section

### NMR characterization of products

**N-(Phenyl-4-<sup>2</sup>H)acetamide (2).** White crystals; m.p. 110.2–111.8 °C (data are in agreement with the literature reference: 110–112 °C)<sup>72</sup>

**Scheme 1** Proposed mechanism for the catalytic deuteration.

In the context of green chemistry criteria, catalyst recycling is an important issue. Therefore, the robustness of the reaction was also tested (Fig. 3). The deuteration reaction of **1** was repeated multiple times with the same catalyst bed. In the first 6 cycles, the conversion value did not change significantly. However, from run 7 onward, considerable decreases in the catalytic activity were observed. Thus, the catalyst used in the CF deuteration reaction proved to be moderately robust.<sup>71</sup>

The catalyst recycling data were utilized for a careful design of the large scale reaction. Since the catalyst activity did not decrease significantly until 5 cycles and one cycle was carried out with 100 mg of compound **1**, it was planned that after the pumping of 500 mg of **1** through the system, the catalyst cartridge will be replaced by a new one. In total a CF deuteration reaction was carried out with 1.5 g of compound **1**.



$^1\text{H}$  NMR (400 MHz,  $\text{DMSO}-d_6$ )  $\delta$  9.91 (s, 1H), 7.56 (d,  $J = 8.2$  Hz, 2H), 7.27 (d,  $J = 8.2$  Hz, 2H), 2.03 (s, 3H);  $^{13}\text{C}$  NMR (100 MHz,  $\text{DMSO}-d_6$ )  $\delta$  168.3, 139.3, 128.6, 123.0, 118.9, 24.0.

**Benzoic-4- $^2\text{H}$  acid (4).** White crystals; m.p. 119.1–121.4 °C (data are in agreement with the literature reference: 119–121 °C)<sup>72</sup>

$^1\text{H}$  NMR (400 MHz,  $\text{DMSO}-d_6$ )  $\delta$  7.94 (d,  $J = 7.5$  Hz, 2H), 7.50 (d,  $J = 7.5$  Hz, 2H).  $^{13}\text{C}$  NMR (100 MHz,  $\text{DMSO}-d_6$ )  $\delta$  167.4, 132.9, 130.8, 129.3, 128.6.

**Benzoic-3- $^2\text{H}$  acid (6).** White crystals; m.p. 119.6–121.3 °C (data are in agreement with the literature reference: 121 °C)<sup>73</sup>

$^1\text{H}$  NMR (400 MHz,  $\text{DMSO}-d_6$ )  $\delta$  7.91–7.95 (m, 2H), 7.58–7.62 (m, 1H), 7.47 (t,  $J = 8.3$  Hz, 1H).  $^{13}\text{C}$  NMR (100 MHz,  $\text{DMSO}-d_6$ )  $\delta$  167.3, 132.9, 130.7, 129.3, 128.6.

**Benzoic-2- $^2\text{H}$  acid (8).** White crystals; m.p. 119.3–121.1 °C (data are in agreement with the literature reference: 121 °C)<sup>73</sup>

$^1\text{H}$  NMR (400 MHz,  $\text{DMSO}-d_6$ )  $\delta$  7.94 (d,  $J = 7.3$ , 1H), 7.58–7.65 (m, 1H), 7.47–7.54 (m, 1H).  $^{13}\text{C}$  NMR (100 MHz,  $\text{DMSO}-d_6$ )  $\delta$  167.3, 132.9, 130.6, 129.2, 128.6.

**N-Benzylbenzamide-4- $^2\text{H}$  (10).** White crystals; m.p. 104.1–106.2 °C (compound is known,<sup>74</sup> but m.p. not published)

$^1\text{H}$  NMR (400 MHz,  $\text{DMSO}-d_6$ )  $\delta$  9.02 (t,  $J = 5.3$ , 1H), 7.90 (d,  $J = 7.4$ , 2H), 7.47 (d,  $J = 7.4$ , 2H), 7.19–7.28 (m, 1H) 7.28–7.37 (m, 4H), 4.49 (d,  $J = 5.3$ , 2H).  $^{13}\text{C}$  NMR (100 MHz,  $\text{DMSO}-d_6$ )  $\delta$  166.2, 139.7, 134.3, 130.9, 128.3, 128.2, 127.2, 127.1, 126.7, 42.6.

**N-Benzylbenzamide-3- $^2\text{H}$  (12).** White crystals; m.p. 104.1–106.2 °C

$^1\text{H}$  NMR (400 MHz,  $\text{DMSO}-d_6$ )  $\delta$  9.04 (t,  $J = 5.3$ , 1H), 7.87–7.92 (m, 2H), 7.44–7.56 (m, 2H), 7.19–7.28 (m, 1H) 7.28–7.37 (m, 4H), 4.49 (d,  $J = 5.3$ , 2H).  $^{13}\text{C}$  NMR (100 MHz,  $\text{DMSO}-d_6$ )  $\delta$  166.2, 139.7, 134.3, 131.1, 128.3, 128.2, 128.0, 127.2, 127.1, 127.1, 126.7, 42.6.

**N-Benzylbenzamide-2- $^2\text{H}$  (14).** White crystals; m.p. 104.1–106.2 °C

$^1\text{H}$  NMR (400 MHz,  $\text{DMSO}-d_6$ )  $\delta$  9.05 (t,  $J = 5.3$ , 1H), 7.88 (d,  $J = 7.4$ , 1H), 7.43–7.56 (m, 3H), 7.19–7.28 (m, 1H) 7.28–7.37 (m, 4H), 4.48 (d,  $J = 5.3$ , 2H).  $^{13}\text{C}$  NMR (100 MHz,  $\text{DMSO}-d_6$ )  $\delta$  166.4, 139.8, 134.3, 131.4, 128.5, 128.4, 128.3, 127.3, 127.3, 127.0, 126.9, 42.6.

## Conflicts of interest

There are no conflicts to declare.

## Acknowledgements

We are grateful to the Hungarian Research Foundation (OTKA No. K 115731). The financial support of the GINOP-2.3.2-15-2016-00014 project is acknowledged.

## Notes and references

1 E. Stokvis, H. Rosing and J. H. Beijnen, *Rapid Commun. Mass Spectrom.*, 2005, **19**, 401–407.

- H. Frederiksen, N. E. Skakkebaek and A.-M. Andersson, *Mol. Nutr. Food Res.*, 2007, **51**, 899–911.
- D. Wade, *Chem.-Biol. Interact.*, 1999, **117**, 191–217.
- M. E. Wood, S. Bissiriou, C. Lowe and K. M. Windeatt, *Org. Biomol. Chem.*, 2008, **6**, 3048–3051.
- A. K. L. Yuen, O. Lafon, T. Charpentier, M. Roy, F. Brunet, P. Berthault, D. Sakellariou, B. Robert, S. Rimsky, F. Pillon, J.-C. Cintrat and B. Rousseau, *J. Am. Chem. Soc.*, 2010, **132**, 1734–1735.
- T. Traoré, L. Delacour, S. Garcia-Argote, P. Berthault, J.-C. Cintrat and B. Rousseau, *Org. Lett.*, 2010, **12**, 960–962.
- A.-L. Guyard, A. Valleix, B. Rousseau and J.-C. Cintrat, *J. Labelled Comp. Radiopharm.*, 2001, **44**, 529–539.
- Q. Raffy, D.-A. Buisson, J.-C. Cintrat, B. Rousseau, S. Pin and J. P. Renault, *Angew. Chem., Int. Ed.*, 2012, **51**, 2960–2963.
- J.-C. Cintrat, F. Pillon and B. Rousseau, *Tetrahedron Lett.*, 2001, **42**, 5001–5003.
- N. Faucher, Y. Ambroise, J.-C. Cintrat, E. Doris, F. Pillon and B. Rousseau, *J. Org. Chem.*, 2002, **67**, 932–934.
- T. H. Zytovicz, E. F. Fitzgerald, D. Marsden, C. A. Larson, V. E. Shih, D. M. Johnson, A. W. Strauss, A. M. Comeau, R. B. Eaton and G. F. Grady, *A Two-Year Summary from the New England Newborn Screening Program*, 2001, vol. 47, pp. 1945–1955.
- S. Wang, M. Cyronak and E. Yang, *J. Pharm. Biomed. Anal.*, 2007, **43**, 701–707.
- E. M. Simmons and J. F. Hartwig, *Angew. Chem., Int. Ed.*, 2012, **51**, 3066–3072.
- W. W. Cleland, *Arch. Biochem. Biophys.*, 2005, **433**, 2–12.
- D. Crich, *Acc. Chem. Res.*, 2010, **43**, 1144–1153.
- M. Miyashita, M. Sasaki, I. Hattori, M. Sakai and K. Tanino, *Science*, 2004, **305**, 495–499.
- T. G. Gant, *J. Med. Chem.*, 2014, **57**, 3595–3611.
- K. Parcella, K. Eastman, K.-S. Yeung, K. A. Grant-Young, J. Zhu, T. Wang, Z. Zhang, Z. Yin, D. Parker, K. Mosure, H. Fang, Y.-K. Wang, J. Lemm, X. Zhuo, U. Hanumegowda, M. Liu, K. Rigat, M. Donoso, M. Tuttle, T. Zvyaga, Z. Haarhoff, N. A. Meanwell, M. G. Soars, S. B. Roberts and J. F. Kadow, *ACS Med. Chem. Lett.*, 2017, **8**, 771–774.
- G. Huntington Study, *J. Am. Med. Assoc.*, 2016, **316**, 40–50.
- M. D. Geschwind and N. Paras, *J. Am. Med. Assoc.*, 2016, **316**, 33–35.
- K. E. Anderson, D. Stamler, M. D. Davis, S. A. Factor, R. A. Hauser, J. Isojärvi, L. F. Jarskog, J. Jimenez-Shahed, R. Kumar, J. P. McEvoy, S. Ochudlo, W. G. Ondo and H. H. Fernandez, *Lancet Psychiatry*, 2017, **4**, 595–604.
- C. Schmidt, *Nat. Biotechnol.*, 2017, **35**, 493.
- R. V. Jones, L. Godorhazy, N. Varga, D. Szalay, L. Urge and F. Darvas, *J. Comb. Chem.*, 2006, **8**, 110–116.
- B. P. Mason, K. E. Price, J. L. Steinbacher, A. R. Bogdan and D. T. McQuade, *Chem. Rev.*, 2007, **107**, 2300–2318.
- K. Geyer, J. D. C. Codee and P. H. Seeberger, *Chem. – Eur. J.*, 2006, **12**, 8434–8442.
- B. Ahmed-Omer, J. C. Brandt and T. Wirth, *Org. Biomol. Chem.*, 2007, **5**, 733–740.

- 27 C. G. Frost and L. Mutton, *Green Chem.*, 2010, **12**, 1687–1703.
- 28 M. B. Plutschack, B. Pieber, K. Gilmore and P. H. Seeberger, *Chem. Rev.*, 2017, **117**, 11796–11893.
- 29 F. Lévesque and P. H. Seeberger, *Angew. Chem., Int. Ed.*, 2012, **51**, 1706–1709.
- 30 C. A. Correia, K. Gilmore, D. T. McQuade and P. H. Seeberger, *Angew. Chem., Int. Ed.*, 2015, **54**, 4945–4948.
- 31 S. Matthies, D. T. McQuade and P. H. Seeberger, *Org. Lett.*, 2015, **17**, 3670–3673.
- 32 D. Mandala and P. Watts, *ChemistrySelect*, 2017, **2**, 1102–1105.
- 33 F. Chigondo, B. Zeelie and P. Watts, *ACS Sustainable Chem. Eng.*, 2016, **4**, 6237–6243.
- 34 C. Wiles and P. Watts, *Green Chem.*, 2014, **16**, 55–62.
- 35 D. Ott, S. Borukhova and V. Hessel, *Green Chem.*, 2016, **18**, 1096–1116.
- 36 H. P. L. Gemoets, Y. H. Su, M. J. Shang, V. Hessel, R. Luque and T. Noel, *Chem. Soc. Rev.*, 2016, **45**, 83–117.
- 37 A. Talla, B. Driessen, N. J. W. Straathof, L. G. Milroy, L. Brunsveld, V. Hessel and T. Noel, *Adv. Synth. Catal.*, 2015, **357**, 2180–2186.
- 38 J. Wegner, S. Ceylan and A. Kirschning, *Chem. Commun.*, 2011, 4583–4592.
- 39 K. Mennecke, R. Cecilia, T. N. Glasnov, S. Gruhl, C. Vogt, A. Feldhoff, M. A. L. Vargas, C. O. Kappe, U. Kunz and A. Kirschning, *Adv. Synth. Catal.*, 2008, **350**, 717–730.
- 40 J. Wegner, S. Ceylan and A. Kirschning, *Adv. Synth. Catal.*, 2012, **354**, 17–57.
- 41 C. Wiles and P. Watts, *Green Chem.*, 2012, **14**, 38–54.
- 42 M. Sau, C. Rodríguez-Esrich and M. A. Pericàs, *Org. Lett.*, 2011, **13**, 5044–5047.
- 43 E. Alza, S. Sayalero, X. C. Cambeiro, R. Martin-Rapun, P. O. Miranda and M. A. Pericàs, *Synlett*, 2011, 464–468.
- 44 F. Cuevas, A. I. Oliva and M. A. Pericàs, *Synlett*, 2010, 1873–1877.
- 45 I. M. Mándity, T. A. Martinek, F. Darvas and F. Fülöp, *Tetrahedron Lett.*, 2009, **50**, 4372–4374.
- 46 S. B. Otvos, I. M. Mándity and F. Fulop, *Mol. Divers.*, 2011, **15**, 605–611.
- 47 C.-T. Hsieh, S. B. Ötvös, Y.-C. Wu, I. M. Mándity, F.-R. Chang and F. Fülöp, *ChemPlusChem*, 2015, **80**, 859–864.
- 48 S. Chandrasekhar, B. V. D. Vijaykumar, B. Mahesh Chandra, C. Raji Reddy and P. Naresh, *Tetrahedron Lett.*, 2011, **52**, 3865–3867.
- 49 A. Borodziński and G. C. Bond, *Catal. Rev.*, 2008, **50**, 379–469.
- 50 M. Jin, H. Liu, H. Zhang, Z. Xie, J. Liu and Y. Xia, *Nano Res.*, 2011, **4**, 83–91.
- 51 G. Neri, M. G. Musolino, C. Milone, D. Pietropaolo and S. Galvagno, *Appl. Catal., A*, 2001, **208**, 307–316.
- 52 H. Klefer, M. Munoz, A. Modrow, B. Böhringer, P. Wasserscheid and B. J. M. Etzold, *Chem. Eng. Technol.*, 2016, **39**, 276–284.
- 53 S. Fichtner, J. Hofmann, A. Möller, C. Schrage, J. M. Giebelhausen, B. Böhringer and R. Gläser, *J. Hazard. Mater.*, 2013, **262**, 789–795.
- 54 B. Böhringer, O. Guerra Gonzalez, I. Eckle, M. Müller, J.-M. Giebelhausen, C. Schrage and S. Fichtner, *Chem. Ing. Tech.*, 2011, **83**, 53–60.
- 55 P. G. Jessop, *Green Chem.*, 2011, **13**, 1391–1398.
- 56 R. K. Henderson, C. Jiménez-González, D. J. C. Constable, S. R. Alston, G. G. A. Inglis, G. Fisher, J. Sherwood, S. P. Binks and A. D. Curzons, *Green Chem.*, 2011, **13**, 854–862.
- 57 M. North, R. Pasquale and C. Young, *Green Chem.*, 2010, **12**, 1514–1539.
- 58 P. Lenden, P. M. Ylioja, C. González-Rodríguez, D. A. Entwistle and M. C. Willis, *Green Chem.*, 2011, **13**, 1980–1982.
- 59 B. Pieber and C. O. Kappe, *Green Chem.*, 2013, **15**, 320–324.
- 60 S. B. Lawrenson, R. Arav and M. North, *Green Chem.*, 2017, **19**, 1685–1691.
- 61 B. Yu, Z.-F. Diao, C.-X. Guo, C.-L. Zhong, L.-N. He, Y.-N. Zhao, Q.-W. Song, A.-H. Liu and J.-Q. Wang, *Green Chem.*, 2013, **15**, 2401–2407.
- 62 H. L. Parker, J. Sherwood, A. J. Hunt and J. H. Clark, *ACS Sustainable Chem. Eng.*, 2014, **2**, 1739–1742.
- 63 P. Neubert, S. Fuchs and A. Behr, *Green Chem.*, 2015, **17**, 4045–4052.
- 64 B. Jerome, H. Jens, S. Benjamin, A. Vasyl, V. Sergej, P. Angelika and B. Armin, *Angew. Chem., Int. Ed.*, 2007, **46**, 5971–5974.
- 65 S. Benjamin, A. Vasyl, H. Jens, S. P. Verevkin and B. Armin, *ChemSusChem*, 2008, **1**, 934–940.
- 66 P. J. Cossar, L. Hizartidis, M. I. Simone, A. McCluskey and C. P. Gordon, *Org. Biomol. Chem.*, 2015, **13**, 7119–7130.
- 67 T. N. Glasnov and C. O. Kappe, *Adv. Synth. Catal.*, 2010, **352**, 3089–3097.
- 68 A. R. Muci and S. L. Buchwald, Practical Palladium Catalysts for C-N and C-O Bond Formation, ed. N. Miyaoura, *Cross-Coupling Reactions. Topics in Current Chemistry*, 2002, vol. 219, Springer, Berlin, Heidelberg.
- 69 J. L. Kiplinger, T. G. Richmond and C. E. Osterberg, *Chem. Rev.*, 1994, **94**, 373–431.
- 70 A. P. Phillips, *J. Am. Chem. Soc.*, 1950, **72**, 1850–1852.
- 71 Á. Molnár and A. Papp, *Coord. Chem. Rev.*, 2017, **349**, 1–65.
- 72 M. Oba, *J. Labelled Comp. Radiopharm.*, 2015, **58**, 215–219.
- 73 A. I. Meyers, D. L. Temple, D. Haidukewych and E. D. Mihelich, *J. Org. Chem.*, 1974, **39**, 2787–2793.
- 74 J. R. L. Smith, M. W. Nee, J. B. Noar and T. C. Bruice, *J. Chem. Soc., Perkin Trans., 2*, 1984, 255–260.

## 1. General

All solvents and reagents were of analytical grade and used directly without further purification. 5% Pd/C and 5% Pd/BaSO<sub>4</sub> catalysts used in this study were purchased from Sigma-Aldrich, while D<sub>2</sub>O (>99.9%) was from Merck; HPLC-grade solvents from VWR were used without purification. The propylene carbonate was bought from Acros Organics. The cartridge containing 5% Pd/polymer-based spherical activated carbon (PBSAC) was filled in-house.

## 2. General aspects of the CF deuteration

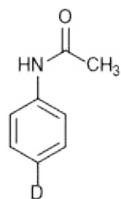
The CF deuteration reactions were carried out in an H-Cube<sup>®</sup> reactor (ThalesNano Inc.) with D<sub>2</sub>O as deuterium source. The catalyst cartridge (with internal dimensions of 30×4 mm) was filled with ca. 100 mg of the heterogeneous hydrogenation catalyst. It was then placed into a thermostat unit controlled by a Peltier system, up to a maximum of 100 °C. The pressure of the system was set by a backpressure regulator to a maximum of 100 bar, and the CF of the solution of the starting material was provided by an HPLC pump (Knauer WellChrom K-120). For the CF reactions, 3 mg mL<sup>-1</sup> solution of the appropriate starting material was prepared in propylene carbonate. The solution was homogenized by sonication for 5 min and then pumped through the CF reactor under the set conditions. A single run was carried out with 100 mg starting material. After the completion of the reaction, the reaction mixture was collected, diluted with water, freeze and lyophilized.

## 3. Product analysis

The products obtained were characterized by NMR spectroscopy. <sup>1</sup>H-NMR and <sup>13</sup>C-NMR spectra were recorded on a Bruker Avance DRX 400 spectrometer, in DMSO-*d*<sub>6</sub> as solvent, at 400.1 MHz. Chemical shifts are expressed in δ and are internally referenced (<sup>1</sup>H NMR: δ 2.50 in DMSO-*d*<sub>6</sub>). Conversion and deuterium incorporation values were determined via the <sup>1</sup>H-NMR spectra of the crude materials. Deuterium contents were determined from the relative intensities of the <sup>1</sup>H-NMR indicator signals. Elemental analyses were performed with a Perkin-Elmer CHNS-2400Ser II Elemental Analyzer.

#### 4. Characterization of products

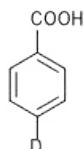
##### *N*-(phenyl-4-<sup>2</sup>H)acetamide (**2**)



White crystals; m.p. 110.2-111.8 °C (data is in agreement with the literature reference: 110-112 °C)<sup>[1]</sup>

<sup>1</sup>H NMR (400 MHz, DMSO-*d*<sub>6</sub>) δ 9.91 (s, 1H), 7.56 (d, *J*=8.2 Hz, 2H), 7.27 (d, *J*=8.2 Hz, 2H), 2.03 (s, 3H); <sup>13</sup>C NMR (100 MHz, DMSO-*d*<sub>6</sub>) δ 168.3, 139.3, 128.6, 123.0, 118.9, 24.0.

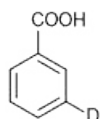
##### Benzoic-4-<sup>2</sup>H acid (**4**)



White crystals; m.p. 119.1-121.4 °C (data is in agreement with the literature reference: 119-121 °C)<sup>[1]</sup>

<sup>1</sup>H NMR (400 MHz, DMSO-*d*<sub>6</sub>) δ 7.94 (d, *J*=7.5 Hz, 2H), 7.50 (d, *J*=7.5 Hz, 2H). <sup>13</sup>C NMR (100 MHz, DMSO-*d*<sub>6</sub>) δ 167.4, 132.9, 130.8, 129.3, 128.6.

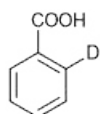
##### Benzoic-3-<sup>2</sup>H acid (**6**)



White crystals; m.p. 119.6-121.3 °C (data is in agreement with the literature reference: 121 °C)<sup>[2]</sup>

<sup>1</sup>H NMR (400 MHz, DMSO-*d*<sub>6</sub>) δ 7.91-7.95 (m, 2H), 7.58-7.62 (m, 1H), 7.47 (t, *J*=8.3 Hz, 1H). <sup>13</sup>C NMR (100 MHz, DMSO-*d*<sub>6</sub>) δ 167.3, 132.9, 130.7, 129.3, 128.6.

##### Benzoic-2-<sup>2</sup>H acid (**8**)

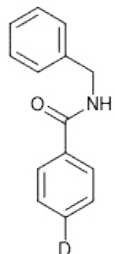


White crystals; m.p. 119.3-121.1 °C (data is in agreement with the literature reference: 121 °C)<sup>[2]</sup>



$^1\text{H}$  NMR (400 MHz,  $\text{DMSO-}d_6$ )  $\delta$  7.94 (d,  $J=7.3$ , 1H), 7.58-7.65 (m, 1H), 7.47-7.54 (m, 1H).  
 $^{13}\text{C}$  NMR (100 MHz,  $\text{DMSO-}d_6$ )  $\delta$  167.3, 132.9, 130.6, 129.2, 128.6.

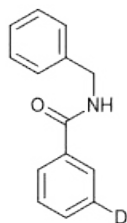
*N*-benzylbenzamide-4- $^2\text{H}$  (**10**)



White crystals; m.p. 104.1-106.2 °C (compound is known,<sup>[3]</sup> but m.p. not published)

$^1\text{H}$  NMR (400 MHz,  $\text{DMSO-}d_6$ )  $\delta$  9.02 (t,  $J=5.3$ , 1H), 7.90 (d,  $J=7.4$ , 2H), 7.47 (d,  $J=7.4$ , 2H), 7.19-7.28 (m, 1H) 7.28-7.37 (m, 4H), 4.49 (d,  $J=5.3$ , 2H).  $^{13}\text{C}$  NMR (100 MHz,  $\text{DMSO-}d_6$ )  $\delta$  166.2, 139.7, 134.3, 130.9, 128.3, 128.2, 127.2, 127.1, 126.7, 42.6.

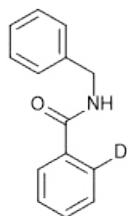
*N*-benzylbenzamide-3- $^2\text{H}$  (**12**)



White crystals; m.p. 104.1-106.2 °C

$^1\text{H}$  NMR (400 MHz,  $\text{DMSO-}d_6$ )  $\delta$  9.04 (t,  $J=5.3$ , 1H), 7.87-7.92 (m, 2H), 7.44-7.56 (m, 2H), 7.19-7.28 (m, 1H) 7.28-7.37 (m, 4H), 4.49 (d,  $J=5.3$ , 2H).  $^{13}\text{C}$  NMR (100 MHz,  $\text{DMSO-}d_6$ )  $\delta$  166.2, 139.7, 134.3, 131.1, 128.3, 128.2, 128.0, 127.2, 127.1, 127.1, 126.7, 42.6.  $\text{C}_{14}\text{H}_{12}\text{DNO}$  (212.11): C, 79.22, H, 6.65, N, 6.60; found C, 79.31, H, 6.61, N, 6.71.

*N*-benzylbenzamide-2- $^2\text{H}$  (**14**)



White crystals; m.p. 104.1-106.2 °C

$^1\text{H}$  NMR (400 MHz,  $\text{DMSO-}d_6$ )  $\delta$  9.05 (t,  $J=5.3$ , 1H), 7.88 (d,  $J=7.4$ , 1H), 7.43-7.56 (m, 3H), 7.19-7.28 (m, 1H) 7.28-7.37 (m, 4H), 4.48 (d,  $J=5.3$ , 2H).  $^{13}\text{C}$  NMR (100 MHz,  $\text{DMSO-}d_6$ )  $\delta$

166.4, 139.8, 134.3, 131.4, 128.5, 128.4, 128.3, 127.3, 127.3, 127.0, 126.9 42.6. C<sub>14</sub>H<sub>12</sub>DNO  
(212.11): C, 79.22, H, 6.65, N, 6.60; found C, 79.29, H, 6.64, N, 6.73.

## 5. $^1\text{H}$ NMR spectra

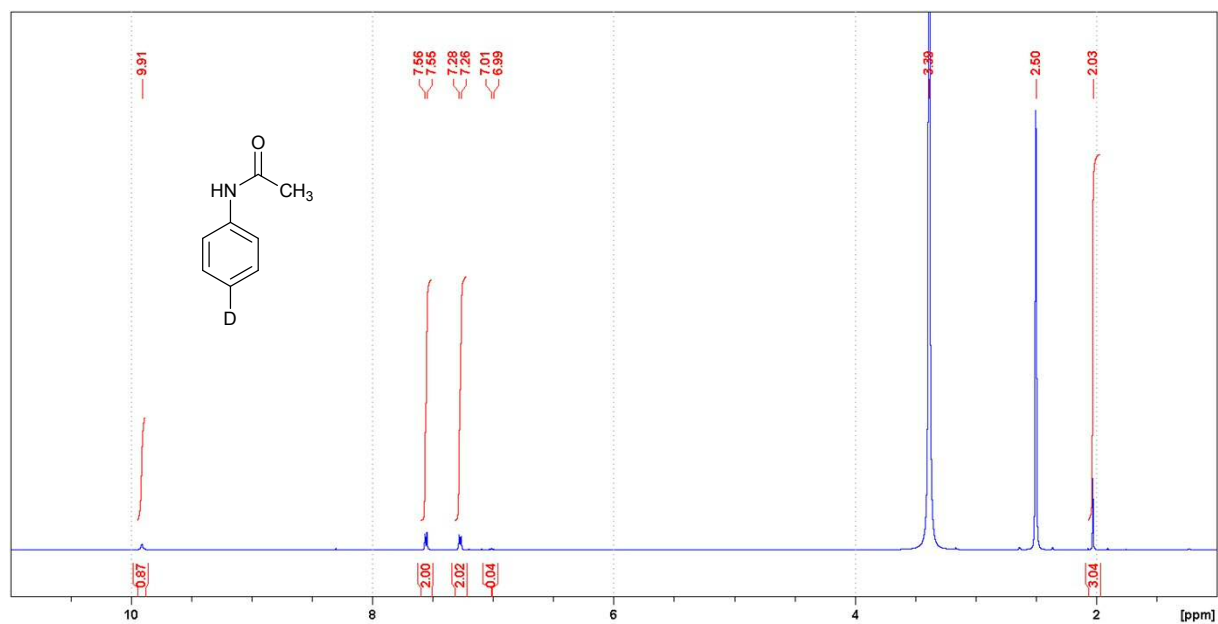


**Figure S1.**  $^1\text{H}$  NMR spectrum of **2** measured in  $\text{DMSO-}d_6$  at 303 K.

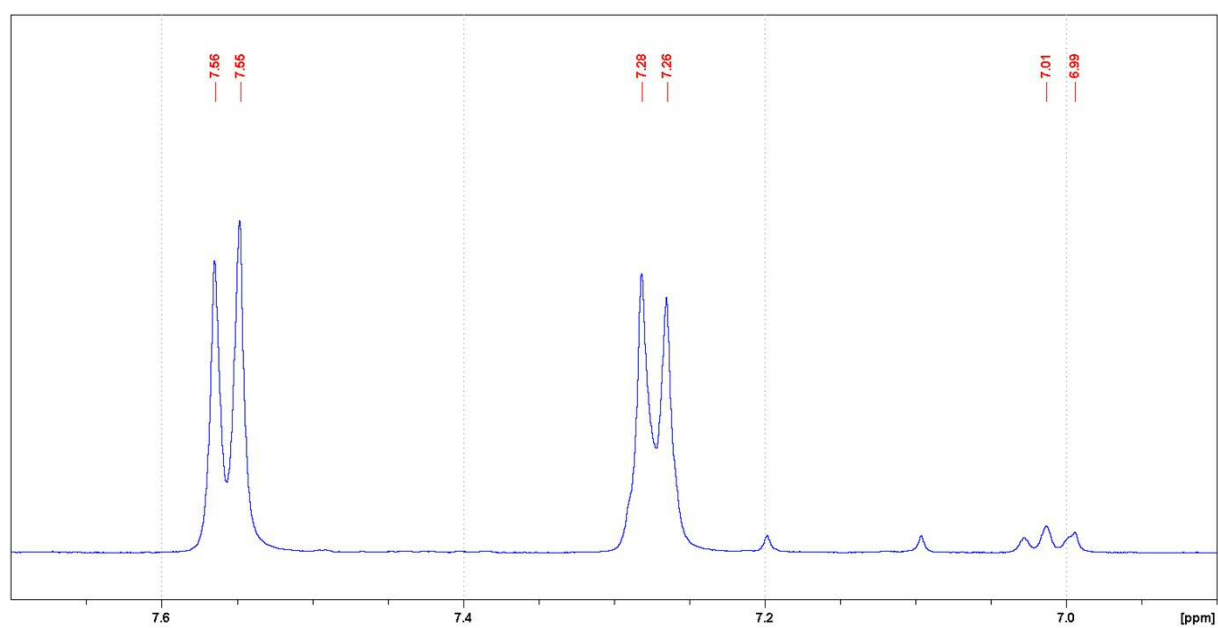


**Figure S2.**  $^1\text{H}$  NMR spectrum of **2** measured in  $\text{DMSO-}d_6$  at 303 K (aromatic section).

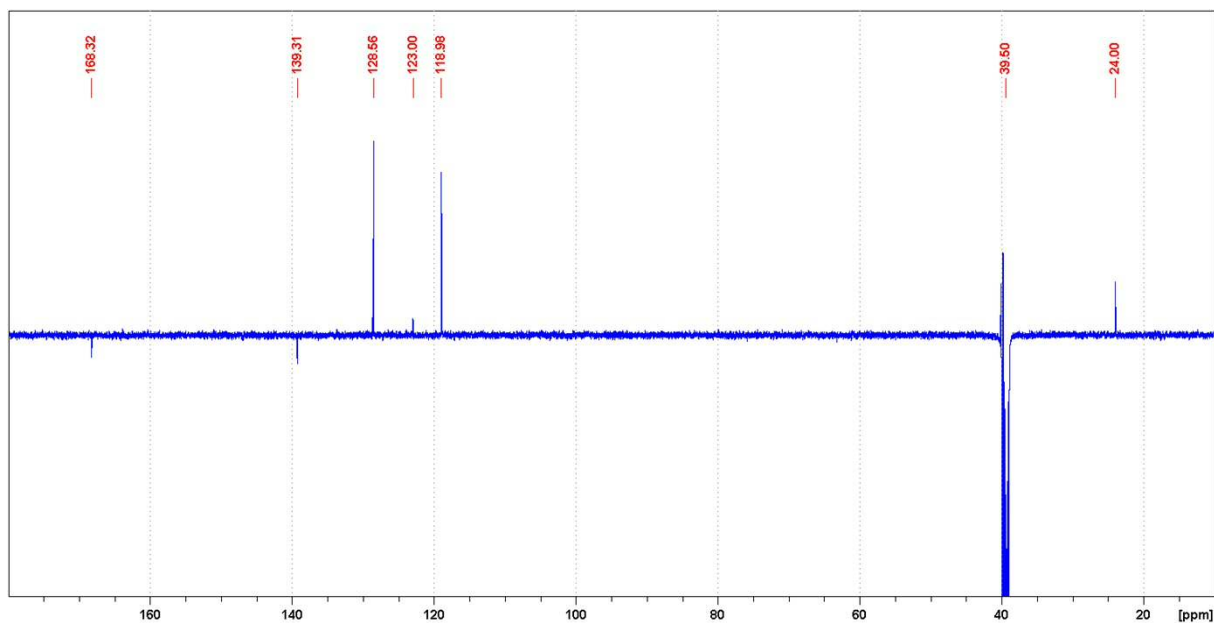


**Figure S3.** APT NMR spectrum of **2** measured in DMSO- $d_6$  at 303 K.

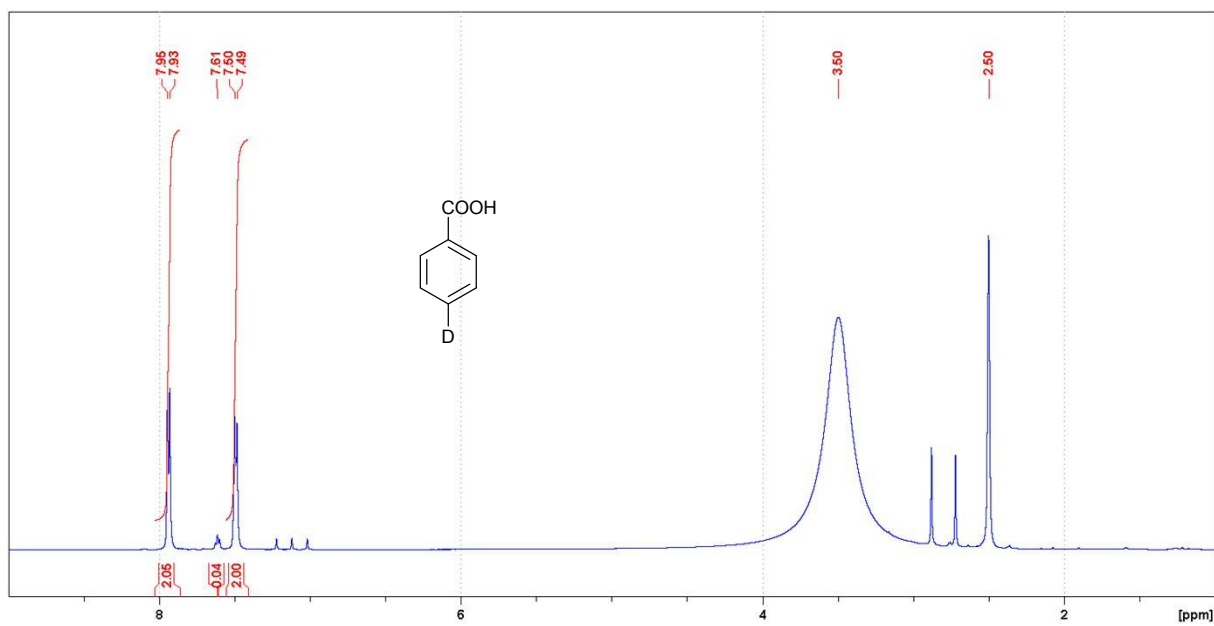


**Figure S4.**  $^1\text{H}$  NMR spectrum of **4** measured in DMSO- $d_6$  at 303 K.

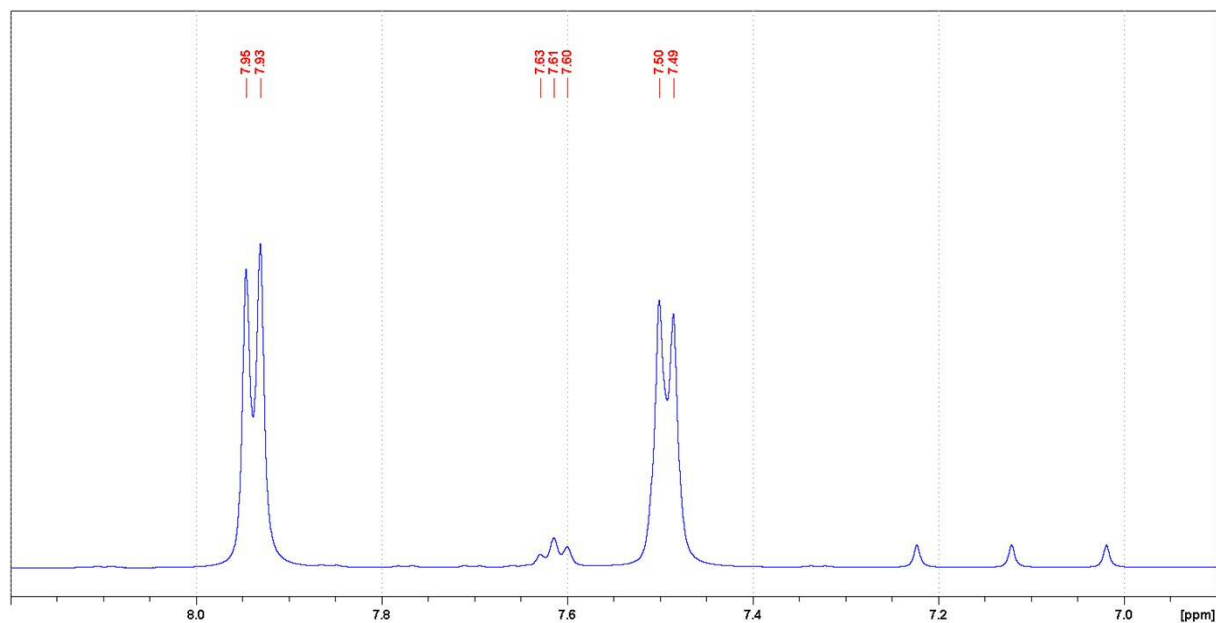


**Figure S5.**  $^1\text{H}$  NMR spectrum of **4** measured in  $\text{DMSO-}d_6$  at 303 K (aromatic section).

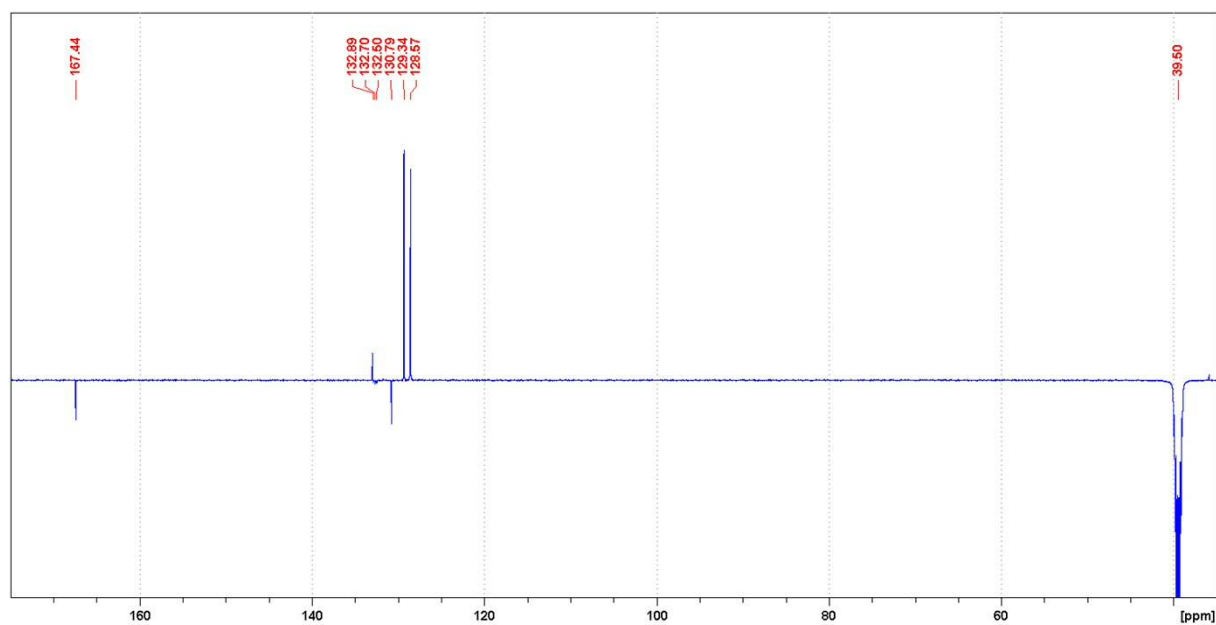


**Figure S6.** APT NMR spectrum of **4** measured in  $\text{DMSO-}d_6$  at 303 K.

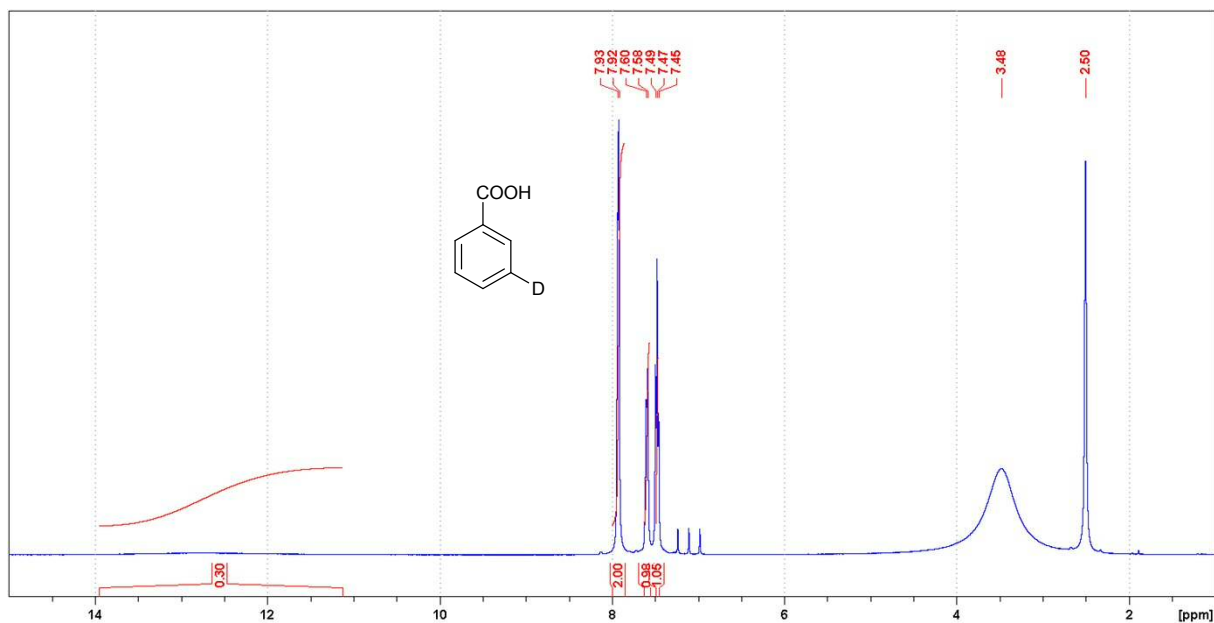


**Figure S7.**  $^1\text{H}$  NMR spectrum of **6** measured in  $\text{DMSO-}d_6$  at 303 K.

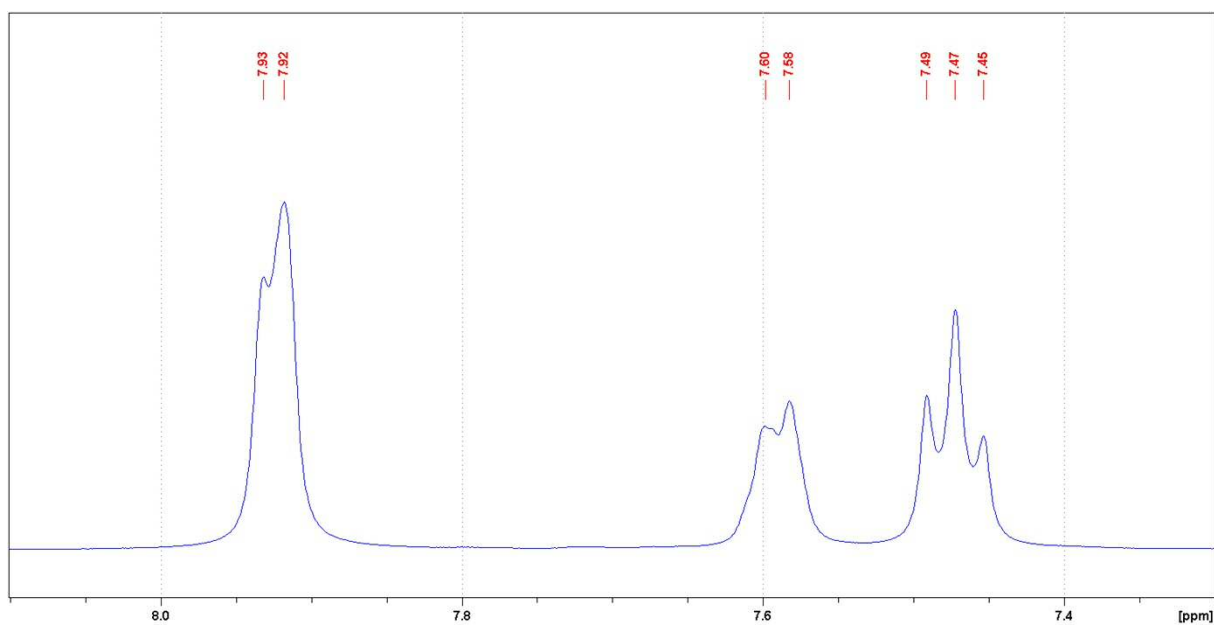


**Figure S8.**  $^1\text{H}$  NMR spectrum of **6** measured in  $\text{DMSO-}d_6$  at 303 K (aromatic section).

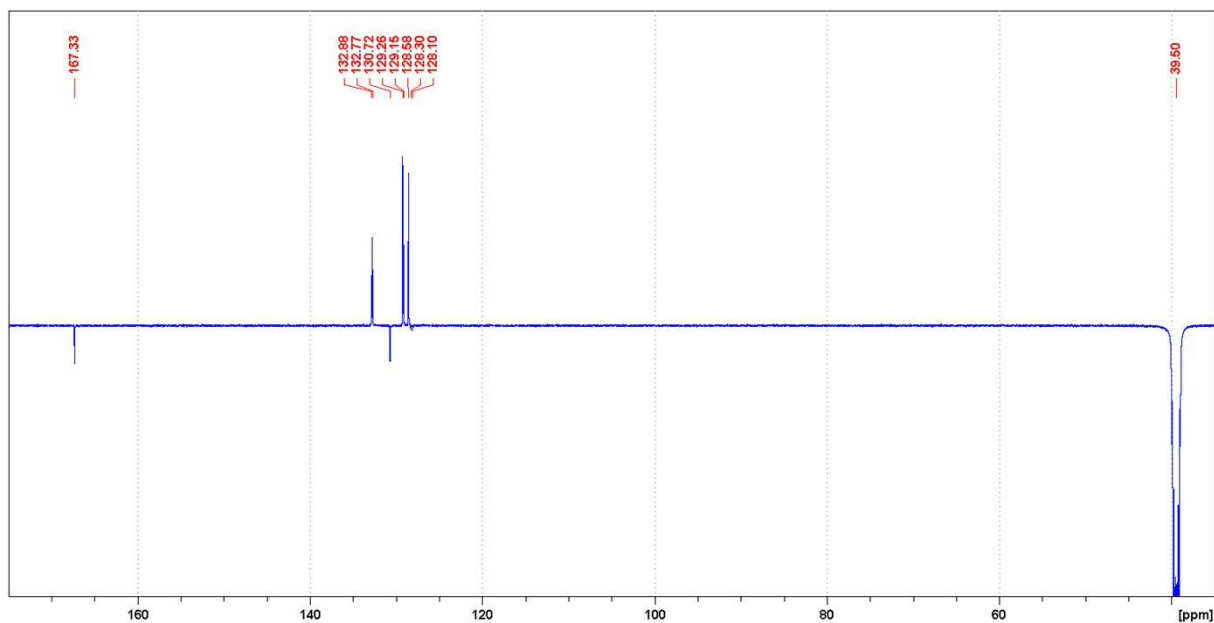


**Figure S9.** APT NMR spectrum of **6** measured in DMSO- $d_6$  at 303 K.

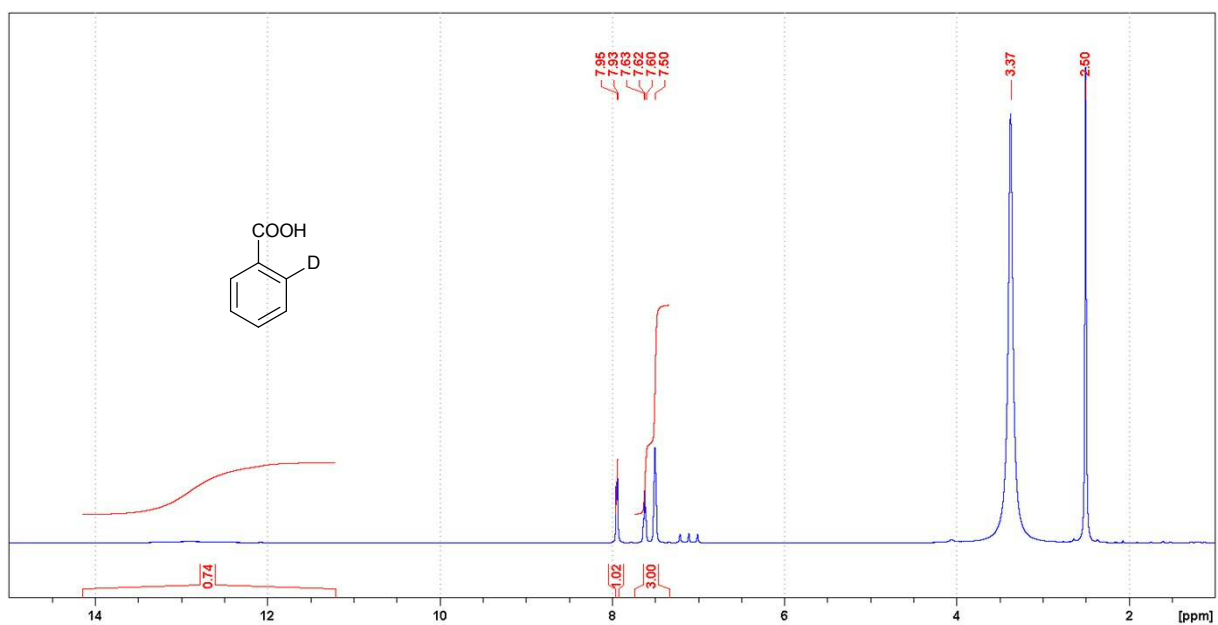


**Figure S10.**  $^1\text{H}$  NMR spectrum of **8** measured in DMSO- $d_6$  at 303 K.

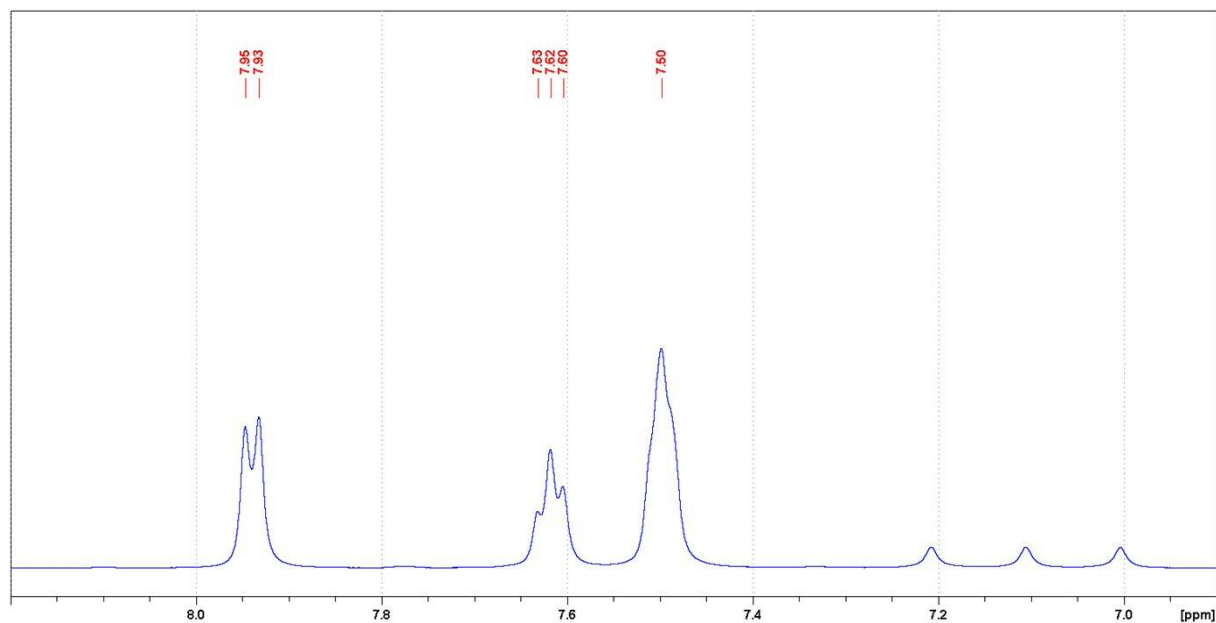


**Figure S11.** <sup>1</sup>H NMR spectrum of **8** measured in DMSO-*d*<sub>6</sub> at 303 K (aromatic section).

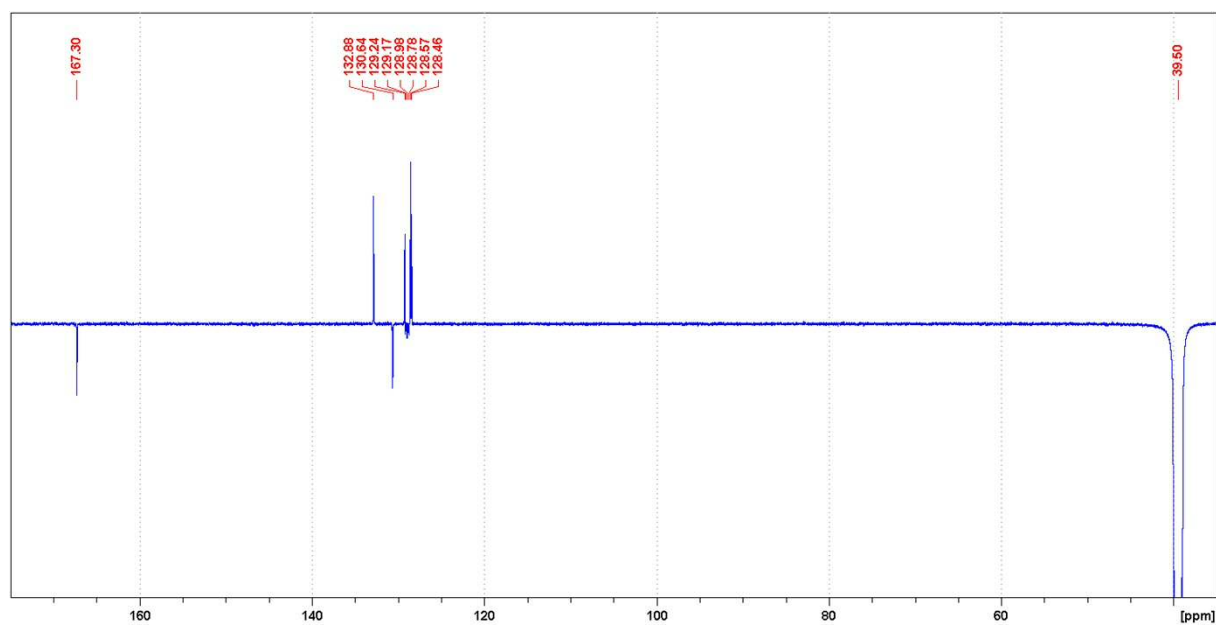


**Figure S12.** APT NMR spectrum of **8** measured in DMSO-*d*<sub>6</sub> at 298 K.



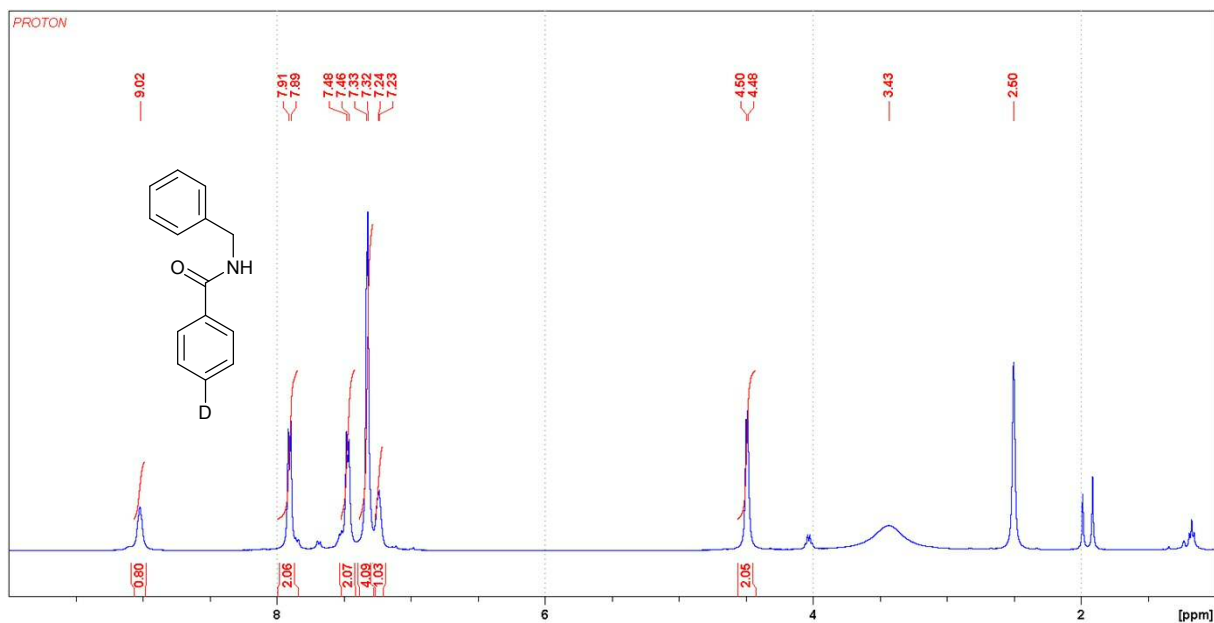


**Figure S13.**  $^1\text{H}$  NMR spectrum of **10** measured in  $\text{DMSO-}d_6$  at 303 K.

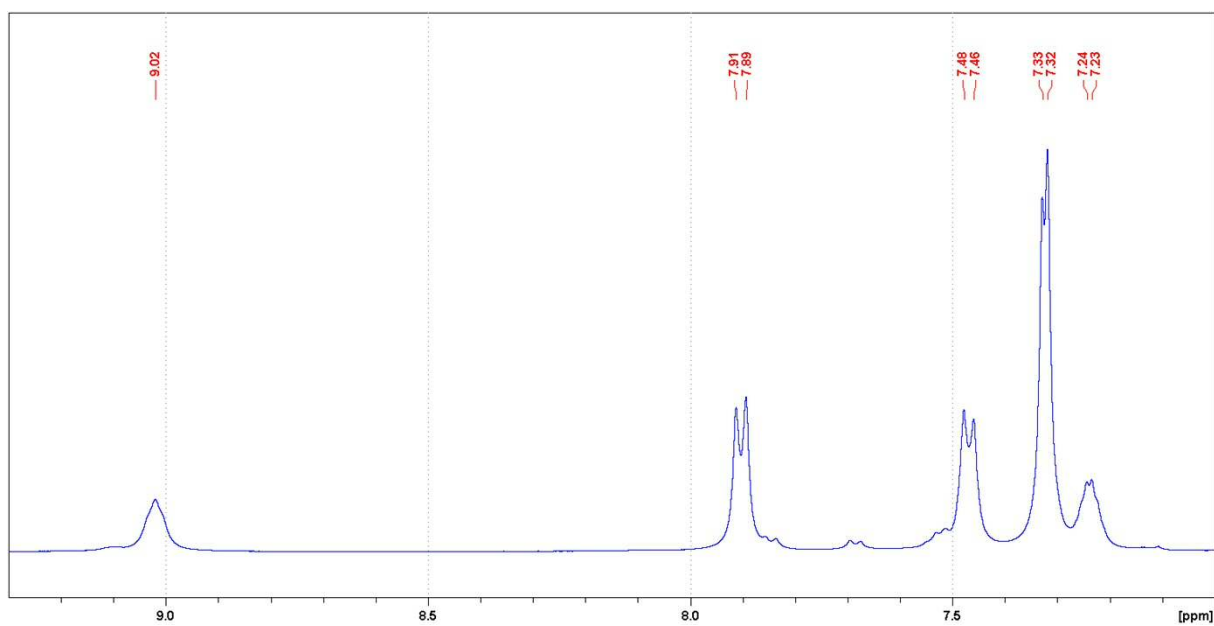


**Figure S14.**  $^1\text{H}$  NMR spectrum of **10** measured in  $\text{DMSO-}d_6$  at 303 K (aromatic section).

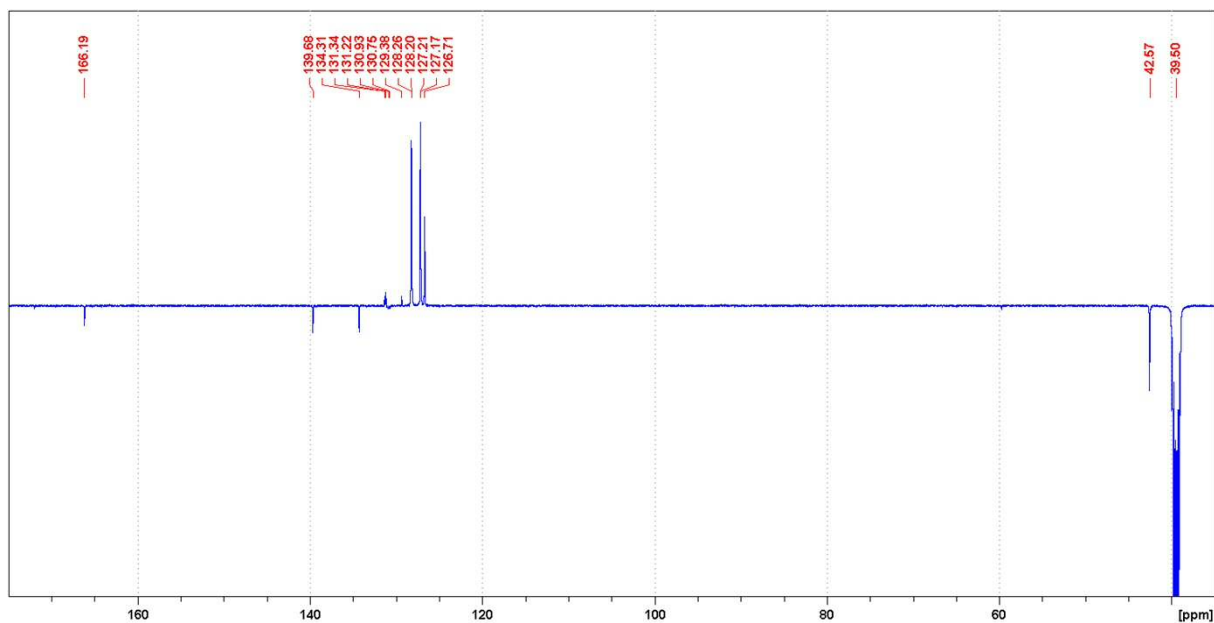


**Figure S15.** APT NMR spectrum of **10** measured in DMSO- $d_6$  at 303 K.

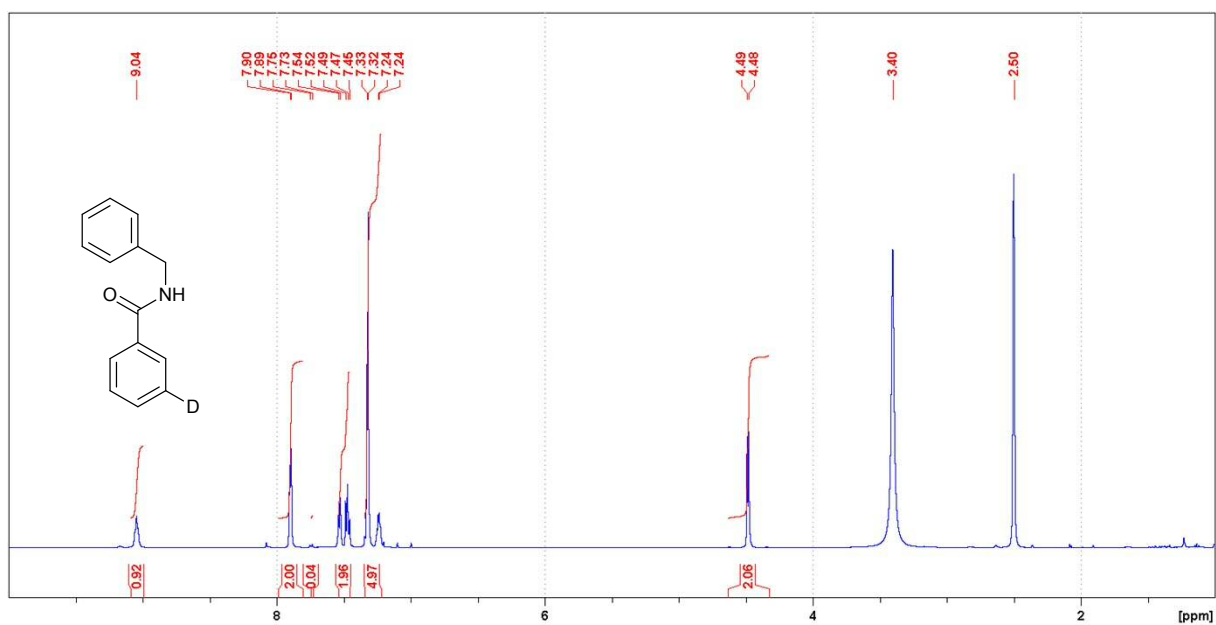


**Figure S16.**  $^1\text{H}$  NMR spectrum of **12** measured in DMSO- $d_6$  at 303 K.

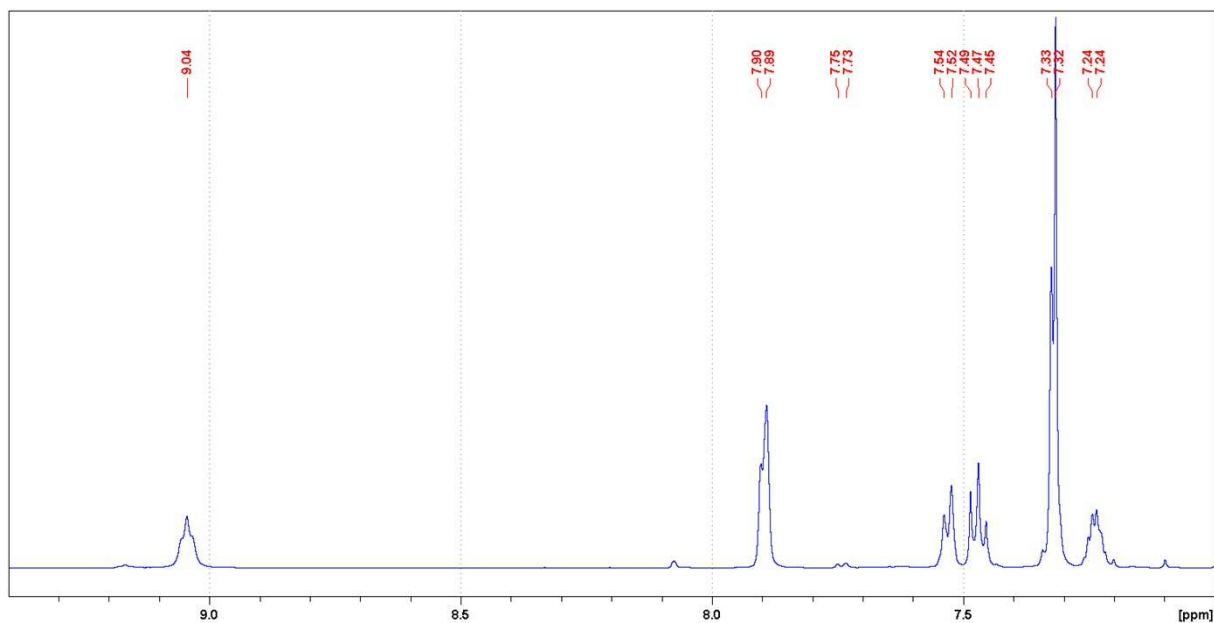


**Figure S17.**  $^1\text{H}$  NMR spectrum of **12** measured in  $\text{DMSO-}d_6$  at 303 K (aromatic section).

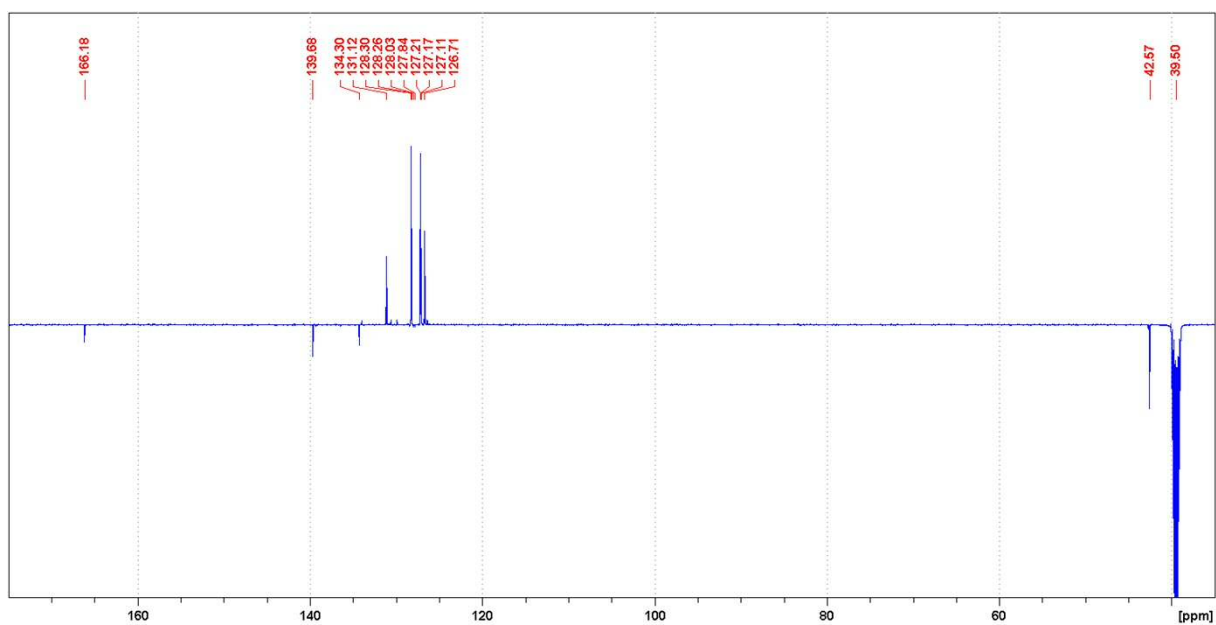


**Figure S18.** APT NMR spectrum of **12** measured in  $\text{DMSO-}d_6$  at 303 K.

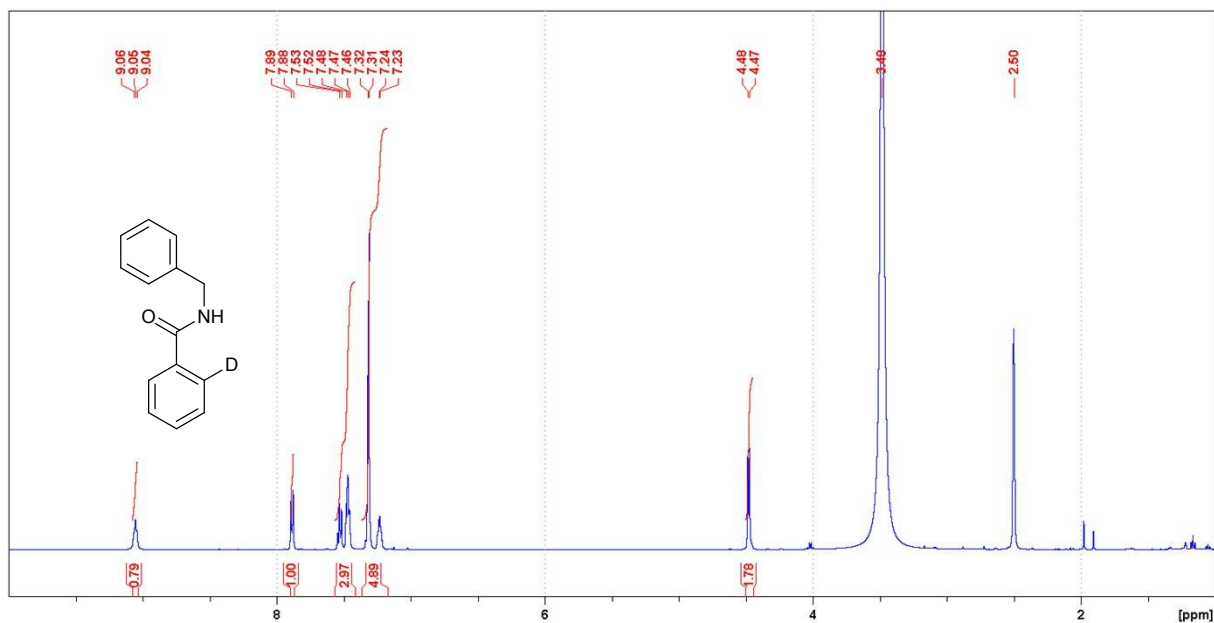


**Figure S19.**  $^1\text{H}$  NMR spectrum of **14** measured in  $\text{DMSO-}d_6$  at 303 K.

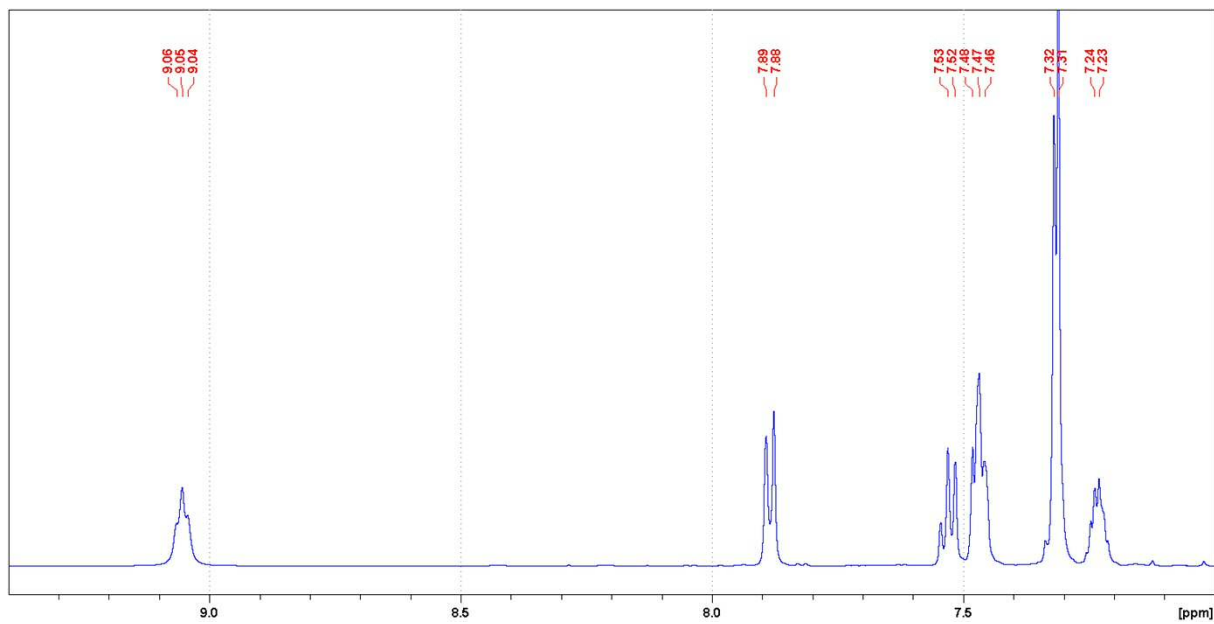


**Figure S20.**  $^1\text{H}$  NMR spectrum of **14** measured in  $\text{DMSO-}d_6$  at 303 K (aromatic section).

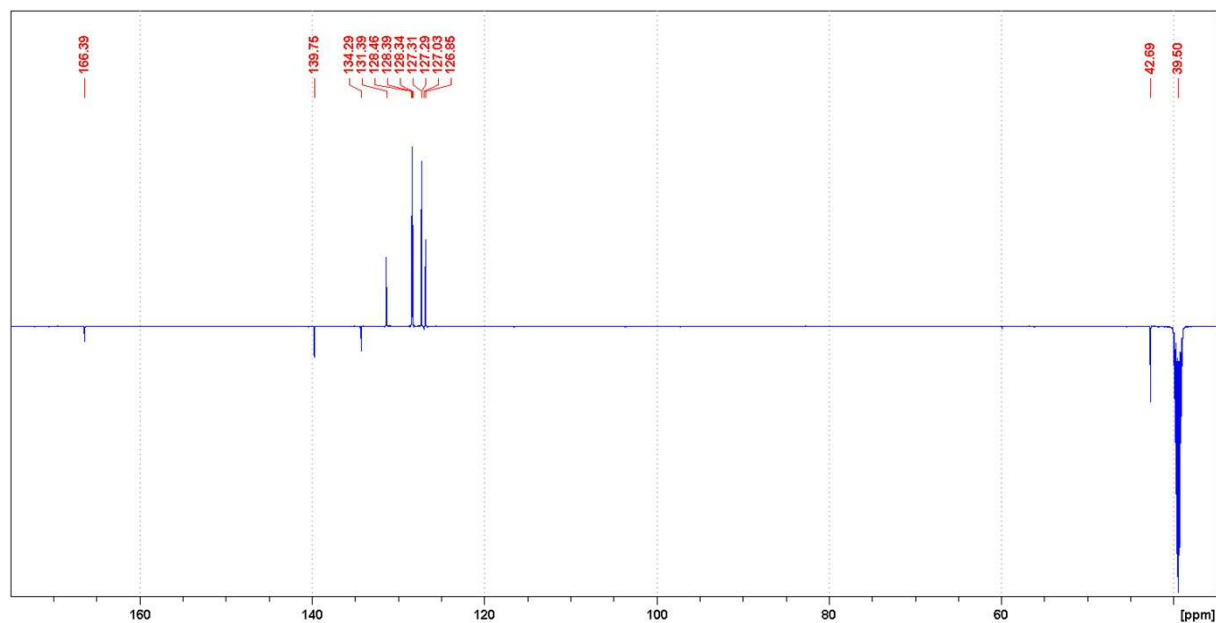




**Figure S21.** APT spectrum of **14** measured in DMSO-*d*<sub>6</sub> at 303 K.

- [1] M. Oba, *J. Lab. Comp. Radiopharm.* **2015**, *58*, 215-219.
- [2] A. I. Meyers, D. L. Temple, D. Haidukewych, E. D. Mihelich, *J. Org. Chem.* **1974**, *39*, 2787-2793.
- [3] J. R. L. Smith, M. W. Nee, J. B. Noar, T. C. Bruice, *J. Chem. Soc. Perkin Transact. 2* **1984**, 255-260.

**II**

Article

# N-Acetylation of Amines in Continuous-Flow with Acetonitrile—No Need for Hazardous and Toxic Carboxylic Acid Derivatives

György Orsy<sup>1,2</sup>, Ferenc Fülöp<sup>1,3,\*</sup>  and István M. Mándity<sup>2,4,\*</sup> 

<sup>1</sup> Institute of Pharmaceutical Chemistry, University of Szeged, Eötvös u. 6, H-6720 Szeged, Hungary; orsy.gyorgy@ttk.hu

<sup>2</sup> MTA TTK Lendület Artificial Transporter Research Group, Institute of Materials and Environmental Chemistry, Research Center for Natural Sciences, Hungarian Academy of Sciences, Magyar Tudosok krt. 2, 1117 Budapest, Hungary

<sup>3</sup> Research Group of Stereochemistry of the Hungarian Academy of Sciences, Dóm tér 8, H-6720 Szeged, Hungary

<sup>4</sup> Department of Organic Chemistry, Faculty of Pharmacy, Semmelweis University, Hőgyes Endre u. 7, H-1092 Budapest, Hungary

\* Correspondence: fulop@pharm.u-szeged.hu (F.F.); mandity.istvan@ttk.mta.hu (I.M.M.); Tel.: +36-1-3826-616 (I.M.M.)

Academic Editor: Maurizio Benaglia

Received: 25 March 2020; Accepted: 21 April 2020; Published: 23 April 2020



**Abstract:** A continuous-flow acetylation reaction was developed, applying cheap and safe reagent, acetonitrile as acetylation agent and alumina as catalyst. The method developed utilizes milder reagent than those used conventionally. The reaction was tested on various aromatic and aliphatic amines with good conversion. The catalyst showed excellent reusability and a scale-up was also carried out. Furthermore, a drug substance (paracetamol) was also synthesized with good conversion and yield.

**Keywords:** flow chemistry; acetylation; acetonitrile; safe; green chemistry

## 1. Introduction

N-acetylation is a widely used chemical reaction in general organic chemistry to build an acetyl functional group on an amine compound [1–4]. The use of the acetyl functional group is widespread, including drug research, the preparation of pharmaceuticals, polymer chemistry and agrochemical applications [5–10]. It can be utilized as a protecting group in many organic reactions and also in peptide synthesis [11]. In addition, it plays a major regulatory role in post-translational protein modification and regulation of DNA expression in all life forms [12,13].

In general, common acetylation reagents such as acetic anhydride and acetyl chloride, are easily accessible in chemical laboratories. Even the most sustainable technologies utilize these reagents in combination with various Lewis acids [14–16] and/or in neat form [17]. Nevertheless, the utilization of acetic anhydride and acetyl chloride have various drawbacks. Both reagents are major irritants and acetyl chloride is considered to be a genotoxic agent [18]. As such, the elimination of their use is of considerable current interest.

Flow chemistry technology is widely used in many synthetic organic reactions at both laboratory and industrial scale [19–35]. There are a number of benefits of using continuous-flow (CF) chemistry. A wide range of reactions are much faster in flow processes, and fewer substrates and reagents are required [36–40]. Furthermore, more efficient and selective reaction can be carried out in continuous systems than in regular batch operations [41–46]. Additionally, flow reaction conditions can enable

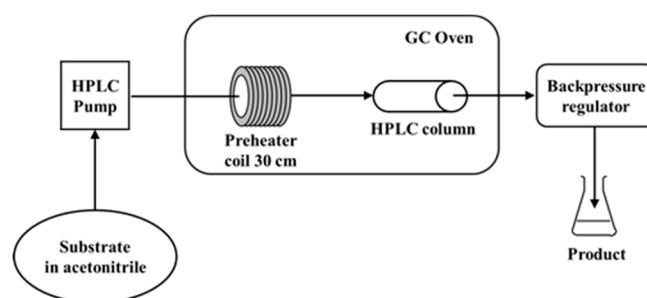
reaction routes that would otherwise only be feasible under regular batch conditions, e.g., higher temperature and pressure than can be used under safe conditions [47–57].

Whilst acetonitrile is a common solvent and is generally used in various fields of chemistry as eluent [41] and polar aprotic organic solvent [58], it is rarely used as reagent in organic chemistry. A few studies on acetonitrile as an acylation agent have been reported [59–64] thus far, for example Saikia et al., [65] presenting an unusual attempt to synthesize *N*-acylated aromatic amines. Acetonitrile was utilized as reagent and solvent with several Lewis acids (e.g.,  $\text{Cu}(\text{OAc})_2$ ,  $\text{Mn}(\text{OAc})_2$ ,  $\text{FeCl}_3$ ,  $\text{InCl}_3$ ). The most promising catalyst was the trimethylsilyl iodide (TMSI), which activated the acetonitrile by co-ordination. On the other hand, Brahmayya et al. [66] developed a new method for preparing *N*-acetamides with metal-free sulfonated reduced graphene oxide catalyst under sonication.

Herein, we present the efficient utilization of acetonitrile for acetylation. We describe a selective and environmentally friendly CF acetylation of aromatic and aliphatic amines by the use of a low-cost and environmentally friendly Lewis acid catalyst as alumina in acetonitrile solvent with excellent conversions. These observations may open a new and green procedure for the synthesis of acetylated aromatic and aliphatic amines.

## 2. Results and Discussion

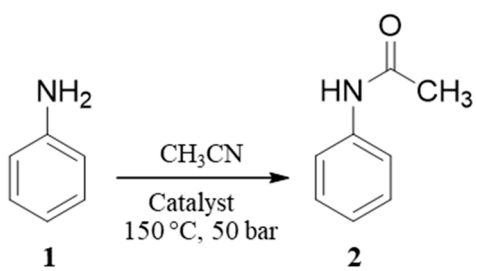
The reactions were carried out in a home-made CF reactor (See Supplementary Material Figure S23). Our equipment consists of an HPLC pump that transports the substrate dissolved in acetonitrile. The solution is feed into a fillable HPLC column where the reaction occurs. The column is filled with solid catalyst. Additionally, there is a GC oven and an in-line back pressure regulator in the system to control the temperature and pressure of the reaction. A schematic outline of the reactor used in this study is shown in Figure 1.



**Figure 1.** Schematic representation of the reactor used in the study.

In order to find the most useful solid Lewis acid catalyst for the flow synthesis, a reagent screen was carried out. Aniline, as a test compound was utilized, and acetonitrile was used both as solvent and acyl donor. The complete study of Lewis acids is shown in Table 1. The study shows that the most promising Lewis acid was the aluminum(III) oxide, other catalysts offered lower yields or no amide product formation was observed. Thus, the further reaction parameter optimization was carried out with aluminum(III) oxide as solid catalyst.



**Table 1.** Lewis acids screen in continuous-flow (CF) acetylation.


Entry	Lewis Acids	Solvent	Conversion (%)
1	Fe <sub>2</sub> O <sub>3</sub>	Acetonitrile	0
2	Boric acid	Acetonitrile	3
3	AlCl <sub>3</sub>	Acetonitrile	19
4	Al <sub>2</sub> O <sub>3</sub>	Acetonitrile	64

Conditions: 150 °C, 50 bar, 0.1 mL min<sup>-1</sup>, 27 min residence time in flow synthesis.

The starting material was dissolved in acetonitrile in a concentration of 100 mM, using aluminum(III) oxide powder as catalyst at a temperature of 25 °C and a pressure of 10–100 bar with 0.1 mL min<sup>-1</sup> flow rate and 27 min residence time. The reaction did not show any pressure dependency and a moderate conversion of 27% was observed without any real pressure dependence. The effect of temperature on the conversion rate was tested at 50 bar pressure. Raising the temperature to 100 °C initiated the product formation with 53% conversion. By applying a higher temperature, the conversion of the reaction improved remarkably. It was found that the optimal temperature is 200 °C. Further increase of the temperature resulted in lower conversion values. In this case, the acetonitrile was in its supercritical state ( $T_c = 275$  °C,  $P_c = 48$  bar) due to the significant solvent expansion produced under supercritical conditions. This is a likely explanation of the decrease of the observed yield above 275 °C. The results obtained for the temperature dependence are summarized in (Figure 2a). The effect of pressure on reaction outcome was also tested (Figure 2b). The results indicate that a modest pressure (50 bar) is needed to increase the reaction conversion, while further pressure increase did not influence the reaction outcome significantly. The flow rate was tested too (Figure 2c). The results show that the optimum flow rate is 0.1 mL min<sup>-1</sup>. Any increase in the flow rate above this value resulted in decreased conversion. The effect of concentration on the reaction outcome was also tested (Figure 2d). The results show that increased concentration results in the decreased conversion.

Under the optimized conditions, the scope of the reaction was explored by a variety of aniline derivatives (Table 2). The anilines containing either electron-donating or electron-withdrawing groups were selected. It must be noted that all reactions were carried out in a single run and the products were analyzed by <sup>1</sup>H and <sup>13</sup>C NMR spectroscopy. Column chromatography purification of the product was only needed for compound 6. For the others, only a simple evaporation of acetonitrile was required.

Importantly, the hydroxyl group possessing aniline 3 was acetylated with excellent yield and the drug substance paracetamol 4 with quantitative yield after a simple recrystallization. Lower yield was observed for 4-methoxyaniline (5), and the acetylated product was isolated after column chromatography with a mere 51% yield. For the halogen atom possessing anilines (7, 9 and 11) excellent yields were achieved. For nitroanilines (13,15 and 17) no conversion was observed and only the starting material was isolated. This fact might be explained by the highly electron-withdrawing nature of the nitro substituent, which reduces the nucleophilicity of the amino group. Besides aromatic amines, aliphatic primary and secondary amines were also tested. The primary benzylic amine (23) was converted to the corresponding acetamide with excellent yield. When secondary amine piperidine (19) and morpholine (21) were tested, the acetylated derivatives (20, 22) were isolated with quantitative yields. The use of this reaction in stereoselective reaction was also tested with acetylation reaction carried out for the two enantiomers of 1-phenylethanamine (25 and 27). For both enantiomers the acetylated derivative was achieved with quantitative yield and the complete retention

of the enantiomeric purity. This was investigated by optical rotation and was found to be identical to literature data.

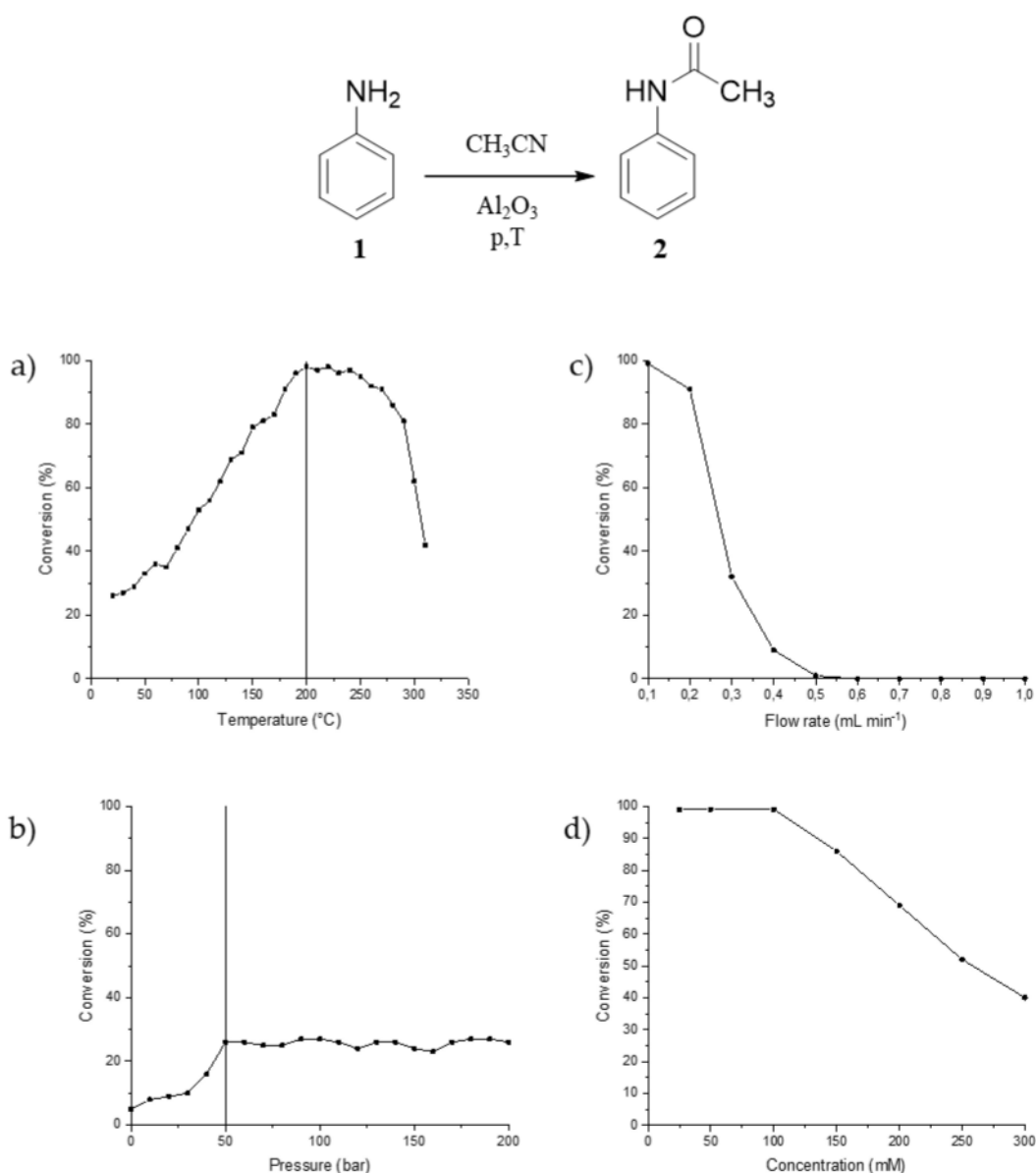


**Figure 2.** The effect of temperature (a), pressure (b), flow rate (c) and concentration (d) on the reaction conversion catalyzed by Al<sub>2</sub>O<sub>3</sub>. The effect of the pressure was measured at room temperature and the effect of temperature was determined at 50 bar, while the effect of the flow rate and concentration was analyzed at the optimized conditions.

The catalyst reusability was also tested. It was an important finding that the activity of the catalyst did not decrease significantly until 10 cycles and one cycle was carried out with 20 mg of benzylamine. This excellent result [67] opened the way to scale up the reaction, which was tested with the same reaction. The acetylation process could be scaled up to 2 g of benzylamine without significant decrease of the conversion. The product (*N*-benzylacetamide, **24**) was isolated with 94% yield after a simple recrystallization. The reaction was completed within 28 hours. This is considerably faster than what has been reported with already known technologies. Results are shown in Figure 3.

**Table 2.** Results of the acetylation of various amines obtained at the optimal conditions: 200 °C, 50 bar, 0.1 mL min<sup>-1</sup> flow rate, 27 min residence time.

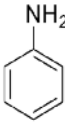
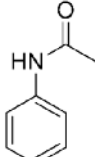
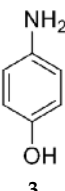
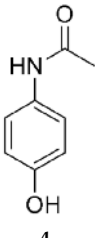
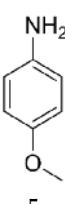
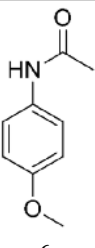
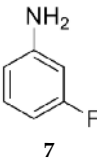
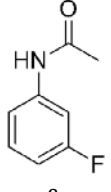
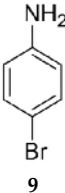
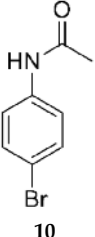
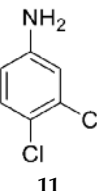
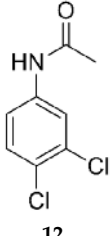
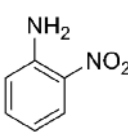
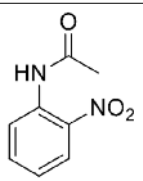
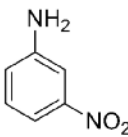
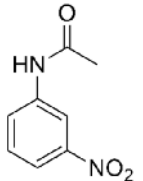
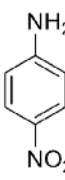
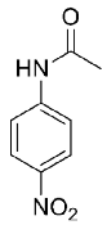
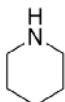
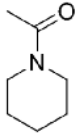
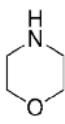
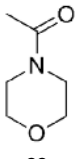
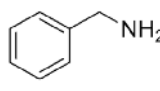
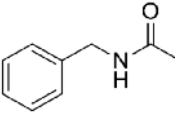
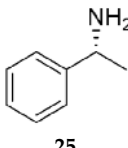
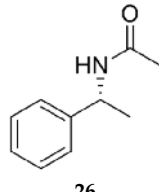
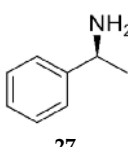
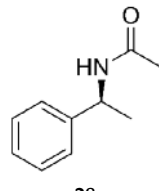
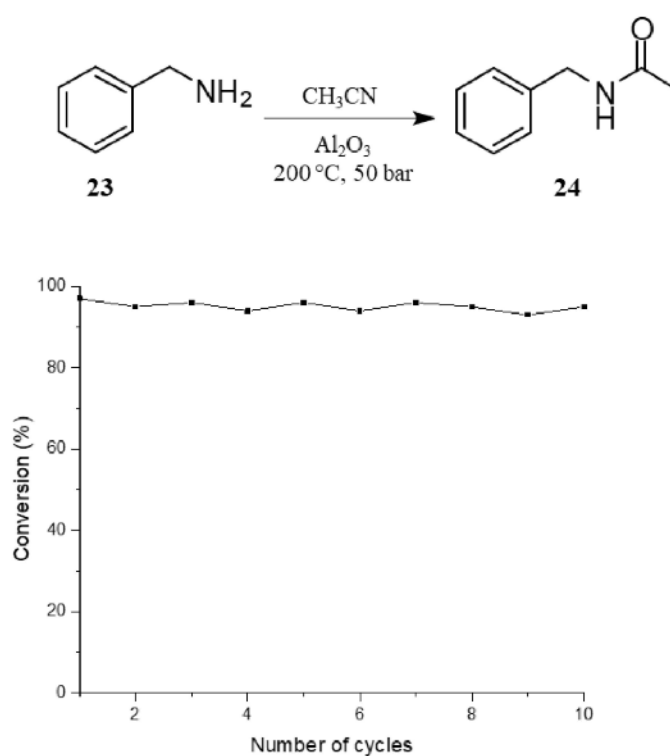
Entry	Substrate	Product	Yield (%)	Space Time Yield (mol kg <sup>-1</sup> h <sup>-1</sup> )
1	 1	 2	> 99	1.5
2	 3	 4	93	1.395
3	 5	 6	51	0.765
4	 7	 8	> 99	1.5
5	 9	 10	> 99	1.5
6	 11	 12	95	1.425

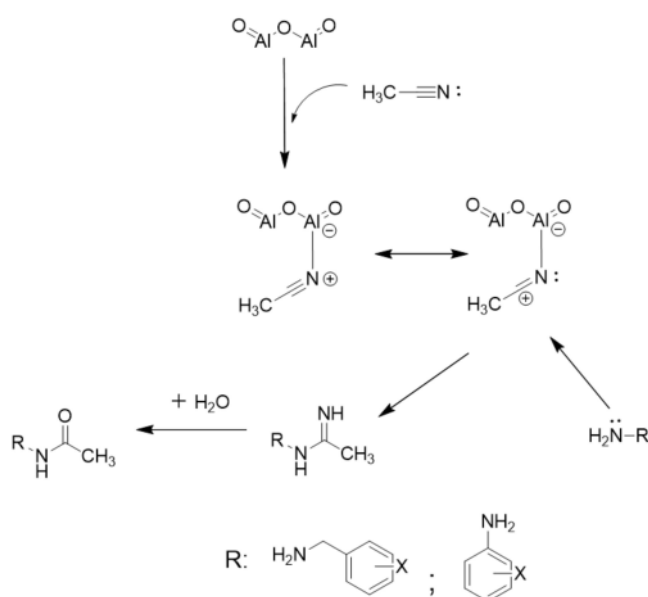
Table 2. Cont.

Entry	Substrate	Product	Yield (%)	Space Time Yield (mol kg <sup>-1</sup> h <sup>-1</sup> )
7	 13	 14	0	0
8	 15	 16	0	0
9	 17	 18	0	0
10	 19	 20	> 99	1.5
11	 21	 22	> 99	1.5
12	 23	 24	> 99	1.5
13	 25	 26	> 99	1.5
14	 27	 28	> 99	1.5



**Figure 3.** Robustness of the acetylation investigated in the reaction of benzylamine. The same reaction was repeated 10 times on the same catalyst.

These results can be explained by the proposed reaction mechanism (Scheme 1) which relies on literature data [63–66]. A key step is the coordination of the lone electron pair of the nitrogen atom of the cyanide group, which yields a positive charge. Due to mesomeric structures, the positive charge might be localized on the carbon atom of the cyanide group. This positively charged carbon atom might be attacked by the lone pair electron of the amine yielding amidine, which is further hydrolyzed to provide the acetamide as shown in Scheme 1. The origin of the water is the residual water content of the solvent and the alumina. The addition of extra amount of water decreased the conversion of the reaction.



**Scheme 1.** The suspected reaction mechanism of acetylation.

### 3. Materials and Methods

#### 3.1. General

All solvents and reagents were of analytical grade and used directly without further purification. Fe<sub>2</sub>O<sub>3</sub>, Boric acid, AlCl<sub>3</sub>, Al<sub>2</sub>O<sub>3</sub> (for chromatography, activated, neutral, Brockmann I, 50–200 μm, 60 A) catalysts used in this study were purchased from Sigma-Aldrich (Budapest, Hungary), while Acetonitrile (100, 0%) was HPLC LC MS-grade solvents from VWR International (Debrecen, Hungary).

#### 3.2. General Aspects of the CF Acetylation

The CF acetylation reactions were carried out in a home-made flow reactor consisting of an HPLC pump (Jasco PU-987 Intelligent Prep. Pump), a stainless steel HPLC column as catalyst bed (internal dimensions 250mm L × 4.6 ID ×  $\frac{1}{4}$  in OD), a stainless steel preheating coil (internal diameter 1 mm and length 30 cm) and a commercially available backpressure regulator (Thalesnano back pressure module 300™, Budapest, Hungary, to a maximum of 300 bar). Parts of the system were connected with stainless steel tubing (internal diameter 1 mm). The HPLC column was charged with 4 g of the alumina catalyst. It was then placed into a GC oven unit (Carlo Erba HR 5300 up to maximum 350 °C). For the CF reactions, 100 mM solution of the appropriate starting material was prepared in acetonitrile. The solution was homogenized by sonication for 5 min and then pumped through the CF reactor under the set conditions. After the completion of the reaction, the reaction mixture was collected and the rest solvent was evaporated by a vacuum rotary evaporator.

#### 3.3. Product Analysis

The products obtained were characterized by NMR spectroscopy. <sup>1</sup>H-NMR and <sup>13</sup>C-NMR spectra were recorded on a Bruker Avance DRX 400 spectrometer (Bruker AVANCE, Billerica, MA, USA), in DMSO-*d*<sub>6</sub> as solvent, at 400.1 MHz. Chemical shifts (δ) are expressed in ppm and are internally referenced (<sup>1</sup>H NMR: 2.50 ppm in DMSO-*d*<sub>6</sub>). Conversion was determined via the <sup>1</sup>H-NMR spectra of the crude materials. A PerkinElmer 341 polarimeter (PerkinElmer, Boston, MA, USA) was used for the determination of optical rotations.

### 4. Conclusions

We have developed a sustainable CF process for the selective N-acetylation of various amines. The obtained chemical process is time and cost efficient, as it utilizes cheap reagent and catalyst and considerably faster with a residence time of only 27 min. Importantly, the well-known, cheap and non-toxic Lewis acid alumina was used as catalyst. Moreover, the acetylation reagent was acetonitrile, which is an industrial side-product with a modest price and it is considerably milder than those for the regular carboxylic acid derivatives used for acetylation, e.g., acetyl chloride, acetic anhydride. In general, under the optimized conditions good or excellent conversions were observed for the aromatic amines, except for the nitro substituted compounds, where no conversion was reached. Importantly, the painkiller drug substance paracetamol was gained with high yield. Mainly complete conversions were also observed for primary and secondary aliphatic amines. The use of this acetylation in stereoselective reactions was also tested and during the course of the reaction no racemization was observed for either enantiomer of enantiomerically pure 1-phenylethylamine.

**Supplementary Materials:** The following are available online, general experimental data, NMR spectra, image of the reactor used.

**Author Contributions:** Conceptualization, I.M.M. and F.F.; Investigation, G.O.; Supervision, I.M.M. and F.F.; Writing—Original draft, G.O.; Writing—Review & editing, I.M.M. and F.F. All authors have read and agreed to the published version of the manuscript.

**Funding:** This research was funded by Hungarian Ministry for Innovation and Technology, grant number 2018-1.2.1-NKP-2018-00005 and by National Research, Development and Innovation Fund of Hungary, grant number 2018-1.2.1-NKP.

**Acknowledgments:** The Lendület grant from the Hungarian Academy of Sciences is gratefully acknowledged. This work was completed in the ELTE Thematic Excellence Programme supported by the Hungarian Ministry for Innovation and Technology. Project no. 2018-1.2.1-NKP-2018-00005 has been implemented with the support provided from the National Research, Development and Innovation Fund of Hungary, financed under the 2018-1.2.1-NKP funding scheme.

**Conflicts of Interest:** The authors declare no conflict of interest.

## References

1. Amić, A.; Molnar, M. An Improved and Efficient N-acetylation of Amines Using Choline Chloride Based Deep Eutectic Solvents. *Org. Prep. Proc. Int.* **2017**, *49*, 249–257. [[CrossRef](#)]
2. Biswas, R.; Mukherjee, A. Introducing the Concept of Green Synthesis in the Undergraduate Laboratory: Two-Step Synthesis of 4-Bromoacetanilide from Aniline. *J. Chem. Ed.* **2017**, *94*, 1391–1394. [[CrossRef](#)]
3. Tajbakhsh, M.; Hosseinzadeh, R.; Alinezhad, H.; Rezaee, P.; Tajbakhsh, M. TiO<sub>2</sub> NPs as Catalyst for N-Formylation and N-Acetylation of Amines under Solvent-Free Conditions. *Lett. Org. Chem.* **2013**, *10*, 657–663. [[CrossRef](#)]
4. Kim, D.H. Acetic anhydride as a synthetic reagent. *J. Het. Chem.* **1976**, *13*, 179–194. [[CrossRef](#)]
5. Baumann, M.; Baxendale, I.R. The synthesis of active pharmaceutical ingredients (APIs) using continuous flow chemistry. *Beilstein J. Org. Chem.* **2015**, *11*, 1194–1219. [[CrossRef](#)]
6. Britton, J.; Raston, C.L. Multi-step continuous-flow synthesis. *Chem. Soc. Rev.* **2017**, *46*, 1250–1271. [[CrossRef](#)]
7. Escobar Carlos, A.; Orellana-Vera, J.; Vega, A.; Sicker, D.; Sieler, J. Regioselective N-Acetylation of 4-(2-Hydroxyphenyl)-2-phenyl-2,3-dihydro-1H-1,5-benzodiazepine Using Protection by an Intramolecular Hydrogen Bond. *Z. Für Nat. B* **2009**, *64*, 969–972. [[CrossRef](#)]
8. Farina, V.; Reeves, J.T.; Senanayake, C.H.; Song, J.J. Asymmetric Synthesis of Active Pharmaceutical Ingredients. *Chem. Rev.* **2006**, *106*, 2734–2793. [[CrossRef](#)]
9. Nakazono, K.; Fukasawa, K.; Sato, T.; Koyama, Y.; Takata, T. Synthesis of acetylene-functionalized [2]rotaxane monomers directed toward side chain-type polyrotaxanes. *Polym. J.* **2010**, *42*, 208–215. [[CrossRef](#)]
10. Xu, G.; Tang, D.; Gai, Y.; Wang, G.; Kim, H.; Chen, Z.; Phan, L.T.; Or, Y.S.; Wang, Z. An Efficient Large-Scale Synthesis of EDP-420, a First-in-Class Bridged Bicyclic Macrolide (BBM) Antibiotic Drug Candidate. *Org. Proc. Res. Dev.* **2010**, *14*, 504–510. [[CrossRef](#)]
11. Isidro-Llobet, A.; Álvarez, M.; Albericio, F. Amino Acid-Protecting Groups. *Chem. Rev.* **2009**, *109*, 2455–2504. [[CrossRef](#)] [[PubMed](#)]
12. Hansen, B.K.; Gupta, R.; Baldus, L.; Lyon, D.; Narita, T.; Lammers, M.; Choudhary, C.; Weinert, B.T. Analysis of human acetylation stoichiometry defines mechanistic constraints on protein regulation. *Nat. Commun.* **2019**, *10*, 1055. [[CrossRef](#)]
13. Zhang, Y.; Zhou, F.; Bai, M.; Liu, Y.; Zhang, L.; Zhu, Q.; Bi, Y.; Ning, G.; Zhou, L.; Wang, X. The pivotal role of protein acetylation in linking glucose and fatty acid metabolism to  $\beta$ -cell function. *Cell Death Dis.* **2019**, *10*, 66. [[CrossRef](#)] [[PubMed](#)]
14. Alletti, R.; Oh, W.S.; Perambuduru, M.; Afrasiabi, Z.; Sinn, E.; Reddy, V.P. Gadolinium triflate immobilized in imidazolium based ionic liquids: A recyclable catalyst and green solvent for acetylation of alcohols and amines. *Green Chem.* **2005**, *7*, 203–206. [[CrossRef](#)]
15. El Seoud, O.A.; Koschella, A.; Fidale, L.C.; Dorn, S.; Heinze, T. Applications of Ionic Liquids in Carbohydrate Chemistry: A Window of Opportunities. *Biomacromolecules* **2007**, *8*, 2629–2647. [[CrossRef](#)]
16. Bartoli, G.; Dalpozzo, R.; De Nino, A.; Maiuolo, L.; Nardi, M.; Procopio, A.; Tagarelli, A. Per-O-acetylation of sugars catalyzed by Ce(OTf)<sub>3</sub>. *Green Chem.* **2004**, *6*, 191–192. [[CrossRef](#)]
17. Deka, N.; Mariotte, A.-M.; Boumendjel, A. Microwave mediated solvent-free acetylation of deactivated and hindered phenols. *Green Chem.* **2001**, *3*, 263–264. [[CrossRef](#)]
18. Snodin, D.J. Genotoxic Impurities: From Structural Alerts to Qualification. *Org. Proc. Res. Dev.* **2010**, *14*, 960–976. [[CrossRef](#)]
19. Plutschack, M.B.; Pieber, B.; Gilmore, K.; Seeberger, P.H. The Hitchhiker’s Guide to Flow Chemistry. *Chem. Rev.* **2017**, *117*, 11796–11893. [[CrossRef](#)]
20. Vukelić, S.; Koksich, B.; Seeberger, P.H.; Gilmore, K. A Sustainable, Semi-Continuous Flow Synthesis of Hydantoins. *Chem. Eur. J.* **2016**, *22*, 13451–13454. [[CrossRef](#)]

21. Ushakov, D.B.; Gilmore, K.; Kopetzki, D.; McQuade, D.T.; Seeberger, P.H. Continuous-Flow Oxidative Cyanation of Primary and Secondary Amines Using Singlet Oxygen. *Angew. Chem. Int. Ed.* **2014**, *45*, 557. [[CrossRef](#)] [[PubMed](#)]
22. McQuade, D.T.; Seeberger, P.H. Applying Flow Chemistry: Methods, Materials, and Multistep Synthesis. *J. Org. Chem.* **2013**, *78*, 6384–6389. [[CrossRef](#)]
23. Watts, K.; Baker, A.; Wirth, T. Electrochemical Synthesis in Microreactors. *J. Flow Chem.* **2015**, *4*, 2–11. [[CrossRef](#)]
24. Wiles, C.; Watts, P. Continuous process technology: A tool for sustainable production. *Green Chem.* **2014**, *16*, 55–62. [[CrossRef](#)]
25. Wiles, C.; Watts, P. Continuous flow reactors: A perspective. *Green Chem.* **2012**, *14*, 38–54. [[CrossRef](#)]
26. Wiles, C.; Watts, P. Solid-Supported Gallium Triflate: An Efficient Catalyst for the Three-Component Ketonic Strecker Reaction. *ChemSusChem* **2012**, *5*, 332–338. [[CrossRef](#)]
27. Osorio-Planes, L.; Rodríguez-Esrich, C.; Pericàs, M.A. Removing the Superfluous: A Supported Squaramide Catalyst with a Minimalistic Linker Applied to the Enantioselective Flow Synthesis of Pyranonaphthoquinones. *Catal. Sci. Technol.* **2016**, *6*, 4686–4689. [[CrossRef](#)]
28. Llanes, P.; Rodríguez-Esrich, C.; Sayalero, S.; Pericàs, M.A. Organocatalytic Enantioselective Continuous-Flow Cyclopropanation. *Org. Lett.* **2016**, *18*, 6292–6295. [[CrossRef](#)]
29. Izquierdo, J.; Pericàs, M.A. A Recyclable, Immobilized Analogue of Benzotetramisole for Catalytic Enantioselective Domino Michael Addition/Cyclization Reactions in Batch and Flow. *ACS Catal.* **2016**, *6*, 348–356. [[CrossRef](#)]
30. Pascanu, V.; Hansen, P.R.; Gómez, A.B.; Ayats, C.; Platero-Prats, A.E.; Johansson, M.J.; Pericàs, M.À.; Martín-Matute, B. Highly Functionalized Biaryls via Suzuki–Miyaura Cross-Coupling Catalyzed by Pd@MOF under Batch and Continuous Flow Regimes. *ChemSusChem* **2015**, *8*, 123–130. [[CrossRef](#)]
31. Martin-Rapun, R.; Sayalero, S.; Pericàs, M.A. Asymmetric anti-Mannich Reactions in Continuous Flow. *Green Chem.* **2013**, *15*, 3295–3301. [[CrossRef](#)]
32. Bottecchia, C.; Rubens, M.; Gunnoo, S.B.; Hessel, V.; Madder, A.; Noël, T. Visible-Light-Mediated Selective Arylation of Cysteine in Batch and Flow. *Angew. Chem. Int. Ed.* **2017**, *56*, 12702–12707. [[CrossRef](#)] [[PubMed](#)]
33. Su, Y.; Kuijpers, K.P.L.; König, N.; Shang, M.; Hessel, V.; Noël, T. A Mechanistic Investigation of the Visible-Light Photocatalytic Trifluoromethylation of Heterocycles Using CF<sub>3</sub>I in Flow. *Chem. Eur. J.* **2016**, *22*, 12295–12300. [[CrossRef](#)] [[PubMed](#)]
34. Su, Y.; Kuijpers, K.; Hessel, V.; Noël, T. A Convenient Numbering-Up Strategy for the Scale-Up of Gas-Liquid Photoredox Catalysis in Flow. *React. Chem. Eng.* **2016**, *1*, 73–81. [[CrossRef](#)]
35. Straathof, N.J.W.; Cramer, S.E.; Hessel, V.; Noël, T. Practical Photocatalytic Trifluoromethylation and Hydrotrifluoromethylation of Styrenes in Batch and Flow. *Angew. Chem. Int. Ed.* **2016**, *55*, 15549–15553. [[CrossRef](#)]
36. Seo, H.; Katcher, M.H.; Jamison, T.F. Photoredox Activation of Carbon Dioxide for Amino Acid Synthesis in Continuous Flow. *Nat. Chem.* **2016**, *9*, 453–456. [[CrossRef](#)]
37. McTeague, T.A.; Jamison, T.F. Photoredox Activation of SF<sub>6</sub> for Fluorination. *Angew. Chem. Int. Ed.* **2016**, *55*, 15072–15075. [[CrossRef](#)]
38. Adamo, A.; Beingessner, R.L.; Behnam, M.; Chen, J.; Jamison, T.F.; Jensen, K.F.; Monbaliu, J.C.M.; Myerson, A.S.; Revalor, E.M.; Snead, D.R. On-Demand Continuous-Flow Production of Pharmaceuticals in a Compact, Reconfigurable System. *Science* **2016**, *352*, 61–67. [[CrossRef](#)]
39. Snead, D.R.; Jamison, T.F. A Three-Minute Synthesis and Purification of Ibuprofen: Pushing the Limits of Continuous-Flow Processing. *Angew. Chem. Int. Ed.* **2015**, *54*, 983–987. [[CrossRef](#)]
40. Wu, J.; Yang, X.; He, Z.; Mao, X.; Hatton, T.A.; Jamison, T.F. Continuous Flow Synthesis of Ketones from Carbon Dioxide and Organolithium or Grignard Reagents. *Angew. Chem. Int. Ed.* **2014**, *53*, 8416–8420. [[CrossRef](#)]
41. Rogers, L.; Jensen, K.F. Continuous manufacturing – the Green Chemistry promise? *Green Chem.* **2019**, *21*, 3481–3498. [[CrossRef](#)]
42. Giri, G.; Yang, L.; Mo, Y.; Jensen, K.F. Adding Crystals to Minimize Clogging in Continuous Flow Synthesis. *Cryst. Growth Des.* **2019**, *19*, 98–105. [[CrossRef](#)]



43. Coley, C.W.; Thomas, D.A.; Lummiss, J.A.M.; Jaworski, J.N.; Breen, C.P.; Schultz, V.; Hart, T.; Fishman, J.S.; Rogers, L.; Gao, H.; et al. A robotic platform for flow synthesis of organic compounds informed by AI planning. *Science* **2019**, *365*. [[CrossRef](#)] [[PubMed](#)]
44. Zhang, P.; Weeranoppanant, N.; Thomas, D.A.; Tahara, K.; Stelzer, T.; Russell, M.G.; O'Mahony, M.; Myerson, A.S.; Lin, H.; Kelly, L.P.; et al. Advanced Continuous Flow Platform for On-Demand Pharmaceutical Manufacturing. *Chem. Eur. J.* **2018**, *24*, 2776–2784. [[CrossRef](#)]
45. Bédard, A.-C.; Adamo, A.; Aroh, K.C.; Russell, M.G.; Bedermann, A.A.; Torosian, J.; Yue, B.; Jensen, K.F.; Jamison, T.F. Reconfigurable system for automated optimization of diverse chemical reactions. *Science* **2018**, *361*, 1220–1225. [[CrossRef](#)]
46. Jensen, K.F. Flow chemistry. Microreaction technology comes of age. *AIChE J.* **2017**, *63*, 858–869. [[CrossRef](#)]
47. Ollivier, N.; Toupy, T.; Hartkoorn, R.C.; Desmet, R.; Monbaliu, J.-C.M.; Melnyk, O. Accelerated microfluidic native chemical ligation at difficult amino acids toward cyclic peptides. *Nat. Commun.* **2018**, *9*, 2847. [[CrossRef](#)]
48. Kreituss, I.; Bode, J.W. Flow chemistry and polymer-supported pseudoenantiomeric acylating agents enable parallel kinetic resolution of chiral saturated N-heterocycles. *Nat. Chem.* **2016**, *9*, 446–452. [[CrossRef](#)]
49. Berton, M.; Huck, L.; Alcázar, J. On-demand synthesis of organozinc halides under continuous flow conditions. *Nat. Protoc.* **2018**, *13*, 324–334. [[CrossRef](#)]
50. Elvira, K.S.; Solvas, X.C.I.; Wootton, R.C.R.; de Mello, A.J. The past, present and potential for microfluidic reactor technology in chemical synthesis. *Nat. Chem.* **2013**, *5*, 905–915. [[CrossRef](#)]
51. Tadele, K.; Verma, S.; Nadagouda, M.N.; Gonzalez, M.A.; Varma, R.S. A rapid flow strategy for the oxidative cyanation of secondary and tertiary amines via C-H activation. *Sci. Rep.* **2017**, *7*, 16311. [[CrossRef](#)] [[PubMed](#)]
52. Fuse, S.; Mifune, Y.; Nakamura, H.; Tanaka, H. Total synthesis of feglymycin based on a linear/convergent hybrid approach using micro-flow amide bond formation. *Nat. Commun.* **2016**, *7*, 13491. [[CrossRef](#)] [[PubMed](#)]
53. Kirschneck, D. Strategies for Using Microreactors and Flow Chemistry: Drivers and Tools. *Chem. Eng. Tech.* **2013**, *36*, 1061–1066. [[CrossRef](#)]
54. Fanelli, F.; Parisi, G.; Degennaro, L.; Luisi, R. Contribution of microreactor technology and flow chemistry to the development of green and sustainable synthesis. *Beilstein J. Org. Chem.* **2017**, *13*, 520–542. [[CrossRef](#)] [[PubMed](#)]
55. De Angelis, S.; Celestini, P.; Purgatorio, R.; Degennaro, L.; Rebuzzini, G.; Luisi, R.; Carlucci, C. Development of a continuous flow synthesis of propranolol: Tackling a competitive side reaction. *J. Flow Chem.* **2019**, *9*, 231–236. [[CrossRef](#)]
56. De Angelis, S.; Hone, C.; Degennaro, L.; Celestini, P.; Luisi, R.; Kappe, C.O. Sequential  $\alpha$ -lithiation and aerobic oxidation of an arylacetic acid-continuous-flow synthesis of cyclopentyl mandelic acid. *J. Flow Chem.* **2018**, *8*, 109–116. [[CrossRef](#)]
57. Movsisyan, M.; Delbeke, E.I.P.; Berton, J.K.E.T.; Battilocchio, C.; Ley, S.V.; Stevens, C.V. Taming hazardous chemistry by continuous flow technology. *Chem. Soc. Rev.* **2016**, *45*, 4892–4928. [[CrossRef](#)]
58. Mellmer, M.A.; Sanpitakseree, C.; Demir, B.; Bai, P.; Ma, K.; Neurock, M.; Dumesic, J.A. Solvent-enabled control of reactivity for liquid-phase reactions of biomass-derived compounds. *Nat. Catal.* **2018**, *1*, 199–207. [[CrossRef](#)]
59. Xiong, B.; Wang, G.; Xiong, T.; Wan, L.; Zhou, C.; Liu, Y.; Zhang, P.; Yang, C.; Tang, K. Direct synthesis of N-arylamides via the coupling of aryl diazonium tetrafluoroborates and nitriles under transition-metal-free conditions. *Tetrahedron Lett.* **2018**, *59*, 3139–3142. [[CrossRef](#)]
60. Lee, Y.M.; Moon, M.E.; Vajpayee, V.; Filimonov, V.D.; Chi, K.-W. Efficient and economic halogenation of aryl amines via arenediazonium tosylate salts. *Tetrahedron* **2010**, *66*, 7418–7422. [[CrossRef](#)]
61. Beller, M. First Amidocarbonylation with Nitriles for the Synthesis of N-Acyl Amino Acids. *Synlett* **1999**, 108–110. [[CrossRef](#)]
62. Enders, D.; Shilvock, J. Some recent applications of  $\alpha$ -amino nitrile chemistry. *Chem. Soc. Rev.* **2000**, *29*, 359–373. [[CrossRef](#)]
63. Jiang, T.-S.; Wang, G.-W. Synthesis of 3-Acylindoles by Palladium-Catalyzed Acylation of Free (N-H) Indoles with Nitriles. *Org. Lett.* **2013**, *15*, 788–791. [[CrossRef](#)] [[PubMed](#)]

64. Jang, W.B.; Shin, W.S.; Hong, J.E.; Lee, S.Y.; Oh, D.Y. Synthesis of Ketones with Alkyl Phosphonates and Nitriles as Acyl Cation Equivalent: Application of Dephosphonylation Reaction of  $\beta$ -Functionalized Phosphonate with Hydride. *Synth. Commun.* **1997**, *27*, 3333–3339. [[CrossRef](#)]
65. Saikia, U.P.; Hussain, F.L.; Suri, M.; Pahari, P. Selective N-acetylation of aromatic amines using acetonitrile as acylating agent. *Tetrahedron Lett.* **2016**, *57*, 1158–1160. [[CrossRef](#)]
66. Brahmayya, M.; Suen, S.-Y.; Dai, S.A. Sulfonated graphene oxide-catalyzed N-acetylation of amines with acetonitrile under sonication. *J. Taiwan Inst. Chem. Eng.* **2018**, *83*, 174–183. [[CrossRef](#)]
67. Molnár, Á.; Papp, A. Catalyst recycling—A survey of recent progress and current status. *Coord. Chem. Rev.* **2017**, *349*, 1–65. [[CrossRef](#)]

**Sample Availability:** Samples of the compounds 1–28 are available from the authors.



© 2020 by the authors. Licensee MDPI, Basel, Switzerland. This article is an open access article distributed under the terms and conditions of the Creative Commons Attribution (CC BY) license (<http://creativecommons.org/licenses/by/4.0/>).

# N-Acylation of Amines in Continuous-Flow with Acetonitrile—No Need for Hazardous and Toxic Carboxylic Acid Derivatives

György Orsy <sup>1,2</sup>, Ferenc Fülöp <sup>1,3,\*</sup> and István M. Mándity <sup>2,4,\*</sup>

<sup>1</sup> Institute of Pharmaceutical Chemistry University of Szeged, Eötvös u. 6, H-6720 Szeged, Hungary; orsy.gyorgy@ttk.hu (G.O.)

<sup>2</sup> MTA TTK Lendület Artificial Transporter Research Group, Institute of Materials and Environmental Chemistry, Research Center for Natural Sciences, Hungarian Academy of Sciences, Magyar Tudosok krt. 2, 1117 Budapest, Hungary

<sup>3</sup> Research Group of Stereochemistry of the Hungarian Academy of Sciences, Dóm tér 8, H-6720 Szeged, Hungary

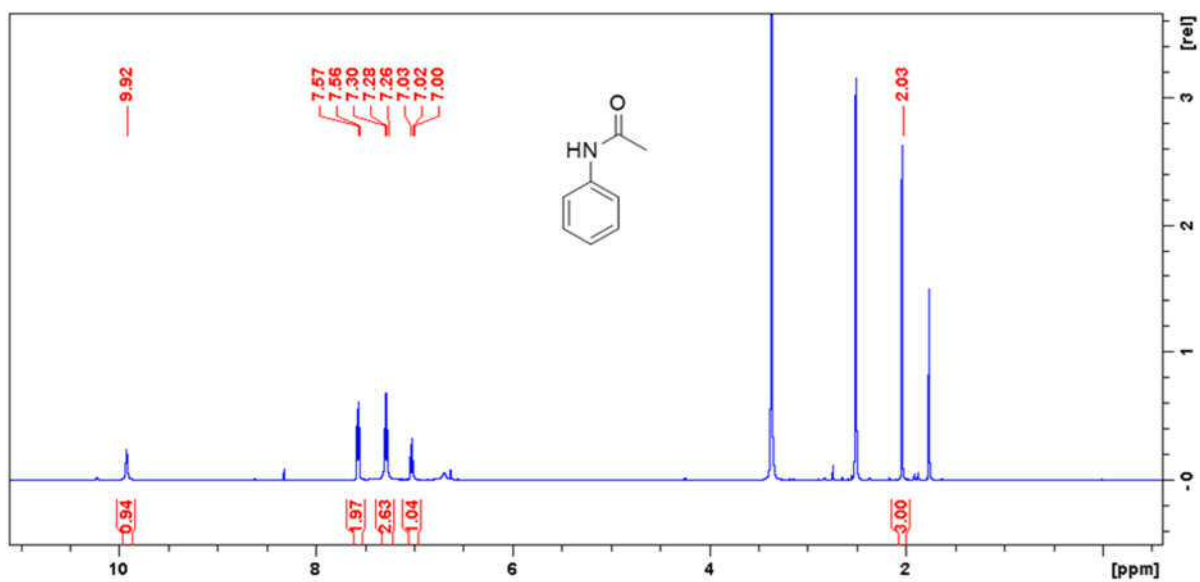
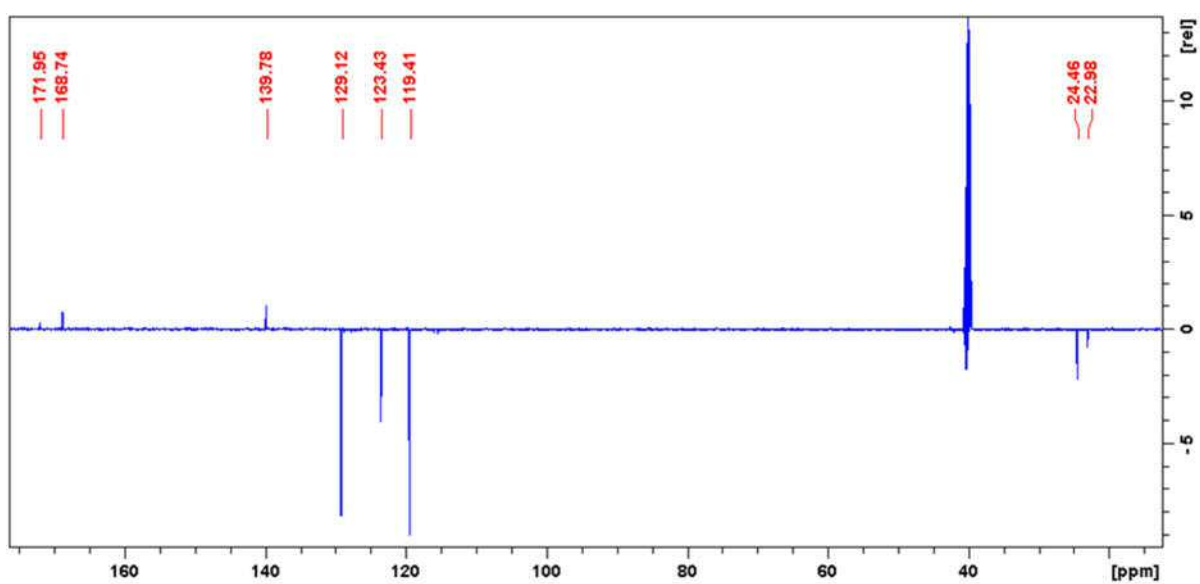
<sup>4</sup> Department of Organic Chemistry, Faculty of Pharmacy, Semmelweis University, Hógyes Endre u. 7, H-1092, Budapest, Hungary

\* Correspondence: fulop@pharm.u-szeged.hu (F.F.); mandity.istvan@ttk.mta.hu (I.M.M.); Tel.: +36 1 3826 616 (I.M.M.)

## Table of Content

1. <sup>1</sup> H and <sup>13</sup> C NMR spectra	S3 – S13
2. Images of the home made reactor	S14

## 1. NMR spectra

Figure S1. <sup>1</sup>H NMR spectrum of acetanilide 2 measured in DMSO-*d*<sub>6</sub> at 298 K.Figure S2. APT NMR spectrum of acetanilide 2 measured in DMSO-*d*<sub>6</sub> at 298 K.

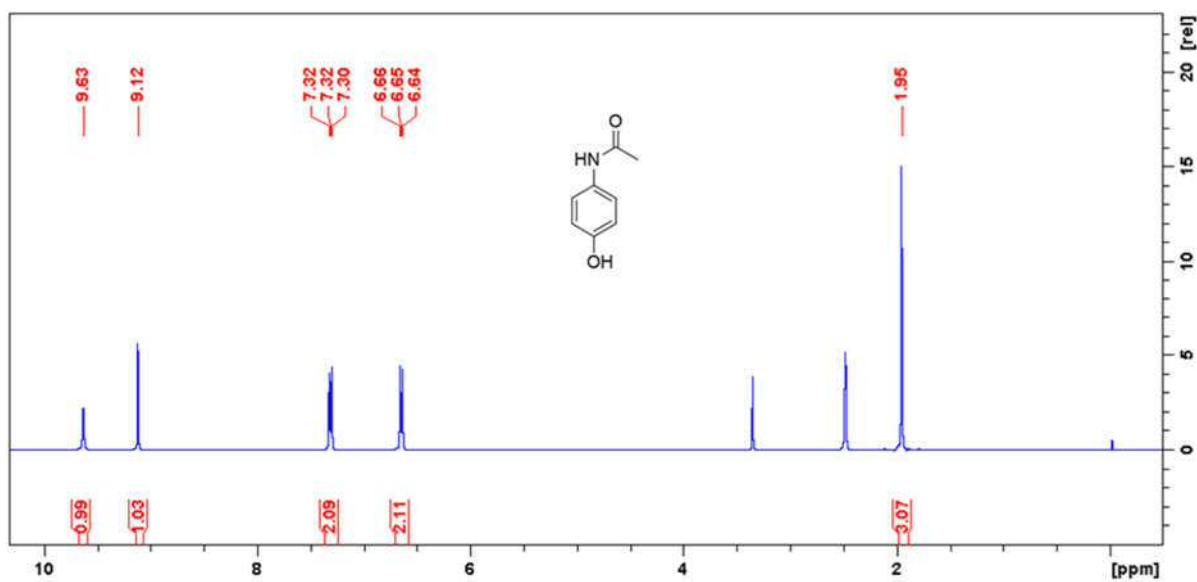


Figure S3. <sup>1</sup>H NMR spectrum of acetaminophen 4 measured in DMSO-*d*<sub>6</sub> at 298 K.

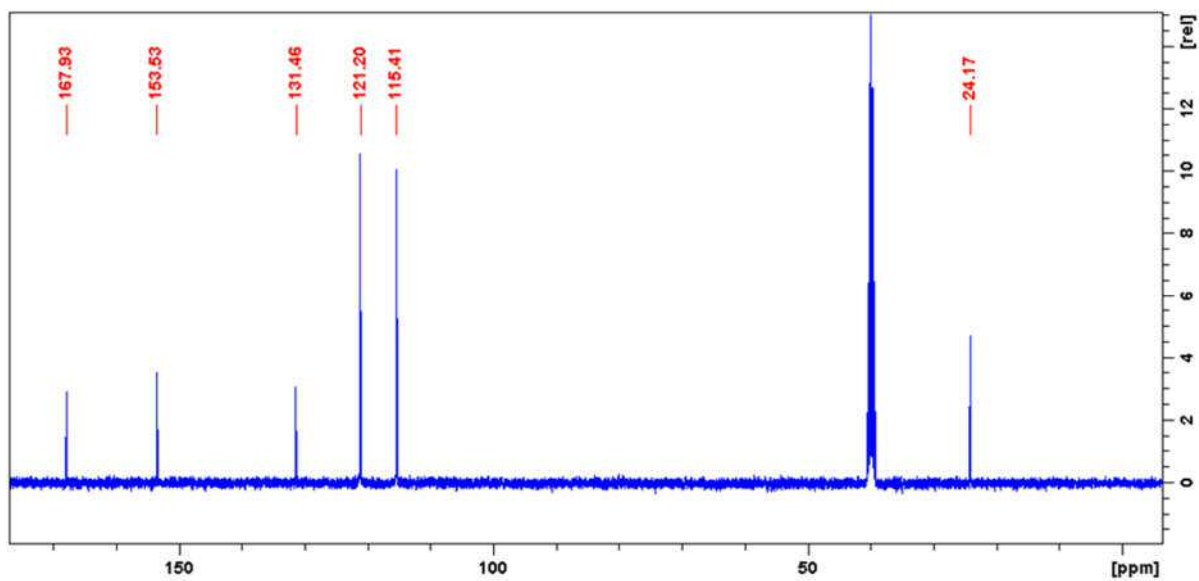


Figure S4. <sup>13</sup>C NMR spectrum of acetaminophen 4 measured in DMSO-*d*<sub>6</sub> at 298 K.

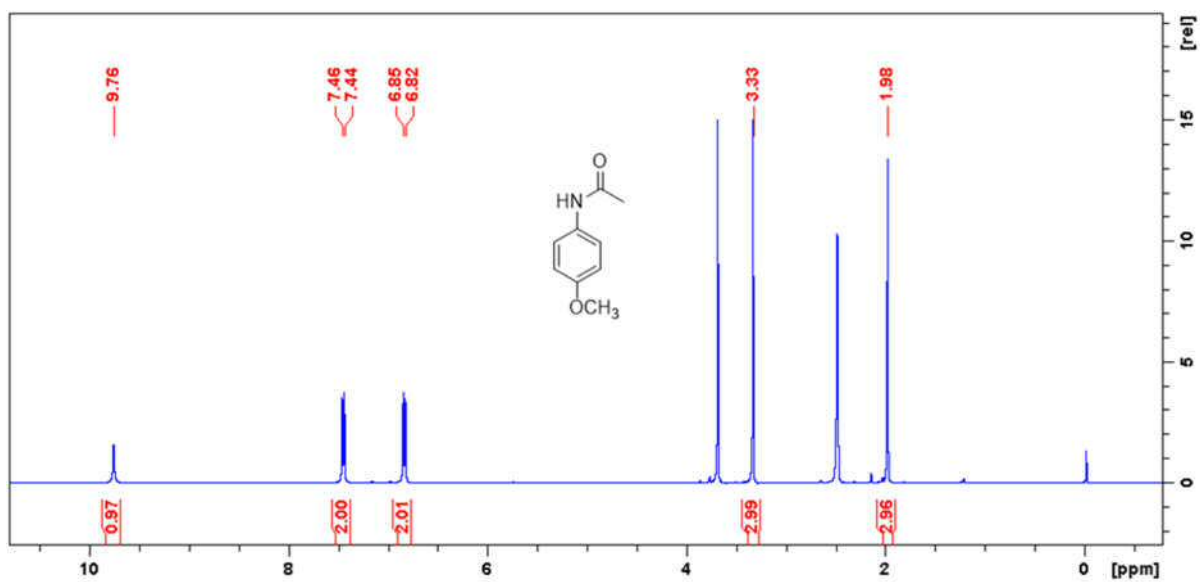


Figure S5. <sup>1</sup>H NMR spectrum of N-(4-methoxyphenyl)acetamide 6 measured in DMSO-*d*<sub>6</sub> at 298 K.

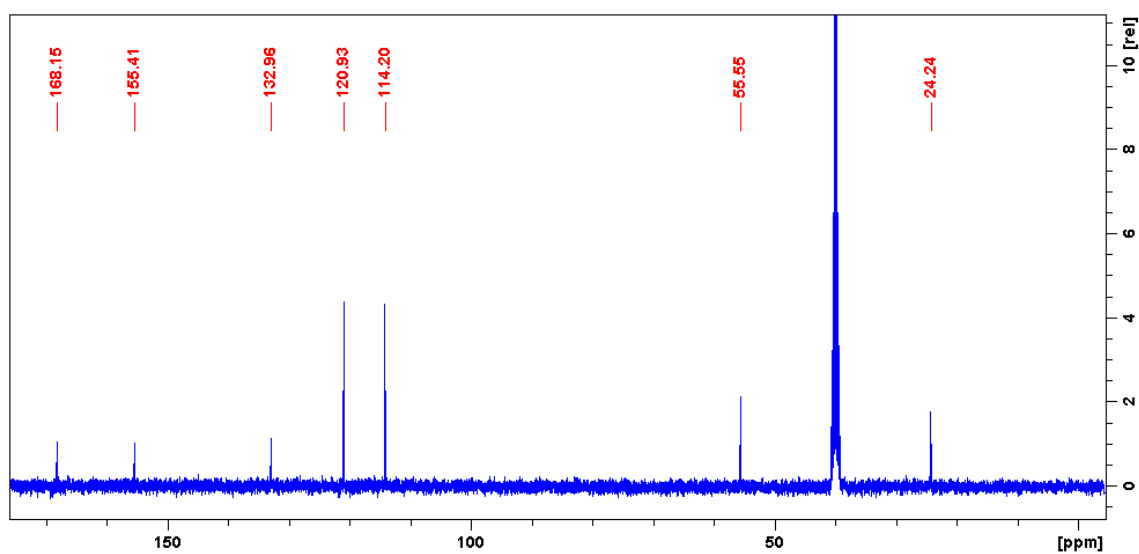
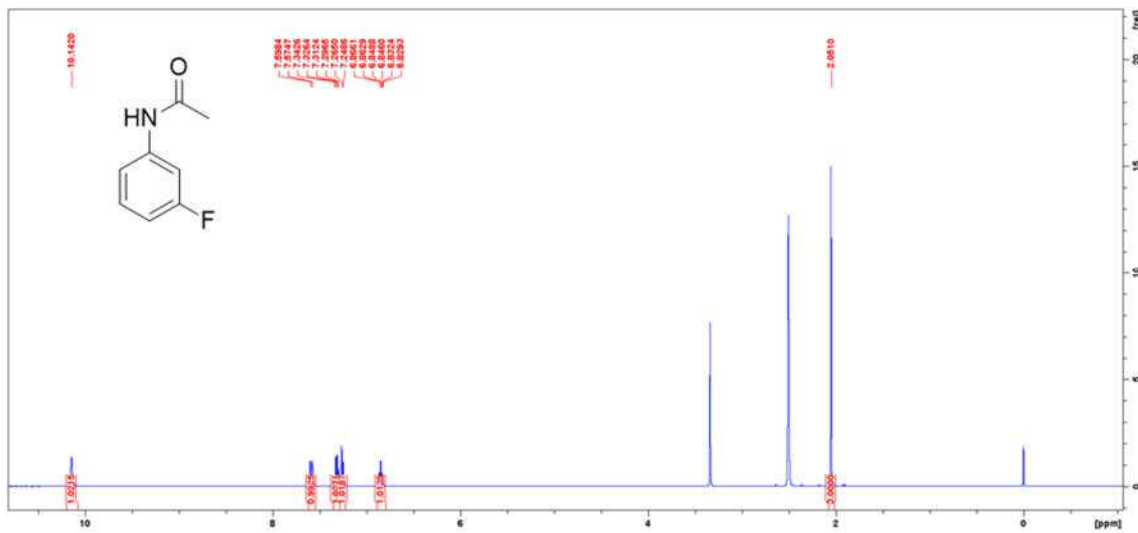
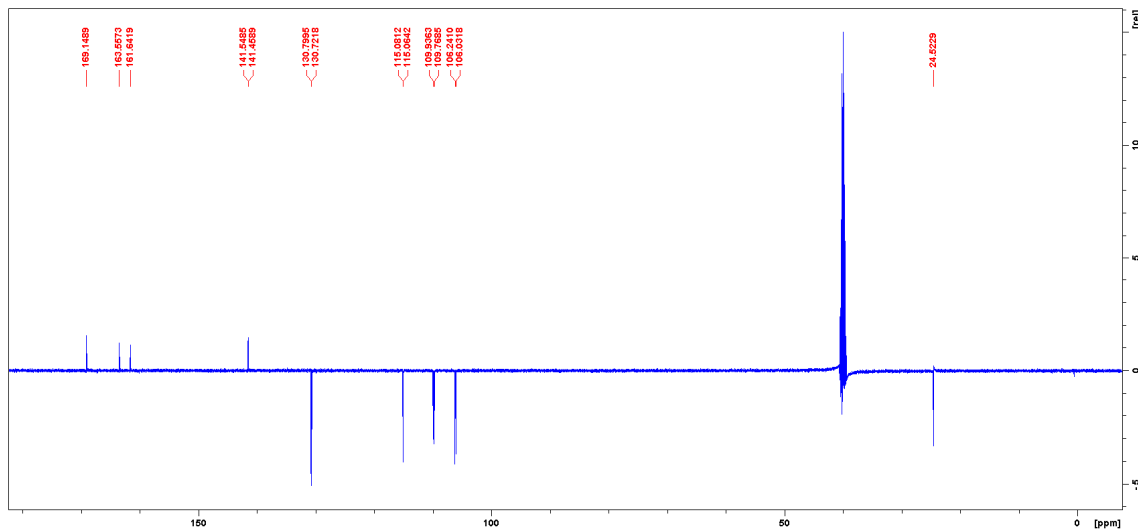


Figure S6. <sup>13</sup>C NMR spectrum of N-(4-methoxyphenyl)acetamide 6 measured in DMSO-*d*<sub>6</sub> at 298 K.



**Figure S7.**  $^1\text{H}$  NMR spectrum of N-(3-fluorophenyl)acetamide **8** measured in DMSO- $d_6$  at 298 K.



**Figure S8.**  $^{13}\text{C}$  NMR spectrum of N-(3-fluorophenyl)acetamide **8** measured in DMSO- $d_6$  at 298 K.

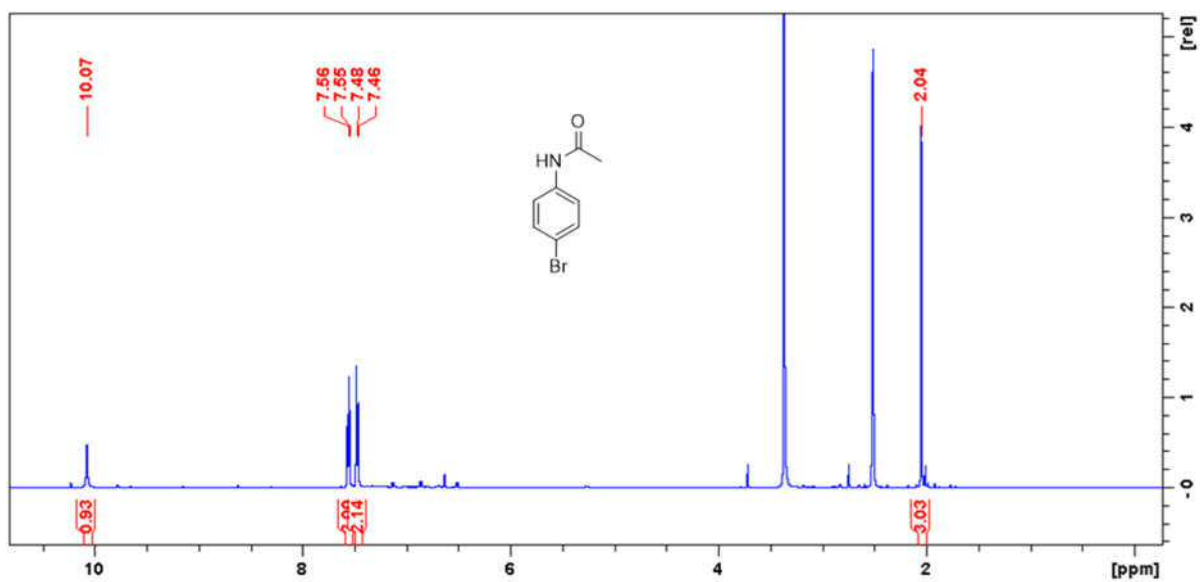


Figure S9. <sup>1</sup>H NMR spectrum of N-(4-Bromophenyl)acetamide 10 measured in DMSO-*d*<sub>6</sub> at 298 K.

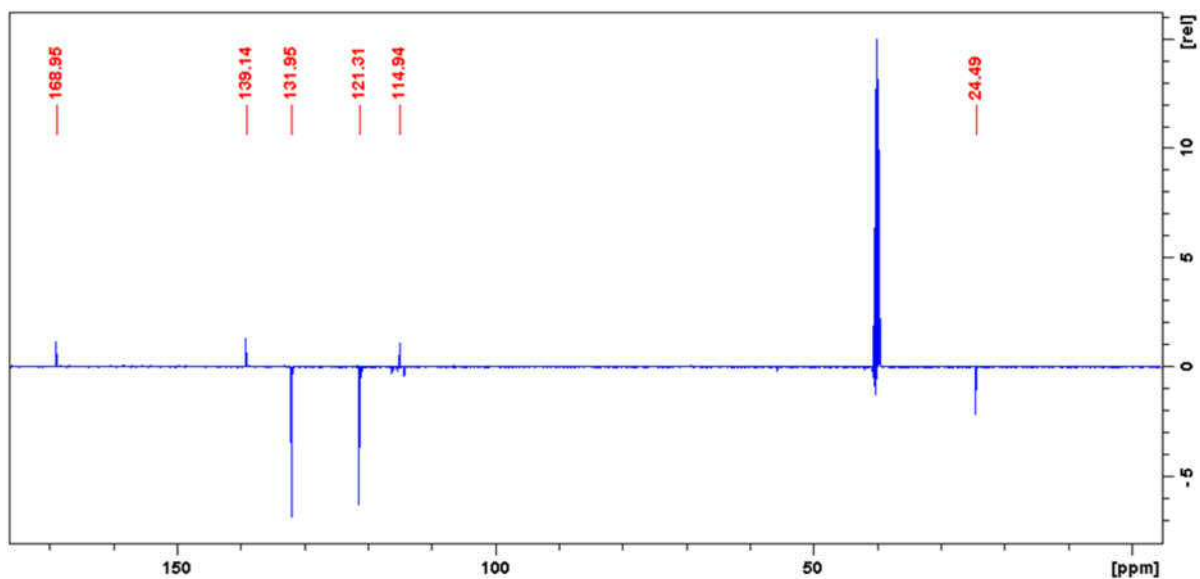


Figure S10. APT NMR spectrum of N-(4-Bromophenyl)acetamide 10 measured in DMSO-*d*<sub>6</sub> at 298 K.



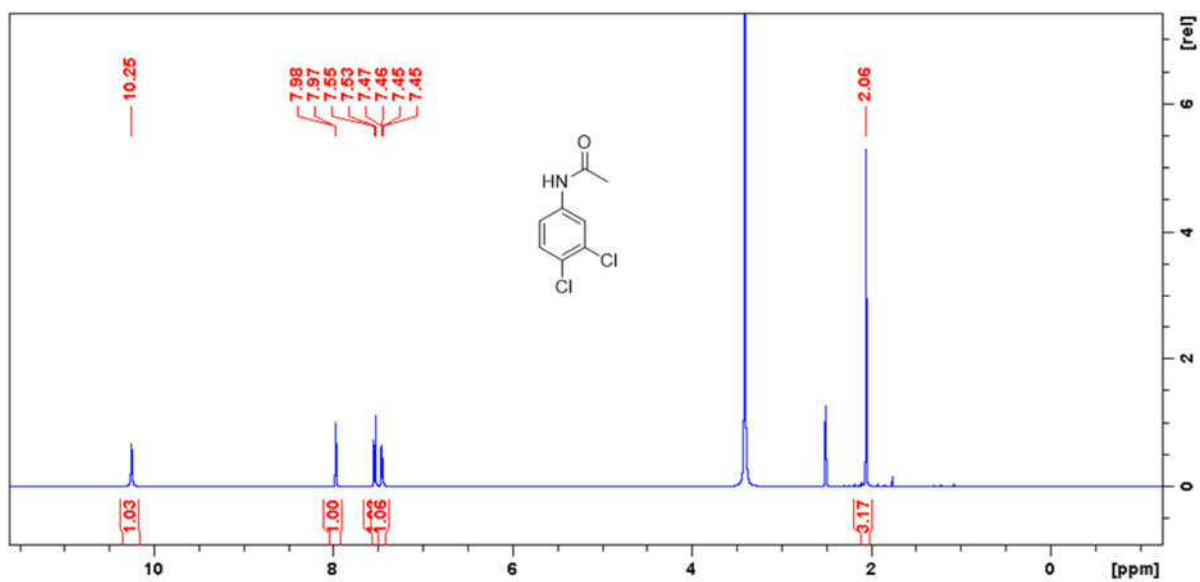


Figure S11.  $^1\text{H}$  NMR spectrum of N-(3,4-dichlorophenyl)acetamide **12** measured in  $\text{DMSO-}d_6$  at 298 K.

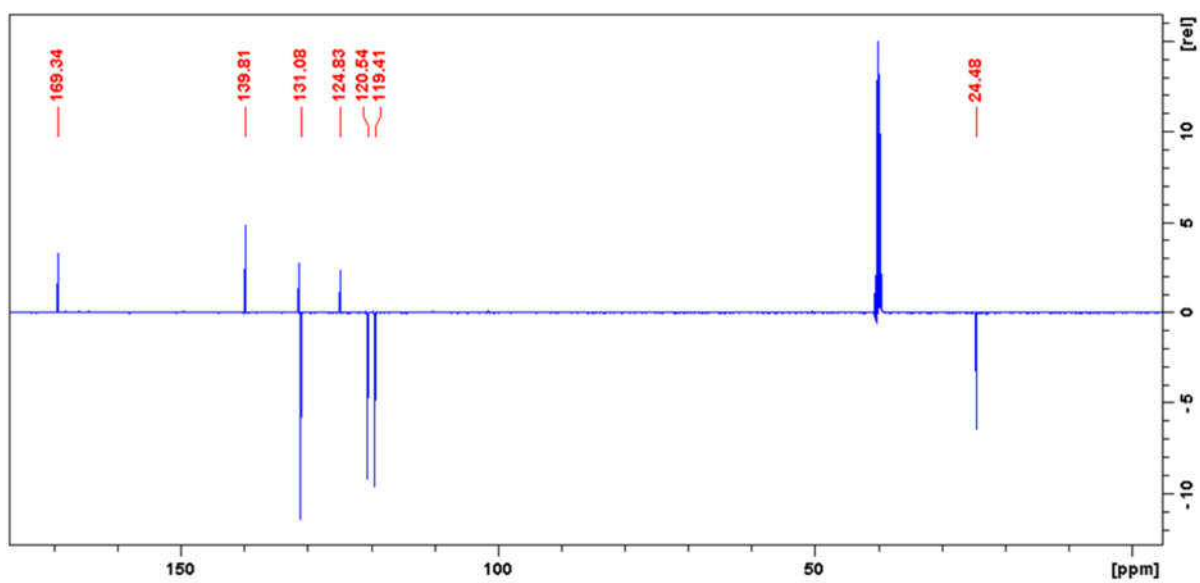


Figure S12. APT NMR spectrum of N-(3,4-dichlorophenyl)acetamide **12** measured in  $\text{DMSO-}d_6$  at 298K.

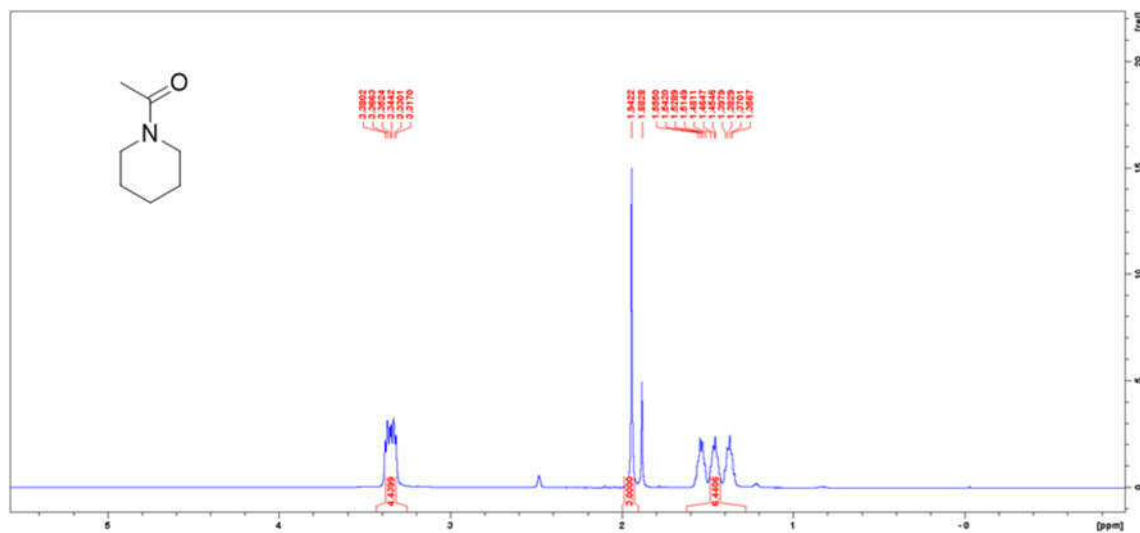


Figure S13. <sup>1</sup>H NMR spectrum of 1-acetylpiperidine 20 measured in DMSO-*d*<sub>6</sub> at 298 K.

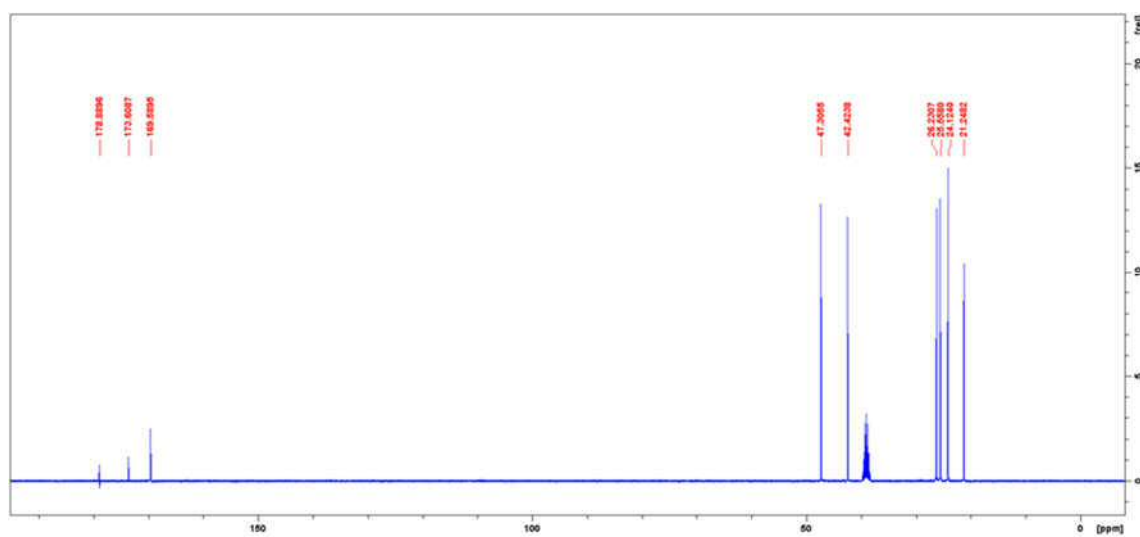


Figure S14. <sup>13</sup>C NMR spectrum of 1-acetylpiperidine 20 measured in DMSO-*d*<sub>6</sub> at 298 K.

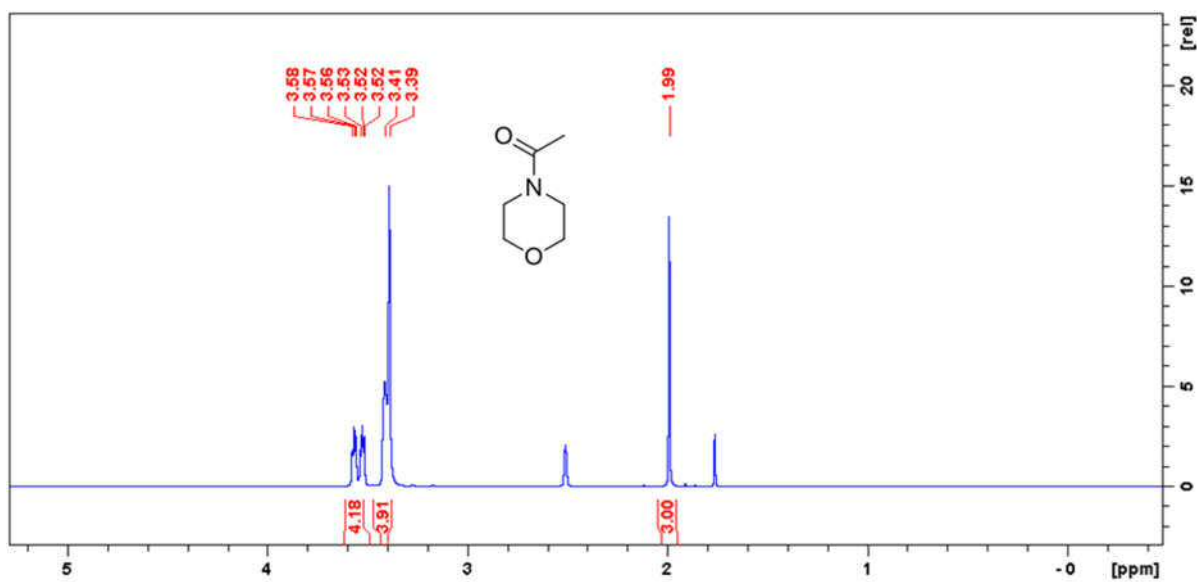


Figure S15. <sup>1</sup>H NMR spectrum of 4-acetylmorpholine 22 measured in DMSO-*d*<sub>6</sub> at 298 K.

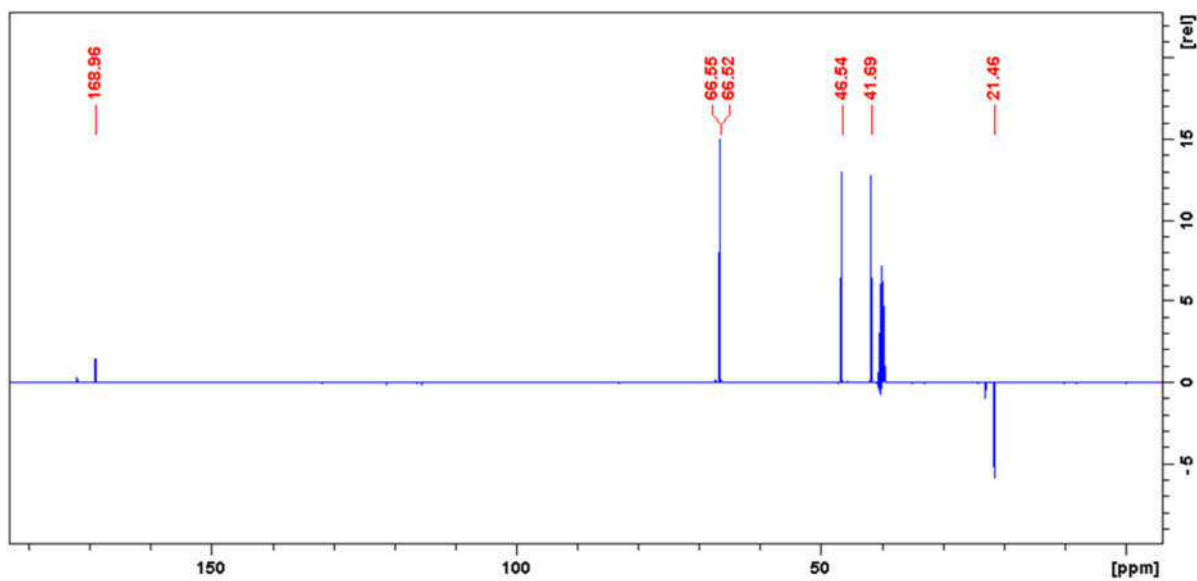


Figure S16. APT NMR spectrum of 4-acetylmorpholine 22 measured in DMSO-*d*<sub>6</sub> at 298 K.

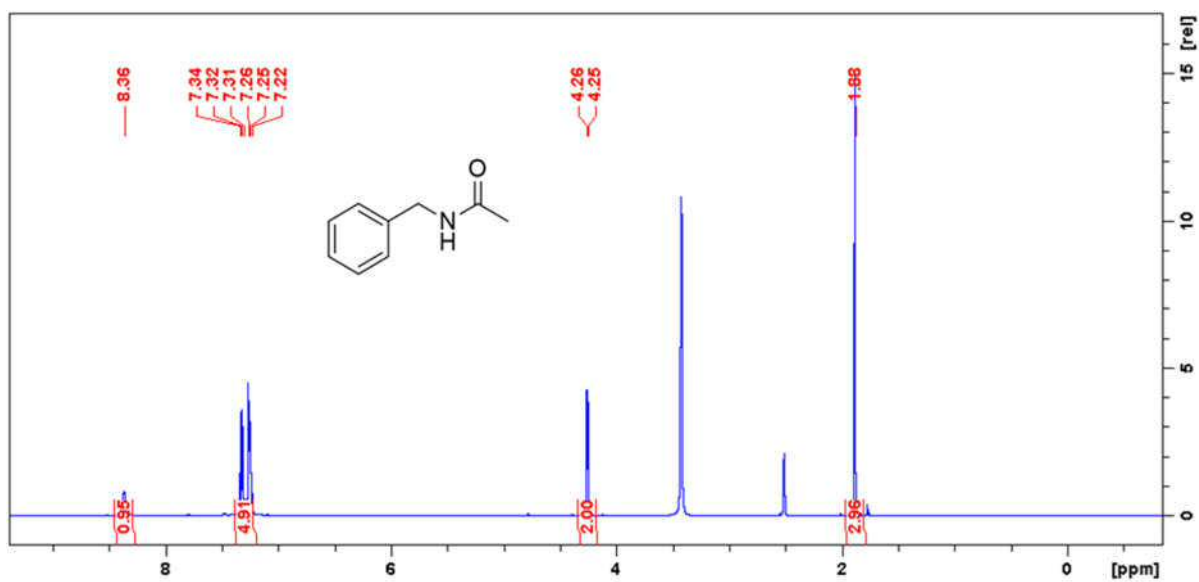


Figure S17. <sup>1</sup>H NMR spectrum of N-benzylacetamide 24 measured in DMSO-*d*<sub>6</sub> at 298 K.

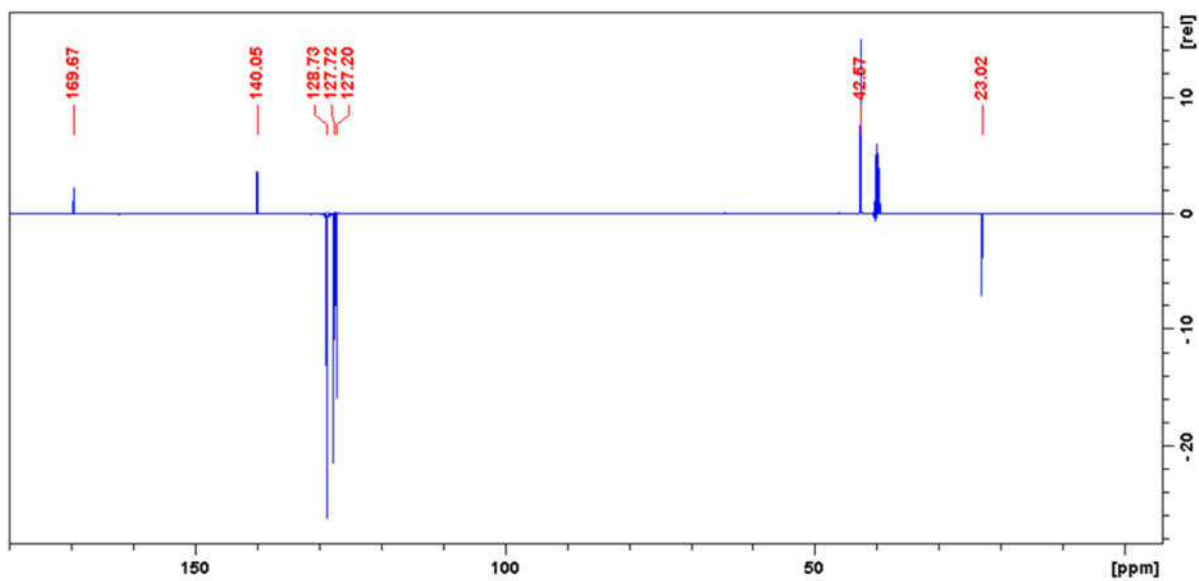


Figure S18. APT NMR spectrum of N-benzylacetamide 24 measured in DMSO-*d*<sub>6</sub> at 298 K.

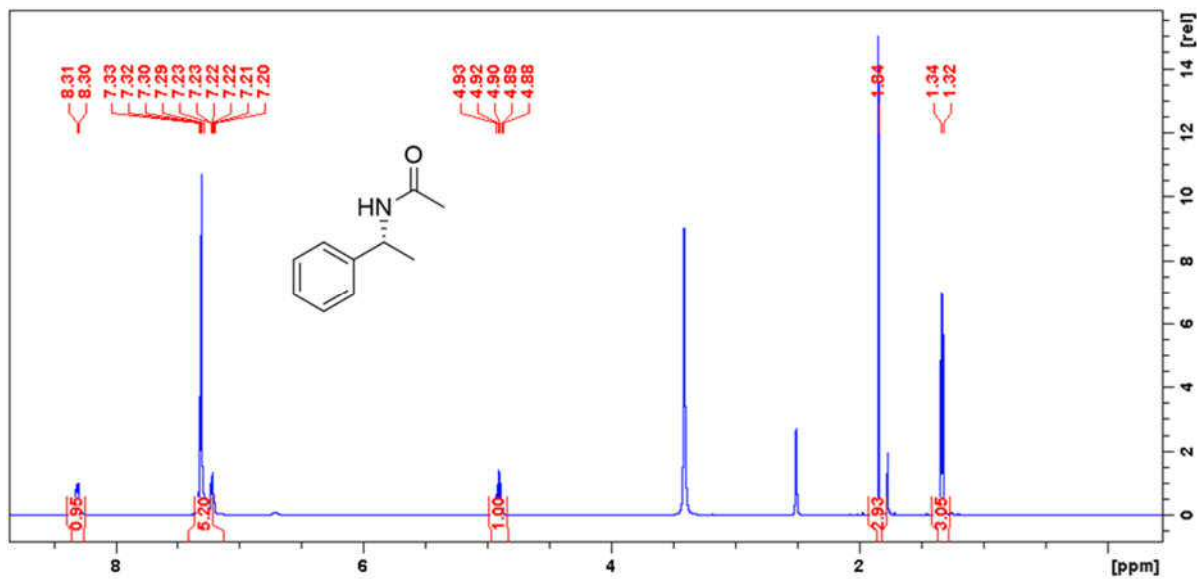


Figure S19.  $^1\text{H}$  NMR spectrum of (R)-N-(1-phenylethyl)acetamide **26** measured in  $\text{DMSO-}d_6$  at 298 K.

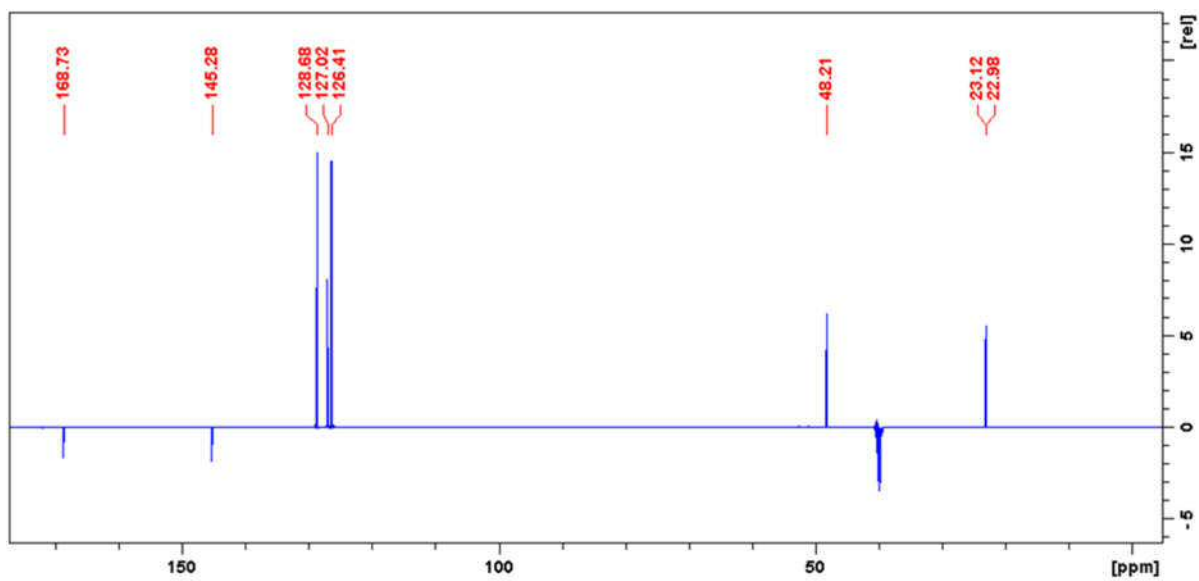


Figure S20. APT NMR spectrum of (R)-N-(1-phenylethyl)acetamide **26** measured in  $\text{DMSO-}d_6$  at 298 K.  $[\alpha]^{20}_{\text{D}} = +149$  ( $c=1.00$ , ethanol).

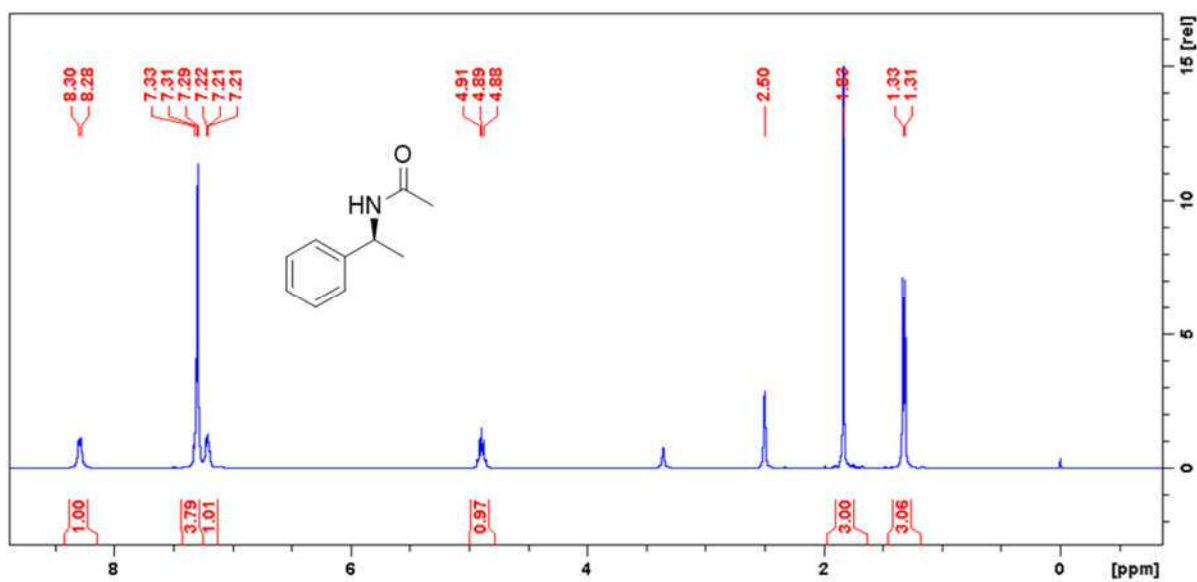


Figure S21. <sup>1</sup>H NMR spectrum of (S)-N-(1-phenylethyl)acetamide 28 measured in DMSO-*d*<sub>6</sub> at 298 K.

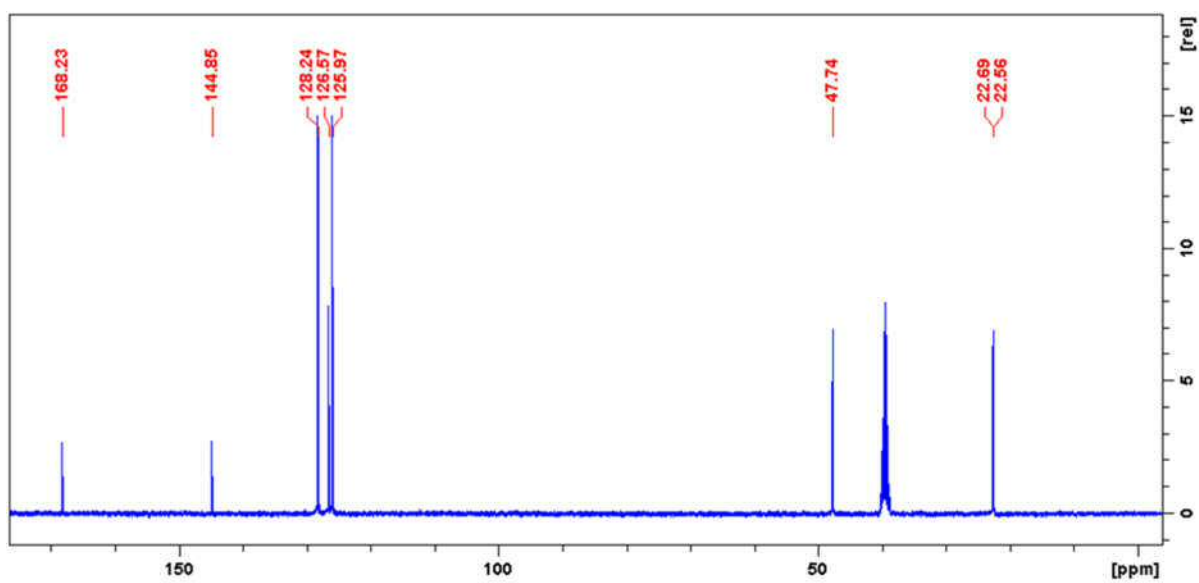


Figure S22. <sup>13</sup>C NMR spectrum of (S)-N-(1-phenylethyl)acetamide 28 measured in DMSO-*d*<sub>6</sub> at 298 K.  $[\alpha]^{20}_{\text{D}} = -150.1$  (c=1.00, ethanol).

## 2. Image of the home made reactor

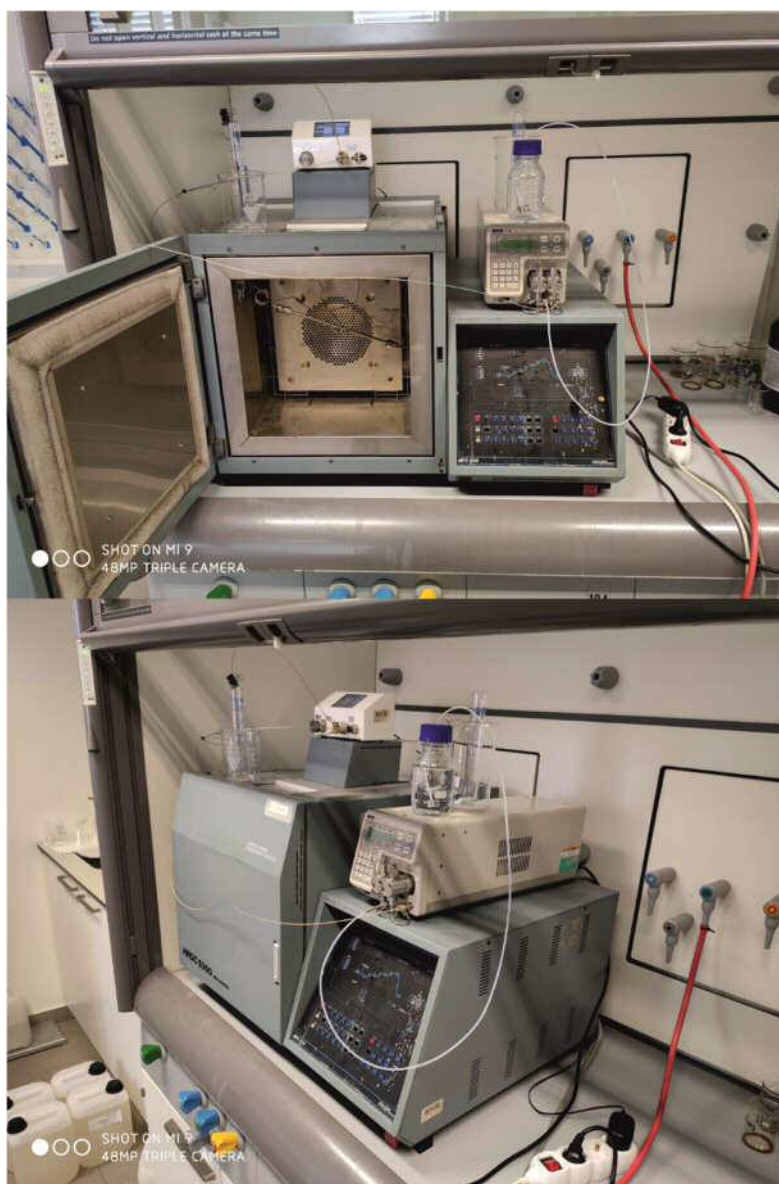


Figure S23. The reactor set-up used.

**III**






Cite this: DOI: 10.1039/d0cy01603a

Received 13th August 2020,  
Accepted 21st September 2020

DOI: 10.1039/d0cy01603a

rsc.li/catalysis

## Direct amide formation in a continuous-flow system mediated by carbon disulfide†

György Orsy,<sup>ab</sup> Ferenc Fülöp<sup>\*ac</sup> and István M. Mándity<sup>ib</sup>  <sup>\*bd</sup>

Amide bonds are ubiquitous in nature. They can be found in proteins, peptides, alkaloids, etc. and they are used in various synthetic drugs too. Amide bonds are mainly made by the use of (i) hazardous carboxylic acid derivatives or (ii) expensive coupling agents. Both ways make the synthetic technology less atom economic. We report a direct flow-based synthesis of amides. The developed approach is prominently simple and various aliphatic and aromatic amides were synthesized with excellent yields. The reaction in itself is carried out in acetonitrile, which is considered as a less problematic dipolar aprotic solvent. The used coupling agent, carbon disulfide, is widely available and has a low price. The utilized heterogeneous Lewis acid, alumina, is a sustainable material and it can be utilized multiple times. The technology is considerably robust and shows excellent reusability and easy scale-up is carried out without the need of any intensive purification protocols.

The amide linkage is one of the most ubiquitous chemical bonds in nature.<sup>1–3</sup> It provides an essential chemical spine-like connection in peptides and proteins. In addition, numerous medicines contain an amide bond from small organic molecules (local anaesthetics, nonsteroidal anti-inflammatory drugs, etc.) through peptides to antibodies,

which are considered to be the therapy of the future.<sup>4–8</sup> Furthermore, the amide moiety is also a crucial connecting bond in synthetic polymers.<sup>9</sup> The natural way of amide formation is a very complex process involving the interplay of many macromolecules such as enzymes, protein factors, mRNAs, and tRNAs in a complex molecular machine, known as the ribosome. Ribosomes and associated molecules are also known as the translational apparatus of biological protein synthesis.<sup>10,11</sup>

There are many different synthetic methods to create amide bonds.<sup>12,13</sup> However, there are only a limited number of methods available for direct amidation resulting in amide bonds without coupling reagents or activating agents.<sup>14–16</sup> These processes utilize greater than the stoichiometric ratio of coupling reagents (carbodiimides, 1*H*-benzotriazoles, etc.). Furthermore, these are generally expensive and harmful materials, and purification of the crude products is complicated due to considerable amounts of by-products.<sup>17–21</sup> Therefore, there is a need for a general technique to access amides directly from free carboxylic acids and amines in an uncomplicated, environmentally friendly, and efficient way.

The direct method route, in general, is hampered by a large activation energy, because the complete thermal dehydration reaction between an amine and a carboxylic acid needs harsh reaction conditions. Thus, the direct method usually requires high temperatures for the dehydration of the intermediate salt to provide the amide compound.<sup>22,23</sup>

There are several boronic acid derivatives studied as catalysts for the amidation reaction.<sup>24–26</sup> One of them, reported by Yihao Du *et al.*,<sup>27</sup> is a solid-supported arylboronic acid catalyst for the direct amidation of a wide range of amine substrates in a continuous-flow system with low yields.

Carbon disulfide has been utilized in the manufacture of viscose rayon,<sup>28</sup> cellophane,<sup>29</sup> and carbon tetrachloride<sup>30</sup> and it is even used as a solvent in extraction processes.<sup>31</sup> On the laboratory scale, it is a reagent and a powerful building block

<sup>a</sup> Institute of Pharmaceutical Chemistry, University of Szeged, Eötvös u. 6, H-6720 Szeged, Hungary. E-mail: fulop@pharm.u-szeged.hu; Tel: +36 1 3826 616

<sup>b</sup> MTA TTK Lendület Artificial Transporter Research Group, Institute of Materials and Environmental Chemistry, Research Center for Natural Sciences, Hungarian Academy of Sciences, Magyar Tudosok krt. 2, 1117 Budapest, Hungary. E-mail: mandity.istvan@ttk.mta.hu

<sup>c</sup> Research Group of Stereochemistry of the Hungarian Academy of Sciences, Dóm tér 8, H-6720 Szeged, Hungary

<sup>d</sup> Department of Organic Chemistry, Faculty of Pharmacy, Semmelweis University, Hógyes Endre u. 7, H-1092, Budapest, Hungary

† Electronic supplementary information (ESI) available. See DOI: 10.1039/d0cy01603a

in preparative synthesis.<sup>32–37</sup> A previous study showed that carbon disulfide might be a possible reagent for amide and peptide coupling synthesis.<sup>38</sup> They produced peptides from unprotected amino acids under prebiotic conditions by the use of carbon disulfide as an additive. The synthesis of poly- $\beta$ -peptides has recently been described through the ring-opening polymerization of  $\beta$ -amino acid *N*-thiocarboxyanhydrides, as carbon disulfide derivatives.<sup>39</sup>

Flow chemistry methods offer many benefits over the use of conventional batch reactors, including improvements in the reaction rate and yield, safety, reliability, and energy efficiency.<sup>40,41</sup> During the last decade, there was a significant increase in the use of flow chemistry either in the laboratory or at the industrial scale.<sup>42–50</sup> Herein we show that the use of carbon disulfide with alumina utilized in continuous flow (CF) allowed the development of a novel, atom-efficient, green, and sustainable catalytic method for the direct synthesis of amides. Thus, the CF approach could offer the possibility of accomplishing direct amide coupling in a new, unique, and efficient way, providing amides with high yields and excellent purity in a single step.

Reactions were carried out in a home-made continuous-flow reactor: a solid catalyst was loaded into an HPLC column, where the reaction takes place, and an organic solution transported by an HPLC pump was used. The system also contained a GC oven and an in-line back pressure regulator that ensure the required temperature and pressure in the reactor zone, respectively. A schematic outline of the reactor used in this study is shown in Fig. 1.

First, a model reaction was selected utilizing benzylamine and 4-phenylbutyric acid as substrates dissolved in acetonitrile to provide a 100 mM solution. Second, the optimization of reaction parameters was carried out. According to our previous study on the acetylation of amines with acetonitrile, high temperature and a modest pressure were used.<sup>51</sup> The first test was performed without either any catalyst or reagent at 200 °C and 50 bar pressure with a flow rate of 0.1 mL min<sup>-1</sup> and a residence time of 27 min. As expected, no trace of the desired amide product was detected (Table S1,† entry 1). A similar result was found when the reaction was repeated under the same conditions in the presence of alumina (Table S1,† entry 2). However, a low conversion of 22% was attained when 1.5 equivalents of carbon disulfide was used as an additive along with numerous by-products (Table S1,† entry 3). According to the literature data, Lewis acids were used in direct amidation reactions as catalysts.<sup>52–56</sup> Thus several Lewis acids were tested too (Table S2,†). The most promising catalyst was alumina and a significant increase of 53% in the conversion

was observed with the formation of the thiourea side product (Table S2,† entry 4). At this point, the effect of solvent on the reaction outcome was tested. Several solvents were investigated and acetonitrile was found to be the most suitable (Table S3,†). But in favor of an even higher conversion, organic bases, such as triethylamine and pyridine, in a catalytic amount, were added to the starting substrate mixture. However, this afforded only slight improvements (Table S1,† entries 5 and 6), although the formation of the thiourea side product was not observed.

Finally, with the use of 4-dimethylaminopyridine (DMAP) as an organic base, full conversion was reached (Table S1,† entry 7). The base additive was removed by simple filtration on a silica gel plug. Conversions were calculated using the relative signal intensities of the carboxylic acid starting compound.

In order to find the optimal conditions for the flow synthesis, the effect of temperature on the outcome of the reaction was tested under conditions established previously. In a reaction carried out at room temperature, no trace of the desired product was found. The increase of temperature resulted in the increase of conversion and a low 9% was reached at 110 °C. Further temperature increases significantly influenced conversion. The optimal temperature was found to be 200 °C, where >99% conversion was obtained. However, reactions at even higher temperatures provided inferior results (Fig. S1a,†). With respect to pressure, tested at 200 °C, the optimal value was found to be 50 bar reaching full conversion. Raising the pressure higher than 50 bar did not influence the conversion (Fig. S1b,†). A similar test about flow rate gave an optimum value of 0.1 mL min<sup>-1</sup>. Any increase in the flow rate resulted in decreasing conversions (Fig. S1c,†). Analyzing the effect of concentration on the reaction outcome indicated full conversions at lower concentrations. The use of higher concentrations of the starting materials, in turn, resulted in lower conversions (Fig. S1d,†). Finally, the results about changing the quantity of carbon disulfide show that the optimal amount is 1.5 equiv.; lower amounts resulted in decreased conversion, whereas higher amounts did not have any significant effect (Table S4,†).

Inspired by the successful direct amide coupling reaction of the model substrates, we expanded the scope of the reaction, testing various aromatic and aliphatic substrates (Table 1).

Using the optimized protocol (200 °C, 50 bar, 0.1 mL min<sup>-1</sup>, and 27 min residence time), we achieved high yields for 15 different amides. Reactions were carried out with three different carboxylic acids and five different amines including primary aromatic and aliphatic amines and secondary aliphatic amines. All reactions were carried out in a single run. After filtration through a silica gel plug and vacuum evaporation of the solvent, the products were analyzed by <sup>1</sup>H and <sup>13</sup>C NMR spectroscopy without any further purification. This fact makes the technology prominently green and sustainable and the isolation of the products is clearly simple. The synthesized amides and the corresponding

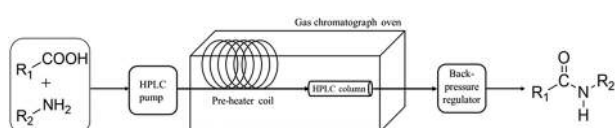
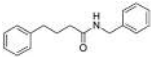
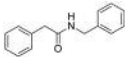
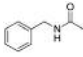
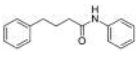
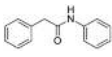
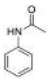
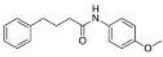
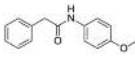
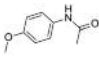
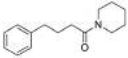
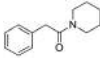
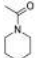
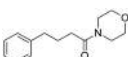
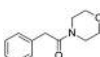
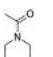


Fig. 1 Schematic illustration of the flow system.

Table 1 Substrate scope of amide formation with isolated yield data<sup>a</sup>

Substrates	4-Phenylbutyric acid	Phenylacetic acid	Acetic acid
Benzylamine	 <b>3</b> 98%	 <b>9</b> 96%	 <b>14</b> 98%
Aniline	 <b>5</b> 96%	 <b>10</b> 95%	 <b>15</b> 98%
<i>p</i> -Anisidine	 <b>6</b> 94%	 <b>11</b> 95%	 <b>16</b> 97%
Piperidine	 <b>7</b> 96%	 <b>12</b> 97%	 <b>17</b> 98%
Morpholine	 <b>8</b> 97%	 <b>13</b> 98%	 <b>18</b> 97%

<sup>a</sup> Reaction conditions: CS<sub>2</sub>, DMAP, Al<sub>2</sub>O<sub>3</sub>, 200 °C, and 50 bar.

isolated yields are shown in Table 1. In all cases, the NMR experiments showed full conversions.

Catalyst reusability with 30 mg of the model starting substrates was tested too. Importantly, the activity of the catalyst did not decrease significantly after 30 cycles (Fig. 2). This result opens the way to scale up the reaction using the model reaction. A scale-up reaction was carried out and 2 grams and 10 grams of the product were isolated after *ca.* 13 hours of working time and *ca.* 3 days of operation, respectively, without a significant loss of productivity of the system.

To establish a reaction mechanism, the literature data and the results gained by the optimization steps were considered.

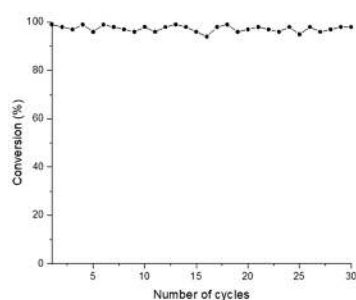
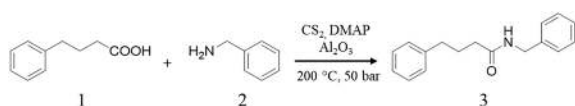


Fig. 2 Robustness of the amide formation reaction was investigated in the reaction of model substrates. The same reaction was repeated 30 times on the same catalyst.

The first step is the reaction of the amine (**m1**) and carbon disulfide (CS<sub>2</sub>).<sup>33,57,58</sup> This provides an *N*-alkyldithiocarbamic acid (**m2**), which decomposes by releasing hydrogen sulfide (H<sub>2</sub>S) and affords an isothiocyanate (**m3**). The formation of H<sub>2</sub>S was confirmed by a simple analytical technology. The lead(II) acetate moistened filter paper turned into brown in the gas space of the reaction mixture collecting baker. This fact indicates the formation of PbS by the reaction of lead(II) ions and H<sub>2</sub>S. According to literature studies,<sup>59–61</sup> we propose

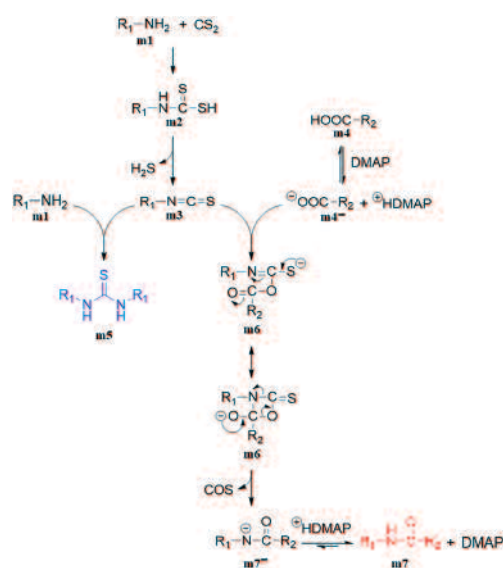


Fig. 3 Plausible mechanism for the alumina-catalyzed amide coupling with carbon disulfide.

that the isothiocyanate (**m3**) is a key element in the direct amidation reaction. In the absence of an organic base, the formation of a thiourea side product (**m5**) was observed. However, if DMAP was present in a catalytic amount, the formation of the desired amide product (**m7**) was detected. This fact can be explained by the deprotonation of the carboxylic acid providing protonated DMAP and **m4**<sup>-</sup>. The latter is more nucleophilic and reacts more rapidly with isothiocyanate **m3** than the amines. The formation of amide product **m7** can be explained by the two mesomeric forms of intermediate **m6**. Furthermore, the necessity of using a catalytic amount of DMAP can be interpreted too, since the last step, when **m7**<sup>-</sup> transforms into **m7**, is a protonation reaction. We suggest that, as indicated, protonated DMAP (+HDMAP) is involved in the last product-forming step. Then, DMAP thus formed is protonated and starts the process again. Therefore, it plays a key role in the proton shuffling (Fig. 3).

## Conclusions

In summary, direct amide synthesis from cheap and easily available carboxylic acids and amines was carried out in CF. The developed technology is time and cost efficient and applies acetonitrile as the solvent, which is a relatively cheap industrial side-product. The utilized additives, alumina and carbon disulfide, are broadly used in several industrial processes too. The scope of the reaction was extended to the preparation of 15 diverse amides. Reactions were carried out with three different carboxylic acids and five amines, including primary and secondary aliphatic amines and primary aromatic amines. In general, full conversions and excellent yields were achieved under the optimized conditions, without the need of any intensive purification step. Catalyst reusability was tested too. The same catalyst bed could be recycled for 30 runs without any significant loss of activity. Additionally, the reaction was successfully scaled up to a 2 gram quantity performed in *ca.* 13 hours. This methodology could become broadly applicable for direct amide synthesis utilizing the industrially reliable continuous technology.

## Conflicts of interest

There are no conflicts to declare.

## Acknowledgements

The Lendület grant from the Hungarian Academy of Sciences is gratefully acknowledged. This work was completed in the ELTE Thematic Excellence Programme supported by the Hungarian Ministry for Innovation and Technology. Project no. 2018-1.2.1-NKP-2018-00005 has been implemented with the support provided by the National Research, Development and Innovation Fund of Hungary, financed under the 2018-1.2.1-NKP funding scheme.

## Notes and references

- V. R. Pattabiraman and J. W. Bode, *Nature*, 2011, **480**, 471–479.
- K. Scheidt, *Nature*, 2010, **465**, 1020–1022.
- B. Shen, D. M. Makley and J. N. Johnston, *Nature*, 2010, **465**, 1027–1032.
- D. Aldeghaither, B. Smaglo and L. Weiner, *J. Clin. Pharmacol.*, 2015, **55**(Suppl 3), S4–S20.
- P. Chames, M. Van Regenmortel, E. Weiss and D. Baty, *Br. J. Pharmacol.*, 2009, **157**, 220–233.
- A. Davenport, C. Scully, C. de Graaf, A. Brown and J. Maguire, *Nat. Rev. Drug Discovery*, 2020, **19**, 389–413.
- D. J. Drucker, *Nat. Rev. Drug Discovery*, 2020, **19**, 277–289.
- J. Lau and M. Dunn, *Bioorg. Med. Chem.*, 2018, **26**, 2700–2707.
- J. M. García, F. C. García, F. Serna and J. L. de la Peña, *Prog. Polym. Sci.*, 2010, **35**, 623–686.
- S. F. Banani, H. O. Lee, A. A. Hyman and M. K. Rosen, *Nat. Rev. Mol. Cell Biol.*, 2017, **18**, 285–298.
- D. Mazia and D. M. Prescott, *Nature*, 1955, **175**, 300–301.
- C. L. Allen and J. M. J. Williams, *Chem. Soc. Rev.*, 2011, **40**, 3405–3415.
- E. Valeur and M. Bradley, *Chem. Soc. Rev.*, 2009, **38**, 606–631.
- H. Xu, X. Qiao, S. Yang and Z. Shen, *J. Org. Chem.*, 2014, **79**, 4414–4422.
- R. M. Lanigan and T. D. Sheppard, *Eur. J. Org. Chem.*, 2013, **2013**, 7453–7465.
- C. A. G. N. Montalbetti and V. Falque, *Tetrahedron*, 2005, **61**, 10827–10852.
- J. Dunetz, J. Magano and G. Weisenburger, *Org. Process Res. Dev.*, 2016, **20**, 140–177.
- B. Mahjour, Y. Shen, W. Liu and T. Cernak, *Nature*, 2020, **580**, 71–75.
- M. Sabatini, L. Boulton, H. Sneddon and T. Sheppard, *Nat. Catal.*, 2019, **2**, 10–17.
- X. Wang, *Nat. Catal.*, 2019, **2**, 98–102.
- K. Wehrstedt, P. A. Wandrey and D. Heitkamp, *J. Hazard. Mater.*, 2005, **126**, 1–7.
- H. Sigel and R. B. Martin, *Chem. Rev.*, 1982, **82**, 385–426.
- J. A. Mitchell and E. E. Reid, *J. Am. Chem. Soc.*, 1931, **53**, 1879–1883.
- N. Gernigon, R. M. Al-Zoubi and D. G. Hall, *J. Org. Chem.*, 2012, **77**, 8386–8400.
- H. Charville, D. Jackson, G. Hodges and A. Whiting, *Chem. Commun.*, 2010, **46**, 1813–1823.
- R. M. Al-Zoubi, O. Marion and D. G. Hall, *Angew. Chem., Int. Ed.*, 2008, **47**, 2876–2879.
- Y. Du, T. Barber, S. E. Lim, H. S. Rzepa, I. R. Baxendale and A. Whiting, *Chem. Commun.*, 2019, **55**, 2916–2919.
- C. Tian, L. Zheng, Q. Miao, C. Cao and Y. Ni, *Cellulose*, 2014, **21**, 3647–3654.
- J. Brasier, *Mater. Des.*, 1986, **7**, 65–67.
- J. F. Devlin and D. Müller, *Environ. Sci. Technol.*, 1999, **33**, 1021–1027.
- R. Cucciniello, A. Proto, F. Rossi, N. Marchettini and O. Motta, *Anal. Methods*, 2015, **7**, 4811–4815.

- 32 M. Gholinejad, *Eur. J. Org. Chem.*, 2013, **2013**, 257–259.
- 33 W.-D. Rudolf, *J. Sulfur Chem.*, 2007, **28**, 295–339.
- 34 N. Azizi, B. Pourhasan, F. Aryanasab and M. Saidi, *Synlett*, 2007, **8**, 1239–1242.
- 35 P. Svoronos and T. Bruno, *Ind. Eng. Chem. Res.*, 2002, **41**, 5321–5336.
- 36 N. Kihara, Y. Nakawaki and T. Endo, *J. Org. Chem.*, 1995, **60**, 473–475.
- 37 R. J. Ferm, *Chem. Rev.*, 1957, **57**, 621–640.
- 38 L. J. Leman, Z.-Z. Huang and M. R. Ghadiri, *Astrobiology*, 2015, **15**, 709–716.
- 39 M. Zhou, X. Xiao, Z. Cong, Y. Wu, W. Zhang, P. Ma, S. Chen, H. Zhang, D. Zhang, D. Zhang, X. Luan, Y. Mai and R. Liu, *Angew. Chem., Int. Ed.*, 2020, **59**, 7240–7244.
- 40 P. Watts, The Application of Flow Chemistry in the Use of Highly Reactive Intermediates and Reagents: Methods and Applications, in *Sustainable Flow Chemistry: Methods and Applications*, Wiley-VCH, 2017, pp. 193–217.
- 41 T. Noel and V. Hessel, Chemical Intensification in Flow Chemistry through Harsh Reaction Conditions and New Reaction Design, in *Microreactors in Preparative Chemistry*, Wiley-VCH, 2013, pp. 273–295.
- 42 M. L. Contente, S. Farris, L. Tamborini, F. Molinari and F. Paradisi, *Green Chem.*, 2019, **21**, 3263–3266.
- 43 C. Gomez, G. Hallot, A. Pastor, S. Laurent, E. Brun, C. Sicard-Roselli and M. Port, *Ultrason. Sonochem.*, 2019, **56**, 167–173.
- 44 T. Ichitsuka, N. Suzuki, M. Sairenji, N. Koumura, S.-Y. Onozawa, K. Sato and S. Kobayashi, *ChemCatChem*, 2019, **11**, 2427–2431.
- 45 H. Koo, H. Y. Kim and K. Oh, *Org. Chem. Front.*, 2019, **6**, 1868–1872.
- 46 G. Laudadio, G. Fusini, G. Casotti, C. Evangelisti, G. Angelici and A. Carpita, *J. Flow Chem.*, 2019, **9**, 133–143.
- 47 V. R. L. J. Bloemendal, S. J. Moons, J. J. A. Heming, M. Chayoua, O. Niesink, J. Hest, T. J. Boltje and F. Rutjes, *Adv. Synth. Catal.*, 2019, **361**, 2443–2447.
- 48 M. Shang and V. Hessel, Synthesis and Application of H<sub>2</sub>O<sub>2</sub> in Flow Reactors, in *Sustainable Flow Chemistry*, Wiley-VCH, 2017, pp. 43–72.
- 49 A. Piskun, J. de Haan, E. Wilbers, H. van de Bovenkamp, Z. Tang and H. J. Heeres, *ACS Sustainable Chem. Eng.*, 2016, **4**, 2939–2950.
- 50 A. Hafner and S. Ley, *Synlett*, 2015, **26**, 1470–1474.
- 51 G. Orsy, F. Fülöp and M. I. Mándity, *Molecules*, 2020, **25**, 1985.
- 52 Y. Du, T. Barber, S. Lim, H. Rzepa, I. Baxendale and A. Whiting, *Chem. Commun.*, 2019, **55**, 2916–2919.
- 53 N. Gernigon, R. Al-Zoubi and D. Hall, *J. Org. Chem.*, 2012, **77**, 8386–8400.
- 54 R. Lanigan and T. Sheppard, *Eur. J. Org. Chem.*, 2013, **20**, 7453–7465.
- 55 M. Sayes and A. Charette, *Green Chem.*, 2017, **19**, 5060–5064.
- 56 H. Xu, X. Qiao, S. Yang and Z. Shen, *J. Org. Chem.*, 2014, **79**, 4414–4422.
- 57 F. E. Critchfield and J. B. Johnson, *Anal. Chem.*, 1956, **28**, 430–436.
- 58 N. Sun, B. Li, J. Shao, W. Mo, B. Hu, Z. Shen and X. Hu, *Beilstein J. Org. Chem.*, 2012, **8**, 61–70.
- 59 V. Delaveau, Z. Mouloungui and E. A. Gaset, *Synth. Commun.*, 1996, **26**, 2341–2348.
- 60 R. N. Ram, P. Kumar and A. K. Mukerjee, *J. Chem. Educ.*, 1983, **60**, 508.
- 61 W. R. Vaughan, M. V. Andersen, H. S. Blanchard, D. I. McCane and W. L. Meyer, *J. Org. Chem.*, 1955, **20**, 819–822.



## Direct amide formation in a continuous-flow system mediated by carbon disulfide

György Orsy<sup>a,b</sup>, Ferenc Fülöp<sup>\*a,c</sup>, István M. Mándity<sup>\*b,d</sup>

---

<sup>a.</sup> *Institute of Pharmaceutical Chemistry University of Szeged, Eötvös u. 6, H-6720 Szeged, Hungary.*

<sup>b.</sup> *TTK Lendület Artificial Transporter Research Group, Institute of Materials and Environmental Chemistry, Research Center for Natural Sciences, Hungarian Academy of Sciences, Magyar Tudosok krt. 2, 1117 Budapest, Hungary.*

<sup>c.</sup> *Research Group of Stereochemistry of the Hungarian Academy of Sciences, Dóm tér 8, H-6720 Szeged, Hungary.*

<sup>d.</sup> *Department of Organic Chemistry, Faculty of Pharmacy, Semmelweis University, Hőgyes Endre u. 7, H-1092, Budapest, Hungary.*

### Table of Content

1. General	S2
2. General aspects of the CF direct amidation	S2
3. Product analysis	S2
4. Tables and Figures	S3-S7
5. <sup>1</sup> H and <sup>13</sup> C NMR spectra	S8-S22

## 1. General

All solvents and reagents were of analytical grade and used directly without further purification. Fe, Cu, Fe<sub>2</sub>O<sub>3</sub>, NiO, CuO, Boric acid, AlCl<sub>3</sub>, Al<sub>2</sub>O<sub>3</sub> (for chromatography, activated, neutral, Brockmann I, 50-200 μm, 60 Å) catalysts, carbon disulfide (anhydrous, ≥99%) reagent and organic bases (trimethylamine, pyridine, 4-(dimethylamino)pyridine) used in this study were purchased from Sigma-Aldrich (Budapest, Hungary), while Acetonitrile (100,0%) was HPLC LC MS-grade solvents from VWR International (Debrecen, Hungary).

## 2. General aspects of the Continuous-Flow (CF) amidation

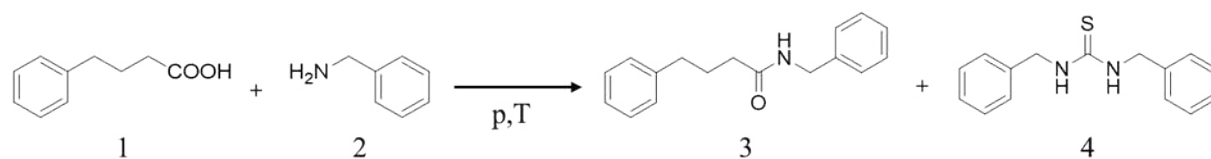
The CF amidation reactions were carried out in a home-made flow reactor consisting of an HPLC pump (Jasco PU-987 Intelligent Prep. Pump), a stainless steel HPLC column as catalyst bed (internal dimensions 250mm L × 4.6 ID × ¼ in OD), a stainless steel preheating coil (internal diameter 1 mm and length 30 cm) and a commercially available backpressure regulator (Thalesnano back pressure module 300™, Budapest, Hungary, to a maximum of 300 bar). Parts of the system were connected with stainless steel tubing (internal diameter 1 mm). The HPLC column was charged with 4 g of the alumina catalyst. It was then placed into a GC oven unit (Carlo Erba HR 5300 up to maximum a 350 °C). For the CF reactions, 100 mM solution of the appropriate starting material was prepared in solvent. The solution was homogenized by sonication for 5 min and then pumped through the CF reactor under the set conditions. After the completion of the reaction, the reaction mixture was collected, and the rest solvent was evaporated by a vacuum rotary evaporator.

## 3. Product analysis

The products obtained were characterized by <sup>1</sup>H NMR spectroscopy. <sup>1</sup>H-NMR and APT-<sup>13</sup>C-NMR spectra were recorded on a Bruker AV NEO Ascend 500 spectrometer and Varian, in DMSO-*d*<sub>6</sub> as applied solvent, at 500.2 MHz. Chemical shifts (δ) are expressed in ppm and are internally referenced (<sup>1</sup>H NMR: 2.50 ppm in DMSO-*d*<sub>6</sub>).

#### 4. Tables and Figures

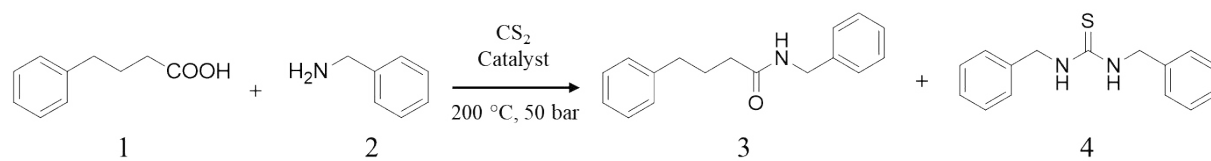
**Table S1.** The model reaction and optimization of amide formation in flow reactor



Entr y	Substrat e A	Substrat e B	Lewis acid	Reagent	Solven t	Conditio n	Conversio n
1	4-PBA	BA	-	-	ACN	200°C 0.1 ml/min 50 bar	0%
2	4-PBA	BA	Alumina	-	ACN	200°C 0.1 ml/min 50 bar	0% <sup>a</sup>
3	4-PBA	BA	-	CS <sub>2</sub>	ACN	200 °C 0.1 ml/min 50 bar	22%
4	4-PBA	BA	Alumina	CS <sub>2</sub>	ACN	200 °C 0.1 ml/min 50 bar	53% <sup>b</sup>
5	4-PBA	BA	Alumina	CS <sub>2</sub> Triethylamine	ACN	200 °C 0.1 ml/min 50 bar	62%
6	4-PBA	BA	Alumina	CS <sub>2</sub> Pyridine	ACN	200 °C 0.1 ml/min 50 bar	58%
7	4-PBA	BA	Alumina	CS <sub>2</sub> DMAP	ACN	200 °C 0.1 ml/min 50 bar	>99%

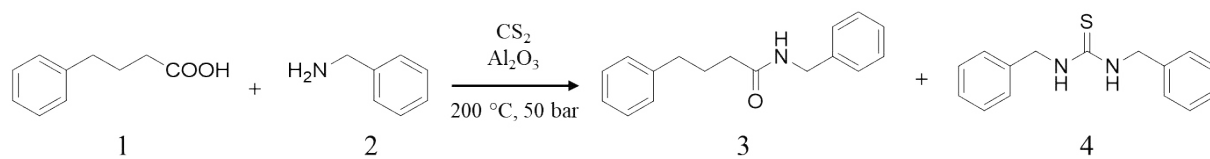
4-PBA: 4-phenylbutyric acid, BA: benzylamine, DMAP: 4-(dimethylamino)pyridine, ACN: acetonitrile, CS<sub>2</sub>: carbon disulfide, a: Acetylation side reaction was only observed; b: 31% thiourea formation was observed.



**Table S2.** Screen of alternative catalysts

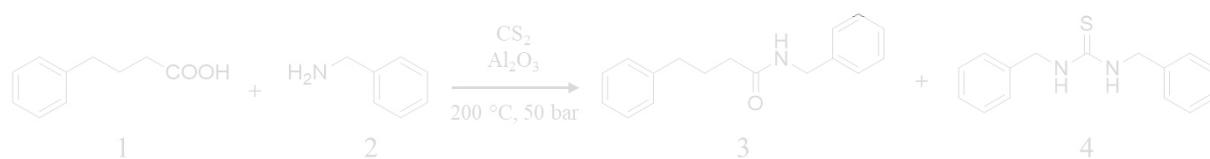
<i>Entry</i>	<i>Lewis acid</i>	<i>Reagent</i>	<i>Solvent</i>	<i>Conversion into 3 (%)</i>
<i>1</i>	boric acid	$\text{CS}_2$	acetonitrile	2%
<i>2</i>	Fe	$\text{CS}_2$	acetonitrile	3%
<i>3</i>	Cu	$\text{CS}_2$	acetonitrile	17%
<i>4</i>	$\text{Fe}_2\text{O}_3$	$\text{CS}_2$	acetonitrile	10%
<i>5</i>	NiO	$\text{CS}_2$	acetonitrile	4%
<i>6</i>	CuO	$\text{CS}_2$	acetonitrile	40%
<i>7</i>	$\text{Al}_2\text{O}_3$	$\text{CS}_2$	acetonitrile	53%

1 equiv. 4-phenylbutyric acid (100 mM), 1 equiv. benzyl amine (100 mM), *Reagent*: 1.5 equiv.  $\text{CS}_2$  *Condition*:  $200\text{ }^\circ\text{C}$ , 50 bar,  $0.1\text{ mL min}^{-1}$ , 27 min residence time

**Table S3.** Direct amide bond formation in a range of solvents

<i>Entry</i>	<i>Solvent</i>	<i>Conversion into 3 (%)</i>
1	Water	0%
2	Methanol	31%
3	Isopropanol	10%
4	Toluene	43%
5	Acetonitrile	53%
6	Dichloromethane	0%
7	Dimethylsulfoxide	4%

1 equiv. 4-phenylbutyric acid (100 mM), 1 equiv. benzyl amine (100 mM), *Lewis acid*: alumina, *Reagent*: 1.5 equiv.  $\text{CS}_2$  *Condition*:  $200\text{ }^\circ\text{C}$ , 50 bar,  $0.1\text{ mL min}^{-1}$ , 27 min residence time

**Table S4.** Effect of the different amount of carbon disulfide

<i>Entry</i>	<i>Lewis acid</i>	<i>Reagent</i>	<i>Solvent</i>	<i>Conversion into 3 (%)</i>
1	$\text{Al}_2\text{O}_3$	0.5 equiv $\text{CS}_2$	acetonitrile	26%
2	$\text{Al}_2\text{O}_3$	1 equiv $\text{CS}_2$	acetonitrile	43%
3	$\text{Al}_2\text{O}_3$	1.5 equiv $\text{CS}_2$	acetonitrile	53%
4	$\text{Al}_2\text{O}_3$	2 equiv $\text{CS}_2$	acetonitrile	49%
5	$\text{Al}_2\text{O}_3$	3 equiv $\text{CS}_2$	acetonitrile	45%

1 equiv. 4-phenylbutyric acid (100 mM), 1 equiv. benzyl amine (100 mM), Lewis acid: alumina, Reagent:  $\text{CS}_2$  Condition:  $200\text{ }^\circ\text{C}$ , 50 bar,  $0.1\text{ mL min}^{-1}$ , 27 min residence time

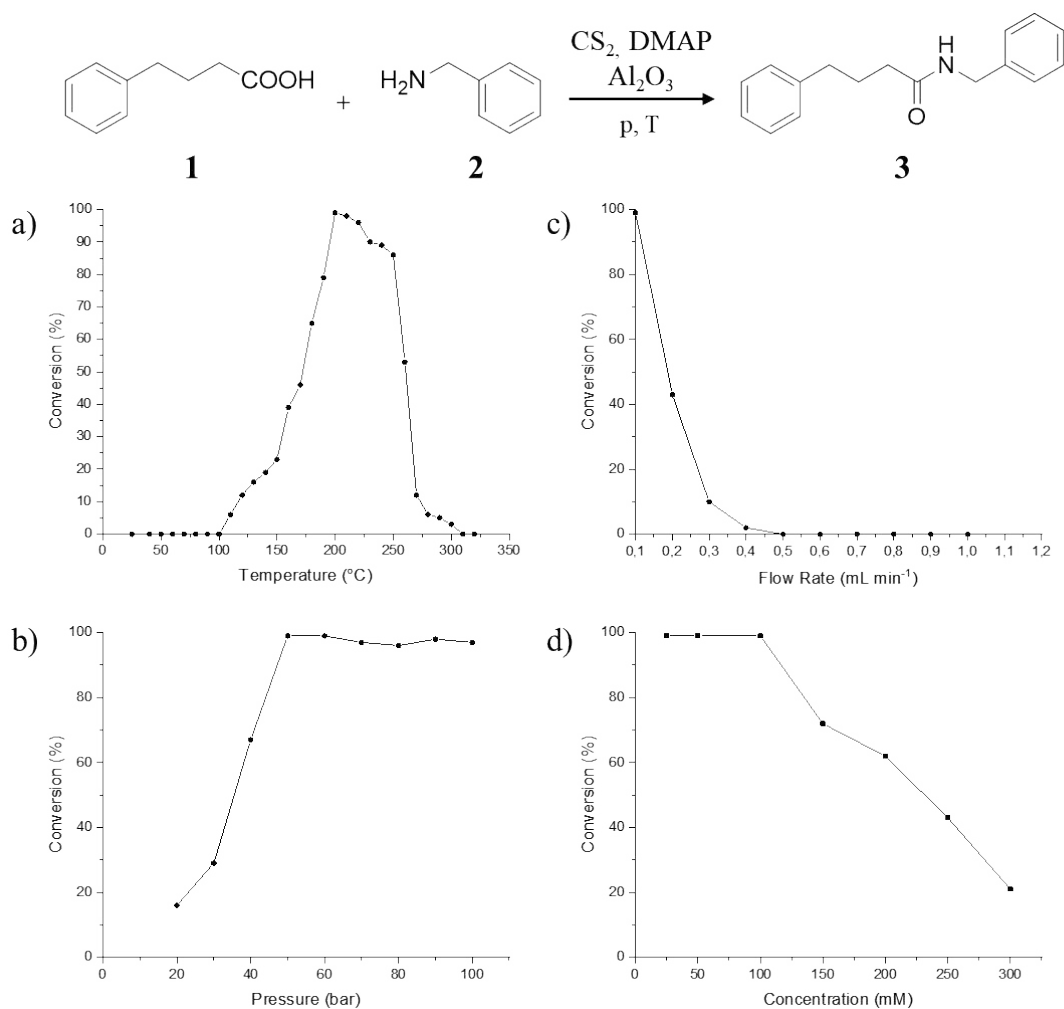
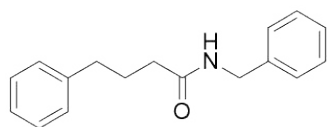


**Fig. S1** The effect of temperature (a), pressure (b), flow rate (c), and concentration of the starting materials (d) on the reaction conversion catalyzed by  $\text{Al}_2\text{O}_3$ . The effect of the pressure was measured at room temperature, the influence of temperature was determined at 50 bar, while the effect of the flow rate and concentration was analyzed under the optimized conditions.

## 5. $^1\text{H}$ and $^{13}\text{C}$ NMR spectra



N-benzyl-4-phenylbutanamide

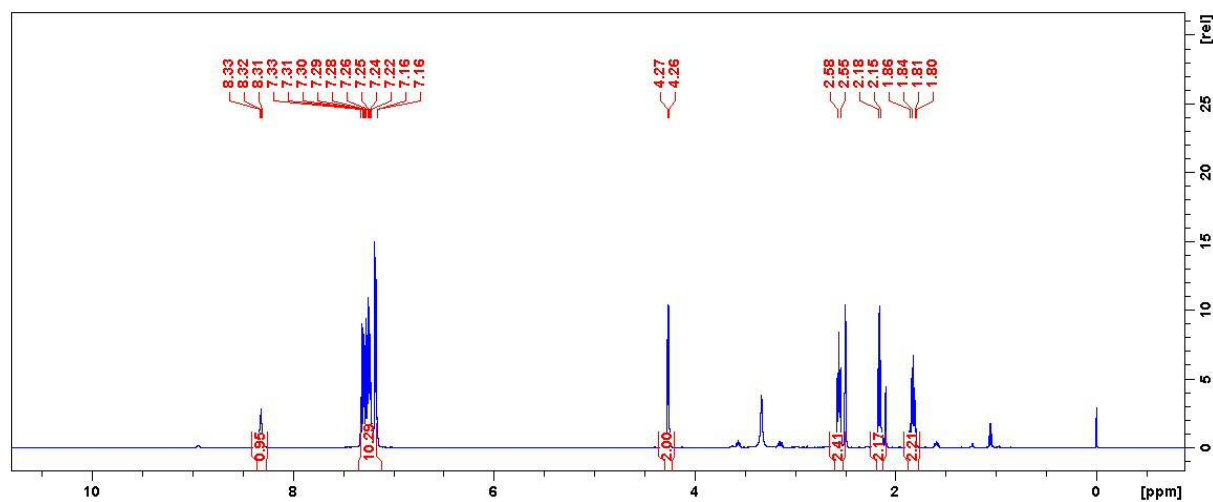


**Figure S2.**  $^1\text{H}$  NMR spectrum of N-benzyl-4-phenylbutanamide measured in DMSO- $d_6$  at 296 K.

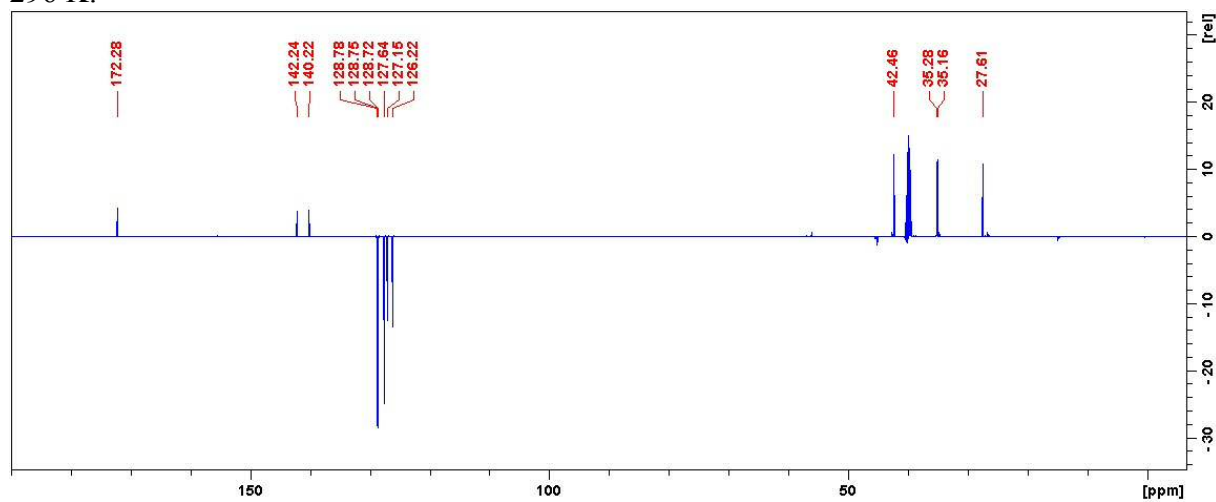
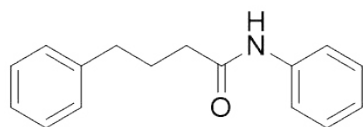


**Figure S3.** APT  $^{13}\text{C}$  NMR spectrum of N-benzyl-4-phenylbutanamide measured in DMSO- $d_6$  at 296 K.



N,4-diphenylbutanamide

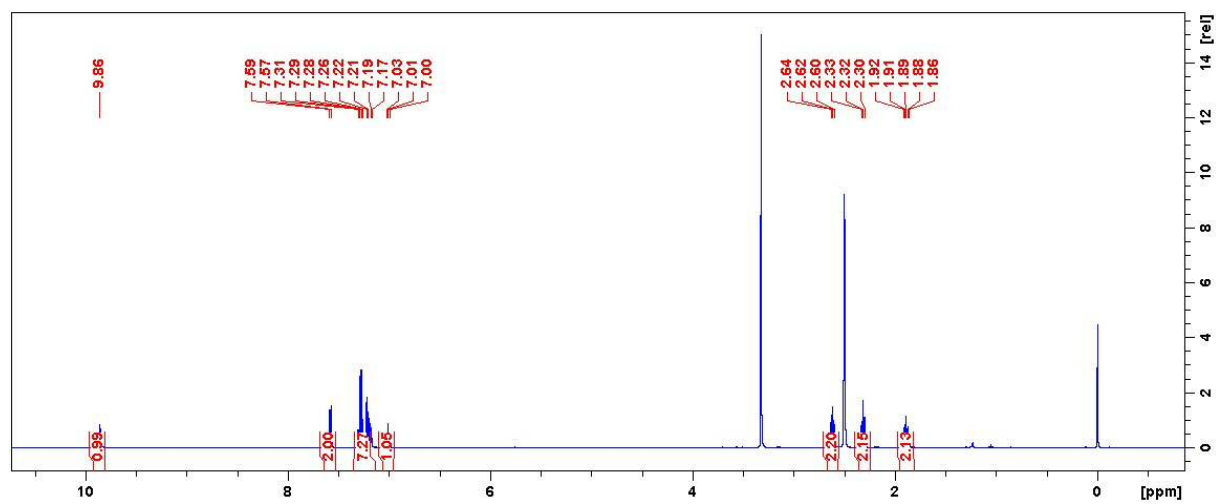


Figure S4.  $^1\text{H}$  NMR spectrum of N,4-diphenylbutanamide measured in DMSO- $d_6$  at 296 K.

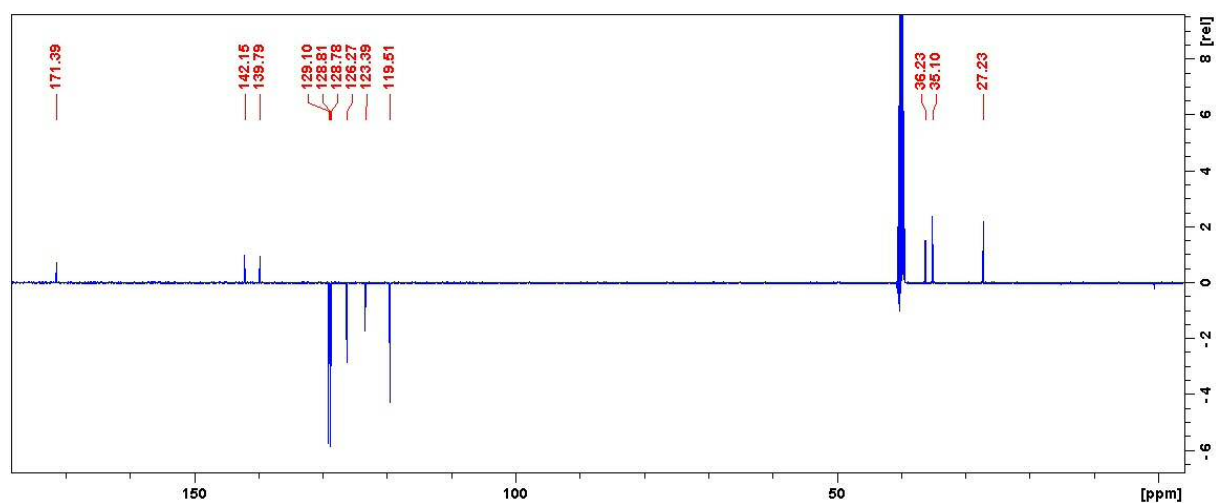
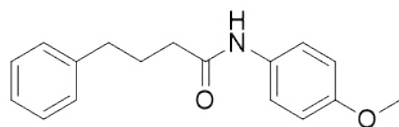
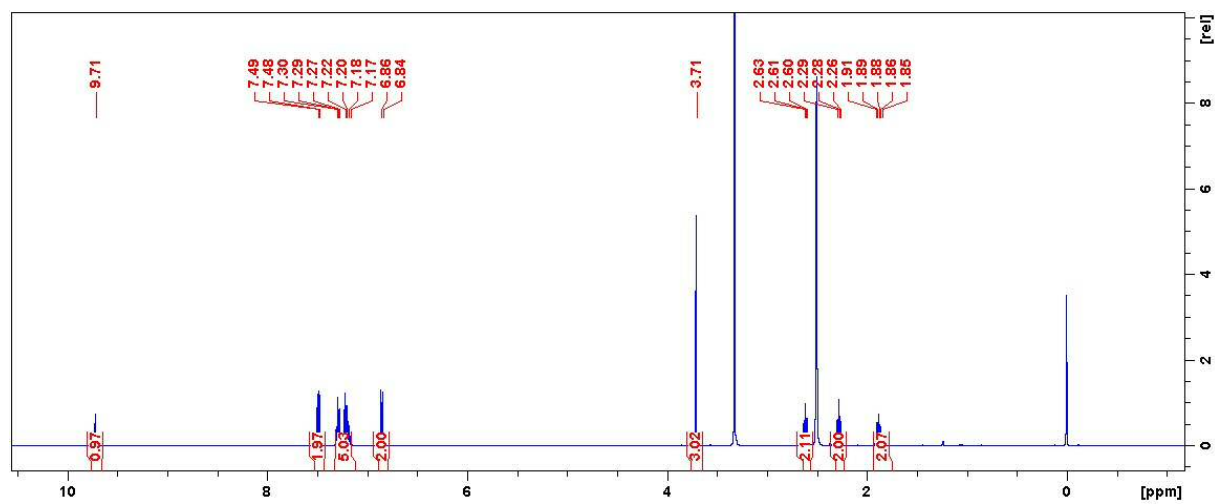


Figure S5. APT NMR spectrum of N,4-diphenylbutanamide measured in DMSO- $d_6$  at 296 K.



N-(4-methoxyphenyl)-4-phenylbutanamide



**Figure S6.**  $^1\text{H}$  NMR spectrum of N-(4-methoxyphenyl)-4-phenylbutanamide measured in DMSO- $d_6$  at 296 K.

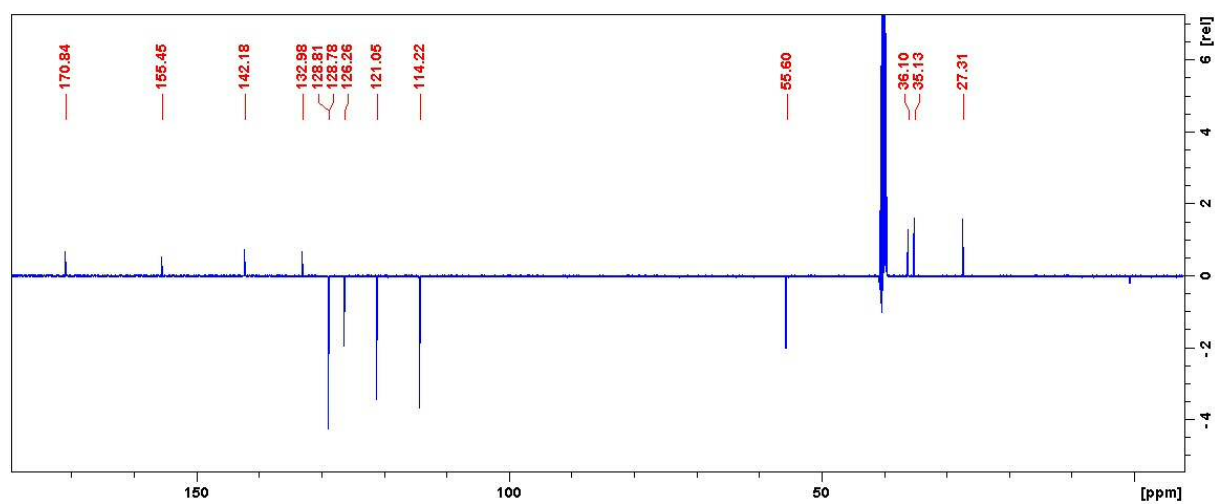
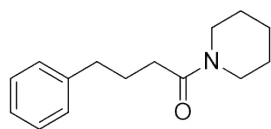


**Figure S7.** ATP NMR spectrum of N-(4-methoxyphenyl)-4-phenylbutanamide measured in DMSO- $d_6$  at 296 K.



4-phenyl-1-(piperidin-1-yl)butan-1-one

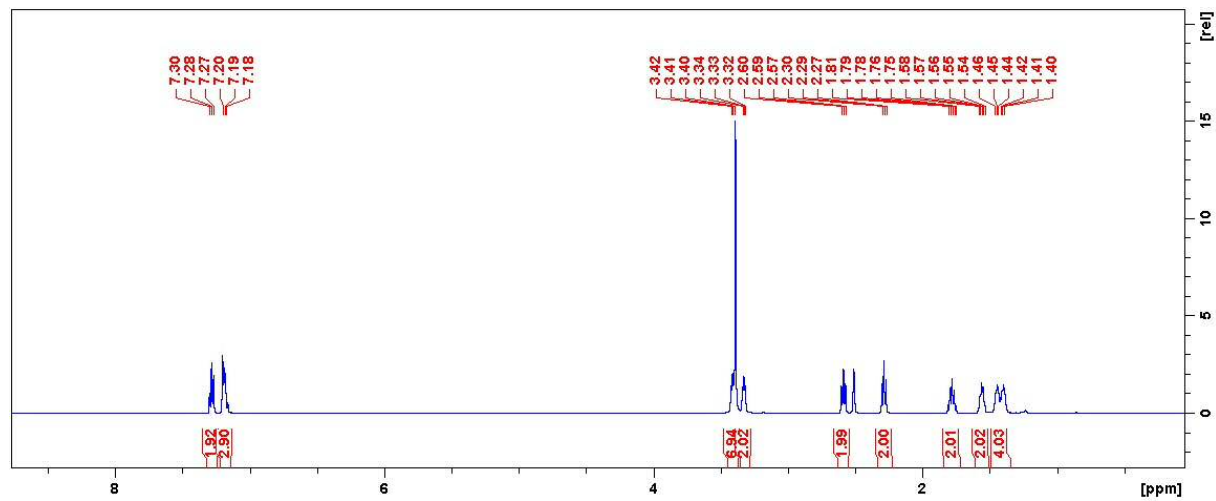


**Figure S8.** <sup>1</sup>H NMR spectrum of 4-phenyl-1-(piperidin-1-yl)butan-1-one measured in DMSO-d<sub>6</sub> at 296 K.

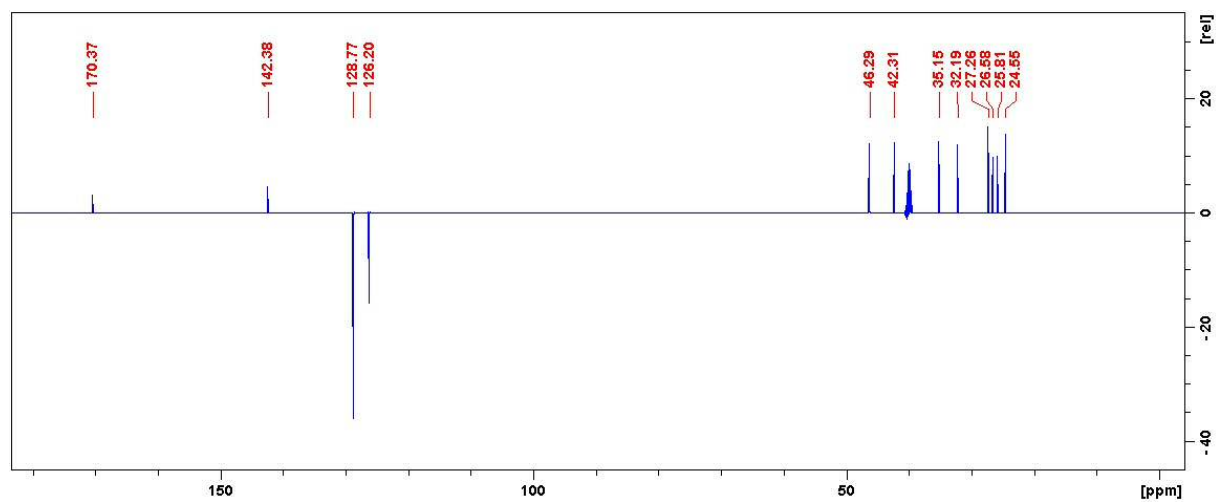
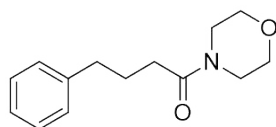


**Figure S9.** APT NMR spectrum of 4-phenyl-1-(piperidin-1-yl)butan-1-one measured in DMSO-d<sub>6</sub> at 296 K.





4-phenyl-1-(piperidin-1-yl)butan-1-one

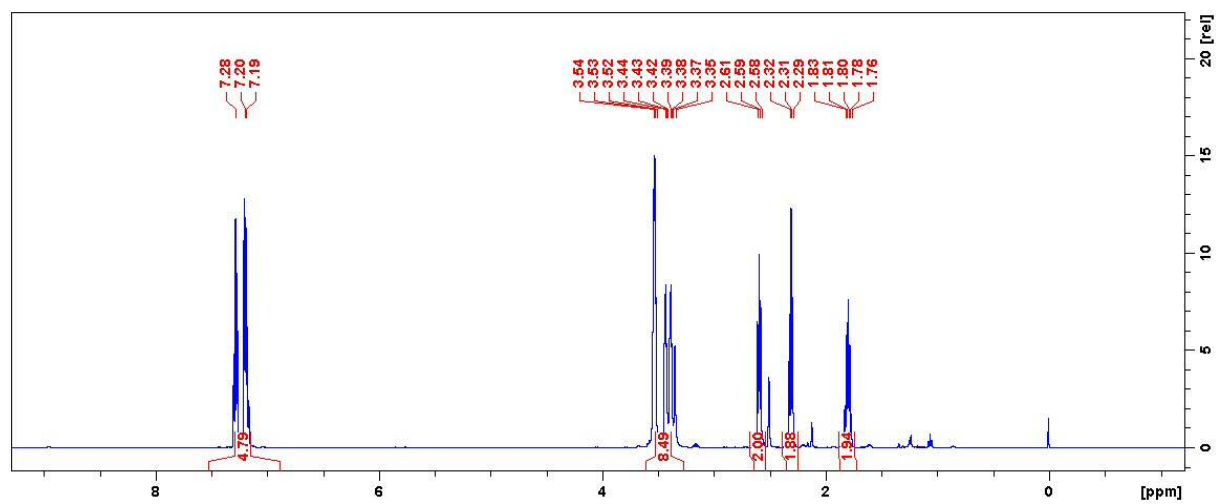


**Figure S10.**  $^1\text{H}$  NMR spectrum of 4-phenyl-1-(piperidin-1-yl)butan-1-one measured in DMSO- $d_6$  at 296 K.

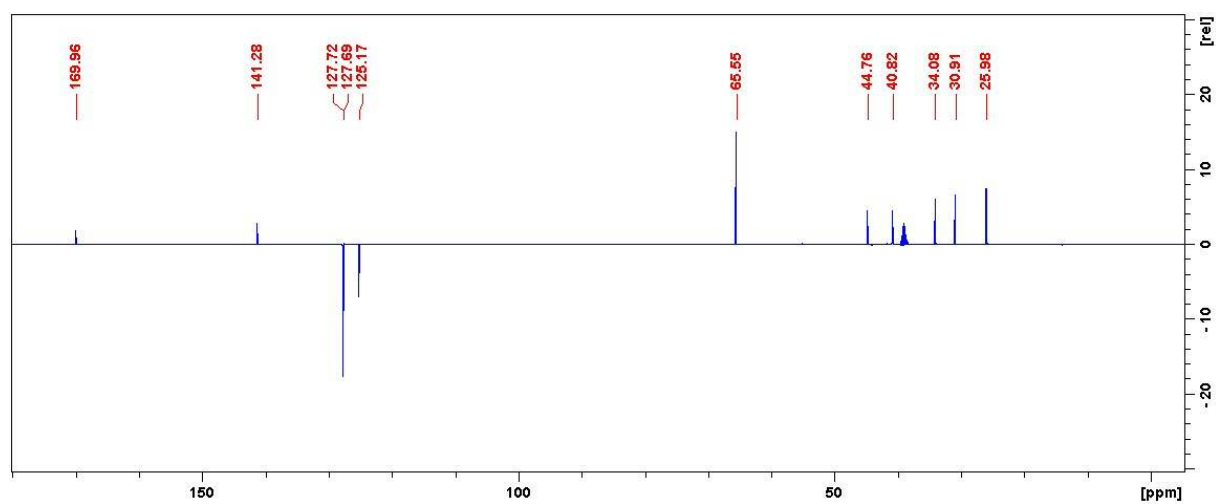
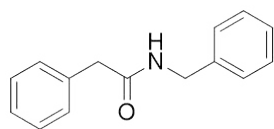


**Figure S11.** ATP NMR spectrum of 4-phenyl-1-(piperidin-1-yl)butan-1-one measured in DMSO- $d_6$  at 296 K.



N-benzyl-2-phenylacetamide

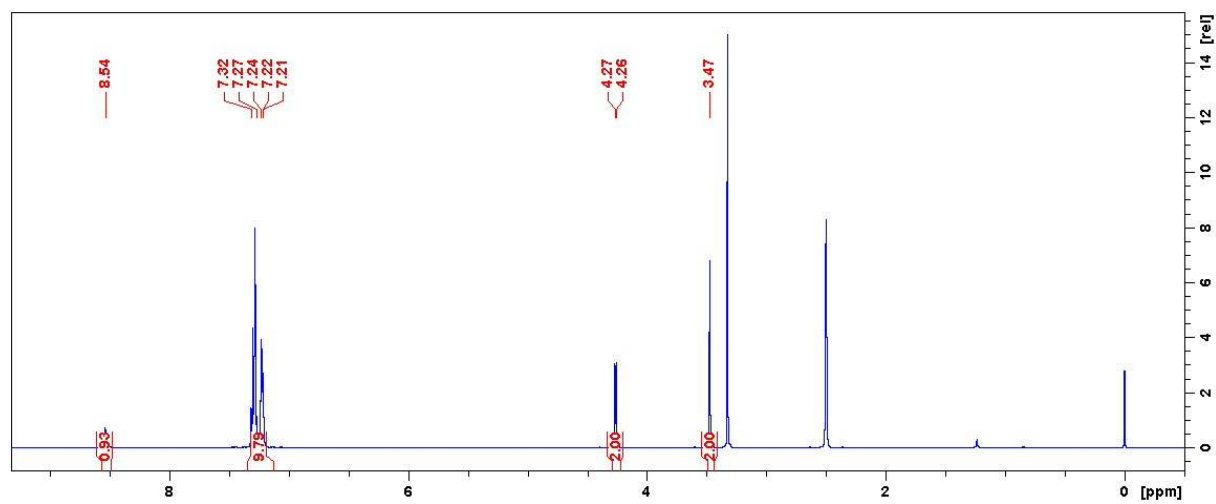


**Figure S12.** <sup>1</sup>H NMR spectrum of N-benzyl-2-phenylacetamide measured in DMSO-d<sub>6</sub> at 296 K.

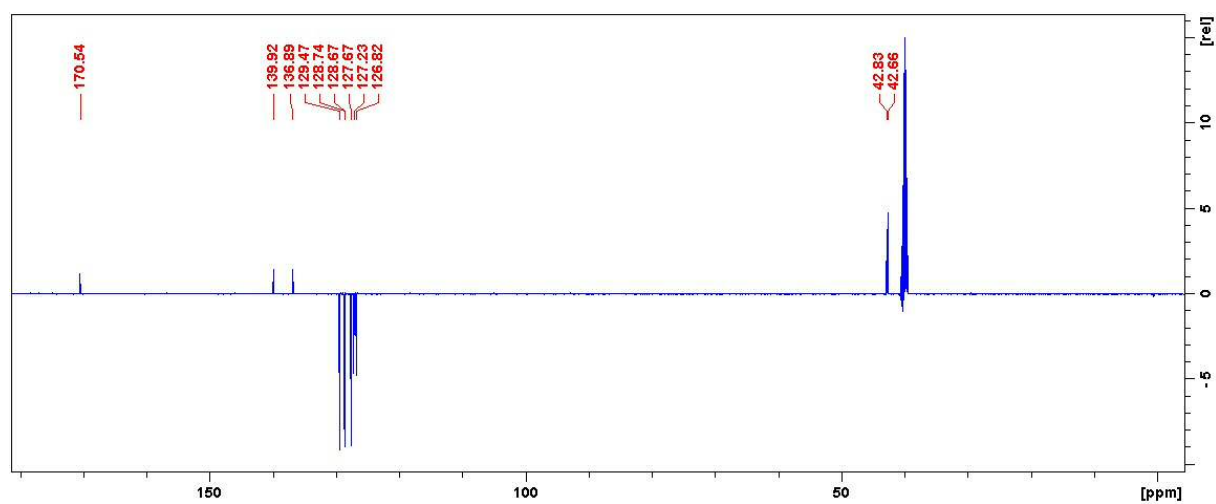
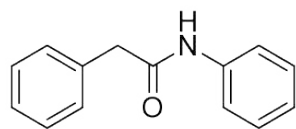


**Figure S13.** APT NMR spectrum of N-benzyl-2-phenylacetamide measured in DMSO-d<sub>6</sub> at 296 K.



N,2-diphenylacetamide

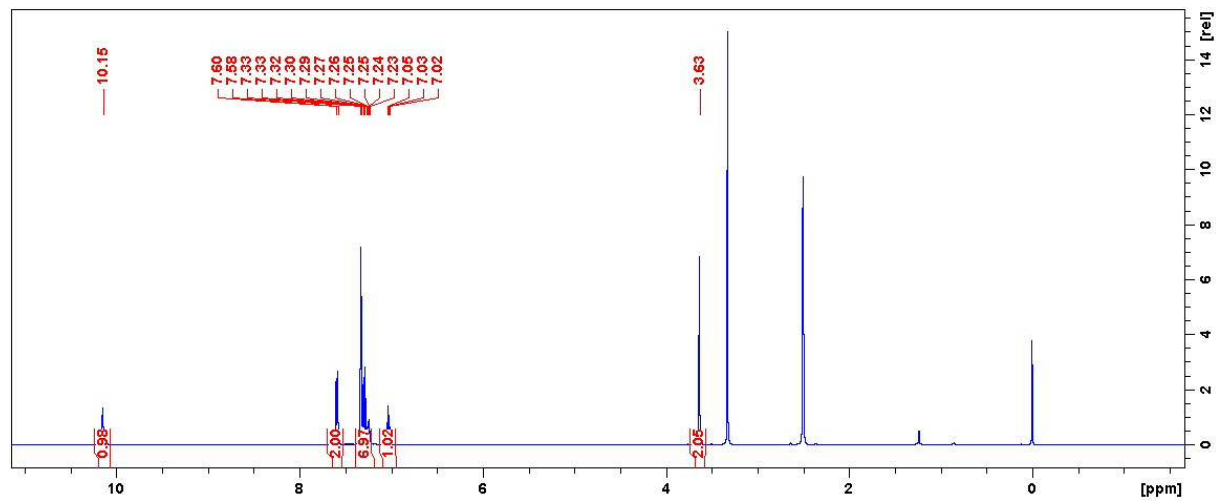


Figure S14.  $^1\text{H}$  NMR spectrum of N,2-diphenylacetamide measured in DMSO- $d_6$  at 296 K.

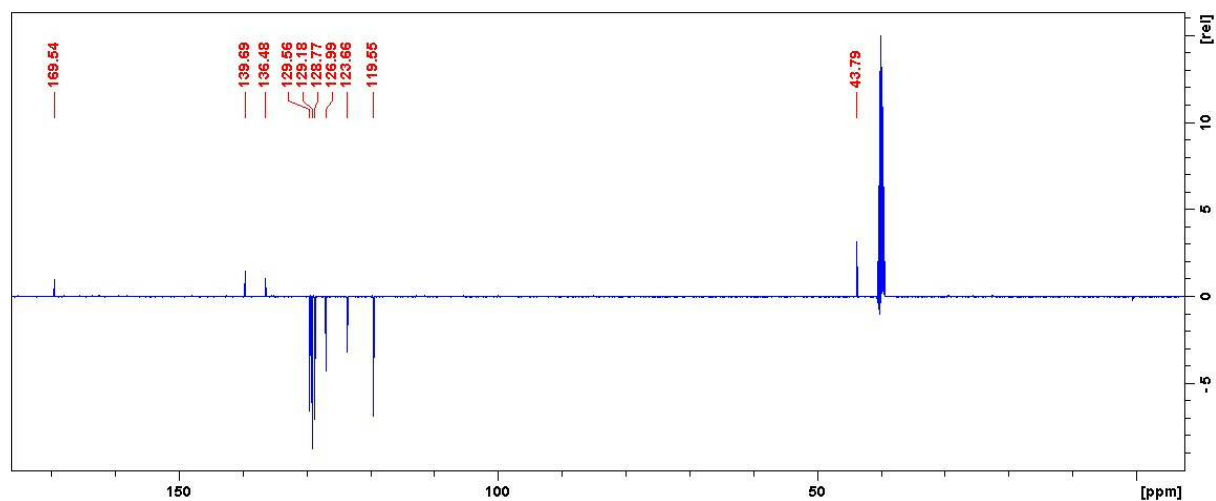
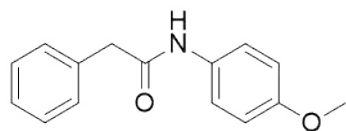
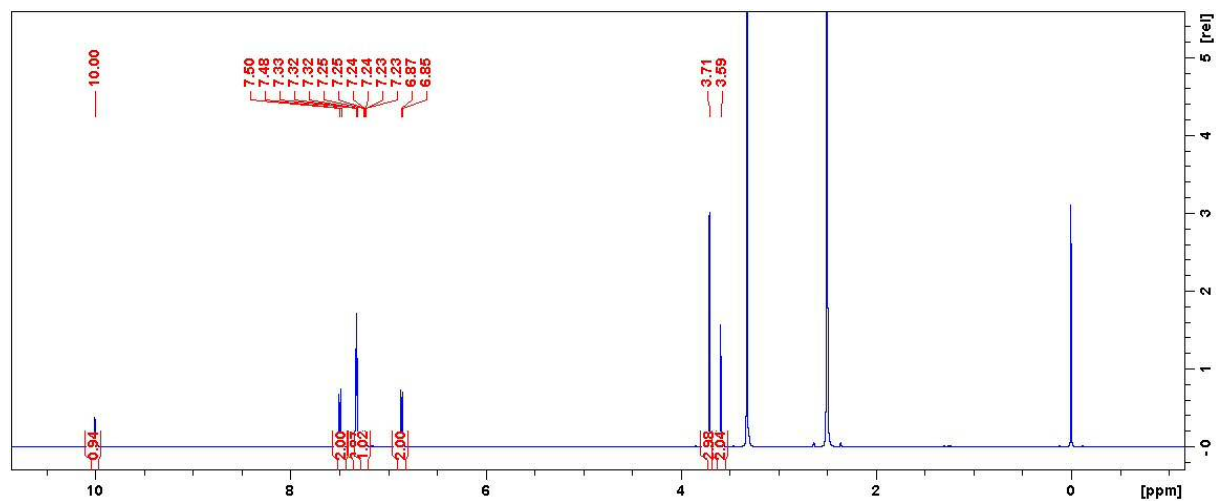


Figure S15. APT NMR spectrum of N,2-diphenylacetamide measured in DMSO- $d_6$  at 296 K.



N-(4-methoxyphenyl)-2-phenylacetamide



**Figure S16.**  $^1\text{H}$  NMR spectrum of N-(4-methoxyphenyl)-2-phenylacetamide measured in DMSO- $d_6$  at 296 K.

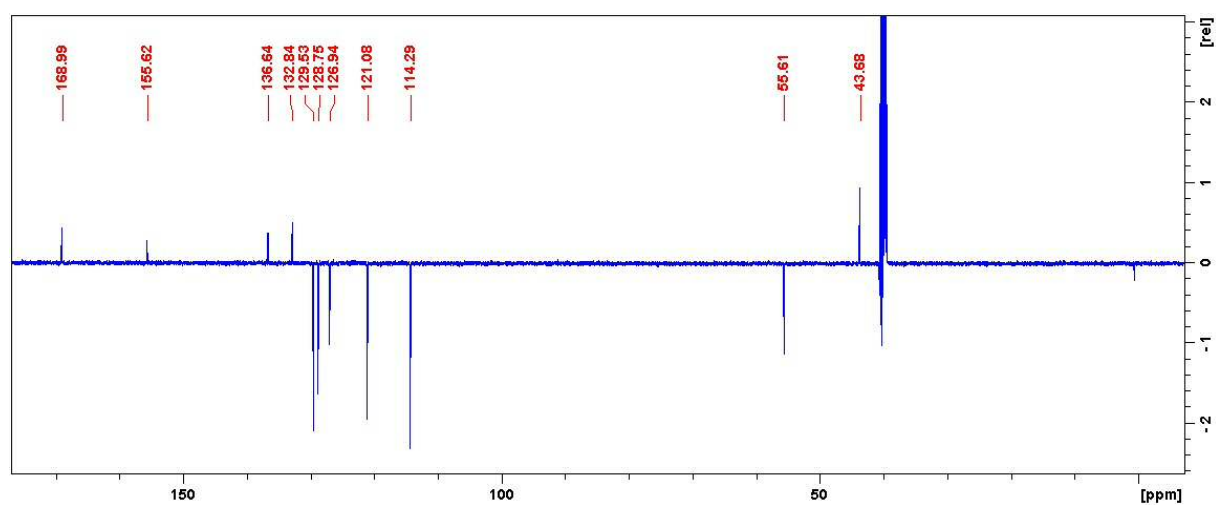
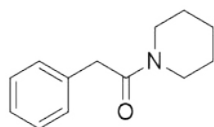


**Figure S17.** APT NMR spectrum of N-(4-methoxyphenyl)-2-phenylacetamide measured in DMSO- $d_6$  at 296 K.



2-phenyl-1-(piperidin-1-yl)ethanone

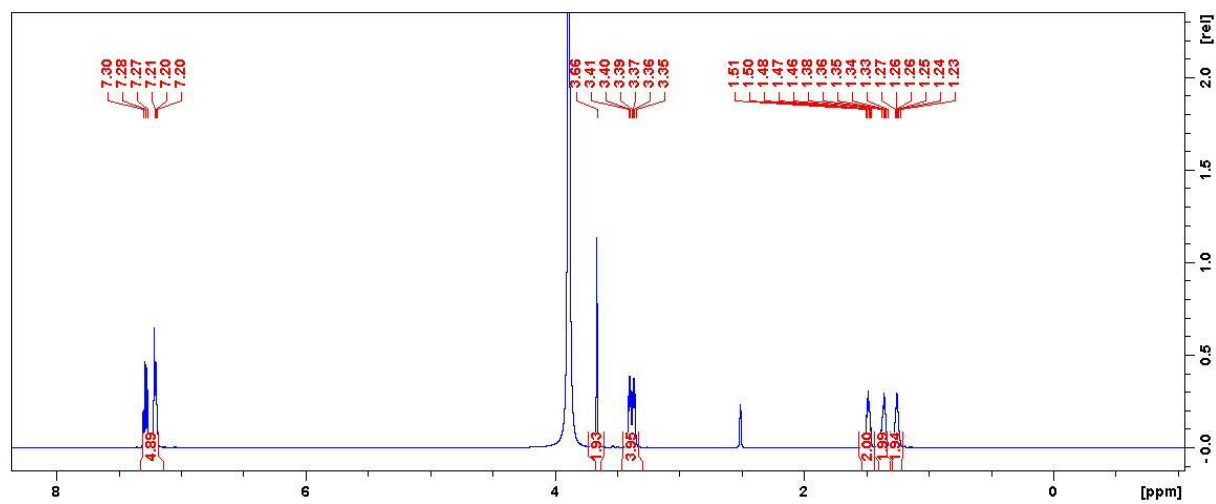


**Figure S18.** <sup>1</sup>H NMR spectrum of 2-phenyl-1-(piperidin-1-yl)ethanone measured in DMSO-d<sub>6</sub> at 296 K.

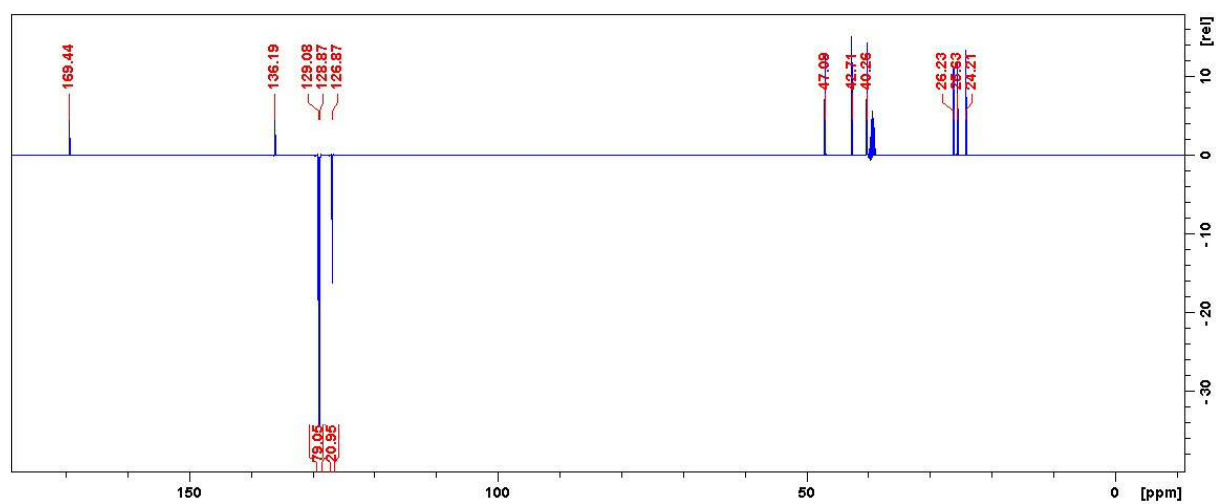
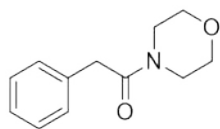


**Figure S19.** APT NMR spectrum of 2-phenyl-1-(piperidin-1-yl)ethanone measured in DMSO-d<sub>6</sub> at 296 K.



1-morpholino-2-phenylethanone

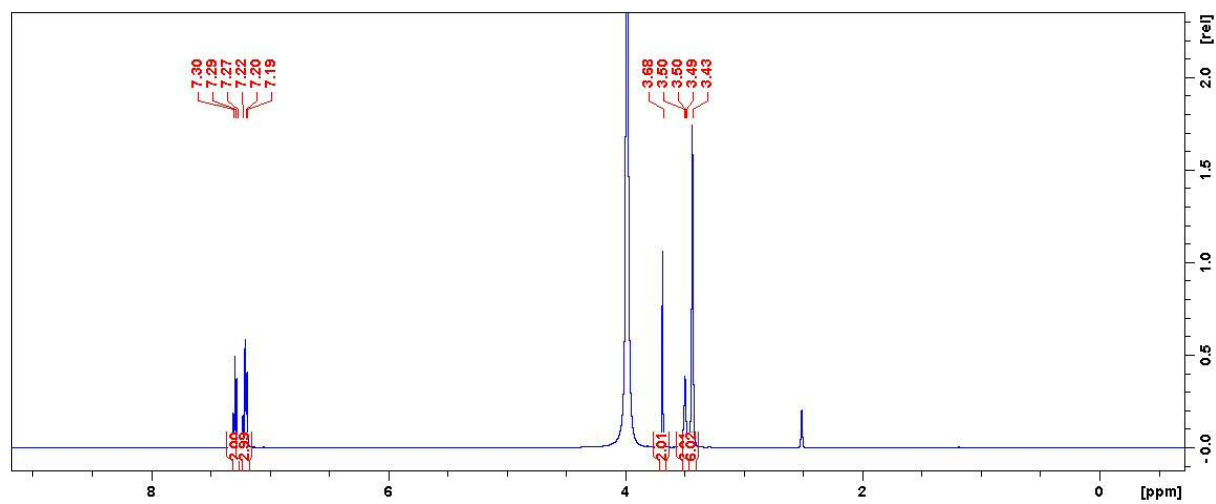


**Figure S20.**  $^1\text{H}$  NMR spectrum of 1-morpholino-2-phenylethanone measured in DMSO- $d_6$  at 296 K.

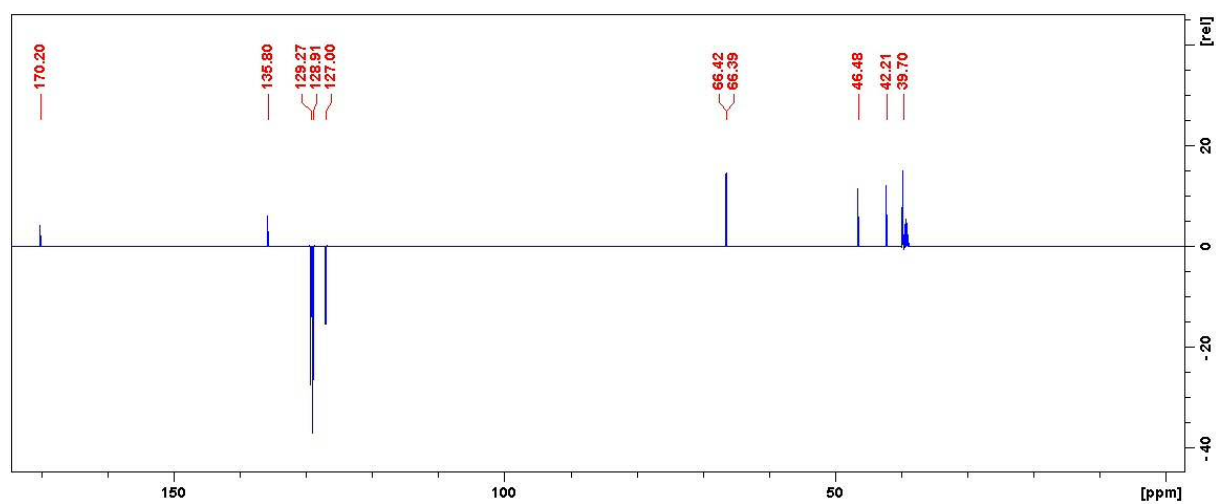
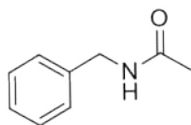


**Figure S21.** APT NMR spectrum of 1-morpholino-2-phenylethanone measured in DMSO- $d_6$  at 296 K.



N-benzylacetamide

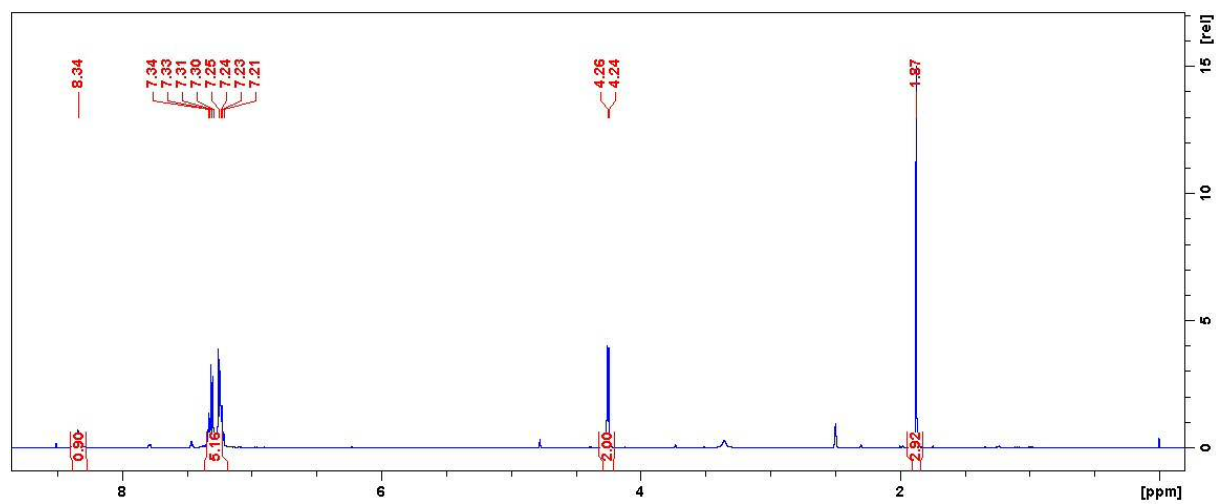


Figure S22.  $^1\text{H}$  NMR spectrum of N-benzylacetamide measured in DMSO-d<sub>6</sub> at 296 K.

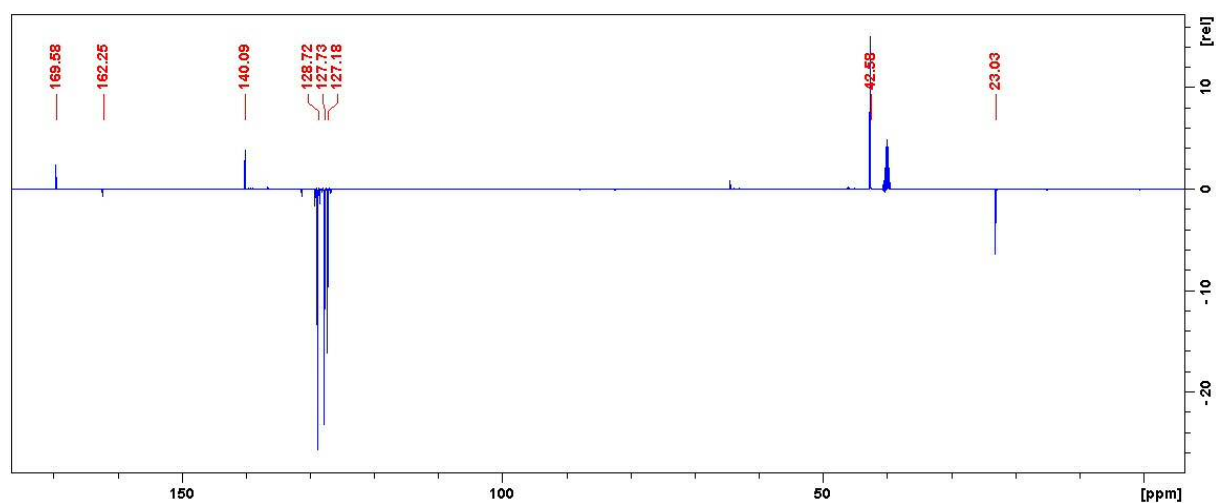
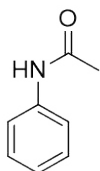


Figure S23. APT NMR spectrum of N-benzylacetamide measured in DMSO-d<sub>6</sub> at 296 K.



N-phenylacetamide

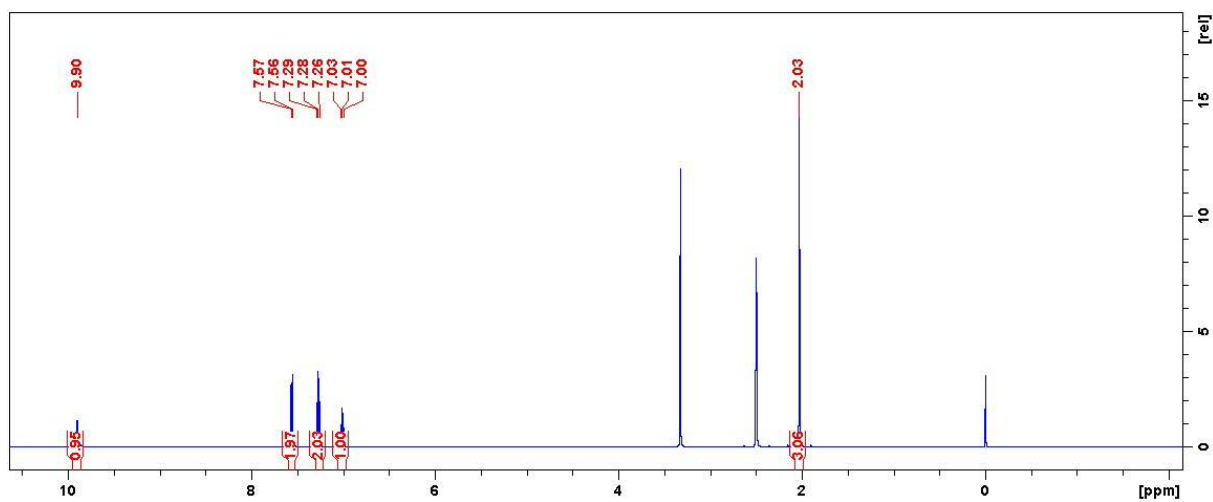


Figure S24. <sup>1</sup>H NMR spectrum of N-phenylacetamide measured in DMSO-d<sub>6</sub> at 296 K.

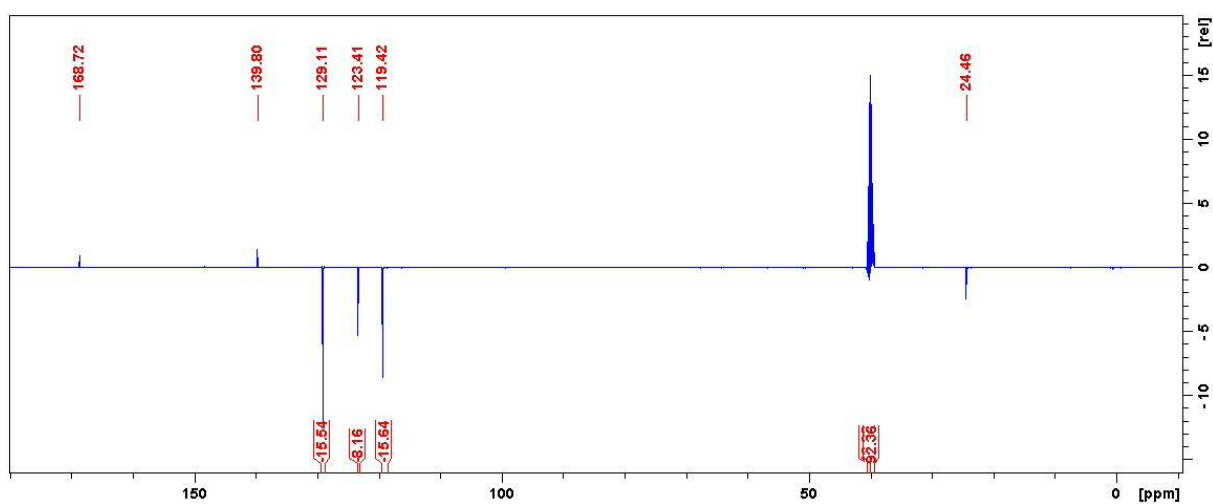
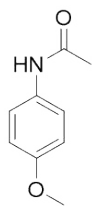
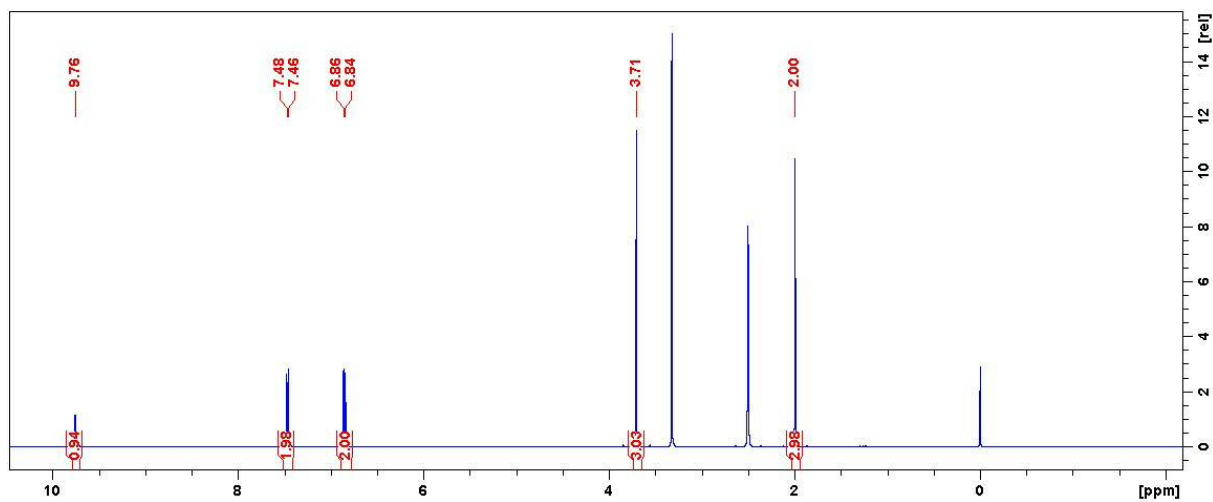


Figure S25. APT NMR spectrum of N-phenylacetamide measured in DMSO-d<sub>6</sub> at 296 K.





N-(4-methoxyphenyl)acetamide



**Figure S26.**  $^1\text{H}$  NMR spectrum of N-(4-methoxyphenyl)acetamide measured in DMSO- $d_6$  at 296 K.

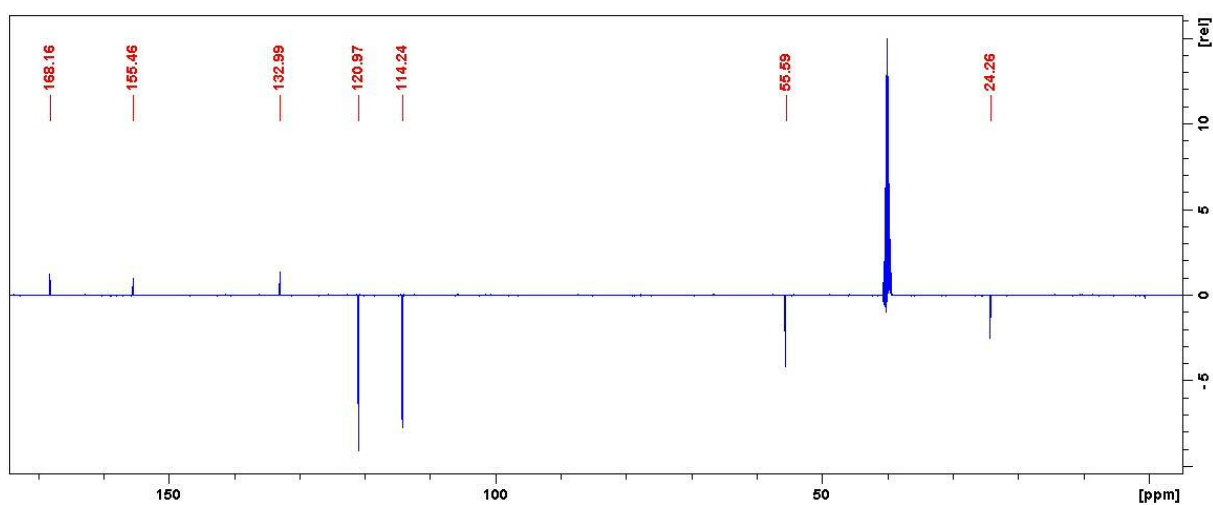
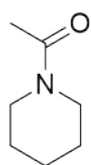


**Figure S27.** APT NMR spectrum of N-(4-methoxyphenyl)acetamide measured in DMSO- $d_6$  at 296 K.



1-(piperidin-1-yl)ethanone

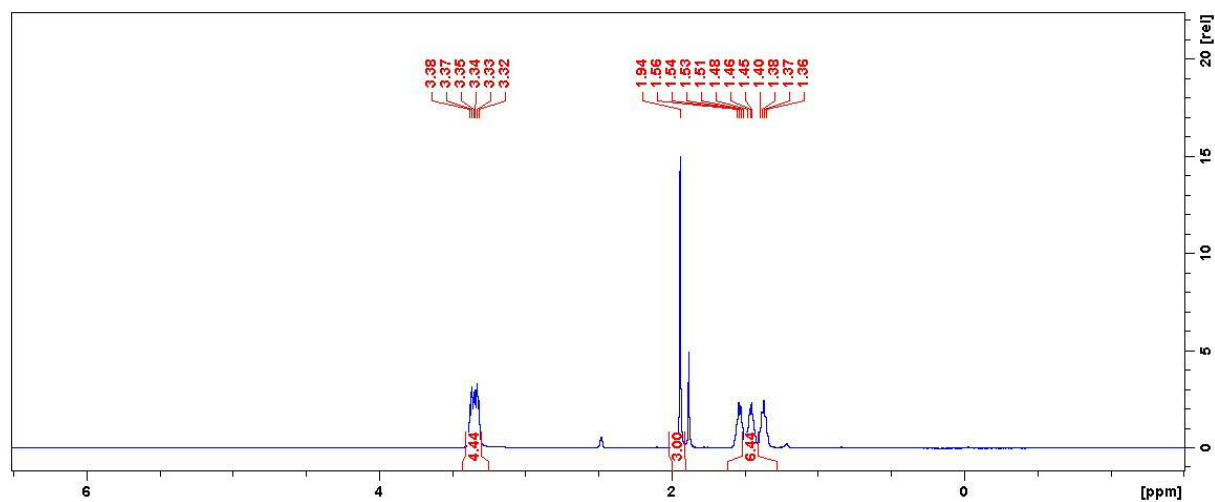


**Figure S28.** <sup>1</sup>H NMR spectrum of 1-(piperidin-1-yl)ethanone measured in DMSO-d<sub>6</sub> at 296 K.

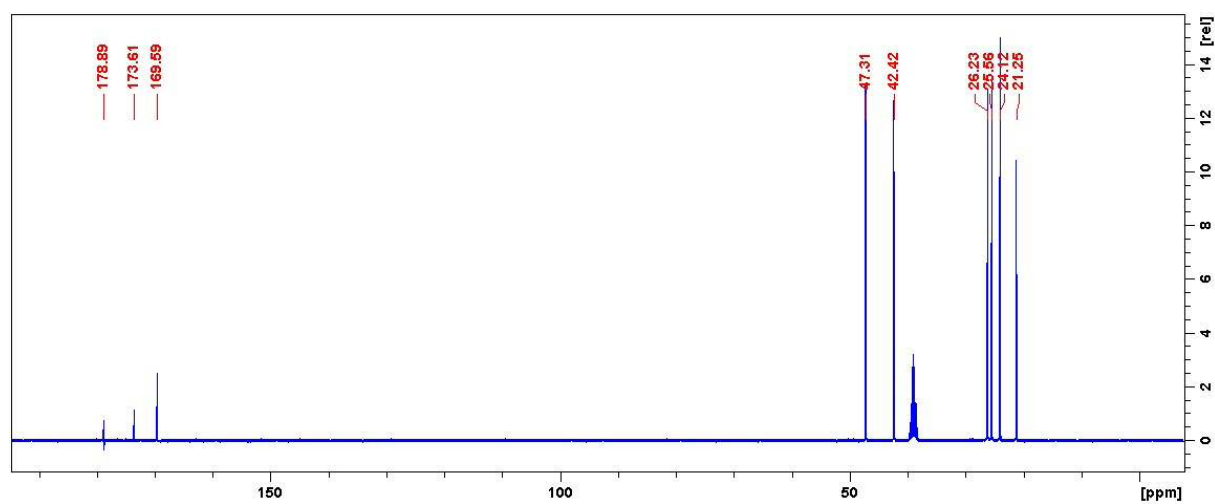
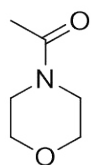


**Figure S29.** <sup>13</sup>C NMR spectrum of 1-(piperidin-1-yl)ethanone measured in DMSO-d<sub>6</sub> at 296 K.



1-morpholinoethanone

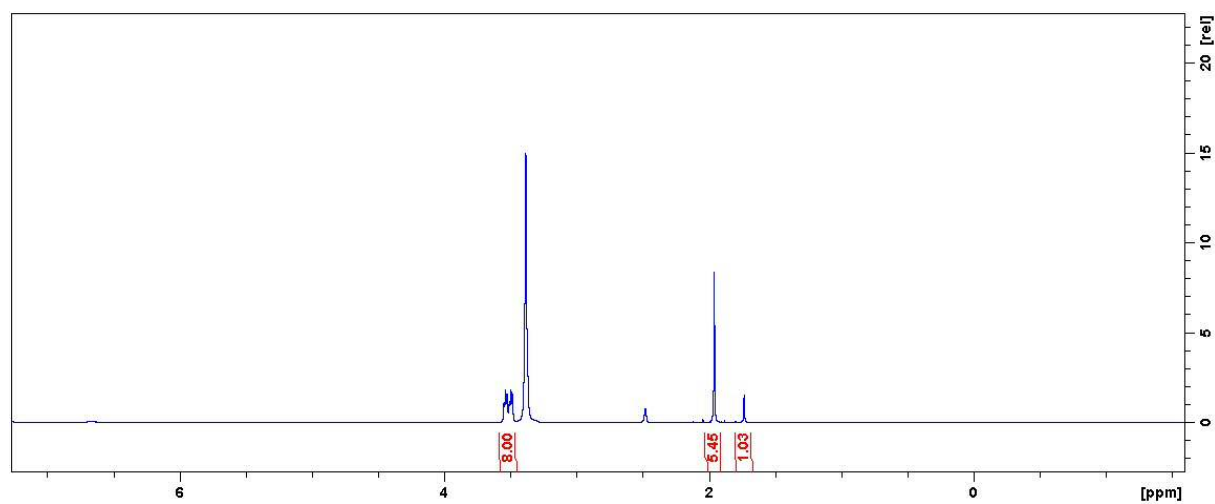


Figure S30.  $^1\text{H}$  NMR spectrum of 1-morpholinoethanone measured in DMSO- $d_6$  at 296 K.

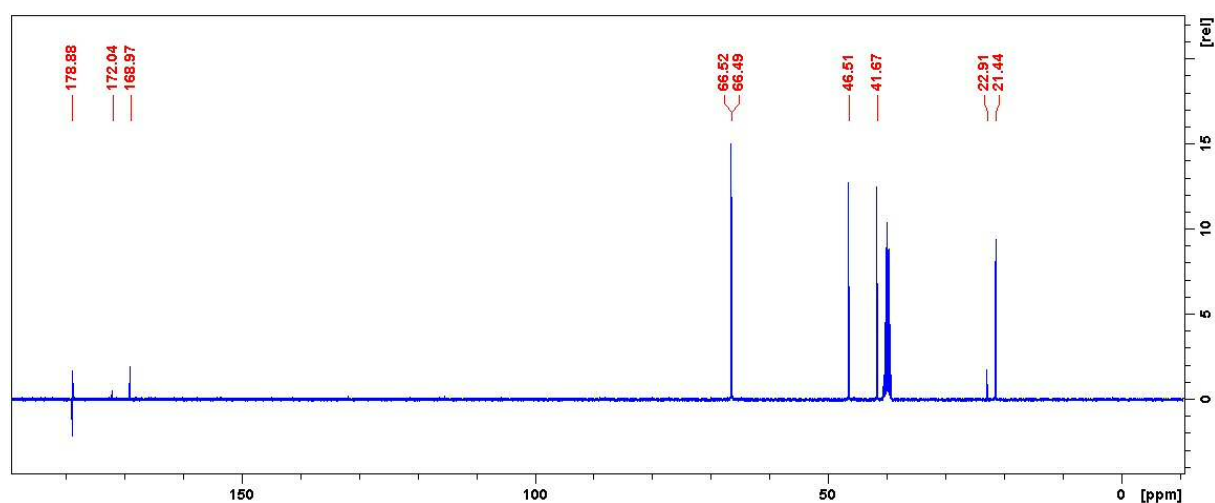
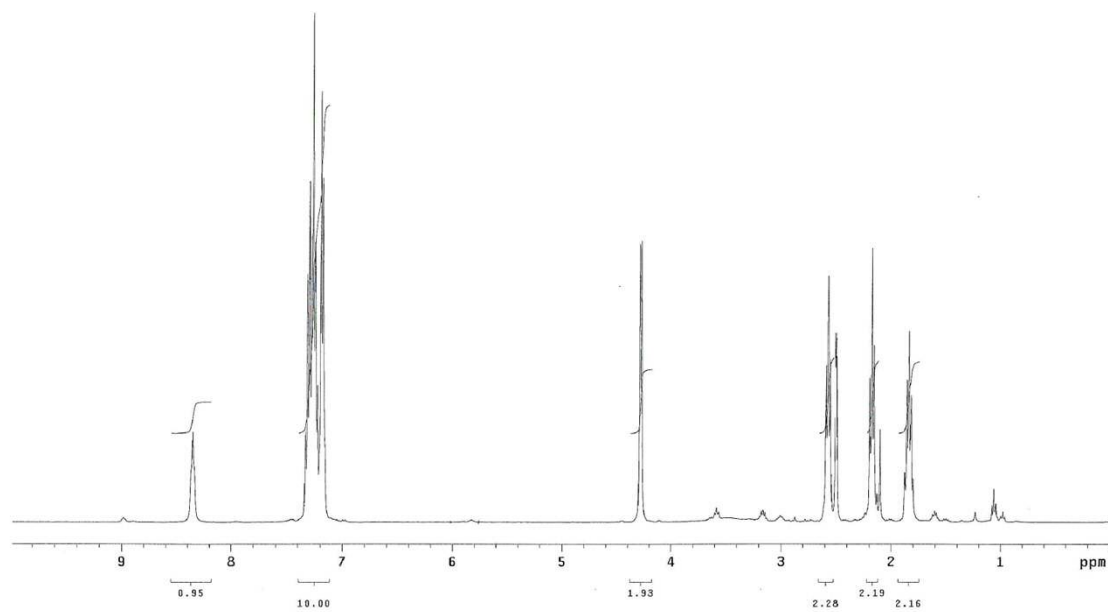


Figure S31.  $^{13}\text{C}$  NMR spectrum of 1-morpholinoethanone measured in DMSO- $d_6$  at 296 K.

<sup>1</sup>H NMR spectrum of Ogy104 in DMSO-d<sub>6</sub> (400 MHz; 32 scans)  
File: exp  
Pulse Sequence: s2pu1



**Figure S32.** <sup>1</sup>H NMR spectrum of N-benzyl-4-phenylbutanamide measured in DMSO-d<sub>6</sub> at 296 K gained by the scale-up reaction.

<sup>13</sup>C NMR spectrum of Ogy104 in DMSO-d<sub>6</sub> (100.6 MHz; 256 scans)  
File: exp  
Pulse Sequence: s2pu1

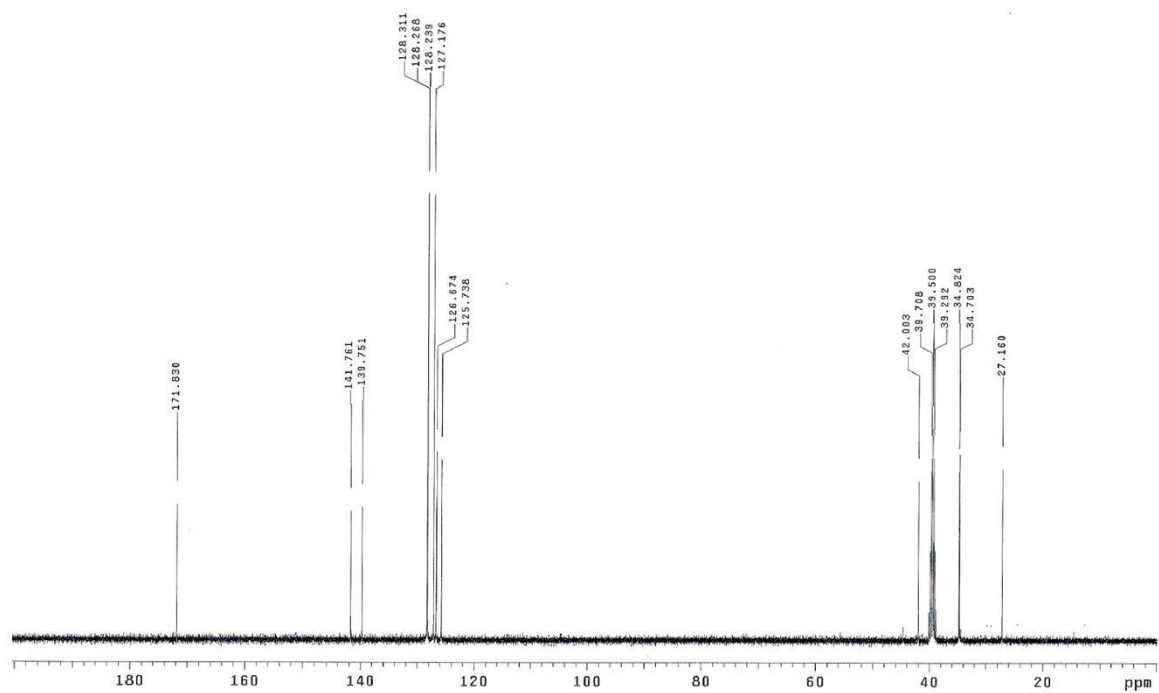


**Figure S33.** <sup>13</sup>C NMR spectrum of N-benzyl-4-phenylbutanamide measured in DMSO-d<sub>6</sub> at 296 K gained by the scale-up reaction.